การวิเคราะห์การแสดงออกและหน้าที่ของจีนและโปรตีนที่เกี่ยวข้องกับการเจริญเต็มที่ของเซลล์ไข่กุ้งกุลาดำ *Penaeus monodon*

นางสาวมหัทธนี ภิญโญ

วิทยานิพนธ์นี้เป็นส่วนหนึ่งของการศึกษาตามหลักสูตรปริญญาวิทยาศาสตรดุษฎีบัณฑิต
สาขาวิชาเทคโนโลยีชีวภาพ
คณะวิทยาศาสตร์ จุฬาลงกรณ์มหาวิทยาลัย
ปีการศึกษา 2556
ลิขสิทธิ์ของจุฬาลงกรณ์มหาวิทยาลัย

EXPRESSION AND FUNCTIONAL ANALYSIS OF GENES AND PROTEINS INVOLVED IN OOCYTE MATURATION OF THE GIANT TIGER SHRIMP *Penaeus monodon*

Miss Mahattanee Phinyo

A Dissertation Submitted in Partial Fulfillment of the Requirements
for the Degree of Doctor of Philosophy Program in Biotechnology
Faculty of Science
Chulalongkorn University
Academic Year 2013

Thesis Title	EXPRESSION AND FUNCTIONAL ANALYSIS OF GENES AND PROTEINS INVOLVED IN OOCYTE MATURATION OF THE GIANT TIGER SHRIMP *Penaeus monodon*
By	Miss Mahattanee Phinyo
Field of Study	Biotechnology
Thesis Advisor	Associate Professor Padermsak Jarayabhand, Ph.D.
Thesis Co-Advisor	Sirawut Klinbunga, Ph.D.

Accepted by the Faculty of Science, Chulalongkorn University in Partial Fulfillment of the Requirements for the Doctoral Degree

.....Dean of the Faculty of Science

(Professor Supot Hannongbua, Dr.rer.nat.)

THESIS COMMITTEE

.....Chairman

(Associate Professor Thaithaworn Lirdwitayaprasit, Ph.D.)

.....Thesis Advisor

(Associate Professor Padermsak Jarayabhand, Ph.D.)

.....Thesis Co-Advisor

(Sirawut Klinbunga, Ph.D.)

.....Examiner

(Kittinan Komolpis, Ph.D.)

.....Examiner

(Assistant Professor Sanit Piyapattanakorn, Ph.D.)

.....External Examiner

(Rachanimuk Hiransuchalert, Ph.D.)

.....External Examiner

(Oraprapai Gajanandana, Ph.D.)

มหัทธนี ภิญโญ : การวิเคราะห์การแสดงออกและหน้าที่ของจีนและโปรตีนที่เกี่ยวข้องกับการเจริญเต็มที่ของเซลล์ไข่กุ้งกุลาดำ *Penaeus monodon*. (EXPRESSION AND FUNCTIONAL ANALYSIS OF GENES AND PROTEINS INVOLVED IN OOCYTE MATURATION OF THE GIANT TIGER SHRIMP *Penaeus monodon*) อ.ที่ปรึกษาวิทยานิพนธ์หลัก: รศ. ดร. เผดิมศักดิ์ จารยะพันธุ์, อ.ที่ปรึกษาวิทยานิพนธ์ร่วม: ดร. ศิราวุธ กลิ่นบุหงา, 213 หน้า.

การค้นหาและพิสูจน์ลักษณะสมบัติของจีนและโปรตีนที่มีการแสดงออกแตกต่างกันในรังไข่มีความสำคัญต่อความเข้าใจกลไกที่เกี่ยวข้องกับการพัฒนารังไข่ของกุ้งกุลาดำ จึงทำการหาลำดับนิวคลีโอไทด์ที่สมบูรณ์ของจีน *PmRpd3, PmCdc16, PmCdk2* and *PmCdk5* ซึ่งมีความยาวเท่า 1949, 2068, 1763 และ 1758 คู่เบส มีส่วนของ ORF เท่ากับ 1452, 1332, 921 และ 1524 คู่เบส แปลงเป็นโปรตีนที่มีความยาว 483, 443, 306 และ 507 กรดอะมิโน ตามลำดับ ศึกษาการแสดงออกของจีนด้วยเทคนิค quantitative real-time PCR พบว่า *PmCdc2, PmCdk2, PmCdk7, PmChk1, PmBystin1* และ *PmRpd3* มีระดับการแสดงออกในรังไข่ของกุ้งวัยเจริญพันธุ์สูงกว่าในรังไข่ของกุ้งวัยรุ่น ($P < 0.05$) ในขณะที่ *PmCdc16* มีระดับการแสดงออกในรังไข่ของกุ้งวัยรุ่นสูงกว่าในกุ้งวัยเจริญพันธุ์ ($P < 0.05$) โดยระดับการแสดงออกของจีน *PmCdc2, PmCdk7, PmChk1* และ *PmBystin1* ในกุ้งที่ตัดก้านตาสูงกว่าในกุ้งที่ไม่ตัดก้านตา ($P > 0.05$) ในขณะ *PmCdk2* และ *PmRpd3* มีระดับการแสดงออกที่ลดลงในกุ้งที่ตัดก้านตา ($P > 0.05$) โดยการตัดก้านตาไม่ส่งผลต่อระดับการแสดงออกของจีน *PmCdc16* ตรวจสอบระดับการแสดงออกของจีน *PmBystin1* หลังการฉีดกระตุ้นด้วย serotonin (5-HT, 50 µg/g น้ำหนักตัว) ของกุ้งอายุ 18 เดือน พบว่ามีการแสดงออกของจีนเพิ่มขึ้นอย่างมีนัยสำคัญทางสถิติที่ 6-48 ชั่วโมงหลังการฉีดกระตุ้น ($P < 0.05$) สำหรับจีน *PmCdc2* มีการแสดงออกที่สูงขึ้นอย่างรวดเร็วที่ชั่วโมงที่ 1 ($P < 0.05$) และกลับสู่สภาวะปกติใน 3-72 ชั่วโมงหลังการฉีดกระตุ้น ส่วนการแสดงออกของจีน *PmCdk7* นั้นเพิ่มสูงขึ้นที่ 6-12 ชั่วโมง ($P < 0.05$) และลดลงสู่ภาวะปกติที่ 24-48 ชั่วโมงหลังการฉีดกระตุ้น นอกจากนี้ระดับการแสดงออกของจีน *PmCdc2* ในชิ้นรังไข่ที่ทำการเลี้ยงเนื้อเยื่อ และบ่มด้วย 5-HT และ 17α, 20β-DHP ในระดับความเข้มข้นต่างๆ นั้น ไม่มีความแตกต่างกัน ($P > 0.05$) ตรวจสอบตำแหน่งการแสดงออกของจีน *PmCdc2* และ *PmCdk7* ด้วยวิธี *in situ* hybridization พบว่ามีการแสดงออกใน ไซโตพลาสซึมของเซลล์ไข่ระยะ previtellogenic ทั้งในกุ้งปกติและกุ้งที่ตัดก้านตา ในขณะที่จีน *PmBystin1* มีตำแหน่งการแสดงออกในโอโอพลาสซึมของเซลล์ไข่ในระยะ previtellogenic และ vitellogenic แต่ไม่พบการแสดงออกในไข่ระยะที่สมบูรณ์พันธุ์มากกว่านี้ ทำการสร้างโปรตีนลูกผสมของ rPmApc11, rPmBystin1, rPmCdc2, rPmCdc20, rPmCdk7, rPmChk1 และ rPmRpd3 และผลิตโพลิโคนอลแอนติบอดีในกระต่าย สามารถผลิตแอนติบอดีของโปรตีนลูกผสมดังกล่าวได้ทั้งหมด ยกเว้น rPmApc11 และ rPmChk1 ผลการทดลองพบว่าโปรตีน PmBystin1 (52 kDa) มีการแสดงออกในไข่ระยะที่ 2-4 และหลังวางไข่ ทั้งในกุ้งปกติและกุ้งที่ตัดก้านตา ส่วนการแสดงออกของโปรตีน PmCdk7 (67 kDa) มีการแสดงออกที่แตกต่างกันในระยะที่ 2-4 เมื่อเปรียบเทียบกับระยะที่ 1 แต่ไม่พบการแสดงออกในรังไข่กุ้งวัยรุ่น ในขณะที่โปรตีน PmCdc2 (34 kDa) และโปรตีนขนาดเล็กขนาด 23 kDa (ribosomal protein S3) มีการแสดงออกทุกระยะของรังไข่ ผลจาก Western blot เมื่อใช้แอนติบอดีที่จำเพาะต่อ Thr161 phosphorylation ของ Cdc2 พบว่ามีกระบวนการ phosphorylation ของ PmCdc2 เกิดขึ้นในทุกระยะของรังไข่แต่มีปริมาณ phosphorylatied Cdc2 มากที่สุดในรังไข่ระยะที่ 4 ผลจาก Immunofluorescence พบโปรตีน PmCdk7 ในโอโอพลาสซึมของไข่ระยะ previtellogenic และมีการเปลี่ยนตำแหน่งของโปรตีนดังกล่าวไปยังนิวเคลียส ระหว่างการพัฒนาของรังไข่ นอกจากนี้ยังพบตำแหน่งของการเกิด phosphorylation ของจีน Cdc2 (Thr 161) ในเซลล์ฟอลลิเคิล และในโอโอพลาสซึมของไข่ระยะ previtellogenic, vitellogenic และรอบๆ cortical rods ในไข่ที่ใกล้เจริญพันธุ์ และไข่เจริญพันธุ์ทั้งในกุ้งปกติและกุ้งที่ตัดก้านตา

สาขาวิชา เทคโนโลยีชีวภาพ ลายมือชื่อนิสิต .....

ปีการศึกษา 2556 ลายมือชื่อ อ.ที่ปรึกษาวิทยานิพนธ์หลัก

ลายมือชื่อ อ.ที่ปรึกษาวิทยานิพนธ์ร่วม .....

5273923923 : MAJOR BIOTECHNOLOGY
KEYWORDS: PENAEUS MONODON / BLACK TIGER SHRIMP / MEIOTIC MATURATION / IMMUNOFLUORESCENCE / PHOSPHORYLATION

MAHATTANEE PHINYO: EXPRESSION AND FUNCTIONAL ANALYSIS OF GENES AND PROTEINS INVOLVED IN OOCYTE MATURATION OF THE GIANT TIGER SHRIMP *Penaeus monodon*. ADVISOR: ASSOC. PROF. PADERMSAK JARAYABHAND, Ph.D., CO-ADVISOR: SIRAWUT KLINBUNGA, Ph.D., 213 pp.

Identification and characterization of genes and proteins differentially expressed in ovaries is necessary for understanding mechanisms involving ovarian developmental processes of the giant tiger shrimp (*Penaeus monodon*). The full-length cDNA of *PmRpd3, PmCdc16, PmCdk2 and PmCdk5* were characterized. They were 1949, 2068, 1763 and 1758 bp in length with an ORFs of 1452, 1332, 921 and 1524 bp corresponding to polypeptides of 483, 443, 306 and 507 amino acids, respectively. Quantitative real-time PCR indicated that the expression level of *PmCdc2, PmCdk2, PmCdk7, PmChk1, PmBystin1,* and *PmRpd3* were more abundantly expressed in ovaries of broodstock than juveniles ($P < 0.05$) while the expression of *PmCdc16* was in the opposite direction ($P < 0.05$). Eyestalk ablation promoted the expression level of *PmCdc2, PmCdk7, PmChk1* and *PmBystin1* ($P < 0.05$) but resulted in a decreased expression level of *PmCdk2* and *PmRpd3* ($P < 0.05$) relative to that in intact broodstock. However, it had no effect on the expressed profile of *PmCdc16*. Expression level of PmBystin1 in ovaries of 18-month-old *P. monodon* upon 5-HT injection (5-HT, 50 µg/g body weight) were significantly increased at 6 - 48 hours post injection (hpi, $P < 0.05$). PmCdc2 was immediately up-regulated at 1 hpi ($P < 0.05$) and its expression returned to the normal level at 3-72 hpi. The expression level of *PmCdk7* was increased at 6 - 12 hpi ($P < 0.05$) and reduced to the previous level at 24 - 48 hpi. However, the expression level of *PmCdc2* in cultured ovarian explants was not affected by different concentrations of 5-HT and 17α, 20β-DHP treatment ($P > 0.05$). *In situ* hybridization indicated that *PmCdc2* and *PmCdk7* were localized in ooplasm of previtellogenic oocytes in both intact and eyestalk-ablated broodstock while *PmBystin1* was localized in the ooplasm of previtellogenic and vitellogenic oocytes but not in more mature stages of oocytes. Recombinant (r) PmApc11, rPmBystin1, rPmCdc2, rPmCdc20, rPmCdk7, rPmChk1 and rPmRpd3 were successfully expressed *in vitro*. Polyclonal antibodies against these proteins except PmApc11 and PmChk1 were successfully produced in rabbit. PmBystin1 (52 kDa) was expressed in stages II-IV and after spawning in both intact and eyestalk-ablated. PmCdk7 (67 kDa) was differential expressed in stages II-IV ovaries when compared with stage I ovaries in intact broodstock but it was comparably expressed among different ovarian developmental stages in eyestalk-ablated broodstock. This protein was not observed in premature ovaries of juveniles. In addition, western blot analysis revealed the expected 34 kDa band (PmCdc2) along with a smaller band of 23 kDa (ribosomal protein S3) in all stages of ovaries. Using phospho-Cdc2 (Thr161) polyclonal antibody, the positive signal of 34 kDa was observed in all ovarian stages but the most intense signal was found in stage IV ovaries. Immunofluorescence revealed the positive signals of PmCdk7 in ooplasm of previtellogenic oocytes and its subsequent nucleo-cytoplasmic translocation during oocyte development. Moreover, Anti-Phospho-Cdc2 (Thr161) PcAb gave the positive imunoreactive signals in ooplasm of follicular cells, previtellogenic and vitellogenic oocyes and around cortical rods of nearly mature and mature oocytes in both intact and eyestalk-ablated shrimp.

Field of Study: Biotechnology
Academic Year: 2013

Student's Signature .....
Advisor's Signature .....
Co-Advisor's Signature .....

ACKNOWLEDGEMENTS

I would like to express my deepest gratitude to my advisor Associate Professor Padermsak Jarayabhand, Ph.D. and my co-advisor Sirawut Klinbunga, Ph.D. for their guidance, supervision, encouragement, invaluable suggestion and supports throughout my study.

My gratitude is also extended to Associate Professor Thaithaworn Lirdwitayaprasit, Ph.D., Kittinan Komolpis, Ph.D., Assistant Professor Sanit Piyapattanakorn, Ph.D., Oraprapai Gajanandana, Ph.D. and Rachanimuk Hiransuchalert, Ph.D. for serving as thesis committee, for their recommendation and also useful suggestion.

I would particularly like to extend my thank to the Marine Biotechnology Research Unit, Aquatic Molecular Genetics and Biotechnology laboratory, National Center for Genetic Engineering and Biotechnology (BIOTEC), National Science and Technology Development Agency (NSTDA) and Thailand Graduate Institute of Science and Technology (TGIST) for my financial support.

Many thanks are also excessively to Pachumporn Nounurai, Ph.D, Ms. Kanchana Sittikhankeaw, Ms. Natechanok Thamneamdee, Ms. Patchari Yocawibun, Ms. Sasithon Petkon, Ms. Pornthip Sawatpanich, Ms. Sirikarn Prasertlux, Ms. Parichat Chumtong and Ms. Witchulada Talakhun everyone in the laboratory for their help, suggestion and kindness friendship that give a happy time during a study periods.

Finally, I would like to express my deepest gratitude to my beloved parents, all members of my family, Mr. Surapong Nontaprasert and for their love, care, understanding and encouragement extended throughout my study.

CONTENTS

Page

Page

Page

Page

Page

Page

LIST OF TABLE

PAGE

LIST OF FIGURE

PAGE

LIST OF ABBREVIATIONS

bp	base pair
^{o}C	degree Celsius
DEPC	Diethylpyrocarbonate
dATP	deoxyadenosine triphosphate
dCTP	deoxycytosine triphosphate
dGTP	deoxyguanosine triphosphate
dTTP	deoxythymidine triphosphate
DNA	deoxyribonucleic acid
EDTA	ethylene diamine tetraacetic acid (disodium salt)
EtBr	ethidium bromide
HCl	hydrochloric acid
IPTG	isopropyl-thiogalactoside
kD	kilodalton
M	Molar
mg	milligram
mRNA	Messenger-Ribonucleic acid
ml	millilitre
mM	millimolar
ng	nanogram

OD	optical density
PCR	polymerase chain reaction
RNA	Ribonucleic acid
rpm	revolution per minute
SDS	sodium dodecyl sulfate
Tm	melting temperature
Tris	Tris (hydroxy methyl) aminomethane
U	unit
UV	ultraviolet
w/v	weight/volume
µg	Microgram
µl	Microlitre

CHAPTER I
INTRODUCTION

1.1 Background information

The giant tiger shrimp (*Penaeus monodon*) is one of the world's most economically important cultured crustaceans. Reduced degrees of reproductive maturation of the *P. monodon* in captivity is the major constraint for the shrimp industry (Withyachumnarnkul et al., 1998; Wongprasert et al., 2006) Therefore, farming of *P. monodon* in Thailand is currently dependent on wild-caught broodstock resulting in overexploitation of wild stock (Klinbunga et al., 1996).

The meiotic maturation of animal oocytes is controlled by the maturation promotion factor (MPF), a complex of Cdc2 and cyclin B. The maturation inducing hormone (MIH; progesterone or its derivatives) induced germinal vesicle breakdown (GVBD) of oocytes. A complex of Cdc2-cyclinB contains abundant phosphorylated inactive MPF (called pre-MPF), that are maintained inactive by two inhibitory phosphorylations of the Thr14 and Tyr15 residues of Cdc2. Oocyte maturation depends on the conversion of pre-MPF into MPF by the Cdc25 phosphatase (Chk1 phosphorylates Cdc25 on a crucial regulatory site, therefore inhibit Cdc25 phosphatase) that directly dephosphorylates Thr14 and Tyr15 residues of Cdc2 (Dunphy et al., 1988; Dunphy and Kumagai, 1991). In most animals, MPF exists in the cytoplasm of immature oocyte as an inactive form (phosphorylation of Thr161, Thr14 and Tyr15 of Cdc2) and activated by dephosphorylation on Thr14/Tyr15 of Cdc2 kinase during oocyte meiotic maturation. Cdc2 protein can be dephosphorylated shortly after hormonal stimulation.

Alternatively, Cdc2 presents as a monomer with no phosphorylated site due to the absence of cyclin B protein in the immature oocytes in most amphibians and fishes. Only Thr161 phosphorylation by Cdk7 complex is required for MPF activation in fish oocyte maturation (De Smedt et al., 2002; Gautier et al., 1990; Honda et al.,

1993; Kobayashi et al., 1991). However, the molecular mechanism for MPF activation is not understood in *P. monodo*n.

Typically, the Cdc2 activity is inhibited by a complex of Cdc20-APC/C-mediated cyclin B degradation that suppressed by Mos/MAPK-dependent activity. Anaphase Promoting Complex/Cyclosome (APC/C) was consist of the components particularly Apc1, Cdc27 and Cdc16, which are importantly phosphorylated in M-phase (Kraft et al., 2003; Whitfield et al., 2013; Yamamoto et al., 2005). The APC/C activity is inhibited by Cdk2-cyclin E. Cyclin E levels rise before meiosis II and Cdk2-cyclin E can inhibit the APC/C (Marston and Amon, 2004). In this study, Apc11, Cdc20 and Cdc16 of *P. monodon* were characterized.

Reproductive physiology in crustaceans is highly controlled and regulated by the nervous and endocrine systems (Engelmann, 1994). Endocrine control of female reproduction is governed by a variety of hormonal and neuronal factors that involve neuropeptide hormones, such as gonad stimulating hormone (GSH) and sex steroids such as estradiol and progesterone (Huberman, 2000; Zapata et al., 2003).

The presence of vertebrate-type steroids has been documented in almost all invertebrate groups including crustaceans (Cardoso et al., 1997; Lafont, 1991; Lehoux and Sandor, 1970). Progesterone (P4) and its derivatives are sex steroid hormones that play important roles in gametogenesis (Fingerman et al., 1993; Miura et al., 2006; Rodríguez et al., 2002). P4 and 17α-hydroxyprogesterone administration induced ovarian maturation and spawning in *Metapenaeus ensis* (Yano, 1985; Yano, 1987). The conversion of progesterone into estradiol-17β was reported in *Marsupenaeus japonicus* (Summavielle et al., 2003). Estradiol-17β and progesterone levels in the hemolymph were shown to fluctuate closely with that of the serum vitellogenin level during ovarian maturation stages of *P. monodon* (Quinitio et al., 1994) implying its controlling role in vitellogenesis.

In female crustaceans, serotonin (5-HT) stimulates the release of several hormones including crustacean hyperglycemic hormone (CHH; (Keller et al., 1984) red pigment dispersing hormone (RPDH; (Rao and Fingerman, 1970), and molt inhibiting hormone (MIH; (Mattson and Spaziani, 1985). 5-HT injection induced ovarian

maturation in the crayfish, *Procambarus clarkii* (Kulkarni et al., 1992; Sarojini et al., 1995) and the Pacific white shrimp, *Litopenaeus vannamei* (Vaca and Alfaro, 2000) at rates lower than unilateral eyestalk ablation.

Alfaro et al. (2004) reported that injection of combined 5-HT and dopamine antagonist, spiperone stimulated ovarian maturation and spawning in *L. stylirostris* and *L. vannamei*.

Genetic improvement of *P. monodon* cannot be achieved without the knowledge on the control of reproduction. Mechanisms controlling ovarian maturation of *P. monodon* at the molecular level are important and can be directly applied to the industry. Understanding how an immature oocyte transforms into an egg during oocyte maturation is critical for the knowledge of reproductive maturation of *P. monodon*. Here, molecular mechanisms on the signal transduction that control meiotic maturation of *P. monodon* oocytes were extensively studied.

1.2 Objectives of this thesis

1.2.1 Characterization of the full-length cDNA of genes functionally related to ovarian development of *P. monodon*.

1.2.2 Examination of the expression profiles of interesting genes/proteins by quantitative real-time PCR and western blot analysis.

1.2.3 Determination of *in vitro* and *in vivo* effect of 5-HT and 17α, 20β-dihydroxyprogesterone on expression of reproduction-related genes in *P. monodon*.

1.2.4 Determining the localization of interesting genes and proteins by *in situ* hybridization and immunofluorescence.

1.3 General introduction

In Thailand, shrimp farming started in the 1970s using locally available *P. monodon* broodstock captured from the sea to produce postlarvae in land-based hatcheries for pond stocking. By the early 1990s, Thailand emerged as the world's leading farmed shrimp producer and exporter based on the main production of *P. monodon*. The intensive farming system has resulted in consistent production of marine shrimp of Thailand. Accordingly, Thailand has been regarded as the leader of

cultivated shrimp for over a decade. Farming of *P. monodon* in Thailand has increased enormously during the last few decades, leading to the production of at least 200,000 metric tons annually during 1989 – 1995 (Lin and Nash, 1996).

However, the production was dropped owing to several relentless outbreaks of pollution and diseases become the lack of high quality wild and domesticated broodstock. These problems has eventually lead the farming to decrease and a replacement of *P. monodon* with the Pacific white shrimp *Litopenaeus vannamei* (Figure 1.1).

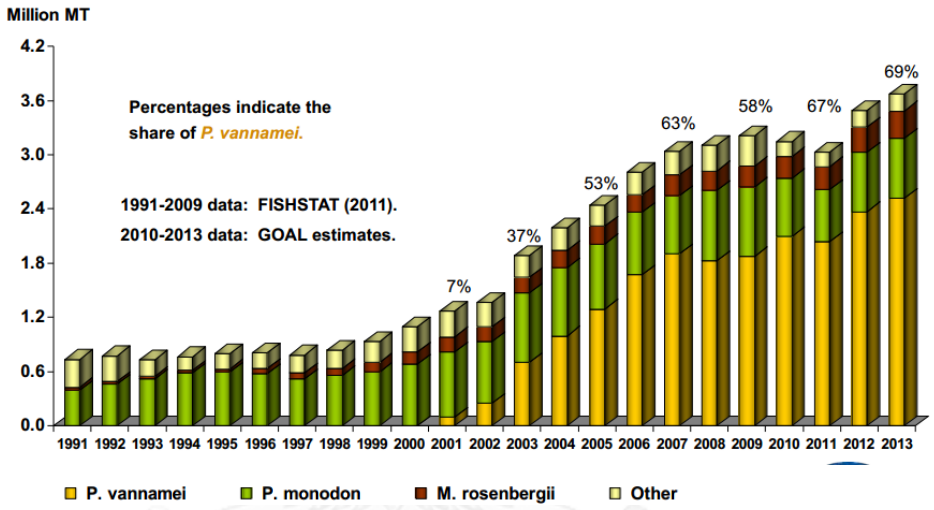

Figure 1. 1 Shrimp aquaculture in Asia during 1991-2013 (www.gaalliance.org)

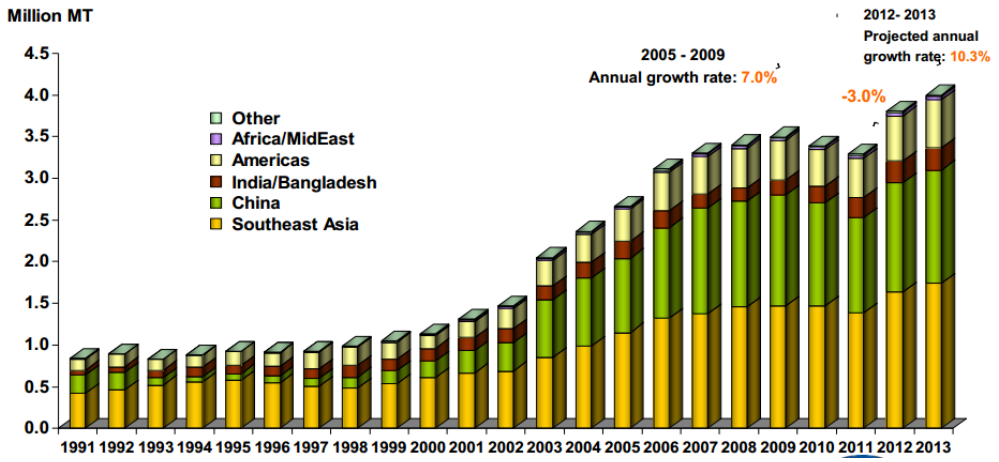

Figure 1. 2 World shrimp aquaculture production during 1991-2013 (www.gaalliance.org)

Table 1. 1 Export of shrimp from Thailand during 2007-2012

Country	2007		2008		2009		2010		2011		2012	
	Quantity (Mkg)	Value (MB)	Quantity (Mkg)	Value (MB)	Quantity (Mkg)	Value (MB)	Quantity (Mkg)	Value (MB)	Quantity (Mkg)	Value (MB)	Quantity (Mkg)	Value (MB)
USA	180	41,736	177	42,496	183	44,750	192	47,207	176	50,576	126	34,719
Japan	58	14,458	63	16,373	70	19,132	76	20,373	77	24,107	80	25,796
EU27	30	7,721	39	9,699	52	12,357	66	14,924	59	15,979	50	14,026
Canada	25	5,525	20	4,837	21	5,038	22	5,446	22	6,554	21	6,249
Australia	8	2,030	7	1,739	9	2,231	10	2,473	9	2,659	10	3,218
Korea	14	2,967	12	2,321	10	1,942	9	1,825	10	2,387	10	2,374
China	3	727	5	681	4	793	11	1,598	5	1,079	8	1,496
ASEAN10	7	1,193	7	1,112	10	1,484	9	1,527	8	1,878	20	3,388
Taiwan	3	638	5	936	5	993	6	1,070	5	1,210	4	1,165
Hong kong	4	1,142	3	905	3	874	3	835	3	774	6	1,159
OTHER	11	2,198	11	2,182	11	2,309	11	2,327	9	2,148	7	1,770
Total	**350**	**80,332**	**354**	**83,285**	**383**	**91,909**	**420**	**99609**	**388**	**109,356**	**348**	**95,365**

Source: Department of Fisheries (2013)

The world shrimp aquaculture production has shown strong increase in subsequent years (Figure 1.2). Several Thai shrimp companies have well-established marketing companies in the major import markets in China and Southeast Asia.

1.4 Penaeid shrimp biology

1.4.1 Taxonomy of *P. monodon*

The giant tiger shrimp is scientific classification as a member of Phylum Arthropoda; Subphylum Crustacea; Class Malacostraca; Subclass Eumalacostraca; Order Decapoda; Suborder Natantia; Infraorder Penaeidea; Superfamily Penaeoidea; Family Penaeidae, Rafinesque, 1985; Genus Penaeus, Fabricius, 1798 (Brusca and Brusca, 1990; Mohamed, 1970) and Subgenus *Penaeus*. The scientific name of shrimp is *Penaeus monodon* where the English common name is giant tiger shrimp or black tiger prawn (Bailey-Brook and Moss, 1992).

1.4.2 External morphology of penaeid shrimp

Shrimp body is divided into 2 parts, the head and body section. The head fused with the chest called the cephalothorax. This section consists of 13 sections. 8 segment the chest and 5 segments on the head. Body and the abdomen consists of 6 segments, each segment has a pair of swimming feet are also segmented (Figure 1.3A). The inner and outer branches are the endopodite and exopodite, respectively (Figure 1.3B). The body surface covered with chromatophores (Figure 1.3C), which are highly branched cell containing pigment granules.

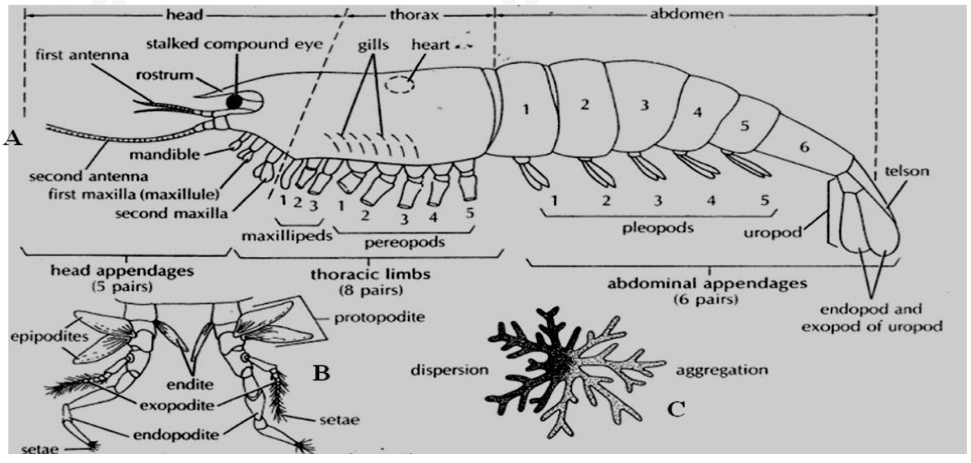

Figure 1. 3 General external anatomy of a crustacean, showing the head, thorax, abdomen and associated appendages. (B) Illustration of biramous appendages. (C) Patterns of pigment dispersion in crustacean chromatophores. In the dispersed configuration, the cuticle become dark; pigment aggregation within the chromatophores cause the cuticle to become lighter in color. Movement of pigment within the chromatophores is under hormonal control in response to changing light intensities (American Society of Zoologists; Weber, 1993).

1.4.3 Life cycle of penaeid shrimp

After spawning, it takes about 12 to 15 hr before *P. monodon* eggs hatch to the nauplius stage. The naupliar substages comprise nauplius1 to nauplius 6 within 48 - 56 hr. The zoea stage has three substages, which are completed within 5 to 6 days. Mysis is the last larval stage composed three stages, which are completed in 4 to 5 days. The postlarva stage follows. Postlarva 4 to postlarva 6 is the normal substage at which postlarvae are harvested for stocking in ponds. *P. monodon* females spawn average 500,000 **-** 1,000,000 eggs in the open sea. Hatching of the eggs were through the planktonic larval stages until the postlarva period of time about 2 weeks. Benthic postlarvae are found along the coast or in mangrove swamps and other estuarine areas where they are collected by fry gatherers for rearing in brackish water ponds up to marketable size (Figure 1.4). Wild fry become juveniles and adults in estuarine areas and return to the sea for spawning (Rosenberry, 1997).

1.4.4 Reproductive system

Reproductive organs consist of gonads which are similar in position, size and general disposition in both the sexes. They are situated in the posterior region of the thorax dorsally above the hepatopancreas and below the pericardium. Fertilization of penaeid shrimp is external. The male reproductive system includes paired, it call petasma (Fig. 1.5 A). Mating of *P. monodon* occurs at night after the female molts. Sperm is deposited into a special structure called the thelycum on the underside of the female's thorax (Fig. 1.5 B).

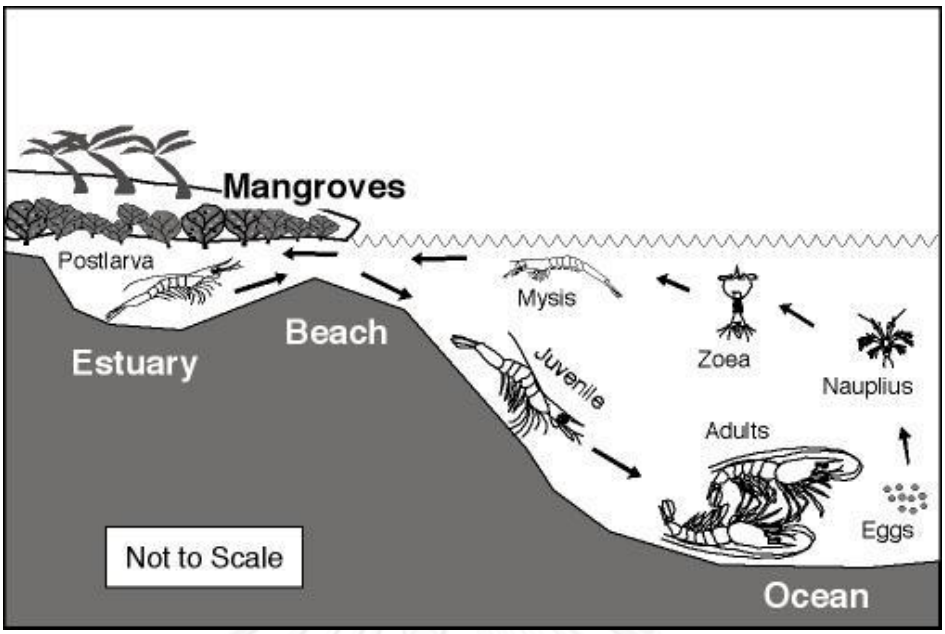

Figure 1. 4 The life cycle and distribution of penaeid shrimp

Source:http://oceanworld.tamu.edu/resources/oceanography-book/invertebrates.htm

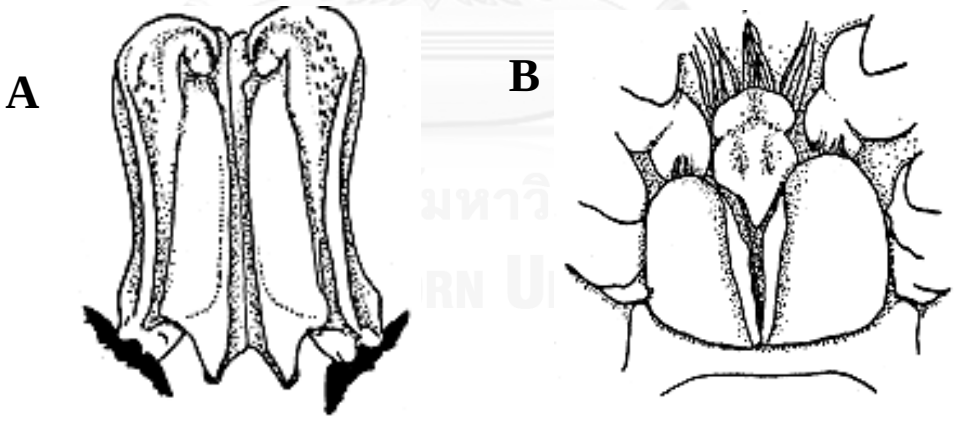

Figure 1. 5 Reproductive systems of male and female (A) petasma, (B) thelycum (King, 1998).

1.4.5 Ovarian development of penaeid shrimp

Fertilization by the males quickly follows ovulation, and generally occurs at night. A mature female (30-60 g weight) will produce about 60,000 to 200,000 eggs per spawning event. At release, the eggs are about 300 μm in size, and they are covered with a cortical granule protein (Bradfield et al., 1989; Quackenbush, 2001; Rankin et al., 1989).

Ovarian maturation in penaeid shrimp is divided into primary and secondary vitellogenesis. Primary vitellogenesis is described by little change in overall size or diameter. Secondary vitellogenesis is where the eggs actually grow in size from around 50 μm to 300 μm. In most crustaceans, the production of primary oocytes derived from oogonia continues throughout adult life. These small eggs undergo several cytological changes during their transition to secondary vitellogenesis. Ribosomes appear and an extensive endoplasmic reticulum develops. The primary oocytes also increase in size. Follicle cells, around the primary oocyte, also hypertrophy. During secondary vitellogenesis, yolk proteins are stored in the oocyte. This yolk protein storage results in the significant expansion of the cell. Yolk proteins produced in follicle cells (*Penaeus japonicas,* (Yano, 1987).

The ovarian development of *P. monodon* is divided in 4 phases according to its histological features and germ cell association as shown in Figure 1.3. It consists of stages I (immature ovaries), II (developing ovaries), III (nearly mature ovaries) and IV (mature ovaries) ovaries. The post-spawning stage may be recognized as stage V ovaries.

For stage I, ovaries are not visible externally from the dorsal exoskeleton. Upon dissection, it appears colorless, white or flesh-colored and devoid of visible egg. The stage II: ovaries are relatively thicker compared to stage I. Color of dissected ovary in stage I and II ranges from grayish green to blue green. Small individual eggs are quite discernible. The stage III ovaries are visible through the dorsal exoskeleton as a thick, solid and dark linear band as it expands at the posterior thoracic and anterior abdominal regions. A slight “butterfly” shape can be seen at the first abdominal segment. The dissected ovary is olive or dark green in color, firm and

granular in texture, with clumps of discernible eggs. The stage IV ovaries are a very prominent, dark band, with the diamond-shape expansion at the first abdominal segment larger and distinct. Upon dissection, the ovary is olive or dark green in color; it fills up all the available space in the body cavity. The ovary is firm and granular in texture with clumps of discernible eggs. Appearance of rod-like bodies, called cortical rods (CRs), arranged radially around the periphery of the oocyte plasma membranes. For the post-spawning stage, ovaries may be similar to that of immature stage (complete spawning) or has clear and dark areas in the different regions. Dissected ovaries are thin and limp and may have white and green patches (Kruevaisayawan et al., 2007b; Tan-Fermin and Pudadera, 1989; Yano, 1987). Histology and histochemistry of ovarian development of *P. monodon* are summarized in Table 1.2.

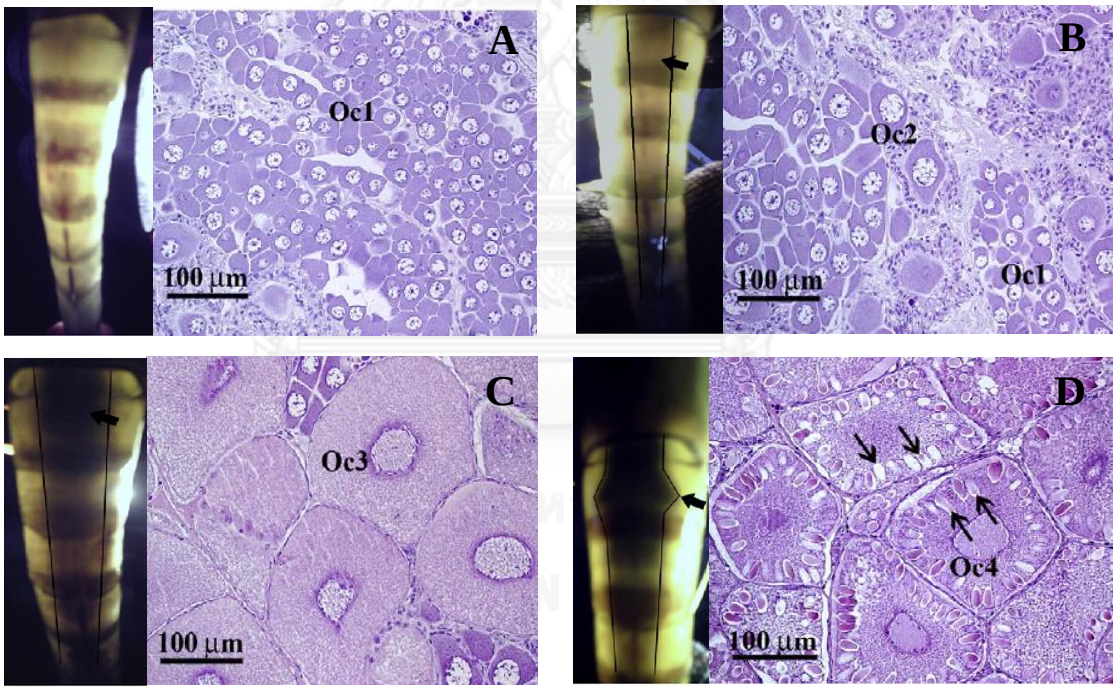

Figure 1. 6 The external appearances light transmission and histology during ovaries development of *P. monodon*. (A) The light transmission in stage I showing clear dorsal surface and the histology, showing predominating step 1 oocytes (Oc1). (B) Stage II ovary as a thin dense midline (arrow), this stage of ovary contained mostly step 2 oocytes. (C) Stage III ovary appeared as a thick band (arrow) and contained mostly step 3 oocytes (Oc3). (D) Stage IV ovary appeared as a thick, broad band with wing-like structure representing lateral lobes (arrow), and it contained a large number of step 4 or mature oocytes (Oc4), with numerous cortical rods (arrows) in their peripheries (Ngernsoungnern *et al.,* 2008)

Table 1. 2 Histology and histochemistry of ovarian development stages in *P. monodon*

ocyte stage/component	Qualitative methods			
	Histology	Histochemistry		
		Mallory	AB-PAS	SB
P:previtellogenic				
a) oocyte	-oogonia and primary oocytes			
1) Nucleus	-chromatin nucleolus and/or perinucleolus stage; single to several nucleoli in nucleoplasm			
2) Cytoplasm	-clear	Basophilic	(-)	(-)
b) follicle cells	-rectangular or cuboidal in shape, if present in oocytes>55µm	Basophilic		
V:vitellogenic				
a) oocyte	-			
1) Nucleus	chromatin materials evenly distributed in nucleoplasm			
2) Cytoplasm	-as in stage P plus oocytes which contain yolky substances in cytoplasm	Red, blue	Magenta	Black
b) follicle cells	-flattened in shape		Light blue	
C; cortical rod				
a) oocytes	-as in stage P plus oocytes with yolky substances and cortical rods in cytoplasm			
1) nucleas	- chromatin materials evenly distributed in nucleoplasm			
2) cytoplasm	- yolky substances in granules	Red, blue	Magenta	Black
3) cortical rods	-spherical or elongated near periphery and extends towards nucleus	Red, blue, purple	Blue near periphery, red towards nucleus	(-)
b) Follicle cells	-spindle-shaped or not distinguishable			
S; spent				
a) oocytes	-remaining oocytes with yolky cortical rods -thicker layers of follicle cells retracted to one side -darkly-stained, irregularly-shaped primary oocytes			
b) follicle cells	-rectangular or cuboidal in shape when enveloping oocytes			

AB-PAS: alcian blue-periodic acid-Schiff. SB: Sudan black (Tan-Fermin and Pudadera, 1989).

1.5 Oogenesis

Oogenesis is the process for production of oocytes, it composed of meiotic cell division, meiosis I and meiosis II. Most animals, oocytes are arrested at prophase of meiosis I (prophase I) during the growth period and resume meiosis near or at the end of growth. The prophase I arrested state is described as immature, and the process of resumption of meiosis is called meiotic maturation and displaying a visible nucleus referred to as germinal vesicle (GV).

When meiosis resumes, the oocytes undergo germinal vesicle breakdown (GVBD; i.e., dissolution of the nuclear envelope). Meiotic maturation is comprised of two consecutive M-phases, meiosis I and meiosis II; as there is no intervening S-phase (DNA replication), haploid gametes are produced. Oocyte nuclear maturation comprises nuclear modifications that chromatin condenses where then homologues chromosomes are paired aligning on the meiotic spindle at metaphase I. During anaphase and telophase bivalents separate as the homologous chromosomes separate and separation is complete when metaphase II occurs, recognizable by presence of 1^{st} polar body. Meiosis is completed following successful fertilization visualized as the presence of 2^{nd} polar body (Figure 1.7) (Grøndahl, 2008).

In many species, oocyte meiosis must arrest again at a certain stage after its resumption to await fertilization (Kishimoto, 2003; Masui, 1985; Nigg, 2001). Thus, from the viewpoint of cell-cycle control, the major questions in meiotic maturation concern the mechanisms underlying prophase I and the subsequent arrests and their release, in addition to those underlying the meiosis I to II transition (Nebreda and Ferby, 2000).

1.6 Oocyte development and maturation

Oocytes are produced in ovaries by the entry of mitotically proliferating oogonia into meiosis. Oocytes stop their meiotic cell cycle at prophase I (prophase I arrest), during which they grow due to the accumulation of vitellogenesis, that substances necessary for early embryonic development. In many vertebrates, fully grown postvitellogenic oocytes under prophase I arrest are unable to be fertilized until they mature (Yamashita, 2000). Fertilization can occur at the prophase stage of

meiosis (clams, marine worms), at metaphase I (MI; some insects, starfish), or at metaphase II (MII; most mammals) of meiosis (Voronina and Wessel, 2003) (Figure 1.8).

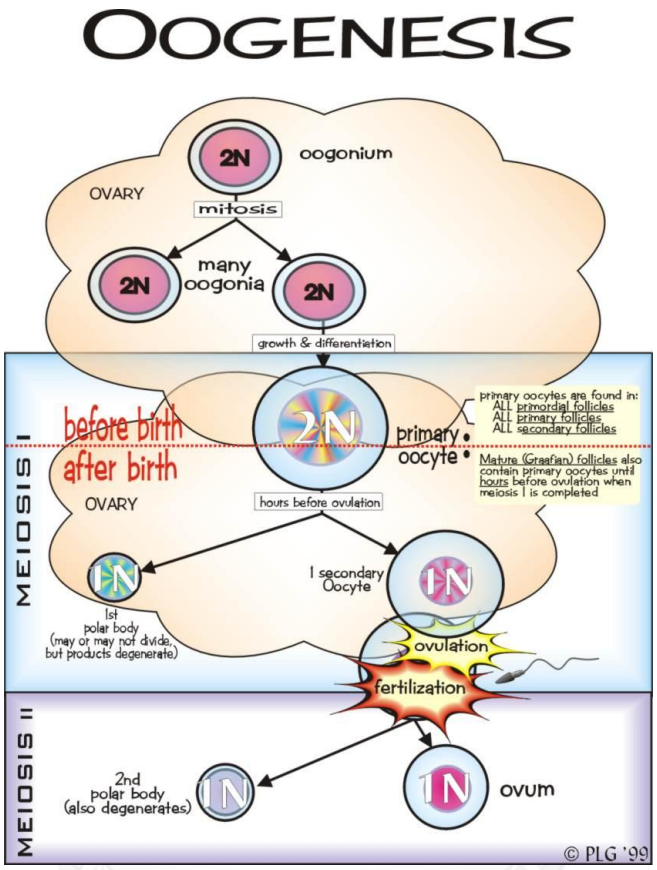

Figure 1. 7 Diagram showing the general of oogenesis
Source: http://alitadisanjaya.blogspot.com/2011/03/spermatogenesis oogenesis.html

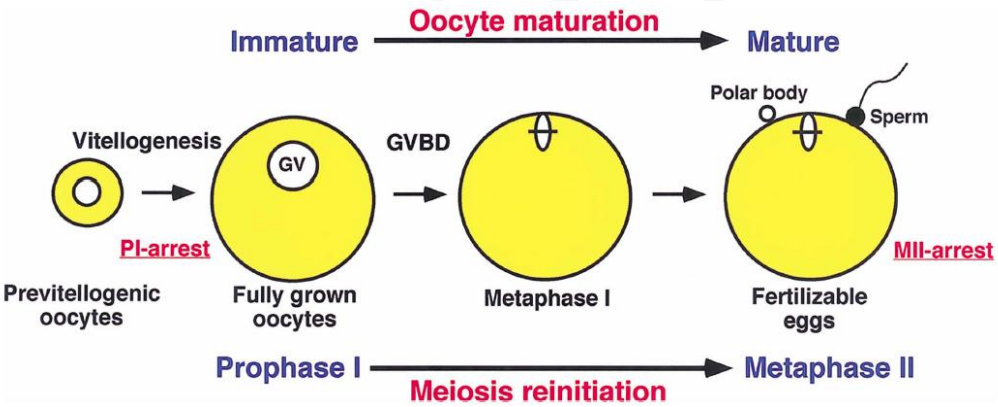

Figure 1. 8 Oocyte maturation and meiotic cell cycle in most animals. During oogenesis, oocytes arrest at two stages, prophase I and metaphase II (PI- and MII-arrest). Oocytes under PI-arrest (characterized by a huge nucleus called a germinal

vesicle) grow due to the accumulation of yolk (vitellogenesis) and become fully grown but are still immature. Upon hormonal stimulation, the immature oocytes are released from the PI-arrest, and after undergoing germinal vesicle breakdown (GVBD) and passing through metaphase I, they reach metaphase II, where they are naturally inseminated. MII-arrested oocytes are usually called mature oocytes or eggs (Yamashita, 2000).

The oocytes of shrimp develop from mitotically dividing oogonia. Development of daughter oogonia, they increase in size and enter the meiotic division in first stage of and migrate away from the zone of proliferation toward the periphery of the ovarian follicles. During oogenesis, the follicular cells around the growing oocytes produce the vitellogenin protein which constitutes the yolk. The yolk vitellogenin is also produced at extraovarian sites, especially the hepatopancreas. The process of synthesis and accumulation of vitellogenin in the oocytes is called vitellogenesis. As vitellogenesis proceeds, oocytes mature synchronously and develop a characteristic dark green color which is due to the deposition of carotenoid pigments (Chen et al., 1999; Hallak et al., 2000; Kruevaisayawan et al., 2010).

1.7 Hormonal regulation of oocytes maturation

The major obstacle in the development of shrimp maturation technology is the limited knowledge of the molecular events of ovarian maturation of shrimp (Benzie, 1998). Over the past few decades, there have been many studies on characterization of vitellogenin/vitellin and the elucidation of the process of vitellogenesis in penaeid shrimp as well as molecular endocrinology of shrimp reproduction, particularly on GIH and methylfarnosoate (MF) (Silva Gunawardene et al., 2001; Yamano et al., 2004).

Reproductive physiology in crustaceans is highly controlled and regulated by the nervous and endocrine systems (Engelmann, 1994). Endocrine control of female reproduction is governed by a variety of hormonal and neuronal factors that involve neuropeptide hormones, such as gonad stimulating hormone (GSH) and sex steroids such as estradiol and progesterone (Huberman, 2000; Zapata et al., 2003). 17β-estradiol have been reported for crabs, *Mictyris brevidactylus*, *Scylla serrata* and

Chasmagnathus granulata (Shih, 1997; Warrier et al., 2001; Zapata et al., 2003) and shrimps, *Marsupenaeus japonicas* (Yano and Hoshino, 2006).

Biogenic amines (e.g. serotonin, 5-HT) and peptide neuroregulators are known to modulate the release of neuropeptide hormones from the sinus gland of penaeid shrimp (Fingerman, 1997; Okumura, 2004; Okumura et al., 2006). For example, 5-HT plays a role in indirect regulation of various physiological processes in crustaceans, including metabolism, reproduction and molting (Keller et al., 1984; Kulkarni et al., 1992; Mattson and Spaziani, 1985; Richardson et al., 1984).

Exogenous serotonin (5-HT) injection induced ovarian maturation in the crayfish, *Procambarus clarkii* (Sarojini et al., 1995) and *Litopenaeus vannamei* (Vaca and Alfaro, 2000) at rates lower than unilateral eyestalk ablation. Simultaneous injections of 5-HT (25 µg/g body weight) and the dopamine antagonist-spiperone (1.5 or 5 µg/g body weight) stimulated ovarian maturation and spawning in wild *Litopenaeus stylirostris* and pond-reared *L. vannamei* (Alfaro et al., 2004). Recently, the effects of exogenous 5-HT on reproductive performance in domesticated *P. monodon* were reported. Shrimp injected with 5-HT (50 µg/g body weight) exhibited ovarian maturation and spawning rates comparable to those in eyestalk-ablated shrimp. Interestingly, the hatching rate and the amount of nauplii produced per brooder were significantly higher in the 5-HT-injected shrimp (Wongprasert et al., 2006).

Understanding the induction mechanisms of reproduction-related genes during ovarian and oocyte maturation will be useful to develop methodologies that to effectively induce ovarian maturation in *P. monodon*. Molecular effects on administration of 5-HT at 50 µg/g body weight in domesticated *P. monodon* adults were recently reported. It clearly promoted the expression of various reproduction-related genes in ovaries of domesticated *P. monodon* for example, *Ovary-Specific Transcript* (*PmOST1*) in cultured 5-month-old shrimp at 12-78 hour post injection (hpi, (Klinbunga et al., 2009), *adipose differentiation-related protein* (*PmADRP*) and *Broad-complex* (*PmBr-c*; (Buaklin, 2010) in domesticated 14-month-old shrimp at 48 (Sittikankaew et al., 2010) and 12 hpi (Buaklin, 2010).

Steroid hormones are functionally involved in shrimp sexual differentiation and reproduction (Cahill, 2007; Miura et al., 2006). Conjugated and unconjugated dehydroepiandrosterone and estrone, conjugated pregnenolone and 17β-estradiol as well as unconjugated progesterone and estrone were detected in ovaries of wild *P. monodon* (Fairs et al., 1990). Quinitio et al. (1994) examined the levels of 17β-estradiol and progesterone in the hemolymph, ovaries and hepatopancreas of captive *P. monodon* females. Levels of 17β-estradiol in ovaries were significantly increased in shrimp possessing vitellogenic (yolky) and cortical rod (mature) ovaries. Interestingly, 17β-estradiol in hemolymph was only observed in mature shrimp while the peak level in hepatopancreas was also observed at this stage. The progesterone level in hemolymph and hepatopancreas was significantly increased in shrimp possessing vitellogenic and cortical rod ovaries while that in ovaries was significantly increased in the mature stage.

Although these studies begin to reveal a better picture of the endocrine control of ovarian maturation in shrimp, reproductive maturation of penaeid shrimp is still not well understood. Accordingly, knowledge of the molecular mechanisms and functional involvement of reproduction-related genes and proteins in ovarian development of *P. monodon* is necessary for better understanding of the reproductive maturation of *P. monodon* to resolve the major constraint of this economically important species in captivity.

1.8 Functionally important genes involved meiotic cell cycle of *P. monodon*

1.8.1 *Cell dision cycle 2 (Cdc2), cyclin B* and *cell-dependent kinase 7 (Cdk7)*

In *Xenopus*, the meiotic oocyte resumption is activated by cyclin B-Cdc2 activation at meiotic resumption (Figure 1.9). Typically, progesterone or its derivatives (collectively called progestins) which is recognized as the maturation inducing hormone (MIH) induced germinal vesicle breakdown (GVBD) of oocytes.

The meiotic maturation of animal oocytes is controlled by the maturation-promoting factor (MPF), a complex of Cdc2 and cyclin B (Okano-Uchida et al., 1998).

In most species, cytoplasmic MPF is maintained in the inactive form (called pre-MPF) by inhibitory phosphorylation of Cdc2 at Thr14 and Tyr15 by Myt1 kinase and at Thr161 by cyclin-activating kinase (CAK), a complex of cyclin-dependent kinase 7 (Cdk7)/cyclin H or Cdk7/cyclin H/Mat 1 (Elledge and Harper, 1998; Patel and Simon, 2010; Tassan et al., 1995). Dephosphorylation of Thr14 and Tyr15 residues of Cdc2 by Cdc25 phosphatase lead to the resumption of meiotic maturation of oocytes (Clarke et al., 1992; Dunphy et al., 1988; Dunphy and Kumagai, 1991; Jessus et al., 1991; Mueller et al., 1995).

Alternatively, a different mechanism of oocyte resumption has been reported in some amphibians and fishes where Cdc2 presents as a monomer with no phosphorylation due to the absence of cyclin B in immature oocytes. Only Thr161 phosphorylation by CAK is required for MPF activation (Hirai et al., 1992; Honda et al., 1993; Kobayashi et al., 1991; Yamashita et al., 1995).

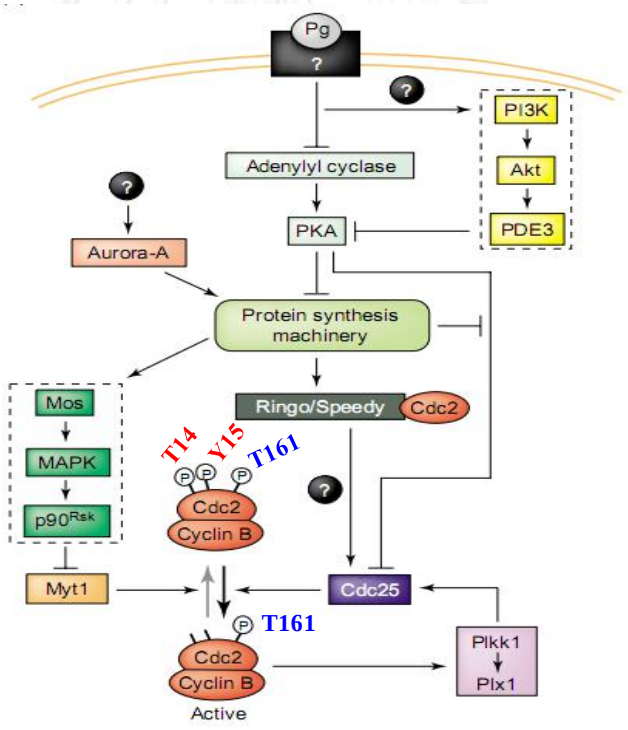

Figure 1. 9 MPF formation of *Xenopus* during oocyte maturation. The progesterone signal received by the surface receptor induces the translation-mediated syntheses. Cdc2 molecules that comprise pre-MPF are phosphorylated on both T14/Y15 and T161. Dephosphorylation of Cdc2-cyclin B by Cdc25C lead to active-MPF (Kishimoto, 2003).

In addition, CAK also acts as a transcriptional regulator in association with the transcription factor II H (TFIIH) (Nigg, 1996; Sclafani, 1996). In zebrafish, the function of CAK is especially important during the early development and *Cdk7* and *cyclin H* mRNAs were shown to be maternally loaded (Liu et al., 2007).

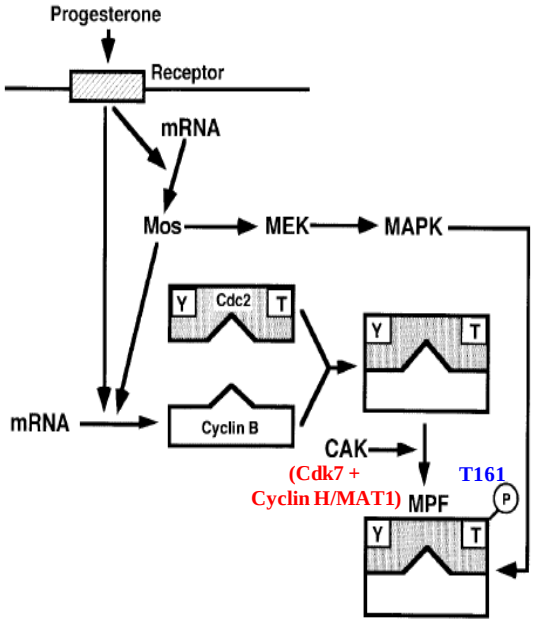

Figure 1. 10 MPF formations during *Rana* and gold fish oocyte maturation. Immature oocytes contain monomeric Cdc2, and cyclin B is synthesized by translational activation of the masked mRNA after progesterone stimulation received by the surface receptor. After the complex formation of the preexisting Cdc2 and the de novo synthesized cyclin B, Cdc2 is activated by CAK-catalyzed (Cdk7, cyclin H and/or MAT1) T161 phosphorylation (Yamashita, 2000).

Qiu and Liu (2009) isolated *Cdc2* of the Chinese mitten crab (*Eriocheir sinensis*) and it was 1364 bp in length containing an ORF of 900 bp deducing to a polypeptide of 299 amino acids with calculated molecular weight of 34.7 kDa. The *Cdc2* mRNAs level was not differentially expressed during ovarian development of *E. sinensis*. In contrast, a greater expression of the Cdc2 protein was found at previtellogenic, late vitellogenic and germinal vesicle breakdown (GVBD) stages. Two forms of the Cdc2 protein (35 and 34 kDa) were simultaneously identified at all

stages of ovaries. Immunohistochemistry (IHC) revealed that the Cdc2 proteins was localized exclusively in ooplasm of previtellogenic oocyte, and then relocate into germinal vesicle at vitellogenesis stage and accumulate on meiotic spindle in mature ovaries.

Subsequently, the full-length cDNA of *Cdc2* in the mud crab (*Scylla paramamosain*) was identified and characterized. The *Sp-Cdc2* was 1593 bp in length with an ORF of 900 bp corresponding to a deduced protein of 299 amino acids. Quantitative real-time PCR analysis revealed that the expression level of *Sp-Cdc2* was not significantly different in different stages of ovarian development ($P > 0.05$). In testes, its expression in the third stage was greater than that in the first and second stages ($P > 0.05$). The positive signals of *Sp-Cdc2* mRNA were localized in the cytoplasm of oogonia and ooplasm of previtellogenic and primary vitellogenic oocytes. In testes, *Sp-Cdc2* had intense signals in spermatids and secondary spermatocytes following primary spermatocytes (Han et al., 2012).

Liu et al. (2007) isolated of *Cdk7* in zebrafish. It was full-length cDNA of 1260 bp with an ORF of 1038 bp encodes a 345 amino acid. The expression profile of various tissue of *Cdk7* mRNA appeared to have highest level ovaries testes and intestine more than brain, fin, eye, kidney and gill.

Recently, Visudtiphole et al. (2009) was characterized the *cyclin B* of *P. monodo*n. Geomic of *PmCyB* consisted of 8 exons and 7 introns. Three isoforms of *PmCyB* with an identical ORF of 1206 bp corresponding to a deduced protein of 401 amino acids but three different 3′ UTR lengths of 416, 543 and 1117 bp, respectively. The expression levels of *PmCyB* were significantly increased from stage I in stage IV ovaries in both intact and eyestalk-ablated broodstock ($P < 0.05$).

Larochelle et al. (1998) cloned and characterized the *Drosophila Cdk7* gene (*DmCdk7*) and it was ORF 1062 bp encoded polypeptide 353 amino acids with calculated molecular mass of 39 kDa. *DmCdk7* function related with meiosis (study in ovaries) and mitosis (study in young embryos). Moreover, results suggest that *Cdk7* was necessary for CAK activity and for complexes of Cdc2/cyclin B.

1.8.2 *Checkpoint kinase1 (Chk1)*

Chk1 is a nuclear kinase, has been shown to enforce the G2 checkpoint by inhibiting Cdc25. Chk1 phosphorylates Cdc25 on a crucial regulatory site (Ser-216 and Ser-287 of human and *Xenopus* Cdc25C, respectively) lead to dephosphorylated Cdc2 of Cdc2-cyclin B complex (Figure 1.11).

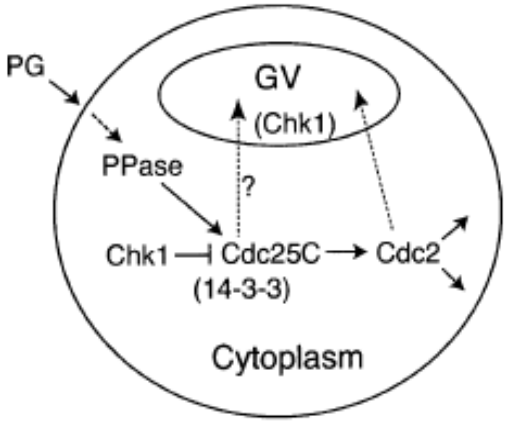

Figure 1. 11 Models of regulation of the Chk1/Cdc25C pathway in *Xenopus* oocytes. In G2-arrested *Xenopus* oocytes, the Chk1/Cdc25C pathway occurs in the cytoplasm. Upon progesterone stimulation of the oocyte, Chk1 activated antagonizing protein phosphatase cause dephosphorylates Ser287 of Cdc25C; this would abrogate the binding of 14-3-3 proteins and allow activation of Cdc25C (and hence Cdc2) in the cytoplasm, thus causing a release from G2 arrest. A portion of the cytoplasmically activated Cdc2 probably enters the germinal vesicle (GV) to induce nuclear events such as GVBD and chromosome condensation. A very small amount of Cdc25C might also enter the GV, although this is unlikely to be essential for a release from G2 arrest (Nebreda and Ferby, 2000; Oe et al., 2001).

Oe et al. (2001) study Chk1 and Cdc25C in the *Xenopus* oocytes. Localization of Cdc25C and Chk1 were found in cytoplasmic throughout oocytes maturation and was not detected at all in the nucleus even just prior to GVBD. The results demonstrate that Chk1 inhibits Cdc25C function in the cytoplasmically in G2-arrested of *Xenopus* oocytes.

1.8.3 *Anaphase-promoting complex (Apc11), Cdc16* and *Cdc20*

The APC is a complex composed of 11 difference subunits that call anaphase-promoting complex/cyclosome (APC/C) oscillates during the cell cycle of both mitotic and meiosis.

The APC/C was being low in S and G2 phase, and high in mitosis and G1. However, during mitosis different APC/C substrates are degraded at highly defined time-points. The APC/C has a large cullin-like subunit, Apc2, which together with a small RING finger protein, Apc11, is sufficient to support E2-dependent E3 activity *in vitro*. The APC/C can use three different E2 enzymes. Specific activity in cells the APC/C critically requires either one of two WD40-domain proteins as activators, Cdc20 or Cdh1 (Yamano et al., 2004). TPR domains are present in the subunits Apc3/Cdc27, Apc6/Cdc16, Apc7 and Apc8/Cdc23, and may directly interact with Cdh1 and Cdc20 (Vodermaier et al., 2003) (Figure 1.12).

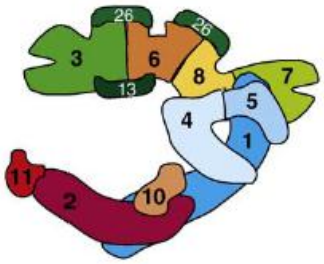

Subunit	Predicted Mw (*H.s.*;kDa)	Functional Aspects
APC1/Tsg24	216	mitotic phosphosites; scaffold?
APC2	94	cullin
APC3/Cdc27	92	TPR; mitotic Phosphosites
APC4	92	connector?
APC5	85	connector?
APC6/Cdc16	72	TPR; mitotic phosphosites
APC7	63	TPR; mitotic phosphosites
APC8/Cdc23	69	TPR; mitotic phosphosites
APC10/Doc1	21	processivity factor
APC11	11	RING-E3
APC13	9	stability factor?
Cdc26	10	stability factor?

Figure 1. 12 Functionally, the APC subunit and compose of the APC/C. APC1 acts as a scaffold for two subcomplexes, a structural block and a catalytical block. The structural block contains TPR subunits catalytical block contains the cullin, the ring finger Apc11 and the Apc10/Doc1 processivity factor. Apc4 and Apc5 may connect the TPR block to the catalytic block (van Leuken et al., 2008).

The release of the metaphase II is mediated by the anaphase-promoting complex (APC)-dependent degradation of cyclin B. This degradation activity requires the APC activator Cdc20 that activates ubiquitination reactions by recruiting substrates to the APC. Cyclin B degradation, which is catalyzed by the 26S proteasome, is regulated through polyubiquitination by the anaphase-promoting complex/cyclosome (APC/C), an E3 ubiquitin ligase, and its activating factor Cdc20. The APC/C–Cdc20 is known to be suppressed in the metaphase arrest caused by the spindle assembly checkpoint (Figure 1.13) (Papin et al., 2004; Yamamoto et al., 2005).

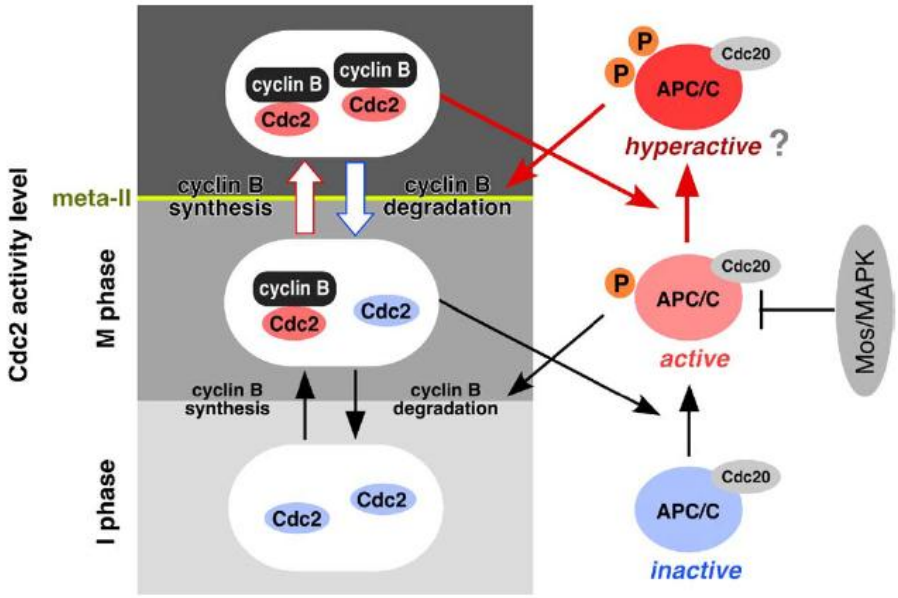

Figure 1. 13 Model for the regulation of cyclin B degradation under cytostatic factor (CSF) arrest. Cyclin B synthesis continues under CSF arrest and Cdc2 activity is elevated (upward open arrow). Complex of APC/C-Cdc20 cause cyclin B degradation is suppressed by a Mos/MAPK activity when Cdc2 activity is lower than the metaphase II level, but activated through hyperphosphorylation of APC/C components when Cdc2 activity is elevated beyond the metaphase II level, resulting in a decline in Cdc2 activity to metaphase II levels (downward open arrow). Cdc2 activity is thus maintained at the metaphase II level through the dynamic regulation for APC/C-Cdc20 mediated cyclin B degradation (Yamamoto et al., 2005).

1.8.4 *Cyclin dependent kinase 2 (Cdk2)*

Cyclin-dependent kinases (Cdks) are a family of Serine/Threonine kinases that involved in the control of the mitotic cycle. Kinase activity is normally controlled by the level of expression of their activator cyclin (Sherr and Roberts, 2004). Cdk enzymes follow the accepted kinase fold and like other S/T-kinases, they must be phosphorylated on a threonine residue in their activation loops. However, unlike other kinases, A-loop phosphorylation of the isolated catalytic subunit is insufficient to assemble the active conformation. The A-loop is frequently referred to as the T-loop (Nelson, 2008). Cdk2 contains PSTAIRE peptide related to the binding of cyclin. In the *Xenopus* model, Cdk2 associating with cyclin E during early G1 phase implicated cytostatic factor (CFS) with inactivated APC/C-Cdc20 (Figure 1.14).

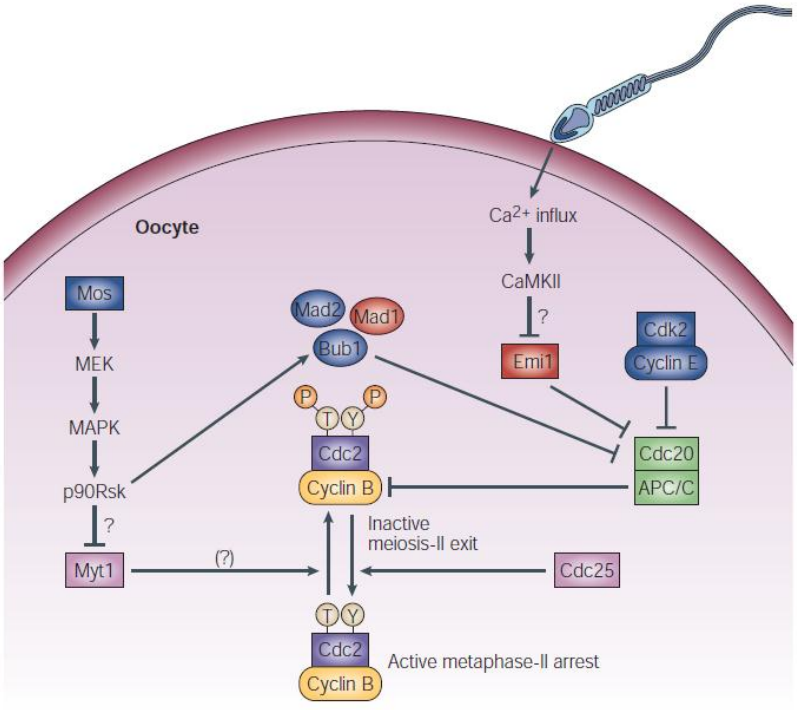

Figure 1. 14 In Xenopus oocytes model, CSF causes arrest in metaphase II. CSF activity comprises pathways that converge on the inhibition of the APC/C-Cdc20, therefore preventing the degradation of cyclin B. Inhibition of the APC/C involves Cdk2-cyclin E. Cyclin E levels rise before meiosis II and Cdk2-cyclin E can inhibit the APC/C (Marston and Amon, 2004).

1.8.5 *Cdk5*

Although Cdk5 is a member of the cyclin kinase family, it is not directly involved in cell cycle control. The essential role of Cdk5 kinase in neurodevelopment and neurodegeneration during brain development. Cdk5 requires the neuronal-specific activator p35 which is a short-lived protein, and phosphorylation by Cdk5 targets it for ubiquitin-mediated proteolysis (Sharma et al., 1999; Wei et al., 2005).

Lozano et al. (2010) characterized Cdk5 in sea urchin and starfish of eggs and embryos. The Cdk5 of sea urchin are highly conserved (92% similarity) with human. Western blot analysis indicated that Cdk5 is present during all stages of sea urchin development.

1.8.6 *Bystin 1*

Originally, bystin was identified as a cytoplasmic protein in human trophoblastic embryonal carcinoma HT-H cells. It has many potential phosphorylation sites indicates its involvement in signal transduction pathways. The bystin protein forms complex with trophinin and tastin (or ErbB4, an ErbB family receptor tyrosine kinase), This complex binds to HB-EGF (heparin-binding EGF-like growth factor) and GWRQ peptide lead to activated tyrosine kinase activity associated with generation of cell (Figure 1.15) (Fukuda et al., 2008; Fukuda and Sugihara, 2007; Sugihara et al., 2007). However, proteins similar to trophinin and tastin were not found in *Drosophila melanogaster*, but bystin was found in the database (Stewart and Nordquist, 2005).

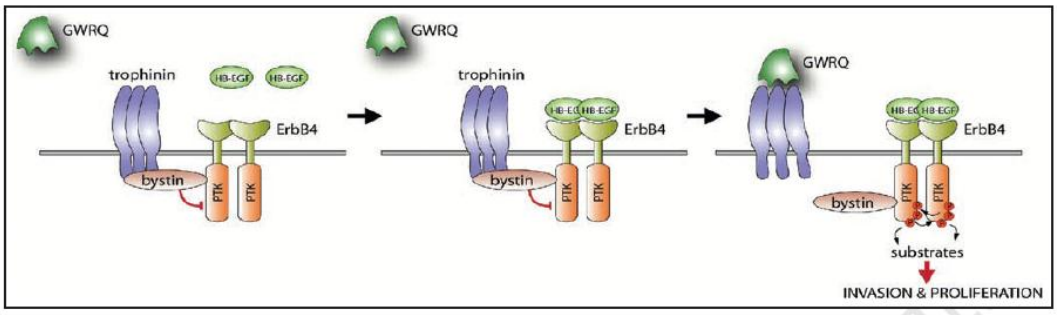

Figure 1. 15 Model of Bystin, (Left) Trophinin and bystin bind in a cytoplasmic complex interacted with ErbB4 and suppressed its tyrosine kinase activity. (Center) HB-EGF binds to ErbB4, but protein kinase activity is suppressed by trophinin/bystin. (Right) Trophinin-mediated cell adhesion is mimicked by binding of GWRQ peptide to trophinin on the cell surface, resulting in dissociation of trophinin from bystin and activation of ErbB4 (Fukuda and Sugihara, 2007).

In *P. monodon*, Karoonuthaisiri et al. (2009) carried out large scale analysis of gene expression using cDNA microarrays and found that *Bystin 1* exhibited a differential expression pattern in different stages of ovaries. Results from that study suggested that *Bystin 1* is functionally involved in ovarian development of *P. monodon*.

1.8.7 *Histone deacetylase Rpd3 (Rpd3)*

Histone deacetylases have crucial roles in the regulation of a variety of biological processes, including cell cycle progression, proliferation, differentiation, and development. Rpd3 encode proteins with Hdac enzymatic activity and disorder of either of this gene causes histone hyperacetylation and changes in transcription (Hassig et al., 1998; Lagger et al., 2010).

To provide further insights into the molecular mechanisms of reproduction-related genes involvement in reproductive development and maturation in *P. monodon*, the full-length cDNA of genes in signal transduction pathway were determined. In addition, their mRNA and protein expression profiles were examined during ovarian development. In addition, effects of progesterone and 5-HT on gene expression were evaluated and localization of reproduction-related genes/proteins in *P. monodon* oocytes at various stages of ovarian development was also examined.

CHAPTER II
MATERIALS AND METHODS

2.1 RNA extraction

2.1.1 Total RNA extraction

Total RNA was extracted from the dissected tissues using TRI Reagent®. A piece of tissue was immediately placed in mortar containing liquid nitrogen and ground to fine powder under the frozen condition. The tissue powder was transferred to 500 µl of TRI Reagent and homogenized. Additional 500 µl of TRI Reagent were later added to the homogenized sample (a final proportion of 1 ml Trizol/ 50-100 mg tissue). The homogenate was left at room temperature for 5 min before 0.2 ml of chloroform was added. The mixture was vortexed for at least 15 s, left at room temperature for 2 - 15 min and centrifuged at 12000 *g* for 15 min at 4°C. The mixture was separated into the lower phenol phase (red), an interphase, and a colorless upper aqueous phase. The aqueous phase (containing the extracted RNA) was carefully collected. RNA was precipitated with 0.5 ml of pre-chilled (-20°C) isopropyl alcohol. The mixture was left at room temperature for 10 - 15 min and centrifuged at 12000 *g* for 10 min at 4°C. The RNA pellet was then collected and washed with 1 ml of pre-chilled (-20°C) 75% ethanol prior to centrifugation at 7500 g for 10 min at 4°C. The washed RNA pellet was air-dried for 5-10 min and then dissolved in DEPC-treated H_2O for immediate use. Alternatively, the RNA pellet was kept in absolute ethanol at -80°C until required. The quality of extracted total RNA was examined by electrophoresis on 1.0% agarose gel.

2.1.2 DNase I treatment of extracted total RNA

Possible contamination of DNA in the extracted total RNA was eliminated by incubation with DNase I (0.5 U/1 µg of RNA) at 37°C for 30 min. After the incubation, the sample was gently mixed with the a sample volume of phenol : chloroform : isoamylalcohol (25:24:1) and thoroughly mixed for 10 min. The samples were then centrifuged for 10 min at 13500 g (4°C), and the upper aqueous phase was

transferred to a fresh, sterilized microcentrifuge tube and repeated extraction process with chloroform:isoamylalcohol (24:1) and one with chloroform. One-tenth volume of 3M sodium acetate (pH 5.2) was added to the aqueous phase followed by 2.5 volume of pre-chilled (-20°C) absolute ethanol. The mixture was incubated at -80°C for 30 min, and the precipitated RNA was recovered by centrifugation at 16000 *g* for 10 min at room temperature. The RNA pellet was washed twice by addition of pre-chilled 75% ethanol. The RNA pellet was kept at -80°C in absolute ethanol until required.

2.1.3 Agarose gel electrophoresis (Sambrook and Russell, 2001)

Appropriate amount of agarose was weighed out and mixed with 1X TBE buffer (89 mM Tris-HCl, 8.9 mM boric acid and 2.5 mM EDTA, pH 8.0). The gel slurry was heated until complete solubilization in the microwave. The gel solution was left at room temperature to approximately 50-55 °C before poured into a gel mould. The comb inserted, the gel was allowed to solidify at room temperature for approximately 45 min. When needed, the gel mould was placed in the gel chamber and sufficient 1X TBE buffer was added to cover the gel for approximately 0.5 cm. The comb was carefully withdrawn. One microliter of total RNA was mixed with 2 µl or one-fourth volume of the gel-loading dye (0.25% bromophenol blue and 25% ficoll, MW 400,000 prepared in sterile deionized H_2O) and loaded into the well. λDNA digested with *Hind* III (λ-*Hind* III) was marker for comparing with RNA extracted. Electrophoresis was carried out at 100 volts for 30 min. After electrophoresis, the gel was stained with ethidium bromide (0.5 µg/ml) for 5 min and destained to remove unbound ethidium bromide by submerged in water for 15-30 min. The RNA fragments were visualized using a UV transilluminator.

2.2 Measurement of nucleic acid concentrations using spectophotometry method and gel electrophoresis

2.2.1 Measurement of nucleic acid concentrations using spectophotometry

DNA and RNA concentration was estimated by measuring the absorbance using spectophotometry method. An OD_{260} of 1.0 corresponds to 50 µg/ml for

double-strand DNA, 40 µg/ml for single-strand RNA and 33 µg/ml for oligonucleotides (Sambrook et al., 2001). Therefore, concentration of nucleic acids was estimated in µg/ml by using the following equation:

$$[\text{Nucleic acid}] = A_{260} \times \text{dilution factor} \times 50 \text{ or } 40 \text{ or } 33$$

(for DNA, RNA and oligonucleotides, respectively)

The ratio between the measuring the absorbance at 260 nm and 280 nm (OD_{260}/OD_{280}) provides an estimate pureness of the nucleic acid. Pure preparations of DNA and RNA have OD_{260}/OD_{280} values of 1.8 and 2.0, respectively (Kirby, 1956).

2.2.2 Estimation quality of nucleic acid using agarose gel electrophoresis

The quality of nucleic acid sample of verifying RNA integrity after extract was estimated from motion of RNA and DNA fragments pass through an agarose gel after electrophoresis. The nucleic acid can roughly estimated on the basic of the direct relationship between the amount of nucleic acid and the level of fluorescent dye (ethidium bromide) was visualized under a UV transilluminator. Nucleic acid was run in 1% agarose gel electrophoresis prepared in 1x TBE buffer (89 mM Tris-HCl, 89 mM boric acid and 2 mM EDTA, pH 8.3) at 4 V/cm. After electrophoresis, the gel was stain with ethidium bromide (0.5 µg/ml). The quality of RNA extracted was estimated from the intensity of the fluorescent band and RNA fragment size by comparing with that of *Hind* III digested λDNA (λ-*Hind* III) was marker.

2.3 First strand cDNA synthesis

One and a half micrograms of DNase-treated total RNA were reverse-transcribed to the first strand cDNA using an ImProm- II™ Reverse Transcription System Kit (Promega, U.S.A.). Total RNA was combined with 0.5 µg of oligo dT_{12-18} and appropriate DEPC-treated H_2O in final volume of 5 µl. The reaction was incubated at 70°C for 5 min and immediately placed on ice for 5 min. Then 5X reaction buffer, $MgCl_2$, dNTP Mix, RNasin were added to final concentrations of 1X, 2.25 mM, 0.5 mM and 20 units, respectively. Finally, 1 µl of ImProm-II™ Reverse transcriptase was add and gently mixed by pipetting. The reaction mixture was incubated at 25°C for 5 min

and at 42°C for 90 min. The reaction mixture was incubated at 70°C for 15 min to terminate the reverse transcriptase activity. Concentration and rough quality of the newly synthesized first strand cDNA was spectrophotometrically examined (OD_{260}/OD_{280}) and electrophoretically analyzed by 1.0% agarose gels, respectively. The first stranded cDNA was 10 fold-diluted and kept at 20°C until required.

2.4 Expression profile of interested reproduction-related genes in ovaries, testes and tissue distribution analysis of *P. monodon* using RT-PCR

2.4.1 Expression analysis of reproduction-related genes in ovaries and testes

For RT-PCR analysis, ovaries and testes of cultured juveniles and wild broodstock (*N* = 5 for each group, Table 2.1) were collected, immediately placed in liquid N_2 and kept at -80°C until needed.

Table 2. 1 Wild and domesticated shrimp used for expression analysis of genes in various tissues of *P. monodon*

Sample	Sex and stage	*N*	Average body weight± SD (g)
Wild shrimp	Male broodstock	5	135.51 ± 21.60
	Female broodstock	5	212.77 ± 43.33
Domesticated shrimp	Male juveniles	5	29.39 ± 5.18
(6-month-old)	Female juveniles	5	36.41 ± 5.17

Primers were designed from EST sequences significantly matched reproduction-related gene homologues using Primer Premier 5.0 (Table 2.2). Expression of genes in ovaries and testes of cultured juveniles and wild broodstock (*N* = 5 for each group) was analyzed. RT-PCR was performed in a 25 μl reaction mixture containing first strand cDNA, 10 mM Tris-HCl, pH 8.8, 50 mM KCl and 0.1% Triton X-100, 2 mM $MgCl_2$, 100 μM each of dATP, dGTP, dTTP and dCTP, 0.2 μM of each primer and 1 unit of Dynazyme™ DNA polymerase (FINNZYMES) using the amplification condition described in Table 2.3. *EF-1*α_{500} (F: 5′-

ATGGTTGTCAACTTTGCCCC-3′ and R: 5′-TTGACCTCCTTGATCACACC-3′) amplified from the same template was included as the positive control. The amplicon was electrophoretically analyzed on 1.5-2.0% agarose gels and visualized with a UV transilluminator after ethidium bromide (0.5 μg/ml) staining (Sambrook and Russell, 2001).

2.4.2 Tissue expression analysis

Tissues were dissected from live shrimps and immediately stored at -80°C until required. Hemolymph was collected using 10% sodium citrate as an anticoagulant. The anticoagulant was removed from the sample by centrifugation at 1000 *g* for 10 min, and the hemocyte pellets were immediately stored at -80°C.

Total RNA extracted from antennal gland, subcuticular epithelium, eyestalk, gill, hemocytes, heart, hepatopancreas, intestine, lymphoid organs, thoracic ganglion, pleopods, stomach and ovaries of female broodstock, ovaries of female juvenile and testes of both juvenile and broodstock of *P. monodon* was reverse-transcribed using the procedure described previously.

RT-PCR was performed in a 25 μl reaction mixture containing first strand cDNA of each tissue, 10 mM Tris-HCl (pH 8.8), 50 mM KCl and 0.1% Triton X–100, 2.0 mM $MgCl_2$, 100 μM each of dNTPs, 0.2 μM of each primer and 1 unit of Dynazyme™ DNA Polymerase (FINNZYMES). The reaction thermal profile of each gene was shown in Table 2.3. Five microliters of the amplification products were electrophoretically analyzed though 1.8-2.0% agarose gel. *EF-1*α_{500} was included as the internal control.

Table 2. 2 Primer sequences and the expected size of the PCR product of gene homologue of *P. monodon*

Gene/Primer	Sequence	Tm (°C)	Size (bp)
1. ***Anaphase promoting complex subunit 11 (Apc11)***			
F:	5' –CATGAAGGTGAAGATTAAATCCT -3'	62	258
R:	5' –GGTTATTCTTTAAACTTCCACTC -3'	62	
2. ***Bystin isoform 1 (Bystin1)***			
F:	5'- ACGAGGAAAGCAGTGACGATGAG -3'	70	330

Gene/Primer	Sequence	Tm (°C)	Size (bp)
R:	5'- TTGGCAAGGGTCCACTTCTGTAT -3'	68	
3. *Cell division cycle 2 (Cdc2) or cyclin dependent kinases 1(Cdk1)*			
F:	5'- ATTCCGTCAAACAGATGGACAGCG -3'	72	114
R:	5'- CATCAAAGTAGGGGTGCTTCAGGG -3'	74	
4. *Cell division cycle 16 (Cdc16)*			
F:	5'- GCTAACTGTGAAGGAAGAGAAAGA -3'	68	148
R:	5'- AGCAGGTTGTGGCAATGGTGTA -3'	66	
5. *Cyclin division cycle 20 (Cdc20)*			
F:	5′- GAGCCGTGTCACCACCCTTTC -3′	68	137
R:	5'- CACAGACCTCCTGCGAATGCC -3'	68	
6. *Cyclin dependent kinases 2 (Cdk2)*			
F:	5'- ATGAAAGCCGTGGAGGATTACC -3'	66	260
R:	5'- GTTTTTGGCACCGAGGAGAATC -3'	66	
7. *Cyclin dependent kinases 5 (Cdk5)*			
F:	5'- ATCCAAGGGGACTCACATACAGG -3'	70	191
R:	5'- CTTTCTCGGCTATTTCGGCAA -3'	62	
8. *Cyclin dependent kinases 7 (Cdk7)*			
F:	5′- TCTTTCCTGCTGCCAGTGAT -3′	60	123
R:	5′- GGACAGGCTTATTGCTGAAAT -3'	60	
9. *Checkpoint kinase 1(Chk1)*			
F:	5'- TGGACAAAGGTGGACAATCTG -3'	62	183
R:	5'- CACACGCTTGGTAGTAGGGGT -3'	66	
10. *Histone deacetylase Rpd3 (Rpd3)*			
F:	5′- ATGAAGCCACACAGGATACG -3′	60	276
R:	5′- AGCACCAGCAATGGAGCCT -3′	60	
11. *Elongation factor-1* α (*EF-1* α_{500})			
F:	5′- ATGGTTGTCAACTTTGCCCC -3′	60	500
R:	5′- TTGACCTCCTTGATCACACC -3′	60	

Table 2. 3 The amplification conditions for RT-PCR and tissue distribution of interesting reproduction-related genes of *P. monodon*.

Gene homologue	Amplification condition	1st cDNA (ng)
Anaphase promoting complex subunit 11 (Apc11)		
	94 °C for 3 min	300
	35 cycles of 94 °C for 30 s, 53 °C for 45 s and 72 °C	
	for 45 s and	
	72 °C for 7 min	
Bystin isoform 1 (Bystin1)		
	94 °C for 3 min	200
	30 cycles of 94 °C for 30 s, 53 °C for 45 s and 72 °C	
	for 45 s and	
	72 °C for 7 min	
Cell division cycle 2 (Cdc2) or*cyclin dependent kinases 1(Cdk1)*		
	94 °C for 3 min	100
	30 cycles of 94 °C for 30 s, 58 °C for 30 s and 72 °C	
	for 45 s and	
	72 °C for 7 min	
Cell division cycle 16 (Cdc16)		
	94 °C for 3 min	200
	30 cycles of 94 °C for 30 s, 58 °C for 45 s and 72 °C	
	for 45 s and	
	72 °C for 7 min	
Cell division cycle 20 (Cdc20)		
	94 °C for 3 min	200
	28 cycles of 94 °C for 30 s, 58 °C for 45 s and 72°C	
	for 45 s and	
	72 °C for 7 min	
cyclin dependent kinases2 (Cdk2)		
	94 °C for 3 min	200
	30 cycles of 94 °C for 30 s, 55 °C for 30 s and 72°C	
	for 45 s and	
	72 °C for 7 min	

Gene homologue	Amplification condition	1st cDNA (ng)
cyclin dependent kinases 5 (Cdk5)		
	94 °C for 3 min	200
	30 cycles of 94 °C for 30 s, 55 °C for 30 s and 72°C	
	for 45 s and	
	72 °C for 7 min	
cyclin dependent kinases 7(Cdk7)		
	94 °C for 3 min	200
	30 cycles of 94 °C for 30 s, 53 °C for 45 s and 72°C	
	for 45 s and	
	72 °C for 7 min	
Checkpoint kinase 1(Chk1)		
	94 °C for 3 min	200
	30 cycles of 94 °C for 30 s, 53 °C for 45 s and 72°C	
	for 30 s and	
	72 °C for 7 min	
Histone deacetylase Rpd3 (Rpd3)		
	94 °C for 3 min	200
	35 cycles of 94 °C for 30 s, 53 °C for 45 s and 72°C	
	for 45 s and	
	72 °C for 7 min	
Elongation factor-1α (EF-1α_{500}) (control)		
	94 °C for 3 min	100
	23 cycles of 94°C for 30 s, 53 °C for 30 s and 72 °C	
	for 30 s and	
	72 °C for 7 min	

2.5 Rapid amplification of cDNA ends-polymerase chain reaction (RACE-PCR) and primer walking of the interesting gene

2.5.1 Purification of mRNA

Messenger (m) RNA was purified from extracted total ovarian RNA using a QuickPrep *micro* mRNA Purification Kit (GE Healthcare). Four hundred microliters of the extraction buffer were added to a microcentrifuge tube containing 25 µl of total

RNA (150 µg) and mixed by pipetting. Two volumes (0.8 ml) of the elution buffer were added and mixed thoroughly. The mixture was centrifuged at 14,000g for 1 min. Concurrently, the tube containing 1 ml of oligo(dT)-cellulose for each purification was centrifuged at the same speed for 1 min. The supernatant was removed. The homogenate was transferred into the microcentrifuge tube containing the oligo(dT)-cellulose pellet. The tube was gently inverted to resuspend the oligo(dT)-cellulose for 3 min and centrifuged at 14,000g for 15 s at room temperature. The supernatant was carefully removed. The high salt buffer (1 ml) was added to a microcentrifuge tube and spun for 15 s at 14,000g. The supernatant was carefully removed. The pellet was washed repeated four more times, as described above. The low salt buffer (1 ml) was added to the oligo(dT)-cellulose pellet. The tube was inverted and spun at 350 g for 2 min. This wash was repeated once. The pellet from the final wash was resuspended in 0.3 ml of the low salt buffer. The slurry was transferred to a MicroSpin column and spun for 5 s. The flow-though solution was discarded. The low salt buffer (0.5 ml) was added and further spun for 10 s. This step was repeated twice. The column was then placed into a sterile 1.5 ml microcentrifuge tube and briefly centrifuged. The mRNA was eluted out by an addition of 0.2 ml of the pre-warmed elution buffer (65°C) to the top of column and centrifuged at 14,000g for 5 s. This step was repeated once before precipitated mRNA pellet by added 10 µl of glycogen solution and 50 µl of K-acetate solution and two point five volume of cold absolute ethanol and mixed thoroughly, whereat incubated mixture at -20 °C for 30 min before centrifuged at 14,000 g for 5 min at 4 °C. The RNA pellet was washed with 1 ml of cold 75% ethanol and left on ice for 30 min before centrifugation at 14,000 g for 5 min. Alternatively, the mRNA pellet was kept under absolute ethanol in a -80 °C freezer (should not exceed 2 weeks).

2.5.2 Preparation of the 5′ and 3′ RACE-PCR template

RACE-PCR templates were prepared using a SMART™ RACE cDNA Amplification Kit (Clontech Laboratories) by combining 1.5 µg of ovarian mRNA with 1 µl of 5′-CDS primer and 1 µl of 10 µM SMART II A oligonucleotide for 5′- RACE-PCR or 1.5 µg of ovarian mRNA with 1 µl of 3′-CDS primer A for 3′- RACE-PCR (Table 2.4). The

components were mixed and spun briefly. The reaction mixture was incubated at 70°C for 2 min and immediately cooled on ice for 2 min. The ingredients composing of 2 µl of 5 X First-Strand buffer, 1 µl of 20 mM DTT, 1 µl of dNTP Mix (10 mM each) and 1 µl of PowerScript Reverse Transcriptase were added to each reaction tube in order, mixed gently and centrifuged briefly to collect reaction mixture at bottom of the tube. The reaction mixture was incubated at 42 °C for 1.5 hr in a thermocycler. The first strand reaction products were diluted with 125 µl of TE buffer (10 mM Tris-HCl; pH 8.0 and 1 mM EDTA) and heated at 72°C for 7 min. The first strand cDNA template was stored at -20°C.

Table 2. 4 Primer sequences for the first strand cDNA synthesis for RACE-PCR

Primer	Sequence
BD SMART II™ A Oligonucleotide (12 µM)	5′- AAGCAGTGGTATCAACGCAGAGTACGCGGG -3′
3′-RACE CDS Primer A (3′-CDS; 12 µM)	5′- AAGCAGTGGTATCAACGCAGAGTAC$(T)_{30}$V N -3′ (N = A, C, G or T; V = A, G or C)
5′-RACE CDS Primer (5′-CDS; 12 µM)	5′- $(T)_{25}$V N -3′ (N = A, C, G or T; V = A, G or C)
10X Universal Primer A Mix (UPM)	Long : 5′- CTAATACGACTCACTATAGGGCAAGCA GTGGTATCAACGCAGAGT -3′ Short : 5′- CTAATACGACTCACTATAGGGC -3′
Nested Universal Primer A (NUP; 12 µM)	5′- AAGCAGTGGTATCAACGCAGAGT -3′

2.5.3 Primer designed for RACE-PCR

The partial sequences of *Rdp3* (clone no. OV-N-S01-2144-W), *Cdc16* (OV-N-S01-1790-W), *Cdk5* (OV-N-S01-2407-W) and *Cdk2* (LP-N-N01-0538-LF) gene homologues from ovarian (OV) and lymphoid organ (LP) cDNA libraries of *P. monodon* were retrieved. Forward and/or reverse primers were designed for isolation of their full-length cDNA (Table 2.5).

Table 2. 5 Gene-specific (GSPs) and internal primers used for characterization of the full length cDNA of functionally important gene homologues in *P. monodon*

Gene/Primer	Sequence	Tm (°C)
Histone deacetylase Rpd3 (PmRpd3)		
3′RACE	5'- CCTGGGACTGGAGACCTAAGGGATA -3'	78
Internal 3'RACE	5'- CAGATTCCGAAGACGAGGGTGACG -3'	76
Cell division cycle 16 (PmCdc16)		
3′RACE	5'- CTGACCCACTCTGTTATGAGGCAA -3'	72
Internal 3′RACE	5'- CAAGGAGGCACTGGACATCGCAC -3'	74
Cyclin dependent kinase 5 (PmCdk5)		
3′RACE	5'- AAACTGCTCTCAGGAACATACATAA -3'	68
Cyclin dependent kinase 2 (PmCdk2)		
5′RACE	5'- CGGTAATCCTCCACGGCTTTCATCA -3'	76
3′RACE	5'- TGATGAAAGCCGTGGAGGATTACCG -3'	76

2.5.4 RACE-PCR amplification products

The master mix which is sufficient for 5′- or 3′- RACE-PCR was prepared as described in Tables 2.6. The 5′- and 3′- RACE-PCR were set up as described in Table 2.7.

Table 2. 6 Composition of 5′- and 3′- RACE-PCR

Component	5′-RACE Sample	3′-RACE Sample	GSP1+UPM (Control)	GSP2+UPM (Control)
5′-RACE-Ready cDNA	3.00 µl	-	-	-
3′-RACE-Ready cDNA	-	3.00 µl	-	-
UPM (10X)	2.5 µl	2.5 µl	2.5 µl	2.5 µl
GSP1 (10 µM)	1.0 µl	-	1.0 µl	-
GSP2 (10 µM)	-	1.0 µl	-	1.0 µl
10X BD adventage® 2 PCR Buffer	2.5 µl	2.5 µl	2.5 µl	2.5 µl
10 µM dNTP mix	0.5 µl	0.5 µl	0.5 µl	0.5 µl
50X BD Advantage® 2 polymerase mix	0.5 µl	0.5 µl	0.5 µl	0.5 µl
H_2O	Up to 25 µl	Up to 25 µl	Up to 25 µl	Up to 25 µl
Final volume	25µl	25µl	25µl	25µl

Table 2. 7 Conditions for RACE-PCR of various gene homologues of *P. monodon*

Gene homologue	Amplification condition
Histone deacetylase Rpd3 (PmRpd3)	
3′RACE	5 cycles of 94°C for 30 s and 72°C for 2 min 5 cycles of 94°C for 30 s, 70°C for 30 s and 72°C for 2 min 20 cycles of 94°C for 30 s, 68°C for 30 s and 72°C for 2 min and 72°C for 7 min
Internal 3′RACE	5 cycles of 94°C for 30 s and 72°C for 2 min 5 cycles of 94°C for 30 s, 70°C for 30 s and 72°C for 2 min 20 cycles of 94°C for 30 s, 68°C for 30 s and 72°C for 2 min and 72°C for 7 min
Cell division cycle 16 (PmCdc16)	
3′RACE	5 cycles of 94°C for 30 s and 72°C for 2 min 5 cycles of 94°C for 30 s, 68°C for 30 s and 72°C for 2 min

Gene homologue	Amplification condition
	20 cycles of 94°C for 30 s, 66°C for 30 s and 72°C for 2 min and 72°C for 7 min
Internal 3′RACE	5 cycles of 94°C for 30 s and 72°C for 2 min
	5 cycles of 94°C for 30 s, 68°C for 30 s and 72°C for 2 min
	20 cycles of 94°C for 30 s, 66°C for 30 s and 72°C for 2 min and 72°C for 7 min
Cyclin dependent kinase 5 (PmCdk5)	
3′RACE	25 cycles of 94°C for 30 s, 62°C for 30 s and 72°C for 3 min and 72°C for 7 min
Cyclin dependent kinase 2 (PmCdk2)	
5′RACE	5 cycles of 94°C for 30 s and 72°C for 2 min
	5 cycles of 94°C for 30 s, 70°C for 30 s and 72°C for 2 min
	20 cycles of 94°C for 30 s, 68°C for 30 s and 72°C for 2 min and 72°C for 7 min
3′RACE	5 cycles of 94°C for 30 s and 72°C for 2 min
	5 cycles of 94°C for 30 s, 70°C for 30 s and 72°C for 2 min
	20 cycles of 94°C for 30 s, 68°C for 30 s and 72°C for 2 min and 72°C for 7 min

2.6 Cloning of PCR products

2.6.1 Elution of PCR products from agarose gels

After electrophoresis, desired individual RACE-PCR bands were excised from agarose gels (200 - 300 mg) using a sterile scalpel. RACE-PCR product was extracted from the gel pieces using illustra™ GFX™ PCR DNA and Gel Band Purification Kit (GE Healthcare). Three to five hundred microliters of the Capture buffer type 3 was added to the sample. The mixture was incubated at 55-60 °C for 15-30 min until the gel slice was completely dissolved. During the incubation period, the tube was inverted every 3 min. A GFX MicroSpin column was placed in a collection tube and

removed mixture was applied into the GFX MicroSpin column and inclubated at room temperature for 1 min before centrifuged at 13,500 rpm for 30 s. The flow-through was discarded. The GFX MicroSpin column was placed back in the collection tube. The column was washed by the addition of 500 µl of the ethanol-added Wash buffer type 1 and centrifuged at 13,500 rpm for 30 s. After discarding the flow-through, the GFX MicroSpin column was centrifuged for 2 min at the full speed (14,000 rpm) to dry the column matrix. The dried column was placed in a new microcentrifuge tube and 10-15 µl of the Elution buffer type 4 was added to the center of the column matrix. The column was left at room temperature for 2 min before centrifuged for 2 min at the full speed to recover the gel-eluted DNA.

2.6.2 Ligation of purified DNA to the pGEM® -T easy vector

The purified PCR product was cloned using the pGEM-T Easy vector (Promega) in 10- µl reactions containing 2x Rapid Ligation buffer (60 mM Tris-HCl, pH 7.8, 20 mM $MgCl_2$, 20 mM DTT, 2 mM ATP and 10% polyethylene glycol), 3 units of T4 DNA ligase, 25 ng of pGEM®-T easy vector and 50 ng of DNA insert. The reaction mixture was incubated overnight at 4°C following transformation into *E. coli* JM109.

2.6.3 Transformation of ligation products into *E. coli* host cells

2.6.3.1 Preparation of competent cells

A single colony of *E. coli* JM109 was inoculated in 3 ml of LB broth (1% Bacto tryptone, 0.5% Bacto yeast extract and 0.5% NaCl, pH 7.0) with vigorous shaking (250 rpm) at 37°C overnight for 12-15 hr. The starting culture (500 µl) was added to 50 ml of fresh LB broth and the OD was monitored at OD_{600} of 0.5 - 0.6. Cells were briefly chilled on ice for 10 min, and recovered the cell by centrifugation at 2700g for 10 min at 4°C. The cell pellets were resuspened in 30 ml of ice-cold $MgCl_2/CaCl_2$ solution (80 mM $MgCl_2$ and 20 mM $CaCl_2$) and centrifuged as above. After resuspended in 2 ml of ice-cold 0.1 M $CaCl_2$, the cell suspension was divided to 200 µl aliquots and stored at -80°C until required.

2.6.3.2 Transformation to competent cell (*E. coli* JM109)

The prepared competent cells were thawed on ice for 5 min and 2-4 µl of the ligation products was added into competent cells and gently mixed by pipetting. The mixture was incubated on ice for 30 min before heat-shocked for 45 s in at 42°C water bath and then immediately placed on ice for 2-3 min. Next, 1 ml of prewarmed SOC medium was added (2% Bacto tryptone, 0.5% Bacto yeast extract, 10 mM NaCl, 2.5 mM KCl, 10 mM $MgCl_2$, 10 mM $MgSO_4$ and 20 mM glucose), and the mixture was incubated at 37°C with shaking for 90 min. The cells culture were collected by centrifuging for 20 s at room temperature, gently resuspended in 100 µl of SOC medium and spread onto a selective LB agar plates containing the appropriate antibiotic (50 µg/ml of ampicillin, 25 µg/ml of IPTG and 20 µg/ml of X-gal) to selected for insert plasmid. The spread plates were incubated at 37°C overnight (Sambrook and Russell, 2001).

2.6.4 Detection of recombinant clones by colony PCR

Clones that contain PCR products, in most cases, produce white colonies, but blue colonies can result from PCR fragments that are cloned in-frame with the *lac*Z gene. Recombinant clones were selected by *lac*Z system following standard protocols (Sambrook and Russell, 2001). Only white colonies containing the inserted DNA were selected. Colony PCR was performed to identify the insert sizes of positive clones.

Colony PCR was performed in 25 ul reactions containing 10 mM Tris-HCl (pH 8.8), 50 mM KCl, 0.1% Triton X – 100, 100 mM of each dNTP, 2 mM $MgCl_2$, 0.1 µM each of pUC1 (5′-CCGGCTCGTATGTTGTGTGGA-3′) and pUC2 (5′-GTG GTGCAAGGCGATTAAGTTGG-3′), 0.5 unit of Dynazyme^{TM} DNA Polymerase (FINNZYMES). Selected colonies were individually picked by pipette tips and resuspended in the reaction mixtures. PCR was conducted in a PCR thermal cycle began with predenaturation at 94°C for 3 min followed by 35 cycles of denaturation at 94°C for 30 s, annealing at 50°C for 1 min and extension at 72°C for 2 min. The final extension was carried out at the same temperature for 7 min. The colony PCR

product was size-fractioated through 1.5% agarose gels and visualized after staining with ethidium bromide.

2.6.5 Extraction of recombinant plasmids

Plasmids were extracted from the *E. coli* host using an illustra plasmid Prep Mini Spin Kit (GE Healthcare). The extraction was carried out according to the manufacturer's protocol. Shortly, *E. coli* cells containing the transformed plasmids were inoculated into 3 ml of LB broth (1% tryptone, 0.5% yeast extract, 1.0 % NaCl containing 50 µg/ml of ampicillin) incubated at 37°C with shaking overnight. Harvesting of bacterial culture from 1.5 ml fresh overnight culture was collected by centrifuging at 16,000 g for 1 min. The cell pellets were lysed and resuspended with 175 µl of the Lysis buffer type 7. The resuspended cells were lysed by gently mixing with 175 µl of the Lysis buffer type 8 and 350 µl of the Lysis buffer type 9. After that, plasmid binding were transferred to column and centrifuged at 16,000 g for 30 s. The column was washed with 400 µl of the Lysis buffer type 9 and centrifuged at 16,000 g for 30 s. The column was washed one more time with 400 µl of the Wash buffer type 1 and subjected to a final spin for 2 min at 16,000 g to remove the residual Wash buffer. Add 30-50 µl Elution buffer to elute the plasmid. The column was then left at room temperature for 2 min and centrifuged at 16000 g for 2 min. Concentrations of the extracted plasmid were spectrophotometrically measured.

2.6.6 Restriction enzyme digestion of the recombinant plasmids

Recombinant plasmid was digested with *Eco R*I to verify whether the ligated PCR product possibly contained one type of sequence. The digestions were set up in a total volume of 12 µl containing an appropriate restriction enzyme buffer (90 mM Tris-HCl; pH 7.5, 10 mM NaCl and 50 mM $MgCl_2$), 5 unit of *Eco R*I (Promega) and 1 µl of recombinant plasmid. The reaction mixtures were incubated at 37°C for 4-6 hr before analyzed by agarose gel electrophoresis.

2.6.7 DNA sequencing

Nucleotide sequences of recombinant plasmids were examined by automated DNA sequencer using forward and/or reverse M13 primer as the

sequencing primer by MACROGEN, Korea. Nucleotide sequences were blasted against data in the GenBank (http://www.ncbi.nlm.nih.gov/blast) using Blast*N* (nucleotide similarity against the nr/nt database) and Blast*X* (translated protein similarity against the non-redundant protein sequences, nr, and database) and the functional domain of the deduced protein was searched using SMART (http://smart.embl-heidelberg.de/).

2.7 Relative expression levels of interesting genes in ovaries of *P. monodon* using quantitative real-time PCR

Expression levels of several transcripts related to ovarian development were examined using quantitative real-time PCR analysis. *EF-1*α_{214} was also amplified from the same template and considered as the positive control.

2.7.1 Experimental animals

2.7.1.1 Examination of expression levels of various genes using ovarian development of *P. monodon*

For gene expression analysis, wild female broodstock were live-caught from the Andaman Sea (west of peninsular Thailand, average body weight = 217.07 ± 47.10 g) and acclimated under the farm conditions for 2-3 days. The post-spawning group was immediately collected after shrimp were ovulated (stage V, *N* = 5). Ovaries were dissected out from each broodstock and weighed. For the eyestalk ablation group, wild broodstock were acclimated for 7 days prior to unilateral eyestalk ablation (average body weight = 209.97 ± 39.45). Ovaries of eyestalk-ablated shrimp were collected at 2-7 days after ablation. The ovarian developmental stages of wild shrimp were classified according to the GSI values (GSI, ovarian weight/body weight x 100). Ovarian developmental stages were divided to previtellogenic (stage I, GSI < 1.5%, *N* = 4 and 5 for intact and eyestalk-ablated broodstock, respectively), vitellogenic (stage II, GSI > 2-4%, *N* = 4 and 9), late vitellogenic (stage III, GSI > 4-6%, *N* = 5 and 9) and mature (stage IV, GSI > 6%, *N* = 9 and 5) ovaries, respectively. The ovarian developmental stages of wild shrimp were confirmed by conventional histology (Qiu et al., 2005). In addition, cultured juveniles (4-month-old, *N* = 4) were

collected from the Broodstock Multiplication Center (BMC), Burapha University (Chanthaburi, Thailand) and included in the experiments.

2.7.1.2 *In vivo* effects of 5-HT injection

In addition, domesticated female *P. monodon* (18-month-old) were also sampled and acclimated for 7 days at the laboratory conditions (28-30ºC, 15 ppt seawater and natural daylight) in 1000-liter fish tanks. Eight groups of female shrimp (average body weight = 106.80 ± 21.42 g) were injected intramuscularly into the first abdominal segment with 5-HT (50 µg/g body weight, *N* = 4 for each group). Specimens were collected at 0, 1, 3, 6, 12, 24 and 48 hr post injection (hpi). Shrimp injected with the 0.85% saline solution (at 0 hpt) were included as the control.

2.7.1.3 *In vitro* effects of 5-HT treatment

Female broodstock were live-caught from the Andaman Sea and acclimated under the laboratory conditions for 3 days. The body weight, total length, standard length of each shrimp was recorded (Table 2.8). An ovarian developmental stage of each shrimp was roughly evaluated externally. Shrimp with previtellogenic ovaries were selected and ovaries were dissected out from each shrimp and weighed. Ovaries were rinsed three times with sterilized 2.8% saline solution containing penicillin G (1,000 IU/ml) and streptomycin (1,000 µg/ml) and four times with the M199 medium containing 5% fetal bovine serum (FBS), 100 U/ml penicillin and 100 µg/ml streptomycin.

For serotonin treatment, piece of ovaries were incubated in M199 (supplemented with 10% FBS, 100 U/ml penicillin and 100 µg/ml streptomycin, 2 mM L-glutamine and 10 mM HEPES, pH 7.3) containing 1 and 15 µg/ml of 5-HT. In the control group, ovarian explants were culture in M199 containing 0.85% NaCl (without 5-HT as the vehicle control). The cultures were incubated in a 5% CO_2 atmosphere at 28°C. Specimens were collected at 0, 0.30, 1, 2, 4, 6, 12, 24 and 48 hr after incubation (*N* = 3 for each time point). Ovarian pieces were fixed in Davidson's fixative or kept in RNAlater at -20°C until further needed.

Table 2. 8 Specimens of *in vitro* effects of serotonin (5-HT) and 17α ,20β-dihydroxyprogesterone (17α, 20β-DHP) treatment

Specimens/ Treatment	Total length (cm)	Standard length (cm)	Body weight (g)	Ovarian weighs (g)	GSI (%)
5-HT					
WFNCOV01	30.0	27.5	242.72	5.04	2.08
WFNCOV02	29.5	27.1	221.94	3.91	1.76
WFNCOV03	29.2	28.0	225.15	6.11	2.71
17α, 20β-DHP					
WFNOV02	29.8	28.2	276.60	5.52	2.00
WFNOV04	28.4	26.6	230.72	4.54	1.97
WFNOV05	30.0	27.2	245.55	3.73	1.52
WFNOV06	29.1	25.6	214.71	3.43	1.50
WFNOV07	29.5	26.8	248.01	3.92	1.58
WFNOV09	29.2	26.7	223.22	3.23	1.45

2.7.1.4 *In vitro* effects of 17α, 20β-DHP treatment

The middle lobes of ovaries was excised into small pieces of approximately 3-5 mm in size in M199 (with Earle's salts supplemented with 10% FBS, 100 U/ml penicillin and 100 µg/ml streptomycin, 2 mM L-glutamine and 10 mM HEPES, pH 7.3). Four pieces of ovarian explants were placed in each well of 24-well plate that contained 1 ml of M199 containing 17α-20 β-DHP (treatment) or propylene glycol (PPG): absolute ethanol (1:1 v/v; the vehicle control). The cultured ovarian explants were incubated in a 5% CO_2 atmosphere at 28°C. Three doses of 17α-20β-DHP (0.1, 1.0 and 10.0 µg/ml) were tested against the ovarian tissue explants. Specimens were collected at 0, 1, 3, 6, 12 and 24 hr after incubation (*N* = 6 for each time point). Each piece were fixed in Davidson's fixative and stained with hematoxylin-eosin (H&E) and viewed using an Olympus BX51 microscope equipped with a Olympus DP71 digital camera. For RNA extraction, the tissue pieces were kept in RNAlater at -20°C until further needed. Total RNA was extracted as described previously.

2.7.2 Construction of standard curves for the quantitative real-time PCR

For construction of the standard curve of each gene, the PCR product of the target gene and *EF-1*α was amplified using gene-specific primers described in Table 2.9, and electrophoretically analyzed through agarose gels. The gel-eluted product was cloned into pGEM-T easy vector and transformed into *E. coli* JM109. Plasmid DNA were extracted and used as the template for construction of the standard curve. Templates of each gene homologues were 10 fold-serial dilution prepared covering 10^2 – 10^8 copy numbers. For *EF-1*α, 10^3 – 10^8 copy numbers were used. Real-time RT-PCR was carried out and each standard point was run in duplicate. The copy number of standard DNA molecules can be calculated using the following equation:

X ng/µl DNA x 6.022x10^{23} / plasmid length in bp x 660 x 10^9 = Y molecules/µl

X is amount of plasmid dsDNA (ng/ul), 6.022x10^{23} is Avogadro's number (molecules/mole), 660 is average molecular weight of one mole of a base pair (bp) average weight 650 g, 10^9 used convert to ng from g of dsDNA and Y is amount molecules of plasmid dsDNA per microliters.

The standard curves (correlation coefficient = 0.995-1.000 or efficiency higher than 95%) were drawn for each run. The standard samples were carried out in a 96 well plate and each standard point was run in duplicate. *EF-1*α_{214} was used as the internal control.

Table 2. 9 Primer sequence, melting temperature (Tm), sizes of the expected amplification products and final concentration of primers used for quantitative real-time PCR

Gene	Sequence primer	Tm (°C)	Size (bp)	Final conc. (μM)
PmBystin1	F: 5'- ACGCACAACCCCAGAGAAAACTA -3'	68	183	0.2
	R: 5'- TTGGCAAGGGTCCACTTCTGTAT -3'	68		0.2
PmCdc2	F: 5'- ATTCCGTCAAACAGATGGACAGCG -3'	72	114	0.2
	R: 5'- CATCAAAGTAGGGGTGCTTCAGGG -3'	74		0.2
PmCdc16	F: 5'- CTGACCCACTCTGTTATGAGGCAA -3'	72	197	0.2
	R: 5'- AGCAGGTTGTGGCAATGGTGTA -3'	66		0.2
PmCdk2	F: 5'- ATGAAAGCCGTGGAGGATTACC -3'	66	260	0.2
	R: 5'- GTTTTTGGCACCGAGGAGAATC -3'	66		0.2
PmCdk7	F: 5'- TCTTTCCTGCTGCCAGTGAT -3'	60	123	0.2
	R: 5'- GGACAGGCTTATTGCTGAAAT- 3'	60		0.2
PmChk1	F: 5′- TGGACAAAGGTGGACAATCTG -3′	62	183	0.2
	R: 5′- CACACGCTTGGTAGTAGGGGT 3′	66		0.2
PmRpd3	F: 5′- ATGAAGCCACACAGGATACG -3′	60	276	0.2
	R: 5′- AGCACCAGCAATGGAGCCT -3′	60		0.2
EF-1α_{214}	F: 5´- GTCTTCCCCTTCAGGACGTC-3´	64	214	0.2
(control)	R: 5´-CTTTACAGACACGTTCTTCACGTTG-3´	72		0.2

2.7.3 Quantitative real-time PCR analysis

The target transcripts and the internal control *EF-1*α_{214} of the synthesized cDNA were amplified in a 10 μl reaction volume contained 5 μl of 2X LightCycler® 480 SYBR Green I Master (Roche, Germany), the first strand cDNA template, 0.2 μM each of gene-specific primers. The thermal profile for quantitative real-time PCR of each gene was shown in Table 2.10. Real-time PCR of each specimen was carried out in duplicate using a LightCycler® 480 Instrument II system (Roche).

2.7.4 Statistical test

The relative expression level (copy number of that target genes/that of *EF-1*α_{214}) between shrimp possessing different stages of ovarian development were statistically tested using one way analysis of variance (ANOVA) followed by a Duncan's new multiple range test. Significant comparisons were considered when the *P* value was < 0.05. To determine effects of treatment on gene expression when the homogeneity test failed, Kruskal-Wallis nonparametric analysis of variance test was applied. Pairwise comparisons were performed by Dunn's multiple comparison test (Kruskal and Wallis, 1952; Dunn, 1964). Results were considered significant when *P* < 0.05.

Table 2. 10 Conditions for quantitative real-time PCR analysis of reproduction-related genes of *P. monodon*

Gene	Template (ng)	Amplification condition
PmBystin1	50	95°C for 10 min 40 cycles of 95°C for 15 s, 58°C for 30 s and at 72°C for 30 s. Melting curve analysis was 95°C for 15 s, 65°C for 1 min and at 98°C for continuation and cooling was 40°C for 30 s.
PmCdc2	50	95°C for 10 min 40 cycles of 95°C for 15 s, 58°C for 30 s and at 72°C for 15 s. Melting curve analysis was 95°C for 15 s, 65°C for 1 min and at 98°C for continuation and cooling was 40°C for 30 s.
PmCdc16	100	95°C for 10 min 40 cycles of 95°C for 15 s, 58°C for 30 s and at 72°C for 15 s. Melting curve analysis was 95°C for 15 s, 65°C for 1 min and at 98°C for continuation and cooling was 40°C for 30 s
PmCdk2	100	95°C for 10 min 40 cycles of 95°C for 15 s, 58°C for 30 s and at 72°C for 30 s. Melting curve analysis was 95°C for 15 s, 65°C for 1 min and at 98°C for continuation and cooling was 40°C for 30 s.

Gene	Template (ng)	Amplification condition
PmCdk7	100	95°C for 10 min 40 cycles of 95°C for 15 s, 55°C for 30 s and at 72°C for 30 s. Melting curve analysis was 95°C for 15 s, 65°C for 1 min and at 98°C for continuation and cooling was 40°C for 30 s.
PmChk1	50	95°C for 10 min 40 cycles of 95°C for 15 s, 55°C for 30 s and at 72°C for 30 s. Melting curve analysis was 95°C for 15 s, 65°C for 1 min and at 98°C for continuation and cooling was 40°C for 30 s.
PmRpd3	50	95°C for 10 min 40 cycles of 95°C for 20 s, 53°C for 30 s and at 72°C for 30 s. Melting curve analysis was 95°C for 15 s, 65°C for 1 min and at 98°C for continuation and cooling was 40°C for 30 s.
EF-1 α_{214} (control)	5	95°C for 10 min 40 cycles of 95°C for 15 s, 58°C for 30 s and at 72°C for 30 s. Melting curve analysis was 95°C for 15 s, 65°C for 1 min and at 98°C for continuation and cooling was 40°C for 10 s.

2.8 *In situ* hybridization

2.8.1 Sample preparation

Ovaries of normal and eyestalk-ablated *P. monodon* broodstock were fixed in 4% paraformaldehyde prepared in 0.1 M sodium phosphate buffered (pH 7.2) overnight at 4°C. The fixed ovarian tissue was washed four times with PBS at room temperature and stored in 70% ethanol at -20°C until used. Tissues were dehydrate using the following washed with series alcohol (twice of 70%, 80%, 95% and absolute ethanol for 50 min each), cleared in BioClear (twice for 50 min) at room temperature after that wax in 100% paraffin (twice for 90 min at 65°C) and infiltrated with the embedding material (paraffin). Conventional paraffin sections (5 µm) on to poly-L-lysine-coated slides were carried out and stained with hematoxylin-eosin

(H&E) and viewed using an Olympus BX51 microscope equipped with a Olympus DP71 digital camera.

2.8.2 Preparation of cRNA probes

Forward (with T7 promoter sequence) and/or reverse (with SP6 promoter sequence) were designed (Table 2.11) and used for amplification of the target gene segment. The amplification product was purified using illustra™ GFX™ PCR DNA and Gel Band Purification Kit (GE Healthcare) following the manufacturer's instructions. The sense and anti-sense cRNA probes of interesting genes containing sequences of the T7 and SP6 promoter, respectively, were synthesized by RNA labeling with digoxigenin-UTP (transcription with SP6 and T7 RNA polymerase) using a DIG RNA labeling mix (Roche, Germany). Approximately 1000 µg of the purified product was used as the template using the protocol recommended by the manufacturer (Roche). The mixture was incubated at 37°C for 2 hr for the sense probe and 40°C for 2 hr for the antisense probe. DNA was eliminated by treated cRNA probes with 2 µl DNase I at 37°C for 15 min. The activity of enzymes was stopped reaction by adding 2 µl of 0.2 M EDTA (pH 8.0). The success of cRNA synthesis was determined by electrophoresis. The synthesized cRNA was purified using an RNeasy Mini Elute Clean up Kit (Qiagen) and the probe concentration was spectrophotometrically measured. The cRNA probe was stored at -80°C until needed.

Table 2. 11 Primer sequences for preparation of *PmBystin1, PmCdc2* and *PmCdk7* antisense and sense cRNA probes of *P. monodon*

Primer combinations for sense and antisense cRNA probe	
Bystin1-T7/F	5'- TAATACGACTCACTATAGGGCGCTTCTTCAACTTGGTCCTCC -3'
Bystin1-SP6/R (520 bp)	5'- ATTTAGGTGACACTATAGAATTCTCTCCTCACCTCGGCAG -3'
Cdc2-T7/F	5'- TAATACGACTCACTATAGGGGAAAGAACTTCAGCATCCCAACA -3'
Cdc2-SP6/R (403 bp)	5'- ATTTAGGTGACACTATAGAAAGACCAAACATCAACAGGACAGG -3'
Cdk7-T7/F	5'- TAATACGACTCACTATAGGGATGTTGGTTCGCTGTCCCTAC -3'
Cdk7-SP6/R (400 bp)	5'- ATTTAGGTGACACTATAGAACTAAGGAACCTCCAAAGCCAG -3'

2.8.3 Dot blot analysis

The quality of cRNA probes was determined before used for *in situ* hybridization using dot blot analysis. Serial dilutions of the pre-diluted probe and control cRNA were made. The diluted probe (1 µl) was spotted on a piece of the Hybond N^+ membrane. The spotted probe was fixed to the membrane by cross-linking with UV-light for 1 min. The membrane was washed with the washing buffer for 1 min and incubated in the blocking solution for 1 min. After that, the membrane was incubated in Anti-DIG-alkaline phosphatase (1:5,000 in the blocking solution) for 3 min, washed with the washing buffer for 1 min and incubates in the detection buffer. The positive hybridization signals was developed using NBT/BCIP solution. The intensities of the control and the dilution of probe were compared to estimate the concentration of the cRNA probe.

2.8.4 Hybridization and detection

Tissue sections were dewaxed in toluene and dehydrated in absolute alcohol. Sections were then prehybridized in 2 x SSC (50% deionized formamide, 1 µg/ µl yeast tRNA, 1 µg/ µl salmon sperm DNA, 1 µg/ µl BSA and 10% (w/v) dextran sulfate) at 50°C for 30 min. *In situ* hybridized with either the sense or antisense probe in the prehybridization solution overnight at 50°C. After hybridization, the tissue sections were washed twice with 4 x SSC for 5 min each and once with 2 x SSC containing 50% formamide at 50°C for 20 min. The sections were then treated with 20 µg/ml RNase A for 30 min at 37°C in a prewarmed RNase A buffer (0.5 M NaCl, 10 mM Tris–HCl, pH 8.0, 1 mM EDTA) at 37 °C for 5 min. The sections were washed four times with the RNase A buffer (37°C, 10 min each) and 2 x SSC (50°C, 15 min each). High stringent washing of decreasing salinity was carried out twice in 0.2 x SSC at 50°C for 20 min each. DIG was immunologically detected (anti-Digoxiginin-AP Fab fragment conjugated with alkaline phosphatase and NBT/BCIP) according to the manufacturer's instructions (Roche, Germany).

2.9 *In vitro* expression of recombinant proteins using the bacterial expression system

2.9.1 Construction of recombinant plasmids in cloning and expression vectors

Primers for amplification of the complete ORF of each transcript were designed (Table 2.12). The purified PCR product was cloned using the pGEM-T Easy vector and transformed into *E. coli* JM109. A recombinant plasmid containing the complete ORF of the interesting gene was used as the template and PCR was carried out using the forward and reverse primers of containing restriction enzyme recognized sites and 6X His residues encoded nucleotides (Table 2.13). The amplification products were carried out in a total volume of 25 µl containing 0.5 µM of each forward and reverse primers, 0.75-1.5 unit *Pfu* DNA polymerase and 0.2 mM of each dNTPs and 1 µl of recombinant plasmid (diluted with sterilized distilled water 1:50). The thermal profiles for amplification of each transcript are shown in Tabel 2.14. The amplification product was digested and analyzed by agarose gel electrophoresis.

The gel-eluted product was ligated into digested restriction enzyme of expression vector and transformed into *E. coli* JM109. The positive clones were sequenced to confirm the orientation of recombinant clones. The corrected direction of recombinant plasmid was subsequently transformed into *E. coli* BL21-CodonPlus (DE3)-RIPL and *E. coli* BL21 (DE3) plyss competent cells, respectively.

Table 2. 12 Nucleotide sequences of primers for amplification of an open reading frame (ORF) of each transcript

Gene	Sequence primer	Tm (°C)	Size (bp)	Final conc. primer (μM)
PmApc11	F: 5'- CATGAAGGTGAAGATTAAATCCT -3'	62	255	0.5
	R: 5'- GGTTATTCTTTAAACTTCCACTC -3'	62		0.5
PmBystin1	F: 5'- CAGAATGGGAAAGATTAAACGT -3'	60	1365	0.5
	R: 5'- TACACTACTCATCAACCATCATT -3'	62		0.5
PmCdc20	F: 5'- GCAAGATGTCCCACCTTCAGTT -3'	66	1626	0.5
	R: 5'- ATACAATTTATCGAATGGTCTGA -3'	60		0.5
PmRpd3	F: 5′- GAAAAATGTCGGCCGCACC -3′	62	1452	0.5
	R: 5′- GCCTCAAGATTCCACTTTGGTTTC -3′	70		0.5

Table 2. 13 Nucleotide sequences of primers used for *in vitro* expression of *PmApc11, PmBystin1, PmCdc2, PmCdc20, PmCdk7, PmChk1* and *PmRpd3* of *P. monodon.*

Primer	Sequence
Full-length / domain cDNA containing *restriction* site and 6 repeated-His encoded nucleotides	
PmApc11- *Nde* I	F: 5'- CCGCATATGAAGGTGAAGATTAAATC -3'
PmApc11- 6His and *Bam* HI	R: 5'- CGGGGATCCTTAATGATGATGATGATGATGTT CTT TAAACTTCCACTCTT -3'
PmBystin1-*Nde* I	F: 5'- CCGCATATGGGAAAGATTAAACGTCT -3'
PmBystin1-6His and *Bam* HI	R: 5'- CGGGGATCCCTAATGATGATGATGATGATGCT CAT CAACCATCATTGGCA -3'
PmCdc2- *Nhe* I and 6His	F: 5'- ATGGCTAGCCACCACCACCACCACCACATGGAGGAT-3'
PmCdc2- *Xho* I	R: 5'- CTCGAGTTAATTCTTGGCTGGAAGAGTGGACTTG -3'
PmCdc20-*Nde* I	F: 5'- CCGCATATGTCCCACCTTCAGTTTGA -3'

Primer	Sequence
Full-length / domain cDNA containing *restriction* site and 6 repeated-His encoded nucleotides	
PmCdc20-6His and *Bam* HI	R: 5'- CGGGGATCCTTAATGATGATGATGATGATGTCGAAT GGTCTGAGCAAGCA -3'
PmCdk7- *Nde* I	F: 5'- CCGCATATGGAAGTAGAACAAGAGAAG -3'
PmCdk7- 6His and *Nco* I	R: 5'- CGGCCATGGCTAATGATGATGATGATGATGGAATT GAAGCTTCTTTGCTA -3'
PmChk1- *Bam* HI	F: 5'- CCGGGATCCATGGCTGGGCCGGTCACCG -3'
PmChk1-6His and Sal I	R: 5'- CGGGTCGACTTAATGATGATGATGATGATGGGCTG GTAGCATATTTGTTG -3'
PmRpd3-*Nde* I (Rpd3 domain)	F: 5'- CCGCATATGAGTGACATTGGAAATTATT -3'
PmRpd3-6His and *Bam* HI (Rpd3 domain)	R: 5'- CGCGGATCCTTAATGATGATGATGATGATGTAAAGC AACAGCCGTTTCATA -3'

*underlined = restriction site, double underlined = start or stop codon, dotted line = histidine tag

2.9.2 Expression of recombinant proteins

A single colony of the recombinant clone was inoculated into 3 ml of LB medium supplemented with 50 µg/ml ampicillin and 50 µg/ml chloramphenicol at 37°C. The overnight culture (50 µl) was transferred to 50 ml of LB medium containing ampicillin and chloramphenicol and further incubated to an OD_{600} of 0.4-0.6. One OD600 milliliter was time-interval taken at 0, 1, 2, 3, 4, 6 h and overnight after IPTG induction (1.0 mM final concentration) suitable volume of the culture corresponding to the OD=1.0 was collected several time intervals (0, 1, 2, 3, 4, 6 hr and overnight at 37°C with shaker incubator) and centrifuged at 12000g for 1 min, resuspended with 1 X PBS buffer and analyzed by 12-18% SDS-PAGE (Laemmli, 1970).

Table 2. 14 Amplification condition used for *in vitro* expression of interesting genes

Gene homologue	Amplification condition
Anaphase promoting complex subunit 11 (Apc11)	95 °C for 3 min 30 cycles of 94°C for 30 s, 58°C for 45 s and 72°C for 1 min and 72°C for 7 min
Bystin isoform 1 (Bystin1)	95°C for 3 min 30 cycles of 94 °C for 30 s, 58°C for 45 s and 72°C for 3 min and 72°C for 7 min
Cell division cycle 2 (Cdc2) or *cyclin dependent kinases 1(Cdk1)*	95°C for 3 min 30 cycles of 94°C for 30 s, 58°C for 45 s and 72°C for 2 min and 72°C for 7 min
Cell division cycle 20 (Cdc20)	95°C for 3 min 30 cycles of 94°C for 30 s, 58°C for 45 s and 72°C for 3.30 min and 72°C for 7 min
cyclin dependent kinases 7(Cdk7)	95°C for 3 min 30 cycles of 94°C for 30 s, 58°C for 45 s and 72°C for 2.30 min and 72°C for 7 min
Checkpoint kinase 1(Chk1)	95°C for 3 min 30 cycles of 94°C for 30 s, 58°C for 45 s and 72°Cfor 3 min and 72°C for 7 min
Histone deacetylase Rpd3 (Rpd3)	95°C for 3 min 30 cycles of 94°C for 30 s, 58°C for 45 s and 72°C for 2 min and 72°C for 7 min

In addition, 50 ml of the IPTG induced-cultured were centrifuged, resuspended in the lysis buffer (0.05 M Tris-HCl; pH 7.5, 0.5 M Urea, 0.05 M NaCl, 0.05 M EDTA; pH 8.0 and 1 mg/ml lysozyme). The cells were broken by sonication in lysis buffer using Digital Sonifier® sonicator Model 250 (BRANSON). The suspension was incubated on ice for 30 min before sonicated 5 times on ice at 15% amplitude for a period of time 3 min (pulsed on 15 s and pulsed off 15 s). Soluble and insoluble fractions were further separated by centrifuged at 14000 rpm for 30 min. Insoluble fractions resuspended with binding buffer (20 mM sodium phosphate, 500 mM NaCl,

20 mM imidazole, 8M urea, pH 7.4). Measurement of protein concentration was used following on the method of Bradford with spectrophotometer (Bradford, 1976). Expression of the recombinant protein was electrophoretically analyzed by 12-18% SDS-PAGE.

2.9.3 Western blot analysis

Recombinant protein was analyzed by 12-18% SDS-PAGE. Electrophoretically separated proteins were transferred onto a PVDF membrane (Hybond P; GE Healthcare) (Towbin et al., 1979). The membrane was washed three times with 1X Tris-buffer saline tween-20 (TBST; 25 mM Tris, 137 mM NaCl, 2.7 mM KCl and 0.05% tween-20) for 15 min, blocked with 20 ml of the blocking buffer (1.0 g of BSA in 20 ml of 1X TBST) and incubated overnight at room temperature with gentle shaking. The membrane was washed three times in 1X TBST and incubated with the first antibody; Anti-His antibody IgG (GE Healthcare; 1:5,000) in the blocking buffer for 1 hr. The membrane was washed three times with 1X TBST and incubated with diluted goat anti-mouse IgG (H+L) conjugated with alkaline phosphatase (Bio-Rad Laboratories; 1:7,500) in the blocking buffer for 1 hr and washed three times with 1X TBST. Immunoreactive signals were visualized using NBT/BCIP (Roche) as a substrate and stopped by transferring the membrane into water.

2.9.4 Purification of recombinant proteins and production of polyclonal antibody

Aliquots of IPTG-induced culture (500-1000 ml) were harvested by centrifugation and resuspended in lysis buffer (1 mg/ml lysozyme in 1 X PBS, pH 7.4) incubated on ice for 30 min. The pellet was purified under denaturing conditions by using a His GraviTrap Chelating HP affinity chromatography (GE Healthcare), sonicated and soluble-insoluble fractions were further separated by centrifuged at 14000 rpm for 30 min. Insoluble fraction was loaded into column and washed with 10 ml of binding buffer containing 20 mM imidazole (20 mM sodium phosphate, 500 mM NaCl, 20 mM imidazole, pH 7.4 with 8M urea), 5 ml of the binding buffer containing 40 mM imidazole (20 mM sodium phosphate, 500 mM NaCl, 40 mM imidazole, pH 7.4 with 8 M urea) and 5 ml of the binding buffer containing 80 mM imidazole (20 mM sodium

phosphate, 500 mM NaCl, 80 mM imidazole, pH 7.4 with 8M urea). Eluting step with 6 ml of the elution buffer (20 mM sodium phosphate, 500 mM NaCl, 500 mM imidazole, pH 7.4 with 8M urea). Each fraction of the washing and eluting step were analyzed by 12-18% SDS-PAGE and western blotting. The purified proteins were stored at 4°C or -20°C for long term storage.

Polyclonal antibody was produced by Faculty of Associated Medical Sciences, Chiangmai University. The polyclonal antibody titer was examined direct enzyme-link immunosorbent assay (ELISA).

2.10 Expression profiles of protein during ovarian development of *P. monodon*

2.10.1 Extraction of total ovarian proteins

Approximately 500 µg of the frozen ovaries of *P. monodon* were ground to fine powder in the presence of liquid N_2 and suspended in 1.2 ml of the TCA-acetone extraction buffer : 10% TCA in acetone containing 0.1% DTT and complete protease inhibitor cocktail (Roche) and left at -20°C for 1 hr. The mixture was centrifuged at 10,000 g for 30 min at 4°C and supernatant was discarded. The protein pellets were washed three times with the acetone solution before centrifuged at 10000 g for 30 min at 4°C. The resulting pellet was air-dried and dissolved in the lysis buffer (30 mM Tris-HCl, 2 M Thiourea, 7 M Urea, 4% CHAPS, w/v). The amount of extracted total proteins was measured by a dye binding assay.

2.10.2 Analyzed of protein expression using western blotting

Twenty micrograms of total ovarian proteins were heated at 100°C for 5 min and immediately cooled on ice for 5 min. Proteins were size-fractionated on a 12-18% SDS-PAGE (Laemmli, 1970). Electrophoretically separated proteins and analyzed described western blot analysis.

2.11 Purification of polyclonal antibody

2.11.1 Purification of polyclonal antibody using protein A

Polyclonal antibody was purified following the protocol recommended by the manufacturer (Thermo Scientific) with some modifications. Approximately 5 ml of

serum was centrifuged at 10000 rpm for 10 min at 4 °C. The supernatant was divided to 2 portions and sequentially added to a column preequilibrated with 3-5 ml of the binding buffer. The column was incubated with serum for 45 and 30 min for each flow through. The column was washed with 5-10 ml of the binding buffer. The protein A-bound polyclonal antibody was eluted with 5-10 ml of the elution buffer and collected in each fraction of 1 ml. Each fraction was spectrophotometrically examined at 280 nm.

2.11.2 Purification of polyclonal antibody using affinity chromatography

Alternatively, polyclonal antibody was purified by affinity chromatography using the protocol recommended by the manufacturer (GE healthcare) with some modifications. The HiTrap NHS-activated HP column was prepared with 5 ml of ice-cold 1 mM HCl. The column was incubated with 1 ml of legends (5-10 mg/ml recombinant proteins dissolved in coupling buffer) for 30 min at room temperature. The column was washed with 15-20 ml of buffer A and buffer B and flow through with 10 ml of the binding buffer. Polyclonal antibody (3 ml) was applied at the flow rate of 0.2-1 ml/min. The column was washed with 5-10 ml of the binding buffer. The column-bound polyclonal antibody was eluted with 3-5 ml of the elution buffer and collected in each fraction of 1 ml. Each fraction was spectrophotometrically examined at 280 nm.

2.12 Sensitivity and specificity of polyclonal antibody

2.12.1 Sensitivity of anti-rPmCdc2 PAb and anti-rPmCdk7 PAb

The sensitivity of detection of purified anti-rPmCdc2 PAb and anti-rPmCdk7 PAb were examined against varying amounts (1.0, 0.8, 0.6, 0.4, 0.2, 0.1, 0.05, 0.03, 0.01 µg) of the rPmCdc2 or rPmCdk7 protein. The electrophoretically separated protein was transferred onto a PVDF membrane (Hybond P, GE Healthcare) (Towbin et al., 1979) in 25 mM Tris, 192 mM glycine (pH 8.3) buffer containing 10% methanol at 100 V for 90 min. The membrane was treated with 5% BSA blocking solution (Sigma) overnight and incubated with purified anti-rPmCdc2 or anti-rPmCdk7 PAb (1:100 in the blocking solution) for 1 hr at room temperature. The membrane was washed 3 times with 1 x Tris Buffered Saline-Tween-20 (TBST; 25 mM Tris-HCl, 0.15 M NaCl, pH

7.4, 0.1% Tween-20) and incubated with goat anti-rabbit IgG (H+L) conjugated with alkaline phosphatase (Bio-Rad Laboratories) at 1:5000 for 1 hr and washed 3 times with 1xTBST. Immunoreactive signals were visualized using NBT/BCIP (Roche) as the substrate.

2.12.2 Specificity of anti-rPmCdc2 PAb anti-rPmCdk7 PAb

Cross reactivity of purified anti-rPmCdc2 and anti-rPmCdk7 PAb was tested against 0.2 µg of other recombinant proteins of *P. monodon* previously produced in our laboratory including Downstream of receptor kinase (rPmDRK), cAMP-dependent protein kinase, catalytic beta a-like (PmPKACB), cell division cycle 2 (rPmCdc2), cyclin B (rPmCyclin B), Semaphorin (rPmSema) and Rpd3 histone deacetylase (rPmRpd3). Western blot analysis was carried out as previously described.

To illustrate the specificity of anti-rPmCdk7 PAb against the positive band of 67 kDa, an antigen-antibody competition experiment was carried out. Briefly, 0 (no competition), 1, 2.5, 5 and 10 µg of rPmCdk7 were separately added to 3.5 ml of purified anti-rPmCdk7 PAb (1:100). The reaction mixture was incubated at room temperature for 1 hr. The resulting antibody was used for blotting against size-fractionated 2.5, 5, 10 and 20 µg total proteins extracted from ovaries of a vitellogenic female.

2.13 Immunofluorescence

The sections were deparaffinized by immerges in toluene three times of for 3 min each and rehydrated with series alcohol (twice of absolute ethanol and 90%) for 3 min each and immersed in 0.1 M PBS containing 1% glycine for 15 min. The sections were then incubated in the blocking solution (10% normal goat serum; NGS in 0.1 M PBST) at room temperature for 2 hr, in a moist chamber and rinsed with PBST three times for 20 min each. Tissue sections were further incubated in primary antibodies (1:10 in blocking solution) overnight at room temperature before washed three times with PBST, then incubated with goat anti-rabbit IgG conjugated with Alexa 488 (1:200 in the blocking solution, Molecular Probes, U.S.A) for 2 hr and rinsed three times with PBST. The slides were viewed and image-captured by a confocal laser scanning microscope (Olympus Fluoview FV1000). Tissue sections were also incubated with preimmune rabbit serum as the negative control.

CHAPTER III
RESULTS

3.1 Isolation and characterization of the full-length cDNA of various cell cycle-regulating genes in *P. monodon*

3.1.1 Total RNA extraction and first strand cDNA synthesis

Total RNA was extracted from ovaries, testes, hemocytes and various tissues of *P. monodon*. The concentration of extracted total RNA was measured spectrophotometrically. The $A_{260/280}$ ratios of the extracted RNA were 1.8-2.0. The quality of total RNA was also examined by agarose gel electrophoresis (Figure 3.1A). The discrete ribosomal RNA bands were observed reflecting good quality of total RNA. The first strand cDNA was successfully synthesized (Figure 3.1B).

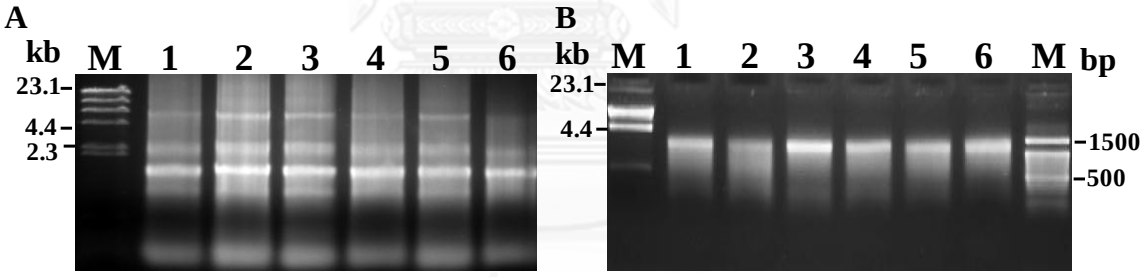

Figure 3. 1 Ethidium bromide-stained 1.0% agarose gel showing the quality of total RNA extracted from ovaries of intact wild broodstock of *P. monodon* (A) and the first stand cDNA synthesized from DNA-free total RNA of ovaries (B). Land M = λDNA-*Hind* III; Lanes 1-6 (A) and (B) = total RNA extracted from ovaries of different individuals of *P. monodon* broodstock and the corresponding first strand cDNA.

3.1.2 Isolation of the full-length cDNAs of *PmRpd3*, *PmCdc16*, *PmCdk5* and *PmCdk2*

In this thesis, several reproduction-related genes including *PmRpd3*, *PmCdc16*, *PmCdk5* and *PmCdk2* were studied. The original nucleotide sequences of these

transcripts were initially identified by EST analysis (http://.pmonodon.biotec.or.th/) of the ovaries cDNA libraries (Preechaphol, 2008; Preechaphol et al., 2007). RACE-PCR was further carried out for isolation of the full-length of these transcripts.

3.1.2.1 *PmRpd3*

Nucleotide sequence of *PmRpd3* fragment was initially obtained from EST analysis of the ovarian cDNA library of *P. monodon* (Figure 3.2A). The partial sequence of EST significantly matched *Histone deacetylase 1* of *Caligus rogercresseyi (E*-value = 5e-152) (Figure 3.2B). 3'RACE-PCR of this transcript was further carried out. The amplification products of 800 and 700 bp were obtained (Figure 3.3A and B). The RACE-PCR product were cloned and sequenced for both directions (Figure 3.3C).

A.

```
GTGTTTTAACTCCTCATTTTACCGCGAAAAATGTCGGCCGCACCGCACAACAGGAAGAAAGTCTGTTAT
TACTATGACAGTGACATTGGAAATTATTACTACGGCCAGGGCCATCCCATGAAGCCACACAGGATACGT
ATGACACACAACCTCCTCTTGAATTATGGGCTGTACCGCAAGATGGAGATATATAGGCCTCATAAAGCA
ACTCAAGATGAAATGACCAAGTTCCATAGTGATGACTACATCAGGTTTATAAGGTCCATTCGTCCAGAT
AACATGAATGAATACAATAAACAGATGCAAAAGTTTAATGTTGGAGAAGATTGCCCAGTCTTTGATGGC
CTGTATGAGTTTTGTCAGTTATCTTCTGGAGGCTCCATTGCTGGTGCTGTGAAGTTGAACAAACAAGCT
TGTGATATTGCTATTAACTGGGCTGGTGGACTTCATCATGCAAAAAAAAGTGAAGCTTCAGGTTTCTGC
TACGTGAATGACATTGTGTTAGCTATTTTGGAGCTCCTTAAGTATCACCAGCGAGTTCTGTACATTGAT
ATTGATATTCATCATGGAGATGGTGTTGAGGAGGCCTTCTACACCACAGACCGTGTAATGACTGTCTCC
                          3'RACE-Hdac Rpd3_1
TTCCACAAGTATGGAGAGTATTTCCCTGGGACTGGAGACCTAAGGGATATTGGTGCTGGGAAGGGTAAA
TATTATGCTGTTAACTTCCCATTAAGAGATGGCATAGAT
```

B.

```
Histone deacetylase 1 [Caligus rogercresseyi]
Sequence ID: gb|ACO11145.1|Length: 322
Score =437 bits, Expect =5e-152
Identities = 219/232(94%), Positives = 228/232(98%), Gaps = 0/232(0%)
Frame = +1


Query  34   SAAPHNRKKVCyyydsdignyyygQGHPMKPHRIRMTHNLLLNYGLYRKMEIYRPHKATQ  213
            S APH+RKK+CYYYDSDIGNYYYGQGHPMKPHRIRMTHNLLLNYGLYRKMEIYRPHKATQ
Sbjct  3    SVAPHSRKKICYYYDSDIGNYYYGQGHPMKPHRIRMTHNLLLNYGLYRKMEIYRPHKATQ  62

Query  214  DEMTKFHSDDYIRFIRSIRPDNMNEYNKQMQKFNVGEDCPVFDGLYEFCQLSSGGSIAGA  393
            +EMTKFHSDDYIRF+RSIRPDNM+EYNKQMQ+FNVGEDCPVFDGLYEFCQLS GGS+A A
Sbjct  63   EEMTKFHSDDYIRFLRSIRPDNMSEYNKQMQRFNVGEDCPVFDGLYEFCQLSGGGSVASA  122

Query  394  VKLNKQACDIAINWAGGLHHAKKSEASGFCYVNDIVLAILELLKYHQRVLYIDIDIHHGD  573
            VKLNKQA DIAINWAGGLHHAKKSEASGFCYVNDIVLAILELLKYHQRVLYIDIDIHHGD
Sbjct  123  VKLNKQAADIAINWAGGLHHAKKSEASGFCYVNDIVLAILELLKYHQRVLYIDIDIHHGD  182
```

```
Query  574  GVEEAFYTTDRVMTVSFHKYGEYFPGTGDLRDIGAGKGKYYAVNFPLRDGMD  729
            GVEEAFYTTDRVMTVSFHKYGEYFPGTGDLRDIGAGKGKYYAVNFP+RDG+D
Sbjct  183  GVEEAFYTTDRVMTVSFHKYGEYFPGTGDLRDIGAGKGKYYAVNFPMRDGID  234
```

Figure 3. 2 Nucleotide sequences of an original EST (A) and its BlastX analysis (B) of *PmRpd3*.

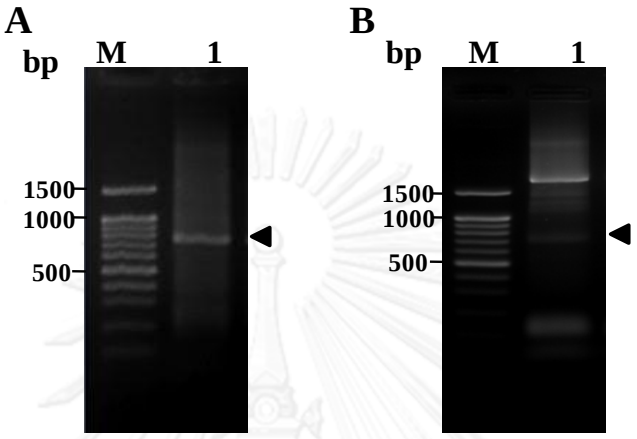

C.

CCTGGGACTGGAGACCTAAGGGATATTGGTGCTGGGAAGGGTAAATATTATGCTGTTAACTTCCCATTAAGAGATGG
CATAGATGATGAGAGCTATGACAGCATATTTGTGCCAATAATGACAAAGGTAATGGAAACCTACCAGCCCTCTGCAA
TTGTTCTTCAGTGTGGTGCTGACTCTCTCAGTGGAGACAGGCTTGGTTGTTTCAACCTCACCCTAAAAGGCCATGCA
AAGTGTGTTGAATTTGTCAAGAAGTACAACCTTCCCCTACTCTTACTTGGTGGAGGAGGATACACCATCCGTAATGT
AGCAAGATGTTGGACTTATGAAACGGCTGTTGCTTTAAATACGGAAATTGCAAATGAACTTCCCTACAATGATTACT
TTGAATACTTTGGACCAGACTTCAAGCTCCATATCAGCCCCTCTAACATGGCCAATCAGAATACACCAGAGTATTTA
GACAAGATCAAAACCAGACTGTTTGAAAACTTGAGGATGTTGCCCCATGCACCTGGTGTACAAAGTATAGCAATTCC
AGAAGATGGTGTAGCAGAAGAGAGTGAAGATGAAGACAAAGCCAGTCCAGATGAGAGAATTTCTATACGTGCTTCTG
ACAAA

3′RACE-Hdac Rpd3_2

CGCATTGCCCCAGATAATGAATATTCAGATTCCGAAGACGAGGGTGACGGGCGAAGAGATGAACGATCCTTCAAGCC
CAAAAAGAAAACAAAGACTGATGAGAGTGCAACCAATAATGGTGCAGGAGAGGACAAGAAGGACACCTCTATTACTT
CTGCAAAGGAGGAAAAGTCTGGTTCTCAGGTTGGACAGAATGAAACCAAAGTGGAATCTTGAGGCAGAGTTAAATTT
TAAGTTCCACTTTTTTCTATATTTTATTCTGTGAATTAGAAAACATAAGGTTAAAGTCAAAGAATACCCTGGAATAT
GCACAGAAATGCTCAGCTGAGATCATATGTAAAAGTAATCATTCCTCACCAAATACCTTTGGGTAGTTTTTTCAAAC
AATGCTTCATGTCACTTGTTGAAAAATCAAGTATACATGTACTGTGTAATTTGTATAAATATATATATGTGCATATA
TATATATATATCTATATATTTAAGGAACTAAACTTGGTCTGTATGGTTTGCAGTCATGCAATATTATATAAACAGTC
AGGACACCTCCTATTCACAATTTTGTTAGCACTGTTTGGAGAAATTGCTCGCAGGAGGGTCATGACCAGAATAGGTA
TATACTCTCATAATGTCAGTATTATCAAAATCTCATGATTCACCAAAAAAAAAAAAAAAAAAAAAA

Figure 3. 3 Results from 3'RACE-PCR of *PmRpd3* (A and B). The amplified fragments (lanes 1, A and B) were cloned and sequenced. Primers for RACE-PCR are underlined. Lane M is 100 bp DNA ladder.

Nucleotide sequences of the original EST and 3'RACE-PCR were assembled The full-length cDNA sequences of *PmRpd3* was 1949 bp in length with an ORF of 1452 bp, corresponding to a polypeptide of 483 amino acids with 5' and 3' UTR of 30 and 467 bp, respectively (Figure 3.4). This characterized sequence was significantly similar to *histone deacetylase Rpd3* of the water fleas (*Daphnia pulex*) (*E*-value = 0.0). The expected MW and pI of the deduced PmRpd3 protein were 54.66 kDa and 5.59, respectively. Two predicted positions of glycosylation sites were found at NLT (positions 275-277) and NET (positions 477-479), respectively.

```
GTGTTTTAACTCCTCATTTTACCGCGAAAAATGTCGGCCGCACCGCACAACAGGAAGAAA  60
                            M  S  A  A  P  H  N  R  K  K     10
GTCTGTTATTACTATGACAGTGACATTGGAAATTATTACTACGGCCAGGGCCATCCCATG  120
V  C  Y  Y  Y  D  S  D  I  G  N  Y  Y  Y  G  Q  G  H  P  M     30
AAGCCACACAGGATACGTATGACACACAACCTCCTCTTGAATTATGGGCTGTACCGCAAG  180
K  P  H  R  I  R  M  T  H  N  L  L  L  N  Y  G  L  Y  R  K     50
ATGGAGATATATAGGCCTCATAAAGCAACTCAAGATGAAATGACCAAGTTCCATAGTGAT  240
M  E  I  Y  R  P  H  K  A  T  Q  D  E  M  T  K  F  H  S  D     70
GACTACATCAGGTTTATAAGGTCCATTCGTCCAGATAACATGAATGAATACAATAAACAG  200
D  Y  I  R  F  I  R  S  I  R  P  D  N  M  N  E  Y  N  K  Q     90
ATGCAAAAGTTTAATGTTGGAGAAGATTGCCCAGTCTTTGATGGCCTGTATGAGTTTTGT  360
M  Q  K  F  N  V  G  E  D  C  P  V  F  D  G  L  Y  E  F  C    110
CAGTTATCTTCTGGAGGCTCCATTGCTGGTGCTGTGAAGTTGAACAAACAAGCTTGTGAT  420
Q  L  S  S  G  G  S  I  A  G  A  V  K  L  N  K  Q  A  C  D    130
ATTGCTATTAACTGGGCTGGTGGACTTCATCATGCAAAAAAAAGTGAAGCTTCAGGTTTC  480
I  A  I  N  W  A  G  G  L  H  H  A  K  K  S  E  A  S  G  F    150
TGCTACGTGAATGACATTGTGTTAGCTATTTTGGAGCTCCTTAAGTATCACCAGCGAGTT  540
C  Y  V  N  D  I  V  L  A  I  L  E  L  L  K  Y  H  Q  R  V    170
CTGTACATTGATATTGATATTCATCATGGAGATGGTGTTGAGGAGGCCTTCTACACCACA  600
L  Y  I  D  I  D  I  H  H  G  D  G  V  E  E  A  F  Y  T  T    190
GACCGTGTAATGACTGTCTCCTTCCACAAGTATGGAGAGTATTTCCCTGGGACTGGAGAC  660
D  R  V  M  T  V  S  F  H  K  Y  G  E  Y  F  P  G  T  G  D    210
CTAAGGGATATTGGTGCTGGGAAGGGTAAATATTATGCTGTTAACTTCCCATTAAGAGAT  720
L  R  D  I  G  A  G  K  G  K  Y  Y  A  V  N  F  P  L  R  D    230
GGCATAGATGATGAGAGCTATGACAGCATATTTGTGCCAATAATGACAAAGGTAATGGAA  780
G  I  D  D  E  S  Y  D  S  I  F  V  P  I  M  T  K  V  M  E    250
ACCTACCAGCCCTCTGCAATTGTTCTTCAGTGTGGTGCTGACTCTCTCAGTGGAGACAGG  840
T  Y  Q  P  S  A  I  V  L  Q  C  G  A  D  S  L  S  G  D  R    270
CTTGGTTGTTTCAACCTCACCCTAAAAGGCCATGCAAAGTGTGTTGAATTTGTCAAGAAG  900
L  G  C  F  N  L  T  L  K  G  H  A  K  C  V  E  F  V  K  K    290
TACAACCTTCCCCTACTCTTACTTGGTGGAGGAGGATACACCATCCGTAATGTAGCAAGA  960
Y  N  L  P  L  L  L  L  G  G  G  G  Y  T  I  R  N  V  A  R    310
TGTTGGACTTATGAAACGGCTGTTGCTTTAAATACGGAAATTGCAAATGAACTTCCCTAC  1020
C  W  T  Y  E  T  A  V  A  L  N  T  E  I  A  N  E  L  P  Y    330
```

```
AATGATTACTTTGAATACTTTGGACCAGACTTCAAGCTCCATATCAGCCCCTCTAACATG  1080
N  D  Y  F  E  Y  F  G  P  D  F  K  L  H  I  S  P  S  N  M    350
GCCAATCAGAATACACCAGAGTATTTAGACAAGATCAAAACCAGACTGTTTGAAAACTTG  1140
A  N  Q  N  T  P  E  Y  L  D  K  I  K  T  R  L  F  E  N  L    370
AGGATGTTGCCCCATGCACCTGGTGTACAAAGTATAGCAATTCCAGAAGATGGTGTAGCA  1200
R  M  L  P  H  A  P  G  V  Q  S  I  A  I  P  E  D  G  V  A    390
GAAGAGAGTGAAGATGAAGACAAAGCCAGTCCAGATGAGAGAATTTCTATACGTGCTTCT  1260
E  E  S  E  D  E  D  K  A  S  P  D  E  R  I  S  I  R  A  S    410
GACAAACGCATTGCCCCAGATAATGAATATTCAGATTCCGAAGACGAGGGTGACGGGCGA  1320
D  K  R  I  A  P  D  N  E  Y  S  D  S  E  D  E  G  D  G  R    430
AGAGATGAACGATCCTTCAAGCCCAAAAAGAAAACAAAGACTGATGAGAGTGCAACCAAT  1380
R  D  E  R  S  F  K  P  K  K  K  T  K  T  D  E  S  A  T  N    450
AATGGTGCAGGAGAGGACAAGAAGGACACCTCTATTACTTCTGCAAAGGAGGAAAAGTCT  1440
N  G  A  G  E  D  K  K  D  T  S  I  T  S  A  K  E  E  K  S    470
GGTTCTCAGGTTGGACAGAATGAAACCAAAGTGGAATCTTGAGGCAGAGTTAAATTTTAA  1500
G  S  Q  V  G  Q  N  E  T  K  V  E  S  *                      483
GTTCCACTTTTTTCTATATTTTATTCTGTGAATTAGAAAACATAAGGTTAAAGTCAAAGA  1560
ATACCCTGGAATATGCACAGAAATGCTCAGCTGAGATCATATGTAAAAGTAATCATTCCT  1620
CACCAAATACCTTTGGGTAGTTTTTTCAAACAATGCTTCATGTCACTTGTTGAAAAATCA  1680
AGTATACATGTACTGTGTAATTTGTATAAATATATATATGTGCATATATATATATATATC  1740
TATATATTTAAGGAACTAAACTTGGTCTGTATGGTTTGCAGTCATGCAATATTATATAAA  1800
CAGTCAGGACACCTCCTATTCACAATTTTGTTAGCACTGTTTGGAGAAATTGCTCGCAGG  1860
AGGGTCATGACCAGAATAGGTATATACTCTCATAATGTCAGTATTATCAAAATCTCATGA  1920
TTCACCAAAAAAAAAAAAAAAAAAAAAAA                                 1949
```

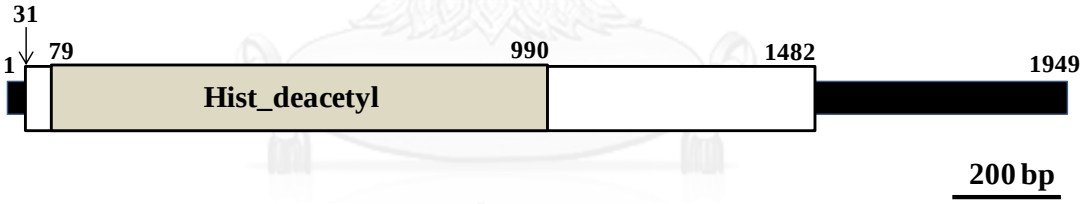

Domain	Position	*E*-value
Hist_deacetyl	79-990	6.50e-87

Figure 3. 4 (A) The full-length cDNA sequences of *PmRpd3*. Start and stop codons are illustrated in boldface and underlined. A Hist_deacetyl domain (positions 17 - 320, *E*-value = 6.50e-87) is highlighted. (B) A schematic diagram showing the full-length cDNA of *PmRpd3* (an ORF of 1452 bp corresponding to a polypeptide of 483 amino acids).

3.1.2.2 *PmCdc16*

The partial cDNA sequence of *PmCdc16* was initially obtained from EST analysis of the ovarian cDNA library of *P. monodon* (Figure 3.5A). It significantly matched *cell division cycle 16* of *Crassostrea gigas (E*-value = 2.0e-52) (Figure 3.5B). The 3'RACE-PCR of *PmCdc16* was further carried out. The amplification product of 1700 bp was obtained (Figure 3.6A). The RACE-PCR product were cloned and sequenced for both directions (Figure 3.6C).

A

```
AACAATATGGCAGAAGATTTTGAATGTATGCCTACTTCTCCCTCAGAATCCATCGATTTGGAGAAGTTT
CGAAAACTCGTTCGAAGTTATATAGAAAGGCACCACTACAAGGCGGCAGTGTTCTGGGCAGACAAAGTA
GTTAGCCTGAGCAATGGATCTCCTGCAGATGTGTACTGGTTAGCACAAAGTTACTACCTCACCAAGCAG
TATCATCGAGCTATTTTGCTAATCAACAGCCACAAACTCACAAGGAATGCTACCTGTCGATACCTGGTG
GCACTGTGCTACTATGAAGTGGGGGAGTATCACTCTGCGTTTGACATCTTGGAGCGCAGTGAGAACAAC
AATGTGTCTCGTATCAAGGCTGAGGGGGAAGCTATTGCTGTTCCAGAGATCGACGACACAATGTCGATT
GAGTGCTCTACACATTTATTGAAAGGCTACATATATGAAGCTAGTGACAATCGAGCATTAGCTGTGGAG
                              3'RACE-Cdc16
AGCTTCCGAGCAGCAGTACAGGCTGACCCACTCTGTTATGAGGCAATACATGCACTAACGCAGCATCAC
ATGCTAACTGTGAAGGAAGAGAAAGACCTGCTGTCATCCTTGCCCCTCTCTCGAACATGCAGCGAAGCA
GAAAGTGCTGTGGTCATGGCAGTATATGAAACGAGAACTAATAAATACAGTTCACCCAGTACACCATTG
CCACAACCTGCTGCTCCACTGGCAACAAACGCTGACTTC
```

B

```
Cell division cycle protein 16-like protein [Crassostrea gigas]
Sequence ID:  gb|EKC23825.1||Length: 594
Score =189 bits, Expect =2e-52
Identities = 93/208(45%), Positives = 135/208(0%), Gaps = 1/208(0%)
Frame = +1

Query  49   SIDLEKFRKLVRSYIERHHYKAAVFWADKVVSLSNGSPADVYWLAQSYYLTKQYHRAILL  228
            I+L + R+ V+ YIE+H Y++A+FWADK+VSLSNG+P DVYW AQ+ YLT QYHRA  L
Sbjct  19   GINLGRLREKVKFYIEKHQYESALFWADKIVSLSNGNPDDVYWYAQTLYLTGQYHRASQL  78

Query  229  INSHKLTR-NATCRYLVALCYYEVGEYHSAFDILERSENNNVSRIKAEGEAIAVPEIDDT  405
            + S KL + N++CRYL A C++E  E+ +A +IL+  +NN+     ++
Sbjct  79   LKSKKLDKTNSSCRYLAAKCHFECKEWQTALNILDMVDNNSYLHSFSKHNLTESLFDQSN  138

Query  406  MSIECSTHLLKGYIYEASDNRALAVESFRAAVQADPLCYEAIHALTQHHMLTVKEEKDLL  585
              +E S +LL+G IYEA DNR LAV+ FR A++ D  C+EA   L  HHML+ +EE++LL
Sbjct  139  KEVEHSINLLRGRIYEAMDNRNLAVDCFREALRQDVYCFEAFDMLVHHHMLSAQEERELL  198

Query  586  SSLPLSRTCSEAESAVVMAVYETRTNKY  669
             +LP +  C   +  ++  +YE R  KY
Sbjct  199  DTLPFAIQCPIEDVELIRYLYENRVKKY  226
```

Figure 3. 5 Nucleotide sequences of an original EST (A) and its BlastX analysis (B) of *PmCdc16*.

A.

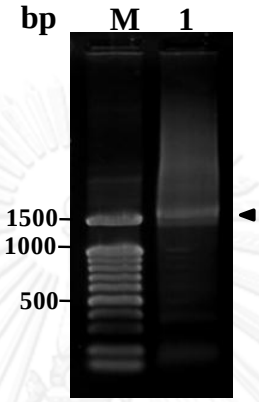

B

CTGACCCACTCTGTTATGAGGCAATACATGCACTAACGCAGCATCACATGCTAACTGTGAAGGAAGAGAAAGACCTG
CTGTCATCCTTGCCCCTCTCTCGAACATGCAGCGAAGCAGAAAGTGCTGTGGTCATGGCAGTATATGAAACGAGAAC
TAATAAATACAGTTCACCCAGTACACCATTGCCACAACCTGCTGCTCCACTGGCAACAAACGCTGACTTCATCACAG
CGCAGGCTGAGAAGCTCTACTACAACTGCAACTTTGCACAGTGTCATCGATTAACACAAGAAGTACTGAAAAAAGAC
CCCTATCATACAGAGTGTCTGCCTATTCATGTTTCCTGCCTAGTGGAGCTAAAACAGTCAAACAGTCTGTTTCTTCT
GGCTCACAAACTTGTTGACCTTTACCCAGAGAGTGCTTTGTCCTGGTTTGCTGTTGGATGTTATTATTATTTGATAG
GTAAGAATGAACAAGCAAGAAGATACCTGAGCAAAGCCACTGCCCTGGACAGAGTTTTTGGCCCAGCCTGGATTGCC
TATGGCCATTCTTTTGCTGCAGAGAATGAGCATGACCAGGCCATGGCAGCATACTTCAAGGCTGCCCAGCCCATGAA
GGGATGCCACCTGCCCCTGCTCTACATTGGTATGGAGTATGGACTCACGAATAACCCGAGGTTTGCTGAGAAGTTCT
TCAAGGAGGCACTGGACATCGCACCTGAGGATCCATTTGTTTTGCATGAATTGGGGGTTGTGTCCTTTTGTAATCAG
GATTACATCTCTGCAGAGTTATACCTCAGAAGAGCTGTGTCATTAGTGGAAGAGAGTGGGGTCGTAGTGGTTCCTGA
GAAGTGAGCAACGCTCTTAAACAAACCTCGCACATACCTGTAGGAAACTTCACAAATAGAAGAGGCATTGCATTTTC
ATCAACAGGCTTTGAAATTATGTCCTGGAGTATCCTCTACGTACTCAGCACTGGGTTTGGTGCAGTCTTTGCTTGGT
GATTATGAGGCAGCAGTTGTGTCACTCCACAAGGCACTCTCTCTGCACCGTGATGACACCACAGCCACCACTCTTCT
CACCACTGTTATGGATCAGCTGATGACACAGACCCCAGCATTCCAAGGAGATGACAACATACCACAGTTAGATCCTC
CCTCTGATATTGTGGGGACTGACACCAACGCAAGTGACATAACCAGTGACATTACTCCAGCCTCAGCAGATGATCCT
CTTAGCGACTCGAAACTACTGGGATCTAGCATAGGTCAGCCCGTGATGCATTCTTCAGATGTTGGGAGAGATTCTCT
AAGCCAGTCCTTAGGTCAGTCAACTGCACTTCTCATTGAGGATATGGTAATGGATGATCAGAGTCCATAAAGAAAAA
AGAAAAAAAAAAATAGAAAAAAAAAATCTAATAGACGTTATTGGTGTTATTTTTTAAGTACTCGTATCTGCAACTAATA
TATTGACAATACATAATGAGTAAGATATATATGTTTCATGAGTTTGAAAATAAAGTGACACTTTAGCTTAAAAAAAA
AAAAAAAAAAAAAAAAAAAAAA

Figure 3. 6 Results from 3'RACE-PCR of *PmCdc16* (A). The amplified fragments (lanes 1, A) were cloned and sequenced (B). Primers for RACE-PCR and internal sequencing are underlined. Lane M is a 100 bp DNA ladder.

The full-length cDNA of *PmCdc16* was 2068 bp in length with an ORF of 1332 bp corresponding to the polypeptides of 443 amino acids with 5' and 3' UTRs of 27 and 709 bp, respectively (Figure 3.7). This characterized sequence was similar to *Cell division cycle 16* of the leaf-cutting ant (*Acromyrmex echinatior*) (*E*-value = 3.0e-175). The expected MW and p*I* of this deduced protein was 50.11 kDa and 5.87, respectively. The poly A additional signal (AATAAA) is boldfaced, italicized and underlined. The predicted signal peptide was not found in the PmCdc16 protein. Three potential positions of glycosylation sites were found at positions 42-44 (NGS), 76-78 (NAT) and 107-109 (NVS).

A

```
AACAATATGGCAGAAGATTTTGAATGTATGCCTACTTCTCCCTCAGAATCCATCGATTTG  60
                          M  P  T  S  P  S  E  S  I  D  L    11
GAGAAGTTTCGAAAACTCGTTCGAAGTTATATAGAAAGGCACCACTACAAGGCGGCAGTG  120
E  K  F  R  K  L  V  R  S  Y  I  E  R  H  H  Y  K  A  A  V    31
TTCTGGGCAGACAAAGTAGTTAGCCTGAGCAATGGATCTCCTGCAGATGTGTACTGGTTA  180
F  W  A  D  K  V  V  S  L  S  N  G  S  P  A  D  V  Y  W  L    51
GCACAAAGTTACTACCTCACCAAGCAGTATCATCGAGCTATTTTGCTAATCAACAGCCAC  240
A  Q  S  Y  Y  L  T  K  Q  Y  H  R  A  I  L  L  I  N  S  H    71
AAACTCACAAGGAATGCTACCTGTCGATACCTGGTGGCACTGTGCTACTATGAAGTGGGG  300
K  L  T  R  N  A  T  C  R  Y  L  V  A  L  C  Y  Y  E  V  G    91
GAGTATCACTCTGCGTTTGACATCTTGGAGCGCAGTGAGAACAACAATGTGTCTCGTATC  360
E  Y  H  S  A  F  D  I  L  E  R  S  E  N  N  N  V  S  R  I   111
AAGGCTGAGGGGGAAGCTATTGCTGTTCCAGAGATCGACGACACAATGTCGATTGAGTGC  420
K  A  E  G  E  A  I  A  V  P  E  I  D  D  T  M  S  I  E  C   131
TCTACACATTTATTGAAAGGCTACATATATGAAGCTAGTGACAATCGAGCATTAGCTGTG  480
S  T  H  L  L  K  G  Y  I  Y  E  A  S  D  N  R  A  L  A  V   151
GAGAGCTTCCGAGCAGCAGTACAGGCTGACCCACTCTGTTATGAGGCAATACATGCACTA  540
E  S  F  R  A  A  V  Q  A  D  P  L  C  Y  E  A  I  H  A  L   171
ACGCAGCATCACATGCTAACTGTGAAGGAAGAGAAAGACCTGCTGTCATCCTTGCCCCTC  600
T  Q  H  H  M  L  T  V  K  E  E  K  D  L  L  S  S  L  P  L   191
TCTCGAACATGCAGCGAAGCAGAAAGTGCTGTGGTCATGGCAGTATATGAAACGAGAACT  660
S  R  T  C  S  E  A  E  S  A  V  V  M  A  V  Y  E  T  R  T   211
AATAAATACAGTTCACCCAGTACACCATTGCCACAACCTGCTGCTCCACTGGCAACAAAC  720
N  K  Y  S  S  P  S  T  P  L  P  Q  P  A  A  P  L  A  T  N   231
GCTGACTTCATCACAGCGCAGGCTGAGAAGCTCTACTACAACTGCAACTTTGCACAGTGT  780
A  D  F  I  T  A  Q  A  E  K  L  Y  Y  N  C  N  F  A  Q  C   251
CATCGATTAACACAAGAAGTACTGAAAAAAGACCCCTATCATACAGAGTGTCTGCCTATT  840
H  R  L  T  Q  E  V  L  K  K  D  P  Y  H  T  E  C  L  P  I   271
CATGTTTCCTGCCTAGTGGAGCTAAAACAGTCAAACAGTCTGTTTCTTCTGGCTCACAAA  900
H  V  S  C  L  V  E  L  K  Q  S  N  S  L  F  L  L  A  H  K   291
CTTGTTGACCTTTACCCAGAGAGTGCTTTGTCCTGGTTTGCTGTTGGATGTTATTATTAT  960
L  V  D  L  Y  P  E  S  A  L  S  W  F  A  V  G  C  Y  Y  Y   311
TTGATAGGTAAGAATGAACAAGCAAGAAGATACCTGAGCAAAGCCACTGCCCTGGACAGA  1020
L  I  G  K  N  E  Q  A  R  R  Y  L  S  K  A  T  A  L  D  R   331
GTTTTTGGCCCAGCCTGGATTGCCTATGGCCATTCTTTTGCTGCAGAGAATGAGCATGAC  1080
V  F  G  P  A  W  I  A  Y  G  H  S  F  A  A  E  N  E  H  D   351
```

```
CAGGCCATGGCAGCATACTTCAAGGCTGCCCAGCCCATGAAGGGATGCCACCTGCCCCTG  1140
Q  A  M  A  A  Y  F  K  A  A  Q  P  M  K  G  C  H  L  P  L     371
CTCTACATTGGTATGGAGTATGGACTCACGAATAACCCGAGGTTTGCTGAGAAGTTCTTC  1200
L  Y  I  G  M  E  Y  G  L  T  N  N  P  R  F  A  E  K  F  F     391
AAGGAGGCACTGGACATCGCACCTGAGGATCCATTTGTTTTGCATGAATTGGGGGTTGTG  1260
K  E  A  L  D  I  A  P  E  D  P  F  V  L  H  E  L  G  V  V     411
TCCTTTTGTAATCAGGATTACATCTCTGCAGAGTTATACCTCAGAAGAGCTGTGTCATTA  1320
S  F  C  N  Q  D  Y  I  S  A  E  L  Y  L  R  R  A  V  S  L     431
GTGGAAGAGAGTGGGGTCGTAGTGGTTCCTGAGAAGTGAGCAACGCTCTTAAACAAACCT  1380
V  E  E  S  G  V  V  V  V  P  E  K  *                          443
CGCACATACCTGTAGGAAACTTCACAAATAGAAGAGGCATTGCATTTTCATCAACAGGCT  1440
TTGAAATTATGTCCTGGAGTATCCTCTACGTACTCAGCACTGGGTTTGGTGCAGTCTTTG  1500
CTTGGTGATTATGAGGCAGCAGTTGTGTCACTCCACAAGGCACTCTCTCTGCACCGTGAT  1560
GACACCACAGCCACCACTCTTCTCACCACTGTTATGGATCAGCTGATGACACAGACCCCA  1620
GCATTCCAAGGAGATGACAACATACCACAGTTAGATCCTCCCTCTGATATTGTGGGGACT  1680
GACACCAACGCAAGTGACATAACCAGTGACATTACTCCAGCCTCAGCAGATGATCCTCTT  1740
AGCGACTCGAAACTACTGGGATCTAGCATAGGTCAGCCCGTGATGCATTCTTCAGATGTT  1800
GGGAGAGATTCTCTAAGCCAGTCCTTAGGTCAGTCAACTGCACTTCTCATTGAGGATATG  1860
GTAATGGATGATCAGAGTCCATAAAGAAAAAAGAAAAAAAAAATAGAAAAAAAAATCTAA  1920
TAGACGTTATTGGTGTTATTTTTTAAGTACTCGTATCTGCAACTAATATATTGACAATAC  1980
ATAATGAGTAAGATATATATGTTTCATGAGTTTGAAAATAAAGTGACACTTTAGCTTAAA  2040
AAAAAAAAAAAAAAAAAAAAAAAAAAAA                                   2068
```

B

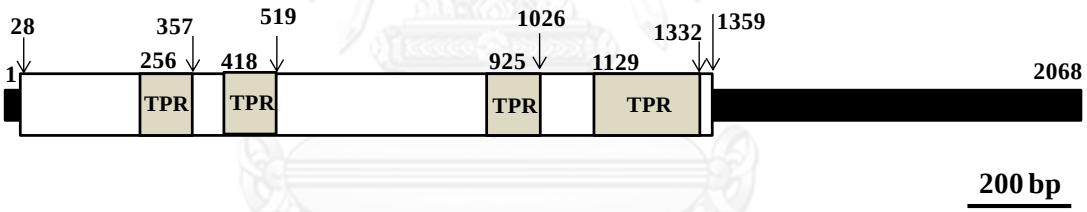

Domain	Position	*E*-value
TPR	256-357	9.99e-01
TPR	418-519	4.03-00
TPR	925-1026	8.17e-01
TPR	1129-1230	1.24e-00
TPR	1231-1332	28.4e-01

Figure 3. 7 The full-length cDNA sequences of *PmCdc16* (an ORF of 1332 bp corresponding to a polypeptides of 443 amino acids). Start and stop codons are illustrated in boldface and underlined. A tetratricopeptide repeat region (TPR) domain (positions 77-110, 131-164, 300-333, 368-401 and 402-435, *E*-value = 9.99e-

01, 4.03e-00, 8.17e-01, 1.24e-00 and 2.84e-01, respectively) are highlighted. The poly A additional signal (AATAAA) is boldfaced, italicized and underlined. (B) A schematic diagram showing the full-length cDNA of *PmCdc16*.

3.1.2.3 *PmCdk5*

The partial sequence of *PmCdk5* CDNA was initially obtained from EST analysis of the ovarian cDNA library of *P. monodon* (Figure 3.8A). This EST was significantly matched *Cyclin-dependent kinase 5* of giant honey bee *Apis dorsata (E-*value = 4.0e-85; Figure 3.8B). 3'RACE-PCR of *PmCdk5* were further carried out and the amplification fragment of 1600 bp was obtained (Figure 3.9A). The RACE-PCR product was cloned and sequenced for both directions (Figure 3.9B).

A

```
AGCAGGGAGGTCAAAAGAGACTGGTCGACAAAGACGCGCATCATAAGAGAGAAGATCAACAATGCCATC
                                3'RACE-Cdk5
CAGGATATGCCTGAACATCCAGAGATCACAAAACTGCTCTCAGGAACATACATAAACTATTTTCACTGCCTGAAAAT
CGTTGAGATCTTGAAGGAGACAGAAAAGGATACCAAGAATATTTTAGGATGGTATGGTTCCCAGCGGATGAAGGATT
GGCAGGAAATTACCCGGTTATATGAGAAGGATAGTGTCTATCTGGCAGAGGCAGCTCACCTTCTGATGCGCAATGTC
AAGTATGACATCCCAGACCTCAAGCAGCAGATATCCAAGGGGACTCACATACAGGAGGAATGTGATCGTAAGGAAGT
GGAATACGTCAAATCAGCTGAGGAGGCCAGGAAAAGATATTCTCAGATGTGTAAACAGATTGGCATTCCTGGAGAGA
AGATAAAGCAAGAAATATTAGCACTGTTAAAGGAGCTTCCAGGGGAGTTTGCCGAAATAGCCGAGAAAGCTAAAACC
CTTCAAGGTGCACGTCAGCTTTACATGGATTTCTTATCTTTTACCCTAGAAGAAGACTGCAACTGCCTTCCGATGTT
GAAGTATATAATGGAACATGGGAATGTGACAACATATGAATGGACGTATGGTGAGCCGCCCTGCCAGATTGAGGAGC
CGCAGATCGAGATAGATCTGGATGATGATCAGAAAGAAGATGC
```

B

```
CDK5 regulatory subunit-associated protein 3-like [Apis dorsata]
Sequence ID:  ref|XP_006612952.1|Length: 513
Score =273 bits, Expect =4e-85
Identities = 138/243(57%), Positives = 177/243(72%), Gaps = 2/243(0%)
Frame = +1


Query  4    REVKRDWSTKTRIIREKINNAIQDMPEHPEITKLLSGTYINYFHCLKIVEILKETEKDTK  183
            R   +DW      IREKINNAIQDMP H  I KLLSG+YINYFHCLKI+EILKETE DTK
Sbjct  23   RHCTKDWHVMVLPIREKINNAIQDMPIHEGIAKLLSGSYINYFHCLKIIEILKETEADTK  82

Query  184  NILGWYGSQRMKDWQEITRLYEKDSVYLAEAAHLLMRNVKYDIPDLKQQISKGTHIQEEC  363
            N+ G YGSQRMKDWQEI RLYEKD++YLAE A +L+RNV Y+IP  K+QI K   IQ E
Sbjct  83   NVFGRYGSQRMKDWQEILRLYEKDNIYLAEVAQILIRNVNYEIPSTKKQIQKLEQIQVEL  142

Query  364  DRKEVEYVKSAEEARKRYSQMCKQIGIPGEKIKQEILALLKELPGEFAEIAEKAKTLQGA  543
            ++KE +Y KS   AR  ++ +CKQ+GIPGE+IKQE+   +KELP  + +IA+K K+L+
Sbjct  143  EKKEADYKKSENIARSEFNLLCKQLGIPGEQIKQELTEKVKELPEIYEKIAKKIKSLEKV  202
```

```
Query  544  RQLYMDFLSFTL--EEDCNCLPMLKYIMEHGNVTTYEWTYGeppcqieepqieiDLDDDQ  717
             + Y  F+++TL  + D  C+PM+KYI++ GN TTYEW YGE P  + EP + I L++D
Sbjct  203  VEFYCAFVNYTLGRQHDGGCVPMVKYIIDKGNTTTYEWIYGEAPLSVSEPSLNISLNNDD  262

Query  718  KED  726
              E+
Sbjct  263  LEN  265
```

Figure 3. 8 Nucleotide sequence of an original EST (A) and its BlastX analysis (B) of *PmCdk5* (B).

A

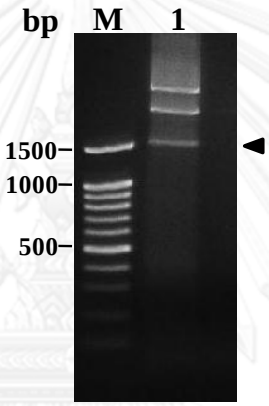

B

AAACTGCTCTCAGGAACATACATAAACTATTTTCACTGCCTGAAAATCGTTGAGATCTTGAAGGAGACA
GAAAAGGATACCAAGAATATTTTAGGATGGTATGGTTCCCAGCGGATGAAGGATTGGCAGGAAATTACC
CGGTTATATGAGAAGGATAGTGTCTATCTGGCAGAGGCAGCTCACCTTCTGATGCGCAATGTCAAGTAT
GACATCCCAGACCTCAAGCAGCAGATATCCAAGGGGACTCACATACAGGAGGAATGTGATCGTAAGGAA
GTGGAATACGTCAAATCAGCTGAGGAGGCCAGGAAAAGATATTCTCAGATGTGTAAACAGATTGGCATT
CCTGGAGAGAAGATAAAGCAAGAAATATTAGCACTGTTAAAGGAGCTTCCAGGGGAGTTTGCCGAAATA
GCCGAGAAAGCTAAAACCCTTCAAGGTGCACGTCAGCTTTACATGGATTTCTTATCTTTTACCCTAGAA
GAAGACTGCAACTGCCTTCCGATGTTGAAGTATATAATGGAACATGGGAATGTGACAACATATGAATGG
ACGTATGGTGAGCCGCCCTGCCAGATTGAGGAGCCGCAGATCGAGATAGATCTGGATGATGATCAGAAA
GAAGATGCTGGTGAAATTGATTTTGGTGATGTTGGGGGCACCATTGACTTCAGTACTGCAGATATTGAG
TTAGCAGAAGACCTGACCACAGGAGATATTGACTGGGGAAATCTTGGTAATGAGGAATCTCAGACAATT
GACTGGGGTGTAGATGTGAATGATGTTGCTACAGTGGATATTGTGGTTGAAGACTCAGGTGTGTCTGGA
GGTGTTGCTAAAGGGACCGAGGCTCTTACATTACTGTACAACCCCAAGACTCGTGCACAACTGATTGAT
GAGTTGTATGAACTGGAAGGATTCTTGAAACAGCGTCTGATAGAACTGGAAAGTGAGGAGTCAAGCTTC
TCAATCAACCAGTTCTCTAGTGCTCCCATCTCCGTGCAAGACCAATCCAAAGAGCAGTTGGAGGTTATG
GTCAGCCACATCCGGAATGTGGTCGACCCTCTTGGCACAAACAAGATGCAGCACCTCTTCCTCATTTAC
TCTTCTCCAAAGTATGTTGATAGGCTTGCTGCGTCACTCAGGTCAAAACTAACAGTTGCTGATAAATTT
GTAATTTCTCAAGAGGGAGTTCGCCAACGTAGGCTGGAAGCTCAACAAGAGCAGCAGAGAGTCCATCCA

AAGTTGGCATTGATGATTGAGAGATCAAAGGAGCTGAAAGTCAATATTGAAGAACACATCTCCAAGCGTTATAAAAA
CAGACCTGTCAATCTGATGGCCCTTGGCCTATCTATGACATAAATTGGGCCTTTCTGACTAGTAGATTAGTATATAT
ACACTTTTTCTGTTTTCCAGTGGGATATATTGTTGTTAGAATTTTTTTTATTATGGTTTAAATAAAGAATATAAGGT
ATAAAAAAAAAAAAAAAAAAAAAAAAAAAAA

Figure 3. 9 Results from 3'RACE-PCR of *PmCdk5* (A). The amplified fragments (lanes 1, A) was cloned and sequenced (B). Primers for RACE-PCR are underlined. Lane M is 100 bp DNA ladder.

The full-length cDNA sequences of *PmCdk5* was 1758 bp in length with an ORF of 1524 bp, corresponding to 507 amino acids and with 5' and 3' UTR of 90 and 144 bp, respectively (Figure 3.10). This characterized sequence was significantly similar to *Cyclin-dependent kinase 5* of the buff-tailed bumblebee (*Bombus terrestris*) (*E*-value = 1.0e-141). The expected MW and p*I* of this deduced protein was 58.25 kDa and 4.90, respectively. The poly A additional signal (AATAAA) is boldfaced, italicized and underlined. The predicted signal peptide was not found in the PmCdk5 protein. The predicted glycosylation sites were found at position 232-234 (NVT) of the deduced PmCdk5.

```
AGCAGTGGTATCAACGCAGAGTAGTCAAAGCGGCGTAAAGAAACCCGAGCAGCTGGGGAG   60
GCGAATTTCTACGACAGATTTTTTGACATAATGGATGAGCAAGACATACCCATTGACATT  120
                            M  D  E  Q  D  I  P  I  D  I     10
CATGGACACAAGCTCCTCGACTGGCTTGTGTCTCGCAGGGAGGTCAAAAGAGACTGGTCG  180
H  G  H  K  L  L  D  W  L  V  S  R  R  E  V  K  R  D  W  S     30
ACAAAGACGCGCATCATAAGAGAGAAGATCAACAATGCCATCCAGGATATGCCTGAACAT  240
T  K  T  R  I  I  R  E  K  I  N  N  A  I  Q  D  M  P  E  H     50
CCAGAGATCACAAAACTGCTCTCAGGAACATACATAAACTATTTTCACTGCCTGAAAATC  300
P  E  I  T  K  L  L  S  G  T  Y  I  N  Y  F  H  C  L  K  I     70
GTTGAGATCTTGAAGGAGACAGAAAAGGATACCAAGAATATTTTAGGATGGTATGGTTCC  360
V  E  I  L  K  E  T  E  K  D  T  K  N  I  L  G  W  Y  G  S     90
CAGCGGATGAAGGATTGGCAGGAAATTACCCGGTTATATGAGAAGGATAGTGTCTATCTG  420
Q  R  M  K  D  W  Q  E  I  T  R  L  Y  E  K  D  S  V  Y  L    110
GCAGAGGCAGCTCACCTTCTGATGCGCAATGTCAAGTATGACATCCCAGACCTCAAGCAG  480
A  E  A  A  H  L  L  M  R  N  V  K  Y  D  I  P  D  L  K  Q    130
CAGATATCCAAGGGGACTCACATACAGGAGGAATGTGATCGTAAGGAAGTGGAATACGTC  540
Q  I  S  K  G  T  H  I  Q  E  E  C  D  R  K  E  V  E  Y  V    150
AAATCAGCTGAGGAGGCCAGGAAAAGATATTCTCAGATGTGTAAACAGATTGGCATTCCT  600
K  S  A  E  E  A  R  K  R  Y  S  Q  M  C  K  Q  I  G  I  P    170
GGAGAGAAGATAAAGCAAGAAATATTAGCACTGTTAAAGGAGCTTCCAGGGGAGTTTGCC  660
G  E  K  I  K  Q  E  I  L  A  L  L  K  E  L  P  G  E  F  A    190
```

```
GAAATAGCCGAGAAAGCTAAAACCCTTCAAGGTGCACGTCAGCTTTACATGGATTTCTTA  720
E  I  A  E  K  A  K  T  L  Q  G  A  R  Q  L  Y  M  D  F  L     210
TCTTTTACCCTAGAAGAAGACTGCAACTGCCTTCCGATGTTGAAGTATATAATGGAACAT  780
S  F  T  L  E  E  D  C  N  C  L  P  M  L  K  Y  I  M  E  H     230
GGGAATGTGACAACATATGAATGGACGTATGGTGAGCCGCCCTGCCAGATTGAGGAGCCG  840
G  N  V  T  T  Y  E  W  T  Y  G  E  P  P  C  Q  I  E  E  P     250
CAGATCGAGATAGATCTGGATGATGATCAGAAAGAAGATGCTGGTGAAATTGATTTTGGT  900
Q  I  E  I  D  L  D  D  D  Q  K  E  D  A  G  E  I  D  F  G     270
GATGTTGGGGGCACCATTGACTTCAGTACTGCAGATATTGAGTTAGCAGAAGACCTGACC  960
D  V  G  G  T  I  D  F  S  T  A  D  I  E  L  A  E  D  L  T     290
ACAGGAGATATTGACTGGGGAAATCTTGGTAATGAGGAATCTCAGACAATTGACTGGGGT  1020
T  G  D  I  D  W  G  N  L  G  N  E  E  S  Q  T  I  D  W  G     310
GTAGATGTGAATGATGTTGCTACAGTGGATATTGTGGTTGAAGACTCAGGTGTGTCTGGA  1080
V  D  V  N  D  V  A  T  V  D  I  V  V  E  D  S  G  V  S  G     330
GGTGTTGCTAAAGGGACCGAGGCTCTTACATTACTGTACAACCCCAAGACTCGTGCACAA  1140
G  V  A  K  G  T  E  A  L  T  L  L  Y  N  P  K  T  R  A  Q     350
CTGATTGATGAGTTGTATGAACTGGAAGGATTCTTGAAACAGCGTCTGATAGAACTGGAA  1200
L  I  D  E  L  Y  E  L  E  G  F  L  K  Q  R  L  I  E  L  E     370
AGTGAGGAGTCAAGCTTCTCAATCAACCAGTTCTCTAGTGCTCCCATCTCCGTGCAAGAC  1260
S  E  E  S  S  F  S  I  N  Q  F  S  S  A  P  I  S  V  Q  D     390
CAATCCAAAGAGCAGTTGGAGGTTATGGTCAGCCACATCCGGAATGTGGTCGACCCTCTT  1320
Q  S  K  E  Q  L  E  V  M  V  S  H  I  R  N  V  V  D  P  L     410
GGCACAAACAAGATGCAGCACCTCTTCCTCATTTACTCTTCTCCAAAGTATGTTGATAGG  1380
G  T  N  K  M  Q  H  L  F  L  I  Y  S  S  P  K  Y  V  D  R     430
CTTGCTGCGTCACTCAGGTCAAAACTAACAGTTGCTGATAAATTTGTAATTTCTCAAGAG  1440
L  A  A  S  L  R  S  K  L  T  V  A  D  K  F  V  I  S  Q  E     450
GGAGTTCGCCAACGTAGGCTGGAAGCTCAACAAGAGCAGCAGAGAGTCCATCCAAAGTTG  1500
G  V  R  Q  R  R  L  E  A  Q  Q  E  Q  Q  R  V  H  P  K  L     470
GCATTGATGATTGAGAGATCAAAGGAGCTGAAAGTCAATATTGAAGAACACATCTCCAAG  1560
A  L  M  I  E  R  S  K  E  L  K  V  N  I  E  E  H  I  S  K     490
CGTTATAAAAACAGACCTGTCAATCTGATGGCCCTTGGCCTATCTATGACATAAATTGGG  1620
R  Y  K  N  R  P  V  N  L  M  A  L  G  L  S  M  T  *           507
CCTTTCTGACTAGTAGATTAGTATATATACACTTTTTCTGTTTTCCAGTGGGATATATTG  1680
TTGTTAGAATTTTTTTTATTATGGTTTAAATAAAGAATATAAGGTATAAAAAAAAAAAAA  1740
AAAAAAAAAAAAAAAAA                                              1758
```

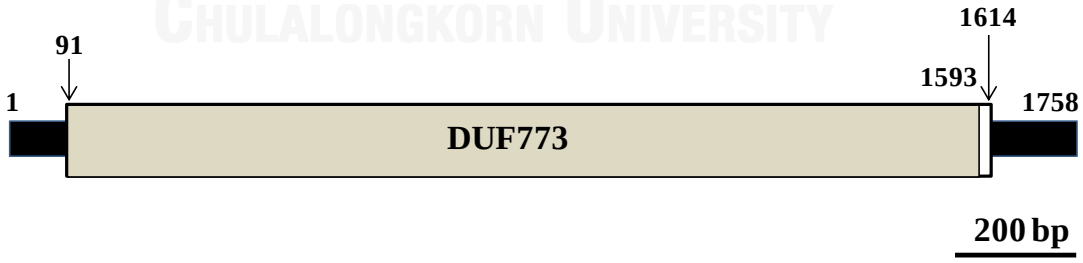

Domain	Position	*E*-value
DUF773	91-1593	6.6e-182

Figure 3. 10 (A) The full-length cDNA sequences of *PmCdk5* (an ORF of 1524 bp corresponding to the polypeptides of 507 amino acids). Start and stop codons are illustrated in boldface and underlined. A domain of unknown function, DUF773 (positions 1 - 501, *E*-value = 6.6e-182) is highlighted. The poly A additional signal (AATAAA) is boldfaced, italicized and underlined. (B) A schematic diagram showing the full-length cDNA of *PmCdk5*.

3.1.2.4 *PmCdk2*

The partial cDNA sequence of *PmCdk2* was initially obtained from analysis of the ovarian cDNA library of *P. monodon* (Figure 3.11A) and it significantly matched *Cyclin-dependent kinase 2* of the giant freshwater prawn *Macrobrachium rosenbergii (E*-value = 2.0e-114) (Figure 3.11 B). 5'- and 3'RACE of *PmCdk2* was further carried (Figure 3.12). The amplification product of 1000 and 700 bp obtained (Figure 3.12A and B) were cloned and sequenced (Figure 3.12C and D).

A

```
GTACGGGGACCACAAGTTGTACATGGTATTTGAATACCTGAATCAGGATCTGAAGAAGCTCTTTGATGA
 3'RACE,5'RACE-Cdk2
AAGCCGTGGAGGATTACCGTTGGATCTGGTGAGGAGTTATATGCAGCAGCTGTTACGAGGCATCGCATTCTGTCATG
CTAATCGTATTCTCCATCGAGACCTGAAGCCGCAAAACCTTCTTATAGATGCCAGAGGGTCAATCAAGCTGGCAGAT
TTTGGATTAGCAAGAGCATTCTGCCTGCCTTTGAGGGTGTACACACATGAAGTTGTCACCTTGTGGTACCGTGCCCC
AGAGATTCTCCTCGGTGCCAAAAACTATTGTACTGCAGTTGATATGTGGAGTCTGGGTGCCATTTTTGCTGAGATGT
TGACGAGAAAAGCACTTTTCCCTGGCGATTCAGAAATAGACCAGCTCTTCCGTATCTTCCGTACTCTGGGAACTCCT
GGGGAGGAAGATTGGCCAGGTGTGATCCAGCTCCCTGACTATAAGAGTTCATTCCCACGGTGGGAGGTTGATGCTGA
AAGTTCCATA
```

B

```
cyclin-dependent kinases 2 [Macrobrachium rosenbergii]
Sequence ID:  gb|AFK65508.1|Length: 305
Score =339 bits, Expect =2e-114
Identities = 161/180(89%), Positives = 169/180(93%), Gaps = 0/180(0%)
Frame = +2

Query  2    YGDHKLYMVFEYLNQDLKKLFDESRGGLPLDLVRSYMQQLLRGIAFCHANRILHRDLKPQ  181
            +GD KLYMVFEYLNQDLKKLFD+  GGLP DLV SYMQQLLRGIAFCHA+RILHRDLKPQ
```

```
Sbjct  73   HGDRKLYMVFEYLNQDLKKLFDQCPGGLPQDLVCSYMQQLLRGIAFCHAHRILHRDLKPQ  132

Query  182  NLLIDARGSIKLADFGLARAFCLPLRVYTHEVVTLWYRAPEILLGAKNYCTAVDMWSLGA  361
            NLLIDA+G IKLADFGLARAFCLPLR YTHEVVTLWYRAPEILLGAKNYCTAVDMWSLGA
Sbjct  133  NLLIDAKGYIKLADFGLARAFCLPLRAYTHEVVTLWYRAPEILLGAKNYCTAVDMWSLGA  192

Query  362  IFAEMLTRKALFPGDSEIDQLFRIFRTLGTPGEEDWPGVIQLPDYKSSFPRWEVDAESSI  541
            IFAEMLT+KALFPGDSEIDQLFRI RTLGTPGEEDWPGV QLPDYK SFPRWEV+A S++
Sbjct  193  IFAEMLTKKALFPGDSEIDQLFRILRTLGTPGEEDWPGVSQLPDYKRSFPRWEVNAASNL  252
```

Figure 3. 11 Nucleotide sequences of an original EST (A) and its BlastX analysis of the partial cDNA sequence of *PmCdk2* (B).

The full-length cDNA sequences of *PmCdk2* was 1763 bp in length with an ORF of 921 bp corresponding to 306 amino acids with 5' and 3' UTR of 342 and 500 bp, respectively (Figure 3.14). This characterized sequence was similar to *Cyclin-dependent kinase 2* of the giant freshwater prawn *(Macrobrachium rosenbergii)* (*E*-value = 6.0e-179). The expected MW and p*I* of the deduced PmCdk2 protein was 34.93 kDa and 7.02, respectively. The predicted signal peptide and glycosylation site were not found in the deduced PmCdk2 protein.

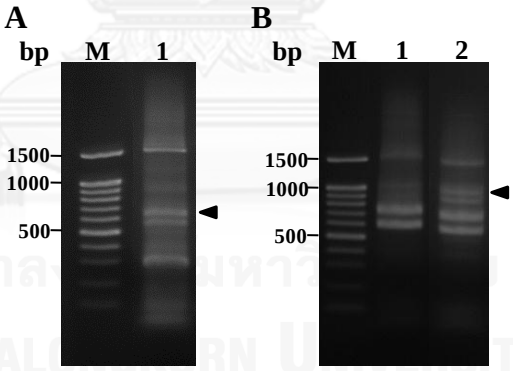

C

```
TTCTTTTTTTATTTTACGGTTTGTTTGTTCCGTTTCTTCGGGTTTTGTTTTGGGTTTGGATTTTTTTTT
TTTTTTTTTTTTCTCTCTCTCTCCTTCGGGGCGAACGAGGAGGCTCGCTTTGCCTTCTCTCTCCCTCTC
TCTCTCTCTCAGAGGAAAACGCACGCCCTTTTCCTCTCTCTCTCTCTCTCTCCTTCTCTCCCTCTCT
TTCTCACTCTCTCATTCTCTCTCTCTCTCTCTCCCTGCGTTTTGTCTCTCCGGGAGCCCTTCCTGTC
TTCGGATTATGCGTTGGGTGTGACGCGCGCGCGTGTGTGAGTGCGTGCGTGCGAGAGAGAGGGAAGATG
TCGGTGCAGAATTACGAGAAAATCGAGAAAATCGGCGAAGGAACTTATGGCGTCGTGTACAAGGCCCAG
GACCGGGCGAGCAAGAGGATTGTGGCGCTCAAGAAAATCCGCCTCGAGAATGAAGCAGACGGAGTACCC
AGTACAGCTTTGAGAGAGATAGCCTTACTCAAGGAACTCGACCATGATAATATTGTTCGACTGCTGGAT
```

GTGGTGTACGGGGACCACAAGTTGTACATGGTATTTGAATACCTGAATCAGGATCTGAAGAAGCTCTTT
GATGAAAGCCGTGGAGGATTACCG

D

TGATGAAAGCCGTGGAGGATTACCGTTGGATCTGGTGAGGAGTTATATGCAGCAGCTGTTACGAGGCATCGCATTCT
GTCATGCTAATCGTATTCTCCATCGAGACCTGAAGCCGCAAAACCTTCTTATAGATGCCAGAGGGTCAATCAAGCTG
GCAGATTTTGGATTAGCAAGAGCATTCTGCCTGCCTTTGAGGGTGTACACACATGAAGTTGTCACCTTGTGGTACCG
TGCCCCAGAGATTCTCCTCGGTGCCAAAAACTATTGTACTGCAGTTGATATGTGGAGTCTGGGTGCCATTTTTGCTG
AGATGTTGACGAGAAAAGCACTTTTCCCTGGCGATTCAGAAATAGACCAGCTCTTCCGTATCTTCCGTACTCTGGGA
ACTCCTGGGGAGGAAGATTGGCCAGGTGTGATCCAGCTCCCTGACTATAAGAGTTCATTCCCACGGTGGGAGGTTGA
TGCTGAAAGTTCCATAGCCCAGCTGGTTCCATTGTTGAATGAAGAGGGACGGTGCTTACTCTTGGCTATGCTGAAAT
ATGACCCACGGCAGCGGATTACTGCAAAGTCGGCCCTCTATCACCCATTCTTCGAACCTCTCTCATCTACTGGCCAA
GTGCTAGTCCCACCAAATCTTAGGTGATCAGAAACAAGGCCTTCAAGATTTTTCTTTTCTTTTTAAGGAATCATGCA
AAAAATGTTGCTTACCCAGTTTTTTTATCATTTAAAGAATATTGTATAGGTTTACACTATTCTTGCATTTTGATATT
TTGACTATGTATAGGTCTAGAGTTTTTGCACATCTACTGTGCTTTTTATATAGAATACAAATAGCTTTTTTACCCAA
AGTTCTACCAACCTTTCCTCTTTTATACAGATATTTGTAAATATACTATATAAGGTCCAAGCTTTTGTGCTTTTATG
TATAGAAAGAAAAATGTTCATTTTACCAAAAGTTTCTGGATCTTGTTTCAAGGAAGTAAGTATAAATTGCTATTTTT
GGAAAAAGTTTCAAGTCTAATTTTATTTTAAAGAATATCATGAATTGATAAAATTGTGTATTTTTTAAATCTATCAA
GTCTGGCTGTGAATATTAGAATAAGAAATAATAGATGGAAAAAAAAAAAAAAAAAAAAAAAAA

Figure 3. 12 Results from 5' RACE-PCR (lane 1A), 3'RACE-PCR (lane 1B) and semi-nested 3'RACE-PCR (lane 2B) of *PmCdk2*. The amplified fragments (lanes 1A and 2B) were cloned and sequenced (C and D). Primers for RACE-PCR are underlined. Lane M is a 100 bp DNA ladder.

A

```
TTCTTTTTTTATTTTACGGTTTGTTTGTTCCGTTTCTTCGGGTTTTGTTTTGGGTTTGGA  60
TTTTTTTTTTTTTTTTTTTTTCTCTCTCTCTCCTTCGGGGCGAACGAGGAGGCTCGCTTT  120
GCCTTCTCTCTCCCTCTCTCTCTCTCTCAGAGGAAAACGCACGCCCTTTTCCTCTCTCTC  180
TCTCTCTCTCTCCTTCTCTCCCTCTCTTTCTCACTCTCTCATTCTCTCTCTCTCTCTC  240
TCCCTGCGTTTTGTCTCTCCGGGAGCCCTTCCTGTCTTCGGATTATGCGTTGGGTGTGAC  300
GCGCGCGCGTGTGTGAGTGCGTGCGTGCGAGAGAGAGGGAAGATGTCGGTGCAGAATTAC  360
                                          M  S  V  Q  N  Y     6
GAGAAAATCGAGAAAATCGGCGAAGGAACTTATGGCGTCGTGTACAAGGCCCAGGACCGG  420
E  K  I  E  K  I  G  E  G  T  Y  G  V  V  Y  K  A  Q  D  R    26
GCGAGCAAGAGGATTGTGGCGCTCAAGAAAATCCGCCTCGAGAATGAAGCAGACGGAGTA  480
A  S  K  R  I  V  A  L  K  K  I  R  L  E  N  E  A  D  G  V    46
CCCAGTACAGCTTTGAGAGAGATAGCCTTACTCAAGGAACTCGACCATGATAATATTGTT  540
P  S  T  A  L  R  E  I  A  L  L  K  E  L  D  H  D  N  I  V    66
CGACTGCTGGATGTGGTGTACGGGGACCACAAGTTGTACATGGTATTTGAATACCTGAAT  600
R  L  L  D  V  V  Y  G  D  H  K  L  Y  M  V  F  E  Y  L  N    86
CAGGATCTGAAGAAGCTCTTTGATGAAAGCCGTGGAGGATTACCGTTGGATCTGGTGAGG  660
Q  D  L  K  K  L  F  D  E  S  R  G  G  L  P  L  D  L  V  R   106
```

```
AGTTATATGCAGCAGCTGTTACGAGGCATCGCATTCTGTCATGCTAATCGTATTCTCCAT  720
S  Y  M  Q  Q  L  L  R  G  I  A  F  C  H  A  N  R  I  L  H     126
CGAGACCTGAAGCCGCAAAACCTTCTTATAGATGCCAGAGGGTCAATCAAGCTGGCAGAT  780
R  D  L  K  P  Q  N  L  L  I  D  A  R  G  S  I  K  L  A  D     146
TTTGGATTAGCAAGAGCATTCTGCCTGCCTTTGAGGGTGTACACACATGAAGTTGTCACC  840
F  G  L  A  R  A  F  C  L  P  L  R  V  Y  T  H  E  V  V  T     166
TTGTGGTACCGTGCCCCAGAGATTCTCCTCGGTGCCAAAAACTATTGTACTGCAGTTGAT  900
L  W  Y  R  A  P  E  I  L  L  G  A  K  N  Y  C  T  A  V  D     186
ATGTGGAGTCTGGGTGCCATTTTTGCTGAGATGTTGACGAGAAAAGCACTTTTCCCTGGC  960
M  W  S  L  G  A  I  F  A  E  M  L  T  R  K  A  L  F  P  G     206
GATTCAGAAATAGACCAGCTCTTCCGTATCTTCCGTACTCTGGGAACTCCTGGGGAGGAA 1020
D  S  E  I  D  Q  L  F  R  I  F  R  T  L  G  T  P  G  E  E     226
GATTGGCCAGGTGTGATCCAGCTCCCTGACTATAAGAGTTCATTCCCACGGTGGGAGGTT 1080
D  W  P  G  V  I  Q  L  P  D  Y  K  S  S  F  P  R  W  E  V     246
GATGCTGAAAGTTCCATAGCCCAGCTGGTTCCATTGTTGAATGAAGAGGGACGGTGCTTA 1140
D  A  E  S  S  I  A  Q  L  V  P  L  L  N  E  E  G  R  C  L     266
CTCTTGGCTATGCTGAAATATGACCCACGGCAGCGGATTACTGCAAAGTCGGCCCTCTAT 1200
L  L  A  M  L  K  Y  D  P  R  Q  R  I  T  A  K  S  A  L  Y     286
CACCCATTCTTCGAACCTCTCTCATCTACTGGCCAAGTGCTAGTCCCACCAAATCTTAGG 1260
H  P  F  F  E  P  L  S  S  T  G  Q  V  L  V  P  P  N  L  R     306
TGATCAGAAACAAGGCCTTCAAGATTTTTCTTTTCTTTTTAAGGAATCATGCAAAAAATG 1320
*
TTGCTTACCCAGTTTTTTTATCATTTAAAGAATATTGTATAGGTTTACACTATTCTTGCA 1380
TTTTGATATTTTGACTATGTATAGGTCTAGAGTTTTTGCACATCTACTGTGCTTTTTATA 1440
TAGAATACAAATAGCTTTTTTACCCAAAGTTCTACCAACCTTTCCTCTTTTATACAGATA 1500
TTTGTAAATATACTATATAAGGTCCAAGCTTTTGTGCTTTTATGTATAGAAAGAAAAATG 1560
TTCATTTTACCAAAAGTTTCTGGATCTTGTTTCAAGGAAGTAAGTATAAATTGCTATTTT 1620
TGGAAAAAGTTTCAAGTCTAATTTTATTTTAAAGAATATCATGAATTGATAAAATTGTGT 1680
ATTTTTTAAATCTATCAAGTCTGGCTGTGAATATTAGAATAAGAAATAATAGATGGAAAA 1740
AAAAAAAAAAAAAAAAAAAAAA                                        1763
```

B

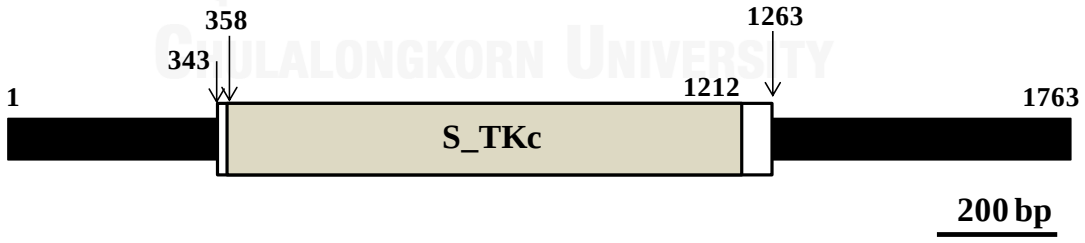

Domain	Position	*E*-value
S_TKc	358-1212	7.46e-105

Figure 3. 13 (A) The full-length cDNA sequences of *PmCdk2* (an ORF of 921 bp corresponding to the polypeptides of 306 amino acids). Start and stop codons are illustrated in boldface and underlined. A serine/threonine kinases catalytic (S_TKc) domain (positions 6 - 290, *E*-value = 7.46e-105) is highlighted. (B) A schematic diagram showing the full-length cDNA of *PmCdk2*.

3.2 Expression profile and tissue distribution analysis of reproduction related genes

3.2.1 Expression level of *PmApc11, PmBystin1, PmCdc2, PmCdc16, PmCdc20, PmCdk2, PmCdk5, PmCdk7, PmChk1* and *PmRpd3* in ovaries and testes of *P. monodon* analyzed by RT-PCR

In this thesis, the expression profiles of several reproduction-related were studied. These included *PmApc11, PmBystin1, PmCdc20, PmCdk7* and *PmChk1* previously isolated from ovaries by Preechaphol (2008) and those successfully characterized in testes such as *PmCdc2* and *PmCdk7* (Leelatanawit, 2008). In addition, expression of *PmRpd3*, *PmCdc16*, *PmCdk5* and *PmCdk2* which were further characterized in this thesis was also examined.

Total RNA was extracted from ovaries and testes of cultured juveniles and wild broodstock of of *P. monodon* and treated with DNase I (0.5 U/µg of total RNA). One and a half microgram of DNase I-treated total RNA was reverse-transcribed (*N* = 5 for each group).

RT-PCR indicated that the relative expression level of *PmApc11* in ovaries was greater than that in testes and its expression in juveniles was greater than that in broodstock (Figure 3.14).

In contrast, *PmBystin1* was less abundantly expressed in testes of juveniles while its expression in ovaries of juvenile and broodstock and testes of broodstock was not significantly different (Figure 3.15).

Based on RT-PCR, the expression of *PmCdc2* in testes of juveniles was greater than that in testes of broodstock and ovaries of both juveniles and broodstock (Figure 3.16).

PmCdc16 was more abundantly expressed in testes than ovaries. Its expression in ovaries of juveniles was greater than that in broodstock. Likewise, the expression of *PmCdc16* in testes of juveniles was also greater than that of broodstock (Figure 3.17).

PmCdc20 and *PmCdk2* was more abundantly expressed in ovaries than testes in both juvenile and broodstock stages. This transcript was expressed at a greater level in ovaries of juveniles than broodstock (Figure 3.18 and 3.19).

Like *PmCdc20, PmCdk5* was more abundantly expressed in ovaries than testes in both juvenile and broodstock stages. This transcript was expressed at a greater level in ovaries of juveniles than broodstock (Figure 3.20).

PmCdk7 was more abundantly expressed in ovaries than that in testes in both cultured juveniles and wild broodstock of *P. monodon* ($P < 0.05$). Its expression in ovaries of juveniles was greater than that in broodstock while the expression in testes was not different between different developmental stages (Figure 3.21).

PmChk1 was more abundantly expressed in ovaries than testes in both juveniles and broodstock. Its expression in testes of juveniles was greater than that of broodstock (Figures 3.22).

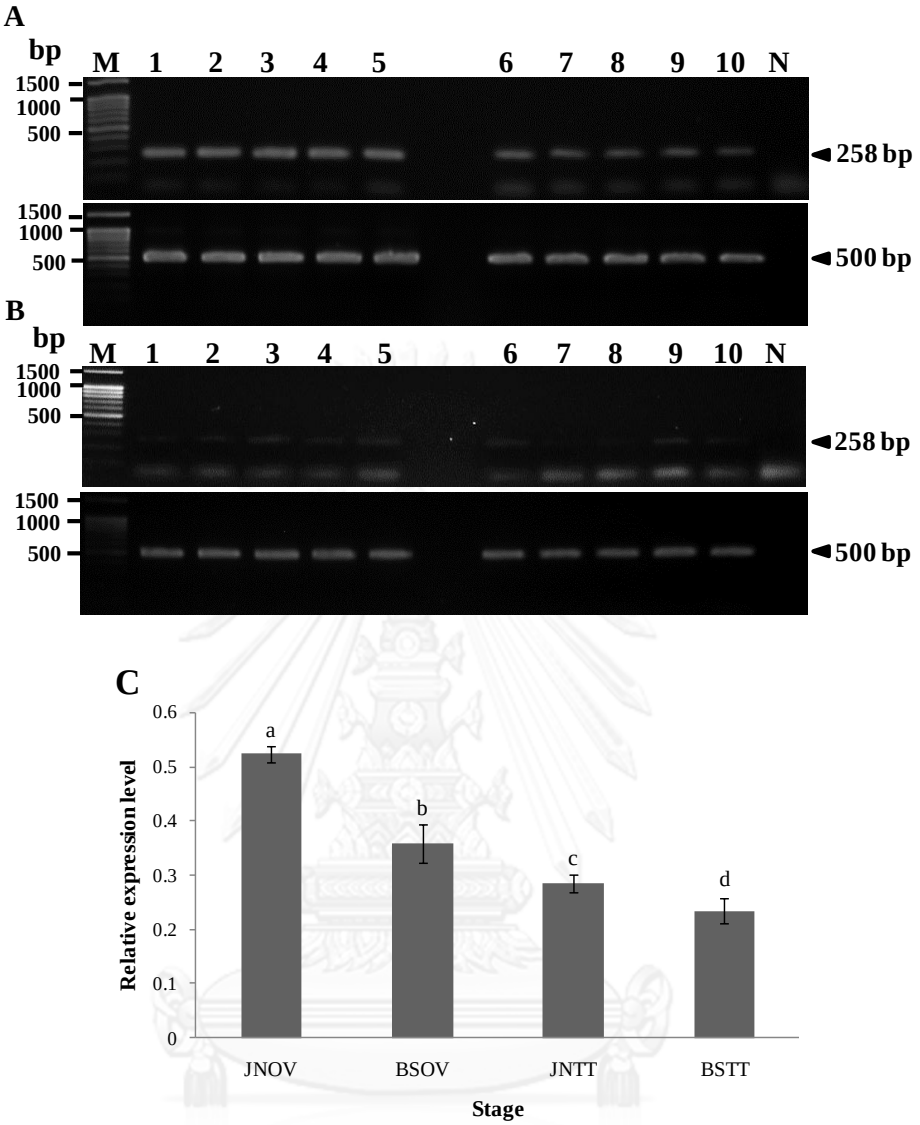

Figure 3. 14 RT-PCR of *PmApc11* using the first strand cDNA from ovaries of domesticated juveniles (lanes 1-5, A) and wild broodstock (lanes 6-10, A) and testes of domesticated juveniles (lanes 1-5, B) and wild broodstock (lanes 6-10, B) of *P. monodon*. *EF-1α* was successfully amplified from the same template (bottom, A and B). Lanes M and N are a 100 bp DNA marker and the negative control (without cDNA template), respectively. (C) Histograms showing the relative expression level of *PmApc11* in ovaries of domesticated juveniles (JNOV) and wild broodstock (BSOV) and testes of domesticated juveniles (JNTT) and wild broodstock (BSTT) of *P. monodon.*

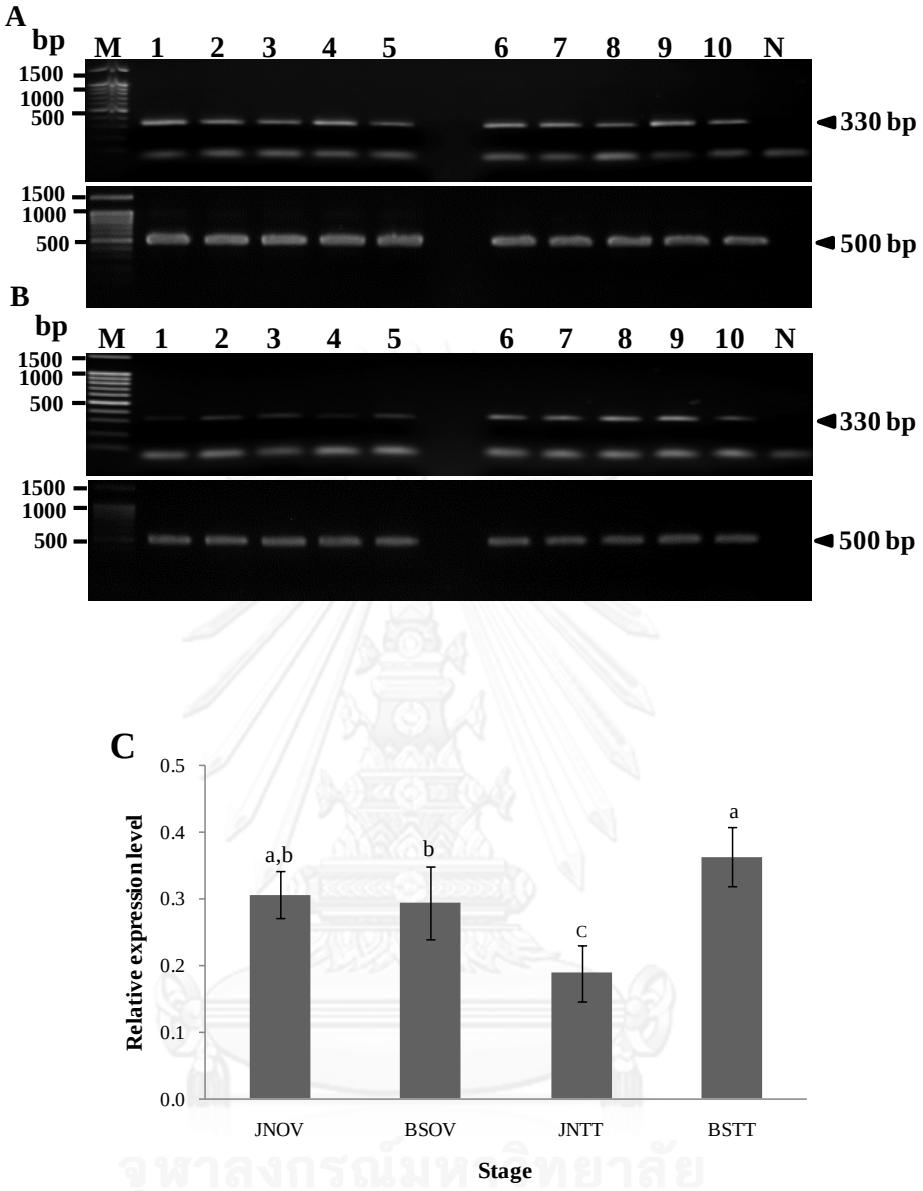

Figure 3. 15 RT-PCR of *PmBystin1* using the first strand cDNA from ovaries of domesticated juveniles (lanes 1-5, A) and wild broodstock (lanes 6-10, A) and testes of domesticated juveniles (lanes 1-5, B) and wild broodstock (lanes 6-10, B) of *P. monodon*. *EF-1α* was successfully amplified from the same template (bottom, A and B). Lanes M and N are a 100 bp DNA marker and the negative control (without cDNA template), respectively. (C) Histograms showing mean relative expression level of *PmBystin1* in ovaries of cultured juveniles (JNOV; 5-month-old) and wild broodstock (BSOV) and testes of cultured juveniles (JNTT; 5-month-old) and wild broodstock (BSTT) of *P. monodon.*

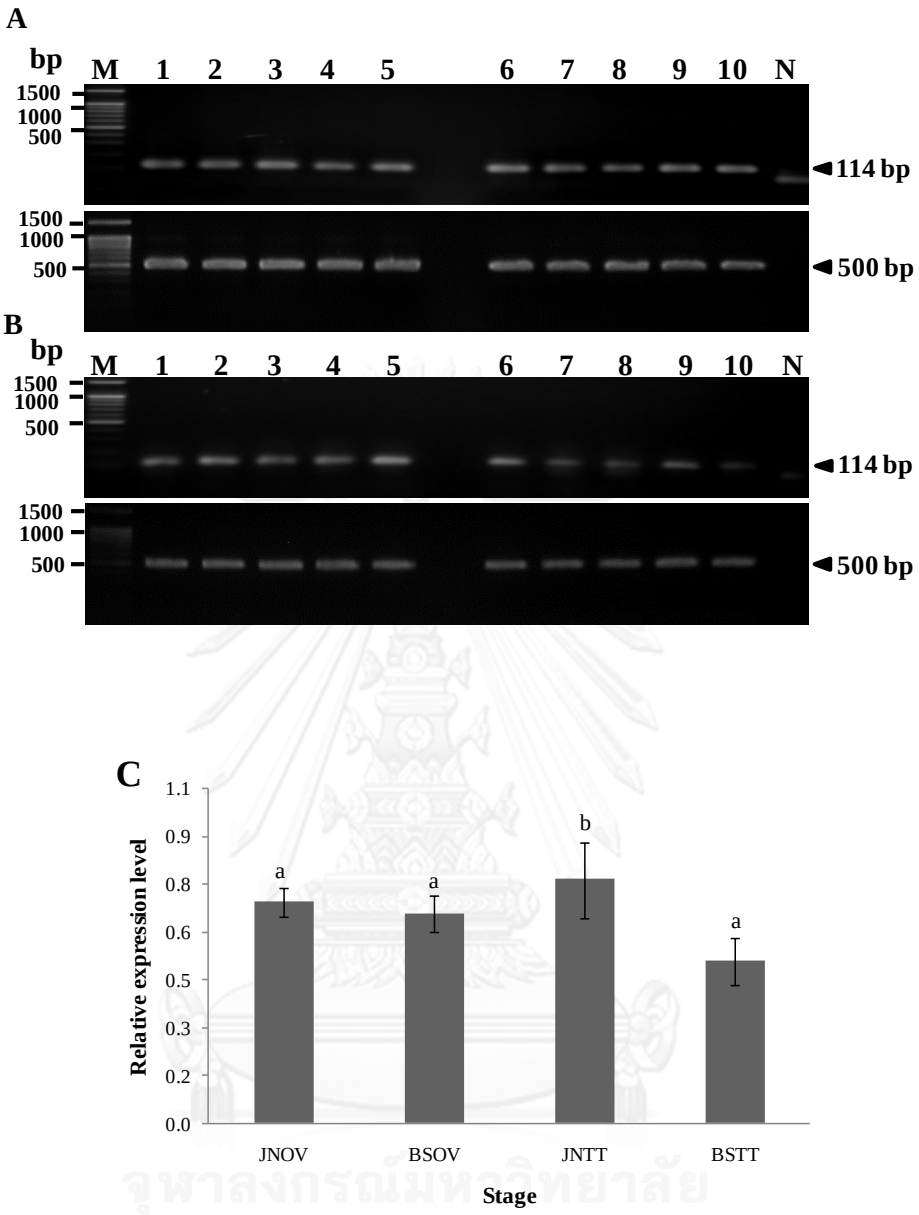

Figure 3. 16 RT-PCR of *PmCdc2* using the first strand cDNA from ovaries of domesticated juveniles (lanes 1-5, A) and wild broodstock (lanes 6-10, A) and testes of domesticated juveniles (lanes 1-5, B) and wild broodstock (lanes 6-10, B) of *P. monodon*. *EF-1α* was successfully amplified from the same template (bottom, A and B). Lanes M and N are a 100 bp DNA marker and the negative control (without cDNA template), respectively. (C) Histograms showing mean relative expression level of *PmCdc2* in ovaries of cultured juveniles (JNOV; 5-month-old) and wild broodstock (BSOV) and testes of cultured juveniles (JNTT; 5-month-old) and wild broodstock (BSTT) of *P. monodon*.

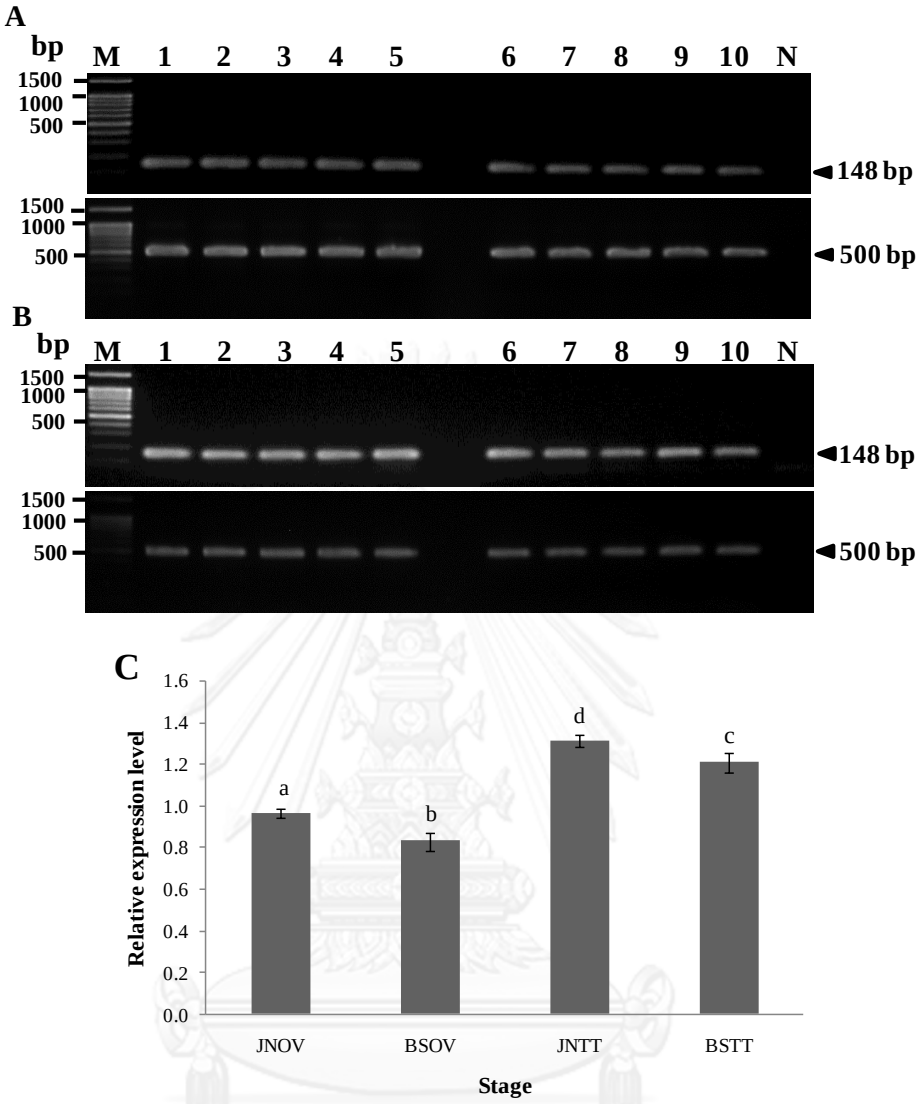

Figure 3. 17 RT-PCR of *PmCdc16* using the first strand cDNA from ovaries of domesticated juveniles (lanes 1-5, A) and wild broodstock (lanes 6-10, A) and testes of domesticated juveniles (lanes 1-5, B) and wild broodstock (lanes 6-10, B) of *P. monodon*. *EF-1α* was successfully amplified from the same template (bottom, A and B). Lanes M and N are a 100 bp DNA marker and the negative control (without cDNA template), respectively. (C) Histograms showing mean relative expression level of *PmCdc16* in ovaries of cultured juveniles (JNOV; 5-month-old) and wild broodstock (BSOV) and testes of cultured juveniles (JNTT; 5-month-old) and wild broodstock (BSTT) of *P. monodon*.

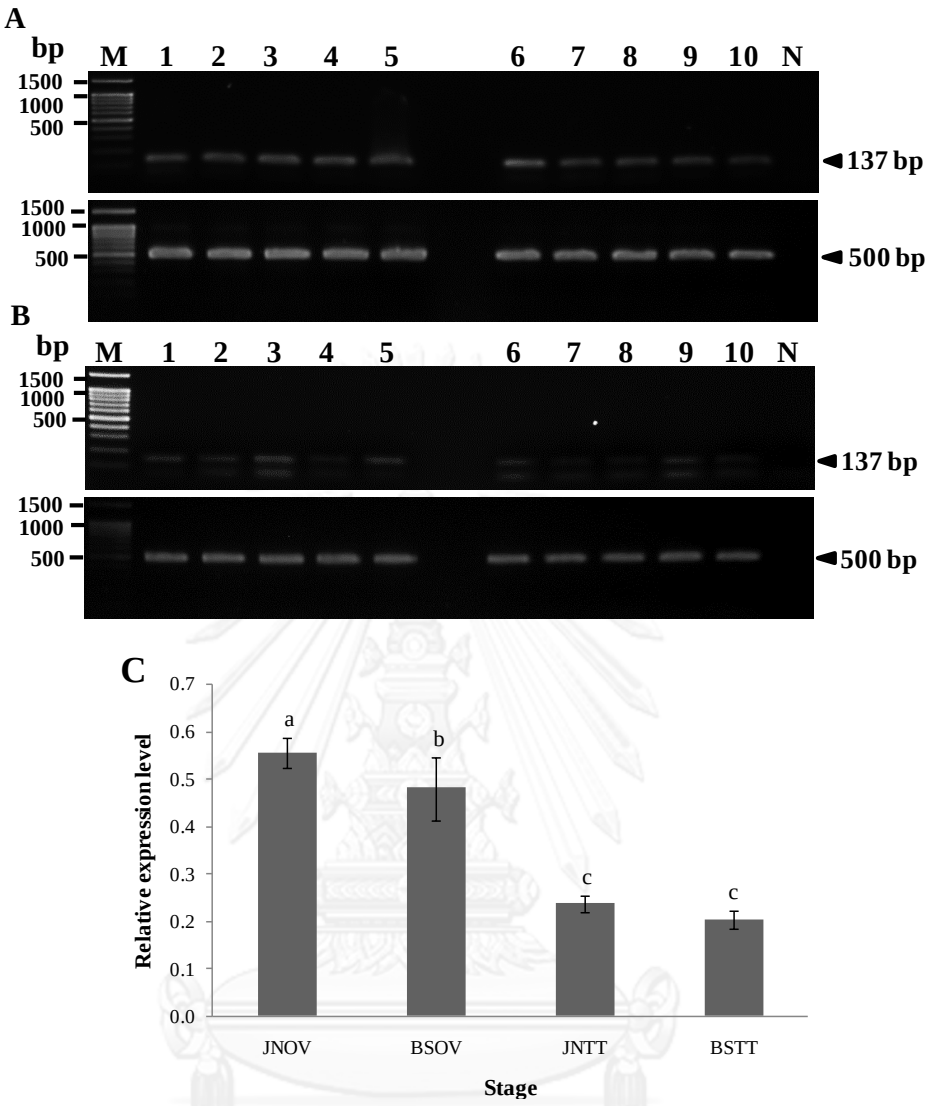

Figure 3. 18 RT-PCR of *PmCdc20* using the first strand cDNA from ovaries of domesticated juveniles (lanes 1-5, A) and wild broodstock (lanes 6-10, A) and testes of domesticated juveniles (lanes 1-5, B) and wild broodstock (lanes 6-10, B) of *P. monodon*. *EF-1α* was successfully amplified from the same template (bottom, A and B). Lanes M and N are a 100 bp DNA marker and the negative control (without cDNA template), respectively. (C) Histograms showing mean relative expression level of *PmCdc20* in ovaries of cultured juveniles (JNOV; 5-month-old) and wild broodstock (BSOV) and testes of cultured juveniles (JNTT; 5-month-old) and wild broodstock (BSTT) of *P. monodon*.

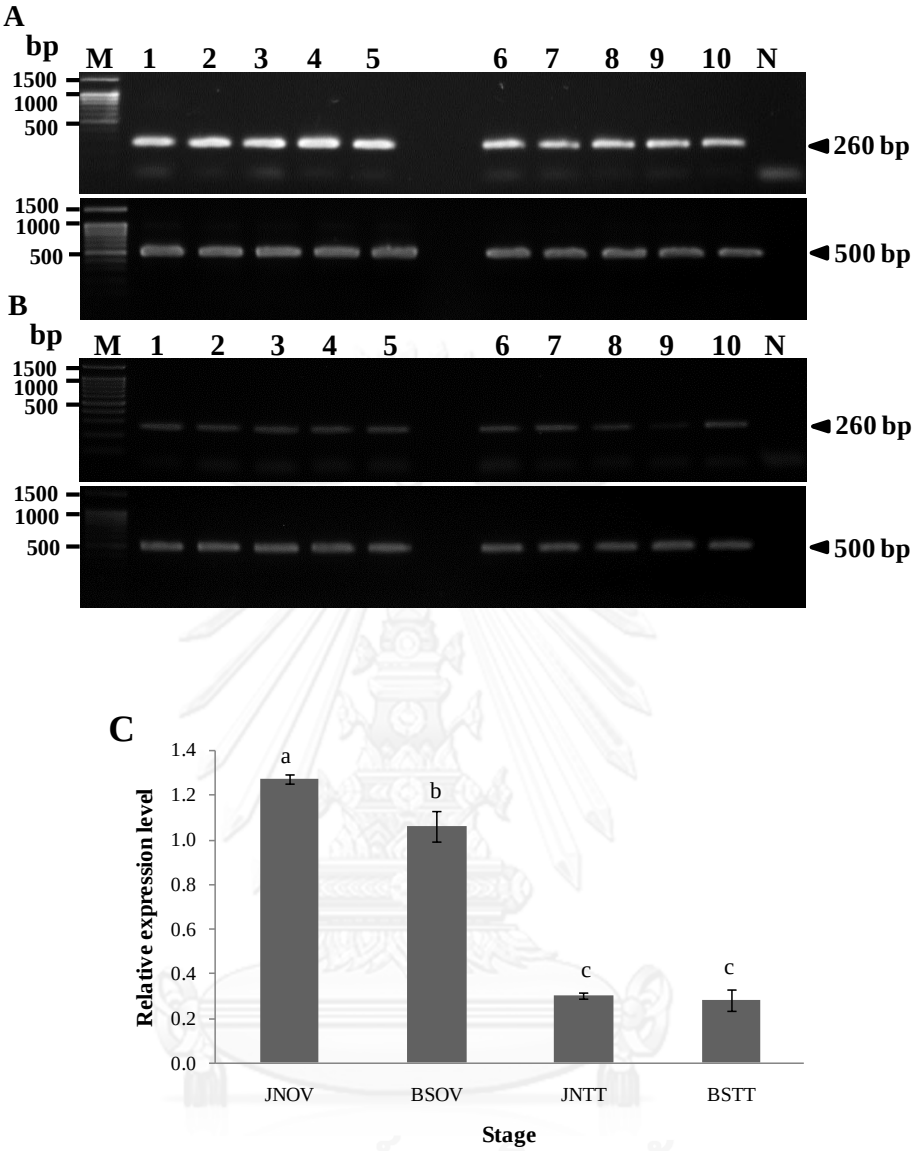

Figure 3. 19 RT-PCR of *PmCdk2* using the first strand cDNA from ovaries of domesticated juveniles (lanes 1-5, A) and wild broodstock (lanes 6-10, A) and testes of domesticated juveniles (lanes 1-5, B) and wild broodstock (lanes 6-10, B) of *P. monodon*. *EF-1α* was successfully amplified from the same template (bottom, A and B). Lanes M and N are a 100 bp DNA marker and the negative control (without cDNA template), respectively. (C) Histograms showing mean expression level of *PmCdk2* in ovaries of cultured juveniles (JNOV; 5-month-old) and wild broodstock (BSOV) and testes of cultured juveniles (JNTT; 5-month-old) and wild broodstock (BSTT) of *P. monodon*.

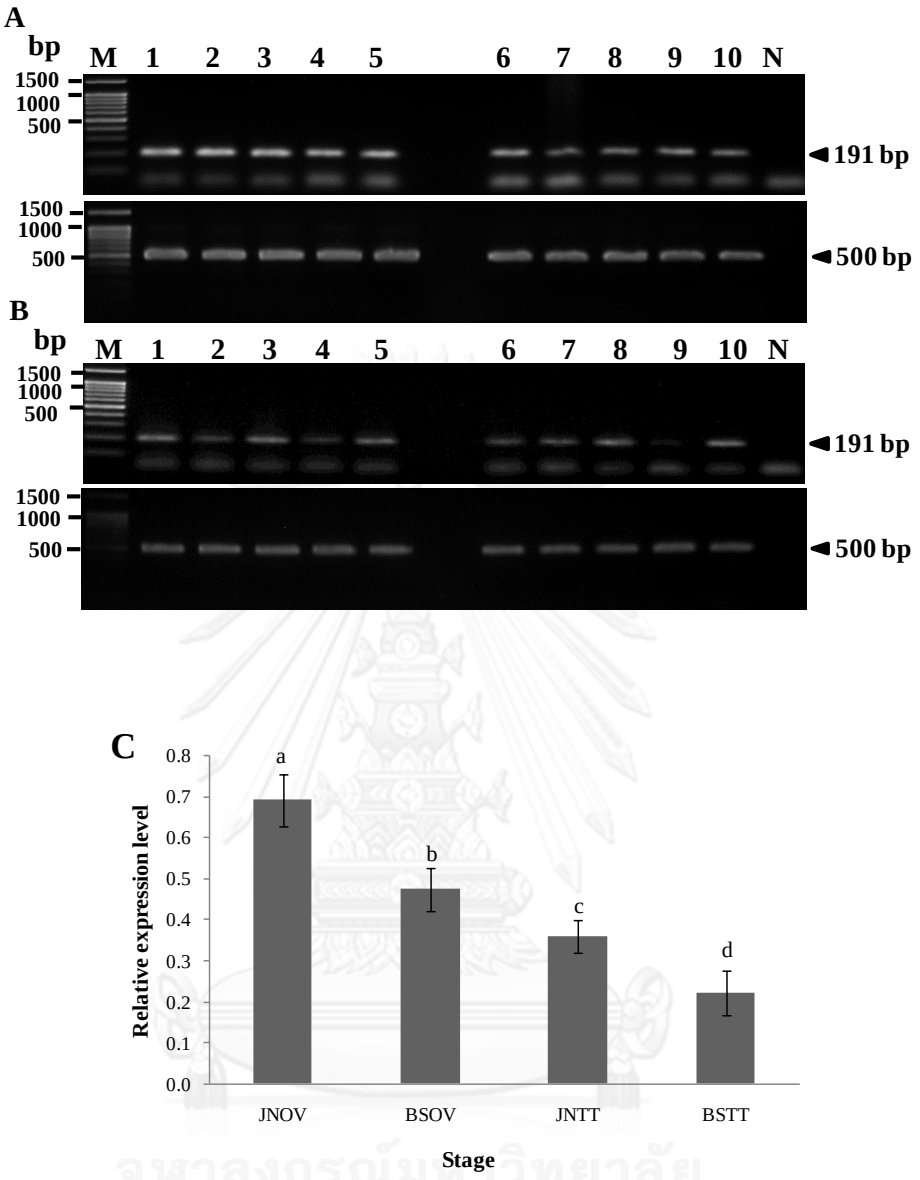

Figure 3. 20 RT-PCR of *PmCdk5* using the first strand cDNA from ovaries of domesticated juveniles (lanes 1-5, A) and wild broodstock (lanes 6-10, A) and testes of domesticated juveniles (lanes 1-5, B) and wild broodstock (lanes 6-10, B) of *P. monodon*. *EF-1α* was successfully amplified from the same template (bottom, A and B). Lanes M and N are a 100 bp DNA marker and the negative control (without cDNA template), respectively. (C) Histograms showing mean relative expression level of *PmCdk5* in ovaries of cultured juveniles (JNOV; 5-month-old) and wild broodstock (BSOV) and testes of cultured juveniles (JNTT; 5-month-old) and wild broodstock (BSTT) of *P. monodon*.

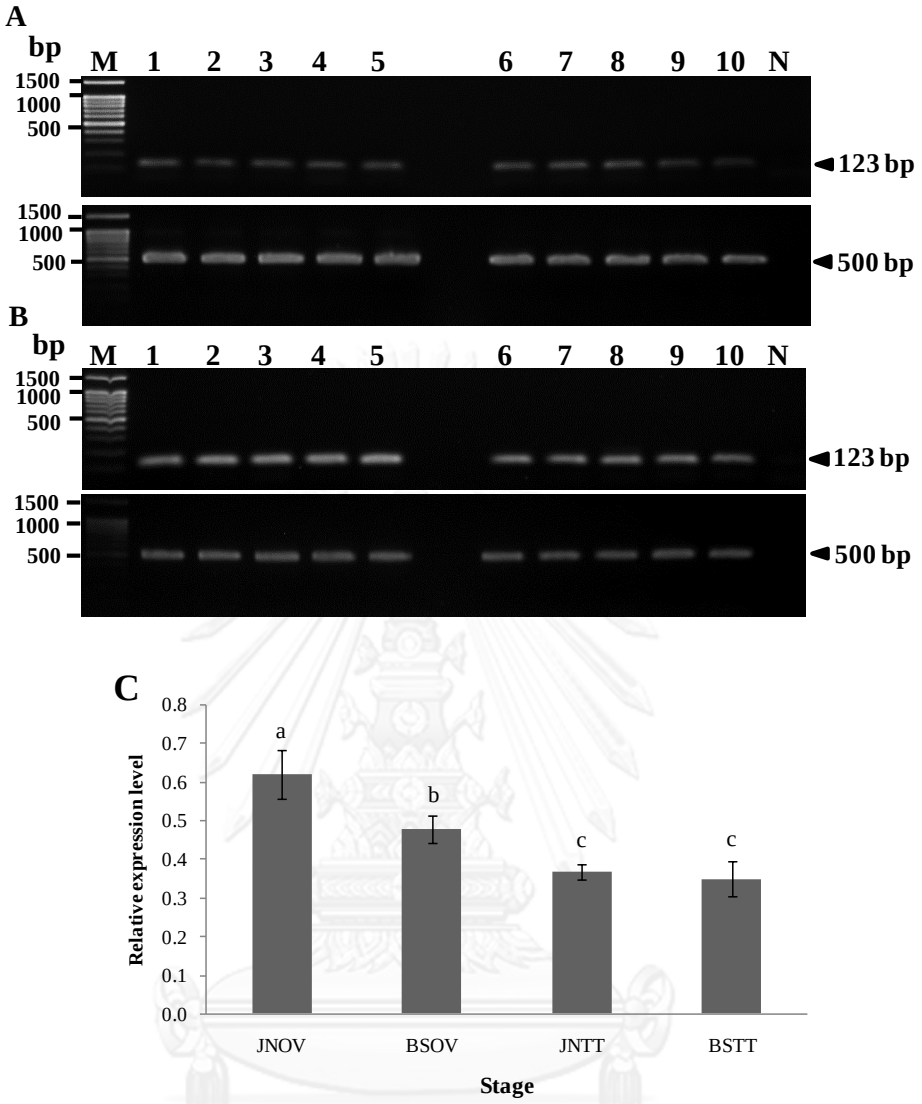

Figure 3. 21 RT-PCR of *PmCdk7* using the first strand cDNA from ovaries of domesticated juveniles (lanes 1-5, A) and wild broodstock (lanes 6-10, A) and testes of domesticated juveniles (lanes 1-5, B) and wild broodstock (lanes 6-10, B) of *P. monodon*. *EF-1α* was successfully amplified from the same template (bottom, A and B). Lanes M and N are a 100 bp DNA marker and the negative control (without cDNA template), respectively. (C) Histograms showing mean relative expression level of *PmCdk7* in ovaries of cultured juveniles (JNOV; 5-month-old) and wild broodstock (BSOV) and testes of cultured juveniles (JNTT; 5-month-old) and wild broodstock (BSTT) of *P. monodon*.

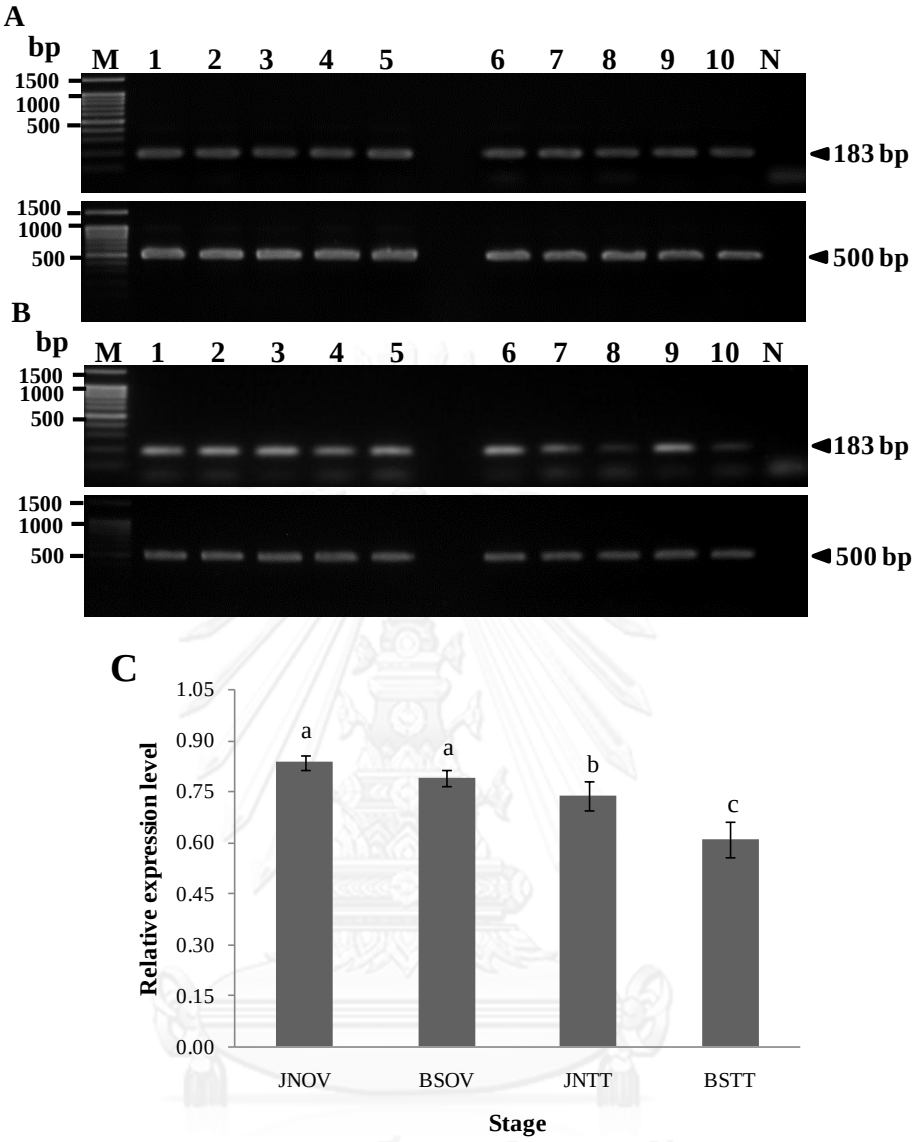

Figure 3. 22 RT-PCR of *PmChk1* using the first strand cDNA from ovaries of domesticated juveniles (lanes 1-5, A) and wild broodstock (lanes 6-10, A) and testes of domesticated juveniles (lanes 1-5, B) and wild broodstock (lanes 6-10, B) of *P. monodon*. *EF-1α* was successfully amplified from the same template (bottom, A and B). Lanes M and N are a 100 bp DNA marker and the negative control (without cDNA template), respectively. (C) Histograms showing mean relative expression level of *PmChk1* in ovaries of cultured juveniles (JNOV; 5-month-old) and wild broodstock (BSOV) and testes of cultured juveniles (JNTT; 5-month-old) and wild broodstock (BSTT) of *P. monodon*.

3.2.2 Tissue distribution analysis of reproduction-related genes of *P. monodon*

Tissue distribution analysis of *PmApc11, PmBystin1, PmCdc2, PmCdc16, PmCdc20, PmCdk2, PmCdk5, PmCdk7, PmChk1* and *PmRpd3* was comparable in various tissues of male cultured juvenile and broodstock and testes of female cultured juvenile and broodstock.

PmApc11 was abundantly expressed in ovaries of broodstock. A lower level of expression was observed in the antennal gland, eyestalk, gills, hemocytes, heart, hepatopancreas, intestine, lymphoid organs, pleopods, stomach, thoracic ganglion, juvenile ovaries and testes of wild male broodstock. *PmApc11* was not expressed in a subcuticular epithelium of wild *P. monodon* broodstock (Figure 3.23A).

PmBystin1 was abundantly expressed in ovaries and testes of wild broodstock and ovaries of cultured juveniles. A lower express pattern was observed in eyestalk, gills hemocytes, hepatopancreas, lymphoid organs, pleopods, stomach and thoracic ganglion. Rare expression was observed in antennal gland, subcuticular epithelium and intestine. *PmBystin1* was not expressed in heart (Figure 3.23B).

PmCdc16 was expressed in all examined tissues and abundantly expressed in testes of wild male and ovaries of both cultured juveniles and broodstock. Lower expression levels of *PmCdc16* were observed in antennal gland, subcuticular epithelium, eyestalk, gills, hemocytes, heart, hepatopancreas, intestine, lymphoid organs, pleopods, stomach, and thoracic ganglion (Figure 3.23C).

PmCdc20 was abundantly expressed in thoracic ganglion, testes and ovaries of both cultured juveniles and broodstock. Lower expression levels of *PmCdc20* was observed in antennal gland, eyestalk, gills, hemocytes, heart, hepatopancreas, intestine, lymphoid organs, and pleopods. Rare expression was observed in subcuticular epithelium and stomach (Figure 3.23D).

PmCdk2 was expressed in all examined tissues and abundantly expressed in antennal gland, eyestalk, gills, hemocytes, heart, hepatopancreas, intestine, lymphoid organs, ovaries, pleopods, stomach, and thoracic ganglion, ovaries of juvenile. Lower expression levels of *PmCdk2* were observed in subcuticular epithelium and testes of wild male broodstock (Figure 3.23E).

PmCdk5 was expressed in all examined tissues and abundantly expressed in gills, hemocytes, heart, hepatopancreas, intestine, lymphoid organs, ovaries, pleopods, stomach, and thoracic ganglion and ovaries of juvenile. Lower expression was found in antennal gland, subcuticular epithelium, eyestalk and testes of wild male broodstock (Figure 3.24A).

PmCdk7 was comparably expressed in antennal gland, subcuticular epithelium, eyestalk, gills, hemocytes, hepatopancreas, intestine, lymphoid organs, ovaries and thoracic ganglion, ovaries of juvenile and testes of wild male whereas low expression levels was observed in heart, pleopods and stomach of *P. monodon* broodstock (Figure 3.24B).

PmChk1 was more expressed in ovaries of broodstock. A lower expression was found in antennal gland, subcuticular epithelium, eyestalk, hemocytes, heart, hepatopancreas, intestine, lymphoid organs, pleopods, and thoracic ganglion, ovaries of juvenile and testes of wild male. This transcript was limited expressed in gills and stomach of *P. monodon* broodstock (Figure 3.24C).

PmRpd3 was expressed in all examined tissues and it was abundantly expressed in ovaries, eyestalk, gills and hemocytes. Lower expressed was observed in heart, hepatopancreas, lymphoid organs, pleopods, stomach, and thoracic ganglion and testes of wild male. This transcript was limited expressed in antennal gland, subcuticular epithelium, intestine and ovaries of juvenile (Figure 3.24D).

PmCdc2 was abundantly expressed in hemocytes, heart, hepatopancreas, ovaries of female and testes of male broodstock. Low expression levels of *PmCdc2* were observed in other tissues including antennal gland, subcuticular epithelium,

eyestalk, gill, intestine, lymphoid organ, thoracic ganglion, pleopods, stomach and ovaries of juvenile (Figure 3.25).

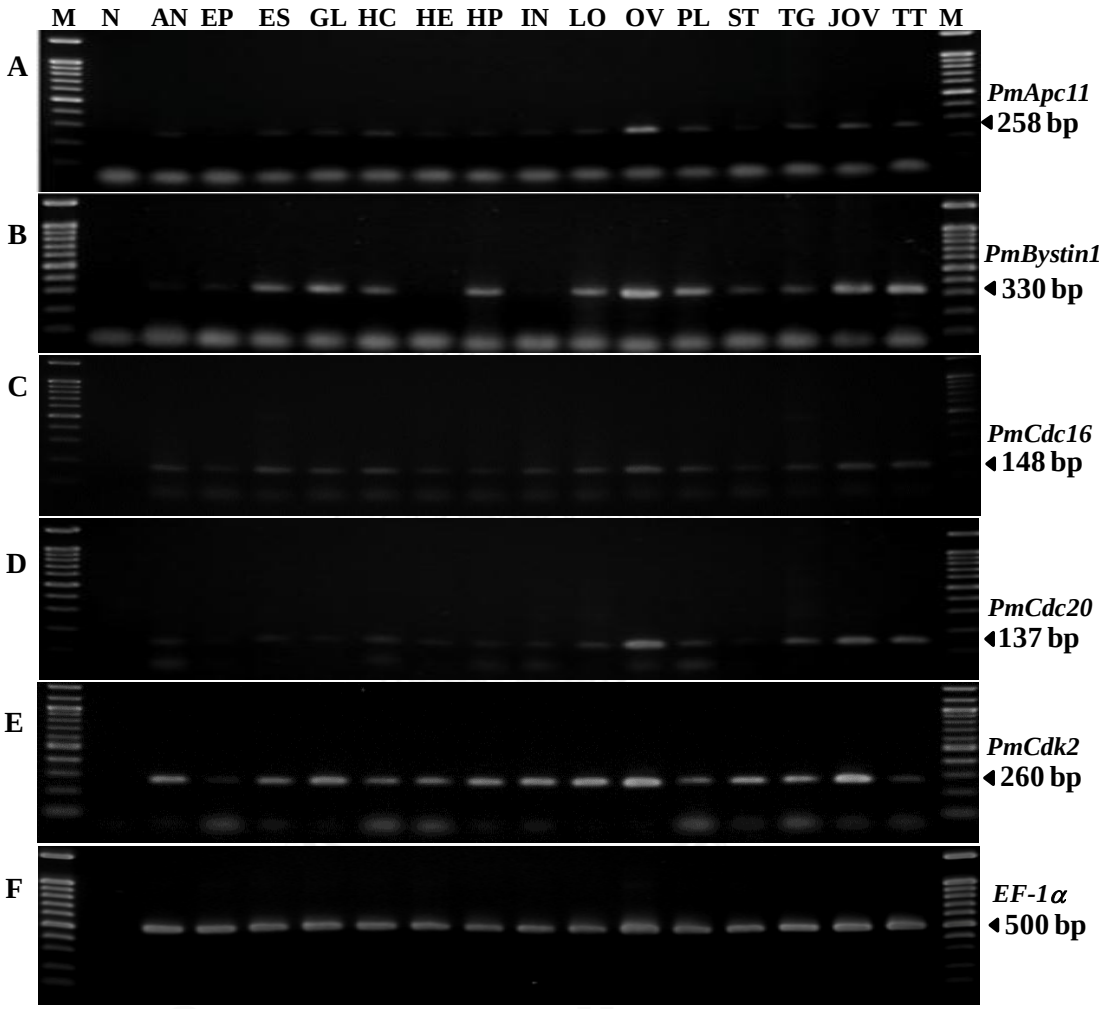

Figure 3. 23 Tissue distribution analysis of *PmApc11* (A)*, PmBystin1* (B)*, PmCdc16* (C)*, PmCdc20* (D) and *PmCdk2* (E). *EF-1α* (F) was successfully amplified from the same template. The first stand cDNA template was from various tissues of wild female *P. monodon* broodstock: antennal gland (AN), subcuticular epithelium (EP), eyestalk (ES), gills (GL), hemocytes (HC), heart (HE), hepatopancreas (HP), intestine (IN), lymphoid organs (LO), ovaries (OV), pleopods (PL), stomach (ST), and thoracic ganglion (TG), ovaries of juvenile (JOV) and testes (TT) of wild male broodstock. Lane M and N are a 100 bp DNA marker and the negative control (without cDNA template), respectively.

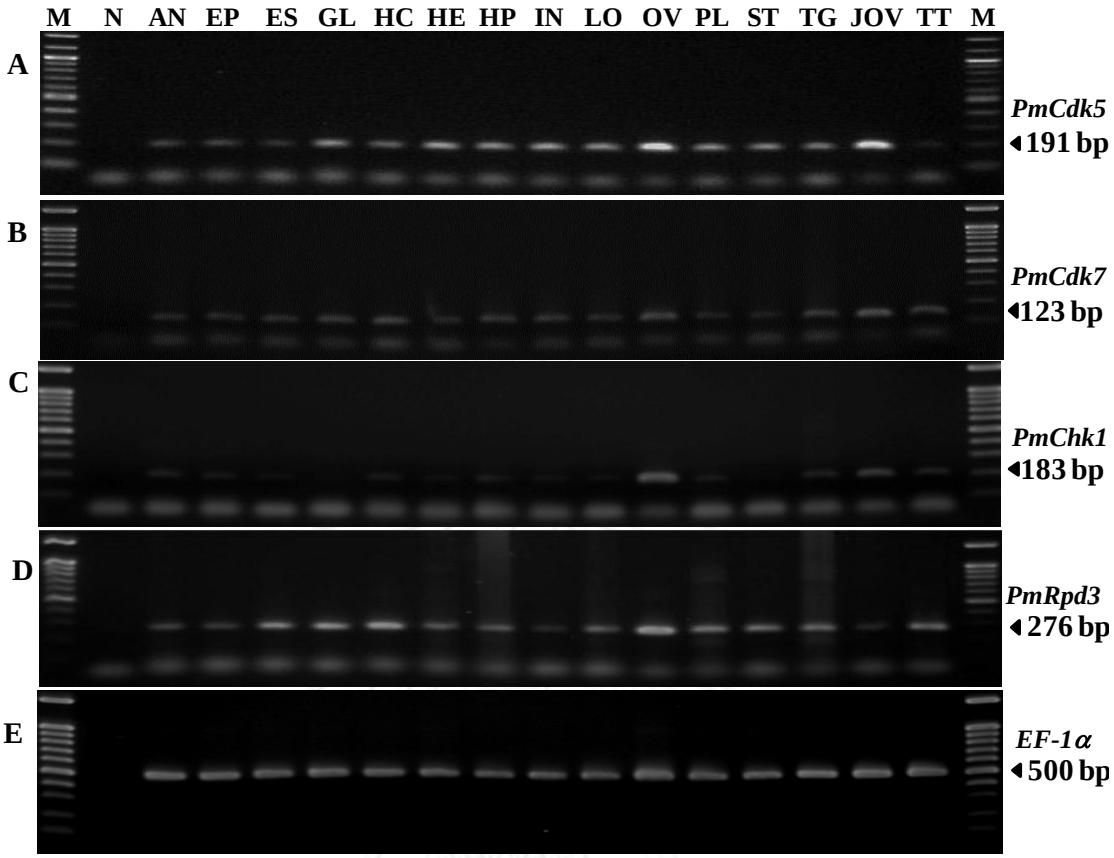

Figure 3. 24 Tissue distribution analysis of *PmCdk5* (A), *PmCdk7* (B), *PmChk1* (C) and *PmRpd3* (D). *EF-1α* (E) was successfully amplified from the same template. The first stand cDNA template was from various tissues of wild female *P. monodon* broodstock: antennal gland (AN), subcuticular epithelium (EP), eyestalk (ES), gills (GL), hemocytes (HC), heart (HE), hepatopancreas (HP), intestine (IN), lymphoid organs (LO), ovaries (OV), pleopods (PL), stomach (ST), and thoracic ganglion (TG), ovaries of juvenile (JOV) and testes (TT) of wild male broodstock. Lane M and N are a 100 bp DNA marker and the negative control (without cDNA template), respectively.

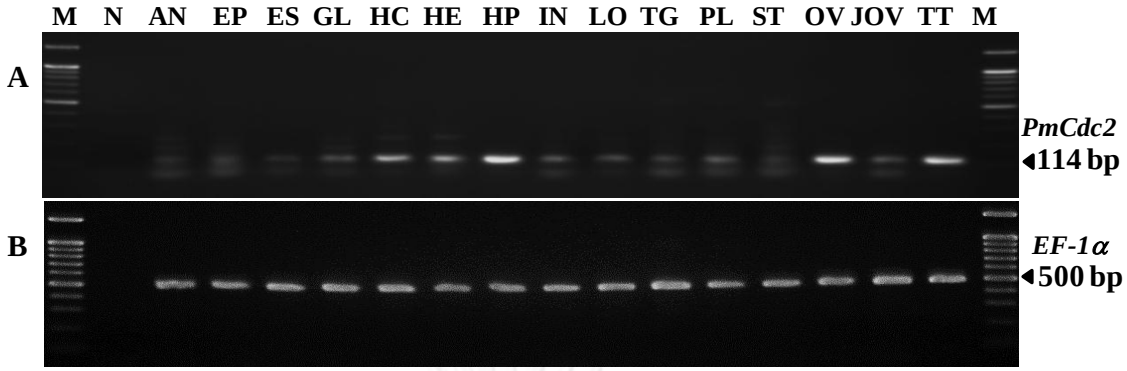

Figure 3. 25 Tissue distribution analysis of *PmCdc2* (A). *EF-1α* (B) was successfully amplified from the same template. The first stand cDNA template was from various tissues of wild female *P. monodon* broodstock: antennal gland (AN), subcuticular epithelium (EP), eyestalk (ES), gills (GL), hemocytes (HC), heart (HE), hepatopancreas (HP), intestine (IN), lymphoid organs (LO), thoracic ganglion (TG), pleopods (PL), stomach (ST), and ovaries (OV), ovaries of juvenile (JOV) and testes (TT) of wild male broodstock. Lane M and N are a 100 bp DNA marker and the negative control (without cDNA template), respectively.

3.3 Expression levels of cell cycle-regulating genes and reproduction-related genes during ovarian development of *P. monodon*

The expression levels of *PmBystin1, PmCdc2, PmCdc16, PmCdc2, PmCdk2, PmCdk7, PmChk1* and *PmRpd3* during ovarian development of *P. monodon* were examined by quantitative real-time PCR analysis. The standard curves of each target gene and the control (*EF-1*α) were constructed from 10-fold dilutions covering 10^3-10^8 copy numbers of *PmBystin1* and 10^2- 10^8 copy numbers of *PmCdc2*, *PmCdc16*, *PmCdk2*, *PmCdk7*, *PmChk1* and *PmRpd3* (Figure 3.26-3.27).

3.3.1 *PmBystin1*

The expression level of *PmBystin1* in ovaries of broodstock was greater than that in premature ovaries of juveniles ($P < 0.05$). In intact broodstock, the expression level of *PmBystin1* was significantly increased from stage I (previtellogenic) in stages II (vitellogenic) and III (early cortical rod), peaked in stage IV (mature) ovaries and slightly reduced after spawning ($P < 0.05$). In eyestalk-ablated broodstock, the expression level of *PmBystin1* was up-regulated from stages I-III ovaries in stage IV ovaries ($P < 0.05$). Its expression level during ovarian development in eyestalk-ablated broodstock (stages I–IV) was greater than that of the same ovarian stages in intact broodstock ($P < 0.05$; Figure 3.28).

3.3.2 *PmCdc2*

Quantitative real-time PCR revealed that the expression level of *PmCdc2* in ovaries of wild broodstock was greater than that of juveniles ($P < 0.05$). In wild intact broodstock, its expression level was significantly increased relative to stage I (previtellogenic) in stages II (vitellogenic) and III (early cortical rod) ovaries, further increased in stage IV (mature) ovaries ($P < 0.05$) and reduced to the basal level after spawning ($P > 0.05$). The expression level of *PmCdc2* in eyestalk-ablated broodstock was significantly increased from stage II in stage IV ovaries ($P < 0.05$). Moreover, the expression level of *PmCdc2* in stages I– IV ovaries of eyestalk-ablated broodstock was greater than that of the same ovarian stages in intact broodstock ($P < 0.05$, Figure 3.29).

-PmBystin1

Error: 0.0163
Efficiency: 1.999
Slope: -3.325
YIntercept: 37.49
Link: 10,150

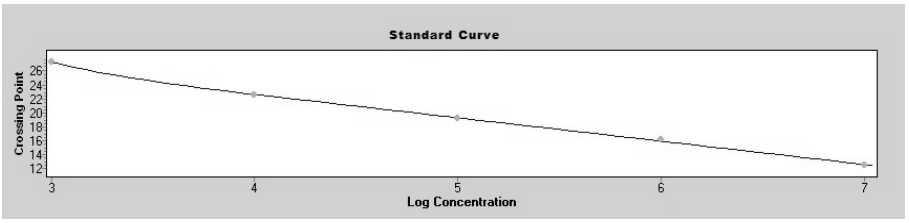

-PmCdc2

Error: 0.0142
Efficiency: 2.020
Slope: -3.275
YIntercept: 35.15
Link: 120.5

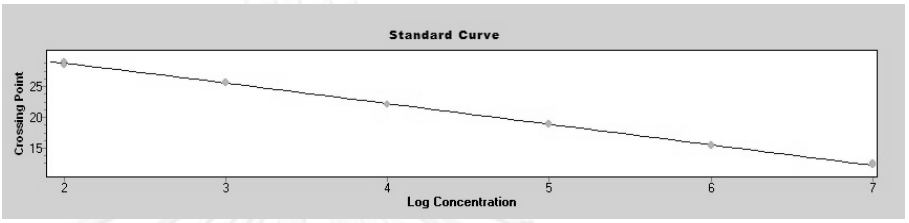

-PmCdc16

Error: 0.0105
Efficiency: 1.952
Slope: -3.441
YIntercept: 37.15
Link: 0.000

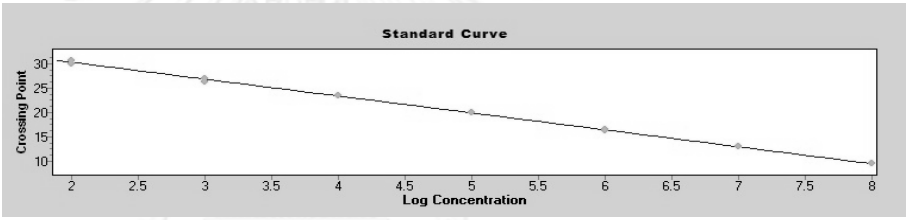

-PmCdk2

Error: 0.0225
Efficiency: 2.017
Slope: -3.282
YIntercept: 34.14
Link: 1,121

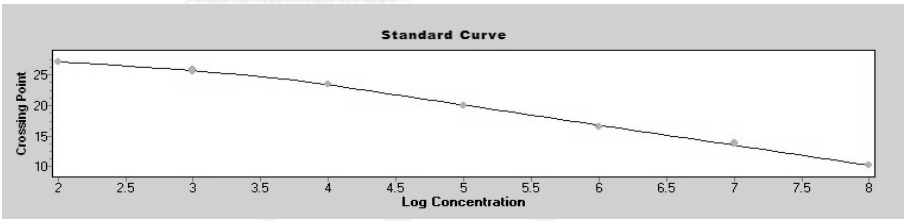

Figure 3. 26 Standard curves of *PmBystin1* (R^2 = 0.994, efficiency = 99.77% or (log_{10}) 1.999 and equation; Y = -3.325 * log(X) + 37.49), *PmCdc2* (R^2 = 1.000, efficiency = 104.71% or (log_{10}) 2.020 and equation; Y = -3.275 * log(X) + 35.15), *PmCdc16* (R^2 = 0.9998, efficiency = 89.54% or (log_{10}) 1.952 and equation; Y = -3.447 * log(X) + 37.15) and *PmCdk2* (R^2 = 0.987, efficiency = 103.99% or (log_{10}) 2.017 and equation; Y = -3.282 * log(X) + 34.14).

-PmCdk7

Error: 0.00771

Efficiency: 1.957

Slope: -3.430

YIntercept: 38.25

Link: 1,010

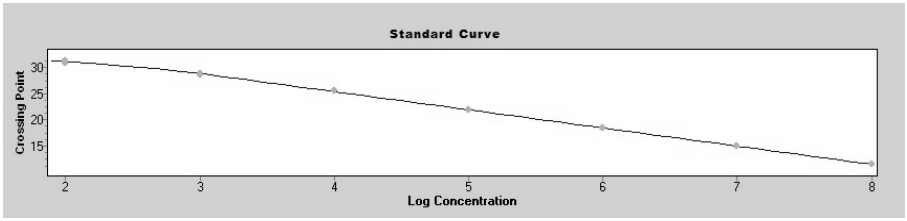

-PmChk1

Error: 0.0146

Efficiency: 1.998

Slope: -3.328

YIntercept: 35.23

Link: 832.1

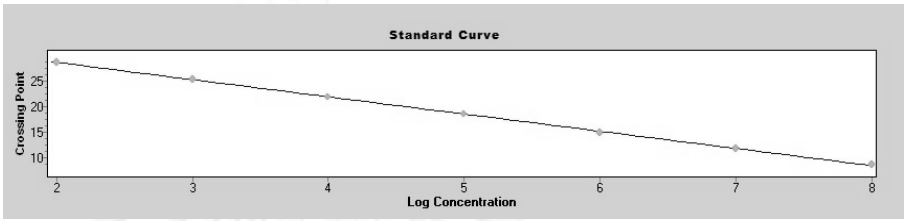

- PmRpd3

Error: 0.0164

Efficiency: 2.038

Slope: -3.235

YIntercept: 35.24

Link: 118.6

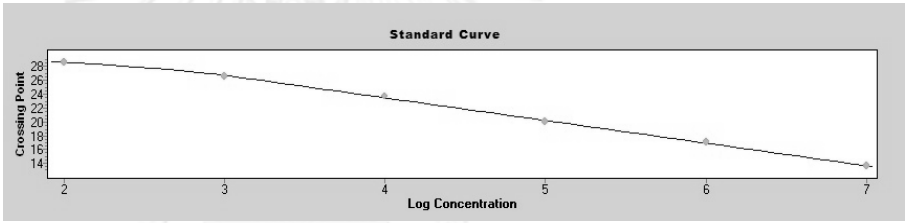

- EF-1α

Error: 0.00609

Efficiency: 1.969

Slope: -3.398

YIntercept: 38.74

Link: 9,793

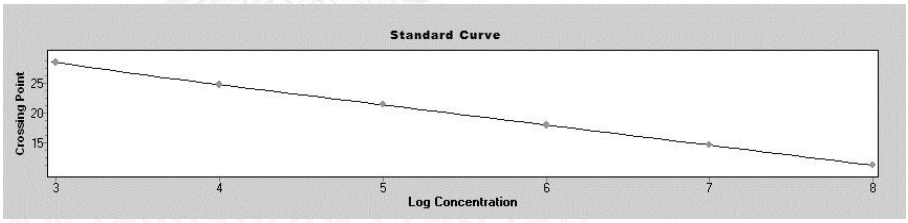

Figure 3. 27 Standard curves of *PmCdk7* (R^2 = 0.998, efficiency = 90.57% or (log_{10}) 1.957 and equation; Y = -3.430 * log(X) + 38.25), *PmChk1* (R^2 = 0.999, efficiency = 99.54% or (log_{10}) 1.998 and equation; Y = -3.328 * log(X) + 35.23), *PmRpd3* (R^2 = 0.995, efficiency = 109.14% or (log_{10}) 2.038 and equation; Y = -3.235 * log(X) + 35.24) and *EF-1α* (R^2 = 0.999, efficiency = 99.11% or (log_{10}) 1.969 and equation; Y = -3.398 * log(X) + 38.74).

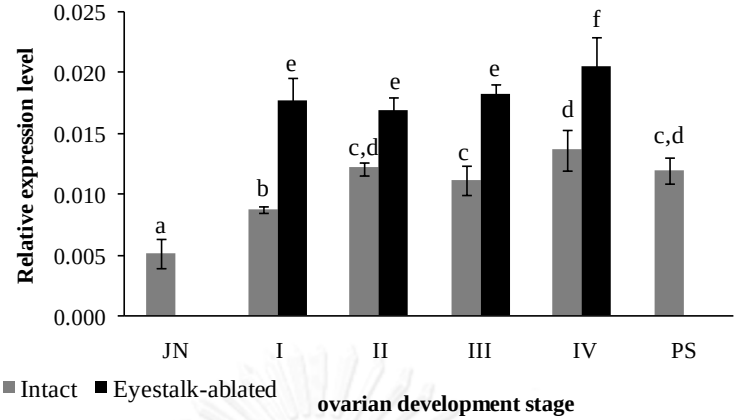

Figure 3. 28 Histograms showing the relative expression level of *PmBystin1* in ovaries of wild intact and eyestalk-ablated *P. monodon*. JN, cultured juveniles (4-month-old); I-IV, different stages of ovarian development (stage I, previtellogenic; II, vitellogenic; III, early cortical rod; IV, mature ovaries; PS, post-spawning broodstock). Bars indicated the standard deviation of the means. Expression levels were measured as the absolute copy number of *PmBystin1* mRNA (50 ng template) normalized by that of *EF-1*α (5 ng template). Each bar corresponds to a particular ovarian stage. The same letters indicate that the expression levels were not significantly different ($P > 0.05$).

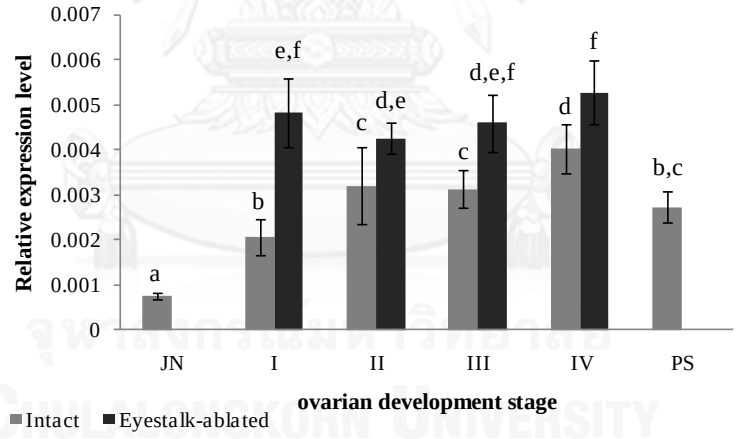

Figure 3. 29 Histograms showing the relative expression level of *PmCdc2* in ovaries of wild intact and eyestalk-ablated *P. monodon*. JN, cultured juveniles (4-month-old); stage I, previtellogenic; II, vitellogenic; III, early cortical rod; IV, mature ovaries; PS, post-spawning broodstock). Bars indicated the standard deviation of the means. Expression levels were measured as the absolute copy number of *PmCdc2* mRNA (50 ng template) normalized by that of *EF-1*α (5 ng template). Each bar corresponds to a particular ovarian stage. The same letters indicate that the expression levels were not significantly different ($P > 0.05$).

3.3.3 *PmCdc16*

PmCdc16 in ovaries of premature ovaries of juveniles was significantly greater than that of intact broodstock ($P < 0.05$). Its expression level was comparable during ovarian development in both wild intact and eyestalk-ablated broodstock (Figure 3.30)

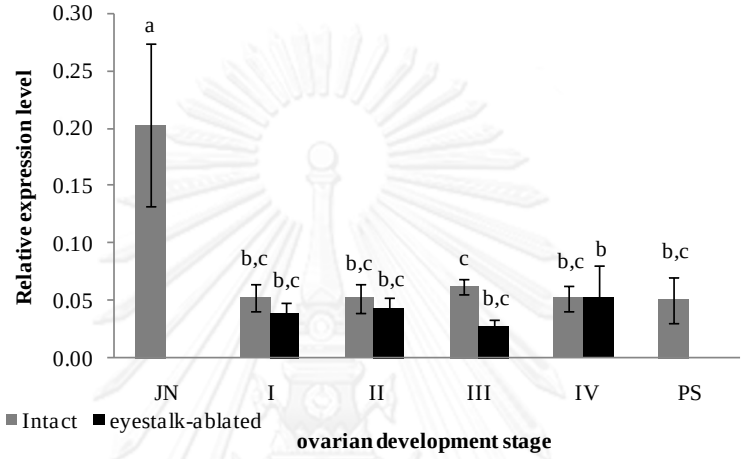

Figure 3. 30 Histograms showing the relative expression level of *PmCdc16* in ovaries of wild intact and eyestalk-ablated *P. monodon*. JN, cultured juveniles (4-month-old); I-IV, different stages of ovarian development (stage I, previtellogenic; II, vitellogenic; III, early cortical rod; IV, mature ovaries; PS, post-spawning broodstock). Bars indicated the standard deviation of the means. Expression levels were measured as the absolute copy number of *PmCdc16* mRNA (100 ng template) normalized by that of *EF-1*α (5 ng template). Each bar corresponds to a particular ovarian stage. The same letters indicate that the expression levels were not significantly different ($P > 0.05$).

3.3.4 *PmCdk2*

The expression level of *PmCdk2* in ovaries of broodstock was greater than that of in premature ovaries of juveniles ($P < 0.05$). In intact broodstock, the expression level of *PmCdk2* was significantly decreased from stages I (previtellogenic) and II (vitellogenic) in stages III (early cortical rod) and IV (mature) ovaries and significantly increased after spawning ($P < 0.05$). The expression level of *PmCdk2* in previtellogenic and vitellogenic ovaries of intact broodstock was greater than that of the same ovarian stages in eyestalk-ablated (Figure 3.31).

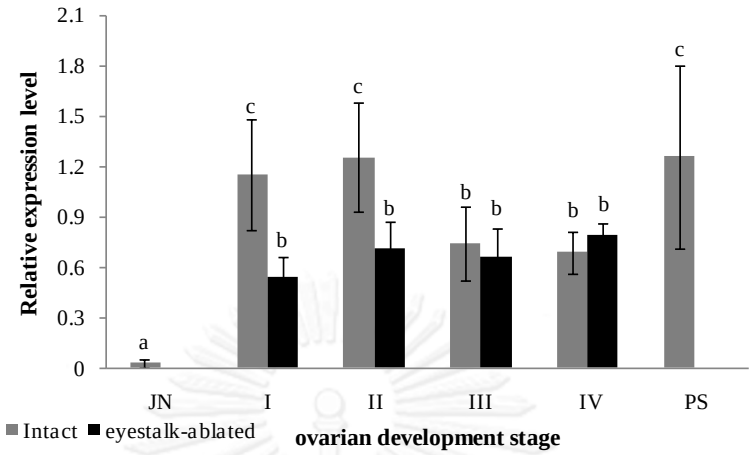

Figure 3. 31 Histograms showing the relative expression level of *PmCdk2* in ovaries of wild intact and eyestalk-ablated *P. monodon*. JN, cultured juveniles (4-month-old); I-IV, different stages of ovarian development (stage I, previtellogenic; II, vitellogenic; III, early cortical rod; IV, mature ovaries; PS, post-spawning broodstock). Bars indicated the standard deviation of the means. Expression levels were measured as the absolute copy number of *PmCdk2* mRNA (100 ng template) normalized by that of *EF-1*α (5 ng template). Each bar corresponds to a particular ovarian stage. The same letters indicate that the expression levels were not significantly different ($P > 0.05$).

3.3.5 *PmCdk7*

The expression level of *PmCdk7* in premature ovaries of juveniles was significantly lower than that in stage IV (mature) ovaries of non-ablated broodstock ($P < 0.05$). In intact broodstock, its expression level was significantly increased relative to stages I (previtellogenic) and II (vitellogenic) in stage IV (mature) ovaries ($P < 0.05$) and slightly reduced after spawning. The expression level of *PmCdk7* was earlier up-regulated in stage III ovaries compared to the previous stages of ovarian development in eyestalk-ablated broodstock ($P < 0.05$). Interesting, the expression level of *PmCdk7* during ovarian development of eyestalk-ablated shrimp was greater than that of the same ovarian stages in intact broodstock ($P < 0.05$, Figure 3.32).

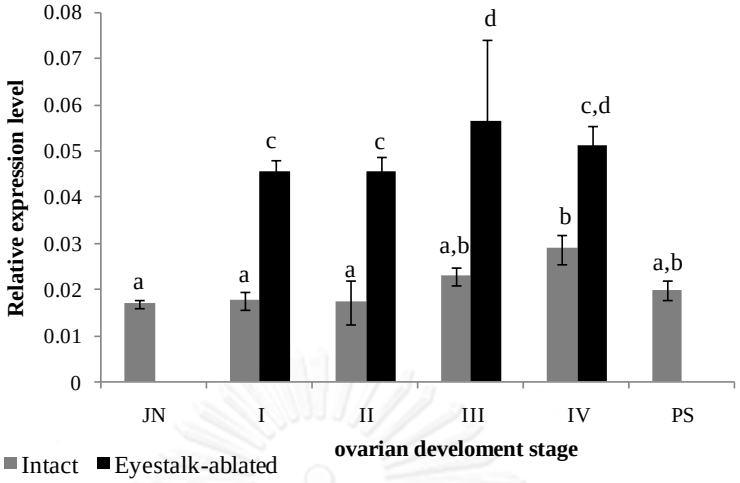

Figure 3. 32 Histograms showing the relative expression level of *PmCdk7* in ovaries of wild intact and eyestalk-ablated *P. monodon*. JN, cultured juveniles (4-month-old); I-IV, different stages of ovarian development (stage I, previtellogenic; II, vitellogenic; III, early cortical rod; IV, mature ovaries; PS, post-spawning broodstock). Bars indicated the standard deviation of the means. Expression levels were measured as the absolute copy number of *PmCdk7* mRNA (100 ng template) normalized by that of *EF-1α* (5 ng template). Each bar corresponds to a particular ovarian stage. The same letters indicate that the expression levels were not significantly different ($P > 0.05$).

3.3.6 *PmChk1*

Quantitative real-time PCR revealed that the expression level of *PmChk1* in ovaries of intact broodstock was greater than that in ovaries of 4-month-old juveniles ($P < 0.05$). The expression level of *PmChk1* was significantly increased relative to stage I (previtellogenic) in stages II (vitellogenic) and IV (mature) ovaries and its expression level was reduced in the basal level after spawning ($P < 0.05$). The expression level of *PmChk1* in stage II was greater than stage I ovaries of eyestalk-ablated broodstock. Its expression level in previtellogenic, vitellogenic, early cortical rod and mature (I–IV) ovaries of eyestalk-ablated broodstock was greater than that of the same ovarian stages in intact broodstock ($P < 0.05$, Figure 3.33).

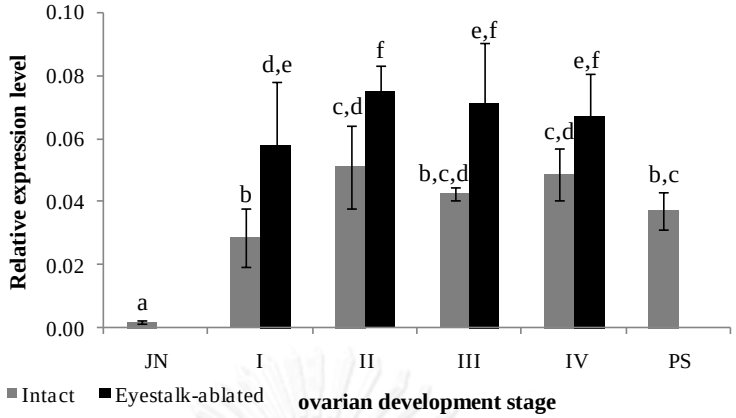

Figure 3. 33 Histograms showing the relative expression level of *PmChk1* in ovaries of wild intact and eyestalk-ablated *P. monodon*. JN, cultured juveniles (4-month-old); I-IV, different stages of ovarian development (stage I, previtellogenic; II, vitellogenic; III, early cortical rod; IV, mature ovaries; PS, post-spawning broodstock). Bars indicated the standard deviation of the means. Expression levels were measured as the absolute copy number of *PmChk1* mRNA (50 ng template) normalized by that of *EF-1*α (5 ng template). Each bar corresponds to a particular ovarian stage. The same letters indicate that the expression levels were not significantly different ($P > 0.05$).

3.3.7 *PmRpd3*

The expression level of *PmRpd3* in premature ovaries of juveniles was significantly lower than that of broodstock ($P < 0.05$). In intact broodstock, its expression level was significantly increased from stage I (previtellogenic) in stages II (vitellogenic), IV (mature) and V (post-spawning) ovaries ($P < 0.05$). The expression level of *PmRpd3* was comparable during ovarian development in eyestalk-ablated broodstock. Unlike other transcripts in this study, the expression level of *PmRpd3* in vitellogenic and mature (II–IV) ovaries of intact broodstock was greater than that of the same ovarian stages in eyestalk-ablated broodstock ($P < 0.05$, Figure 3.34).

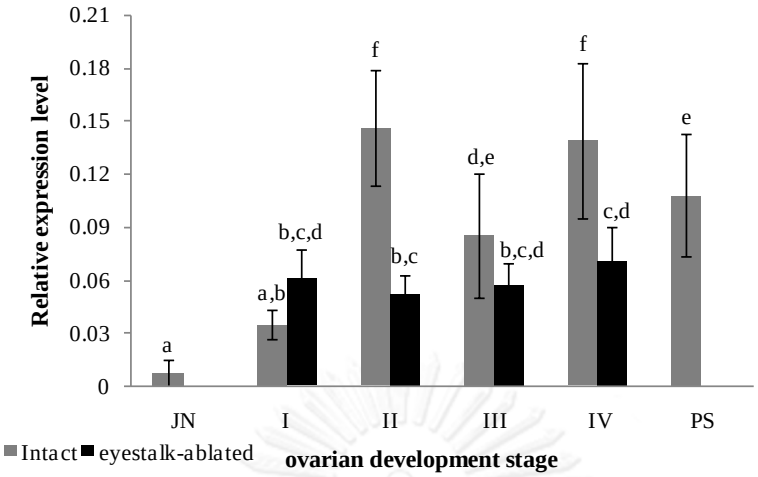

Figure 3. 34 Histograms showing the relative expression level of *PmRpd3* in ovaries of wild intact and eyestalk-ablated *P. monodon*. JN, cultured juveniles (4-month-old); I-IV, different stages of ovarian development (stage I, previtellogenic; II, vitellogenic; III, early cortical rod; IV, mature ovaries; PS, post-spawning broodstock). Bars indicated the standard deviation of the means. Expression levels were measured as the absolute copy number of *PmRpd3* mRNA (50 ng template) normalized by that of *EF-1α* (5 ng template). Each bar corresponds to a particular ovarian stage. The same letters indicate that the expression levels were not significantly different ($P > 0.05$).

3.4 *In vivo* effect of serotonin (5-HT) treatment on transcription of *PmBystin1*, *PmCdc2* and *PmCdk7* in ovaries *P. monodon*.

Effects of exogenous 5-HT injection on the expression level of *PmBystin1, PmCdc2* and *PmCdk7* in ovaries of 18-month-old domesticated *P. monodon* were examined.

The expression level of *PmBystin1* was significantly increased from the vehicle control at 6 - 48 hours post injection (hpi) ($P < 0.05$; Figure 3.35) while *PmCdc2* was immediately up-regulated at 1 hpi ($P < 0.05$) and returned to the normal level at 3 - 48 hpi (Figure 3.36). The expression level of *PmCdk7* was significantly increased at 6 and 12 hpi ($P < 0.05$) and reduced to the previous level at 24 and 48 hpi ($P > 0.05$; Figure 3.37).

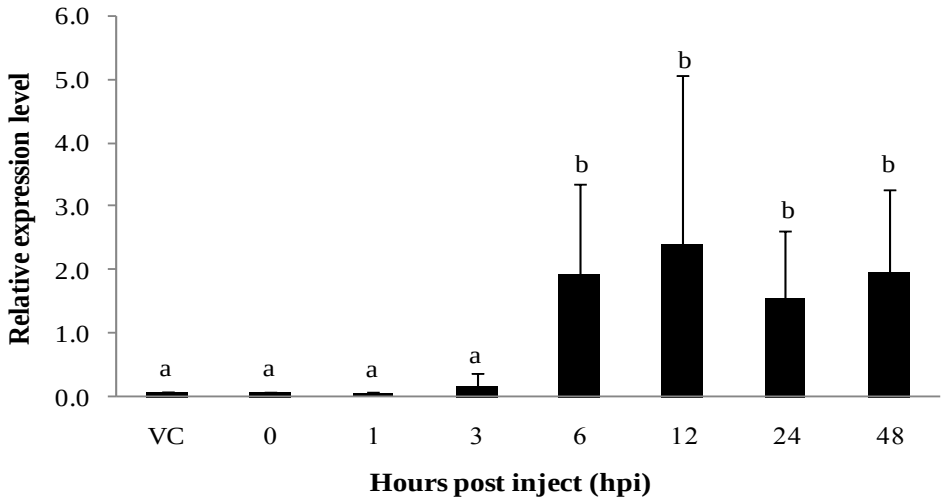

Figure 3. 35 Time-course relative expression levels of *PmBystin1* in ovaries of domesticated shrimp at 0, 1, 3, 6, 12, 24 and 48 hours post injection (hpi) of 5-HT (50 µg/g body weight; 18-month-old, *N* = 4 for each stage). Shrimp injected with 0.85% saline solution at 0 hpi were included as the vehicle control (VC). Bars indicated the standard deviation of the means. The same letters above bars indicate that the expression levels were not significantly different ($P > 0.05$).

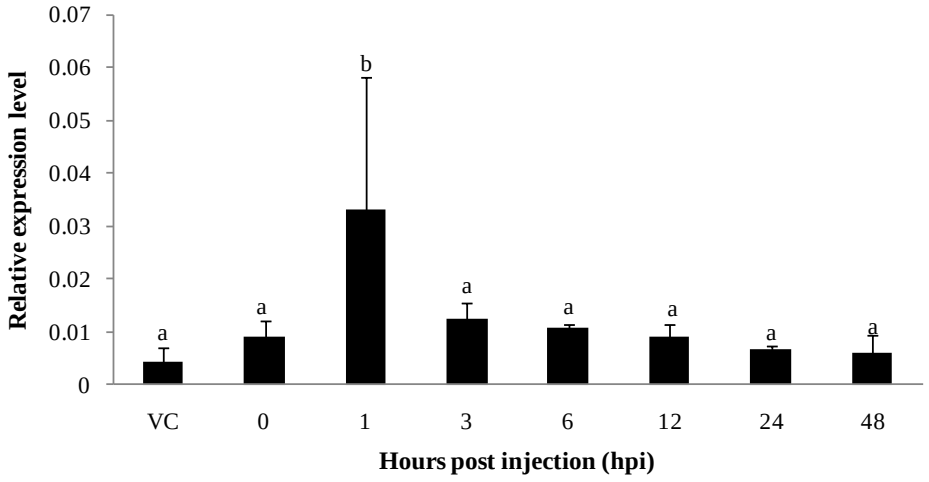

Figure 3. 36 Time-course relative expression levels of *PmCdc2* in ovaries of domesticated shrimp at 0, 1, 3, 6, 12, 24 and 48 hours post injection (hpi) of 5-HT (50 µg/g body weight; 18-month-old, *N* = 4 for each stage). Shrimp injected with 0.85% saline solution at 0 hpi were included as the vehicle control (VC). Bars indicated the standard deviation of the means. The same letters above bars indicate that the expression levels were not significantly different ($P>0.05$).

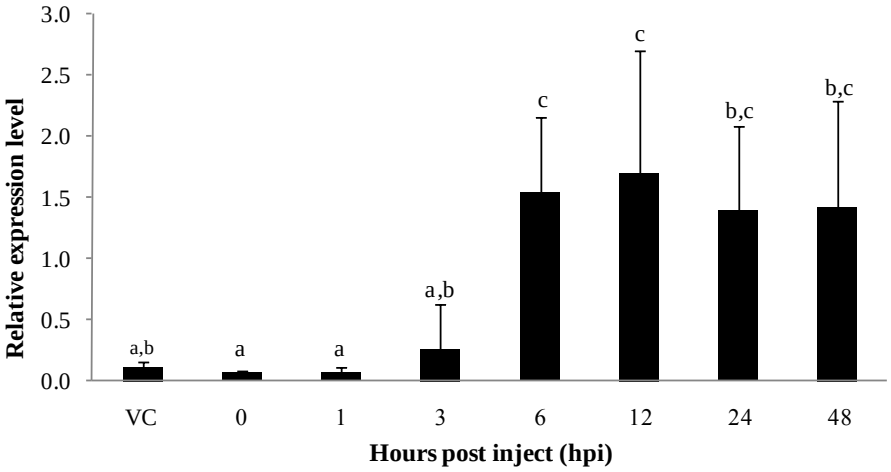

Figure 3. 37 Time-course relative expression levels of *PmCdk7* in ovaries of domesticated shrimp at 0, 1, 3, 6, 12, 24 and 48 hours post injection (hpi) of 5-HT (50 µg/g body weight; 18-month-old, *N* = 4 for each stage). Shrimp injected with 0.85% saline solution at 0 hpi were included as the vehicle control (VC). Bars indicated the standard deviation of the means. The same letters above bars indicate that the expression levels were not significantly different ($P > 0.05$).

3.5 *In vitro* effects of 5-HT and 17α, 20β-dihydroxyprogesterone (17α, 20β-DHP) treatment on transcription of *PmCdc2* in ovaries *P. monodon*

3.5.1 Histology of ovarian organ culture

Conditions for organ culture of *P. monodon* ovaries was preliminary carried out. Previtellogenic ovaries were dissected out from wild females and incubated with M199 or L15 in a CO_2 incubator (5%) at 28°C for 0, 24 and 48 hr. Results indicated morphology of oocytes seemed to be normal when incubated in the M199 medium. However, oocytes seemed to be degenerated when incubated with L15 for 24 and 48 hr. As a result, M199 was selected for determining effects of *in vitro* treatment of 17α, 20β-DHP (Figure 3.38) and serotonin (see below). Three doses of 17α, 20β-DHP (0.1, 1.0 and 10.0 µg/ml) was applied and the tissues were incubated for 0, 1, 3, 6, 12 and 24 hr. Specimens for the conventional histology were collected at 0 and 24 hr post treatment (hpt). Morphological characters of previtellogenic oocytes seemed to be normal in the control but abnormality of oocyte cells were observed at 24 hpt of each treatment dose (Figure 3.39).

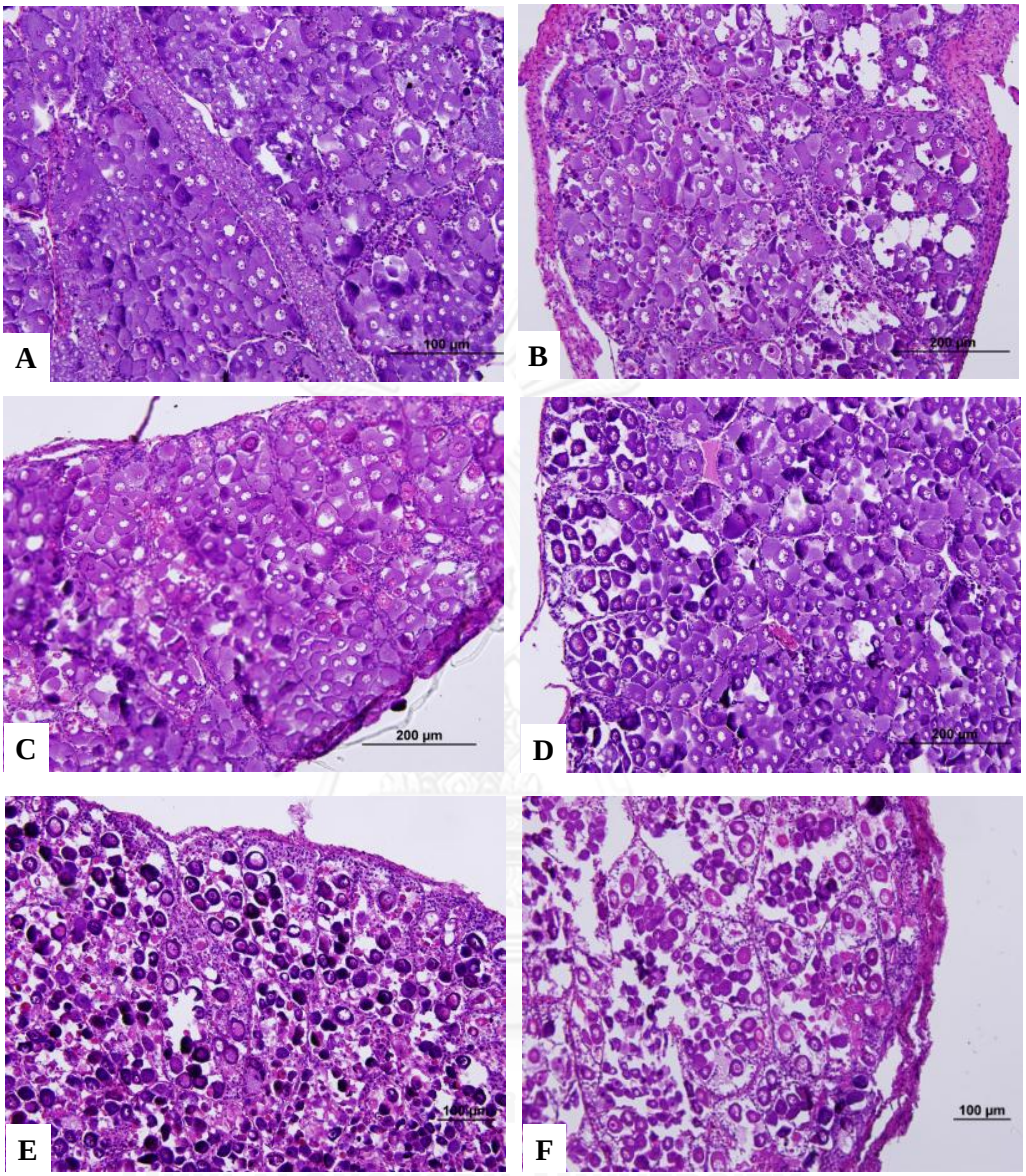

Figure 3. 38 Conventional histology (hematoxylin and eosin staining) of cultured ovarian explants of previtellogenic ovaries of *P. monodon* before (normal, A and D) and after incubated with M199 at 24 and 48 hr (B and C) in a 5% CO_2 incubator at 28°C and after incubated with L15 at 24 and 48 hr (E and F) in a 5% CO_2 incubator at 28°C.

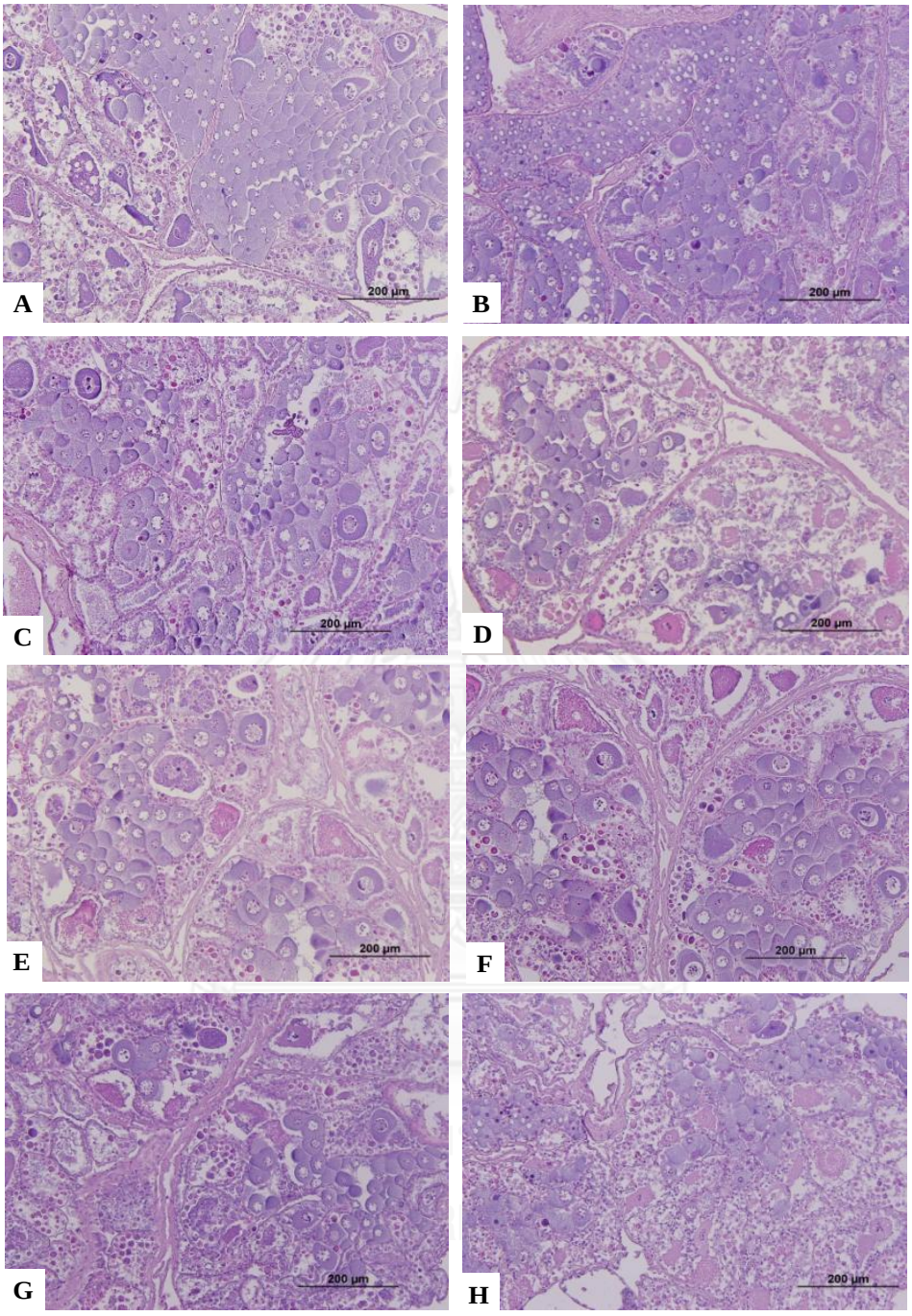

Figure 3. 39 Conventional histology (hematoxylin and eosin staining) of cultured ovarian explants of previtellogenic ovaries of *P. monodon* before (normal, A) and after incubated with M199 containing absolute ethanol at 0 hr (vehicle control, B) and M199 containing 0.1 µg/ml 17α, 20β-DHP at 0 and 24 hr (C and D), 1.0 µg/ml 17α, 20β-DHP at 0 and 24 hr (E and F) and 10 µg/ml 17α, 20β-DHP at 0 and 24 hr (G and H).

3.5.2 The expression level of *PmCdc2* in cultured ovarian explants under 17α, 20β-DHP and 5-HT treatment

The expression level of *PmCdc2* in cultured ovarian explants treated with different concentrations of 17α, 20β-DHP (0.1, 1.0 and 10.0 μg/ml) was examined. The preliminary results did not show significant effects of 17α, 20β-DHP treatment at these concentrations ($P > 0.05$, Figure 3.40). Similarly, treatment of 5-HT (1.0 and 15.0 μg/ml) did not affect the expression of *PmCdc2 in vitro* ($P > 0.05$, Figure 3.41).

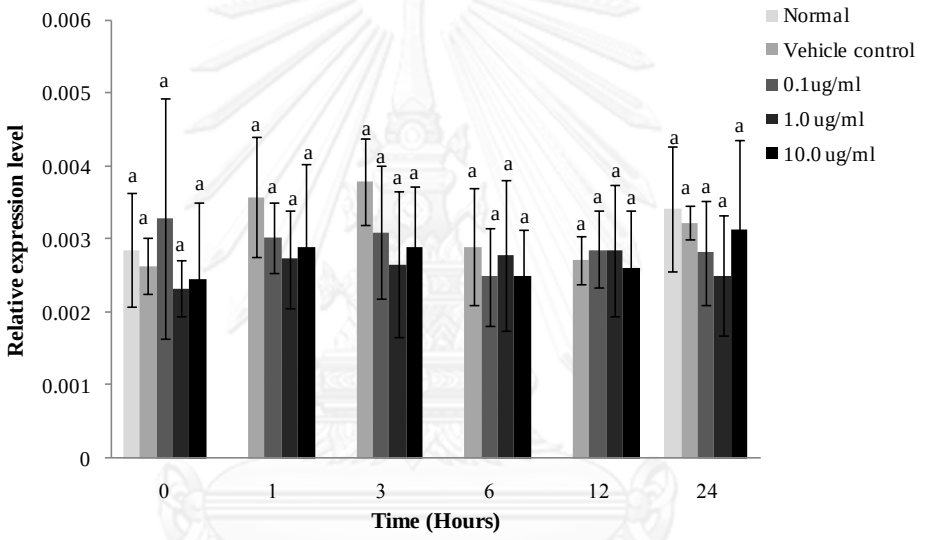

Figure 3. 40 Histograms showing the expression profile of *PmCdc2* in ovaries at different time intervals after treated with different concentrations of 17α, 20β-DHP (0.1, 1.0 and 10.0 μg/ml, $N = 4$ for each group). Ovarian tissues incubated with ethanol were included as the vehicle control (VC). Bars indicated the standard deviation of the means. The same letters above bars indicate that the expression levels were not significantly different ($P > 0.05$).

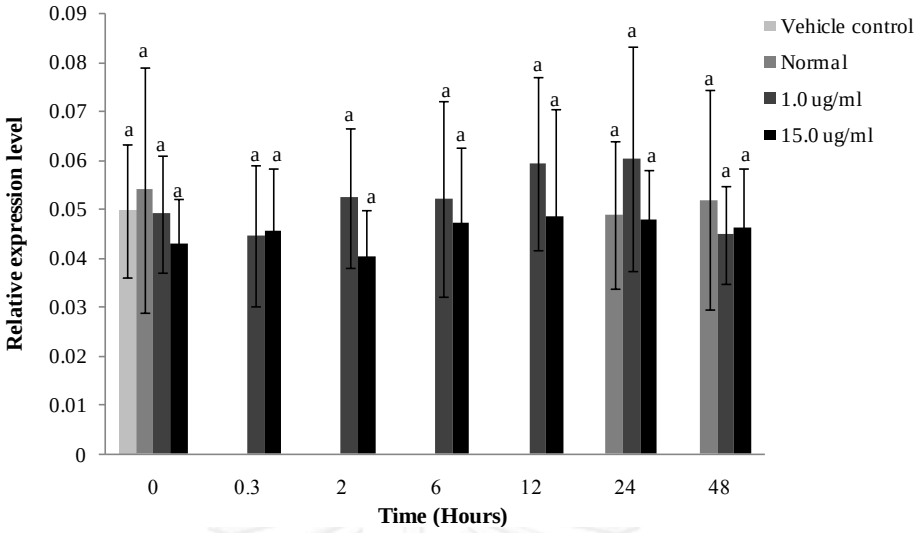

Figure 3. 41 Histograms showing the expression profile of *PmCdc2* in ovaries at different time intervals after treated with different concentrations of 5-HT (1.0 and 15.0 µg/ml, *N* = 3 for each group). Ovarian tissues incubated with 0.85% NaCl were included as the vehicle control (VC). Bars indicated the standard deviation of the means. The same letters above bars indicate that the expression levels were not significantly different (*P* > 0.05).

3.6 Localization of *PmBystin1*, *PmCdc2* and *PmCdk7* transcripts during ovarian development of *P. monodon*

3.6.1 Preparation of a specific RNA probe

RT-PCR of *PmBystin1, PmCdc2* and *PmCdk7* was carried out using the first strand cDNA from ovaries of *P. monodon* broodstock as the template. The purified PCR product of each gene was used for synthesis of sense and antisense cRNA probes (Figure 3.43-3.45, A and B). Dot blot hybridization was carried out for the estimation of the probes obtained. The antisense and sense probes of *PmBystin1* gave the signal lower than 1 ng/µl relative to the control (Figure 3.53C). The amount of *PmCdc2* and *PmCdk7* cRNA probe was approximately 1 ng/µl but that of the antisense probes was lower than 1 ng/µl (Figure 3.54C and 3.55C).

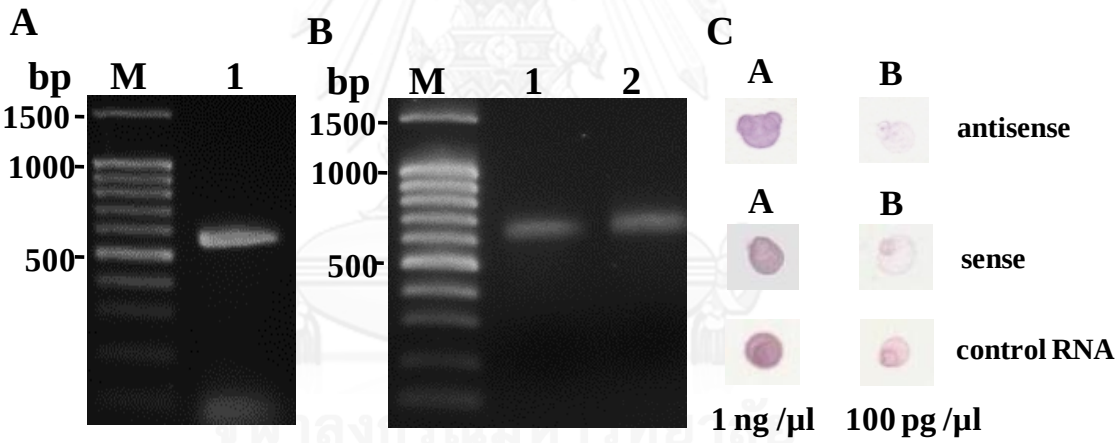

Figure 3. 42 (A) 1.5% ethidium bromide-stained agarose gels showing the RT-PCR product used as the template for synthesis of the sense and antisense cRNA probes of *PmBystin1*. (B) The synthesized antisense (lane 1, B) and sense (lane 2, B) cRNA probes. Lanes M are a 100 bp DNA ladder. (C) The concentration of the antisense and sense *PmBystin1* probes were determined against the control RNA probe by dot blot analysis. (A = 1 ng/µl; B = 100 pg/µl).

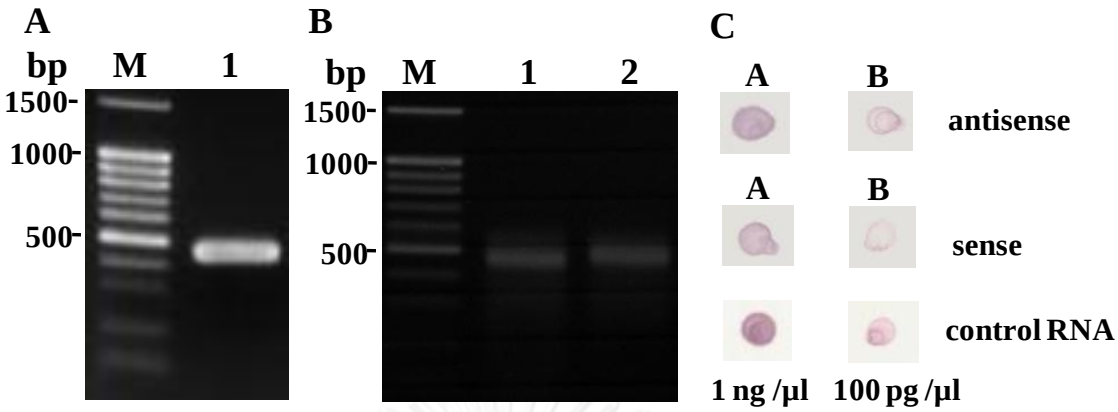

Figure 3. 43 (A) 1.5% ethidium bromide-stained agarose gels showing the RT-PCR product used as the template for synthesis of the sense and antisense cRNA probes of *PmCdc2*. (B) The synthesized antisense (lane 1, B) and sense (lane 2, B) cRNA probes. Lanes M are a 100 bp DNA ladder. (C) The concentration of the antisense and sense *PmCdc2* probes were determined against the control RNA probe by dot blot analysis. (A = 1 ng/µl; B = 100 pg/µl).

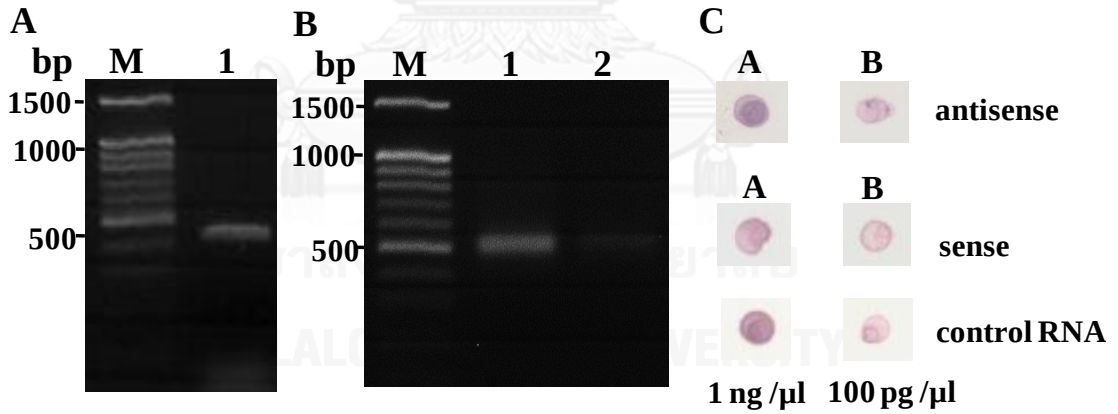

Figure 3. 44 (A) 1.5% ethidium bromide-stained agarose gels showing the RT-PCR product used as the template for synthesis of the sense and antisense cRNA probes of *PmCdk7*. (B) The synthesized antisense (lane 1, B) and sense (lane 2, B) cRNA probes. Lanes M are a 100 bp DNA ladder. (C) The concentration of the antisense and sense *PmCdk7* probes were determined against the control RNA probe by dot blot analysis. (A = 1 ng/µl; B = 100 pg/µl).

3.6.2 *In situ* hybridization (ISH)

Localization of *PmBystin1* in ovaries of wild intact broodstock of *P. monodon* was determined by *in situ* hybridization. The positive signal was observed in ooplasm of previtellogenic and vitellogenic oocytes but not in oogonia and more mature stages of oocytes. No signal was observed with the sense probe (Figure 3.46).

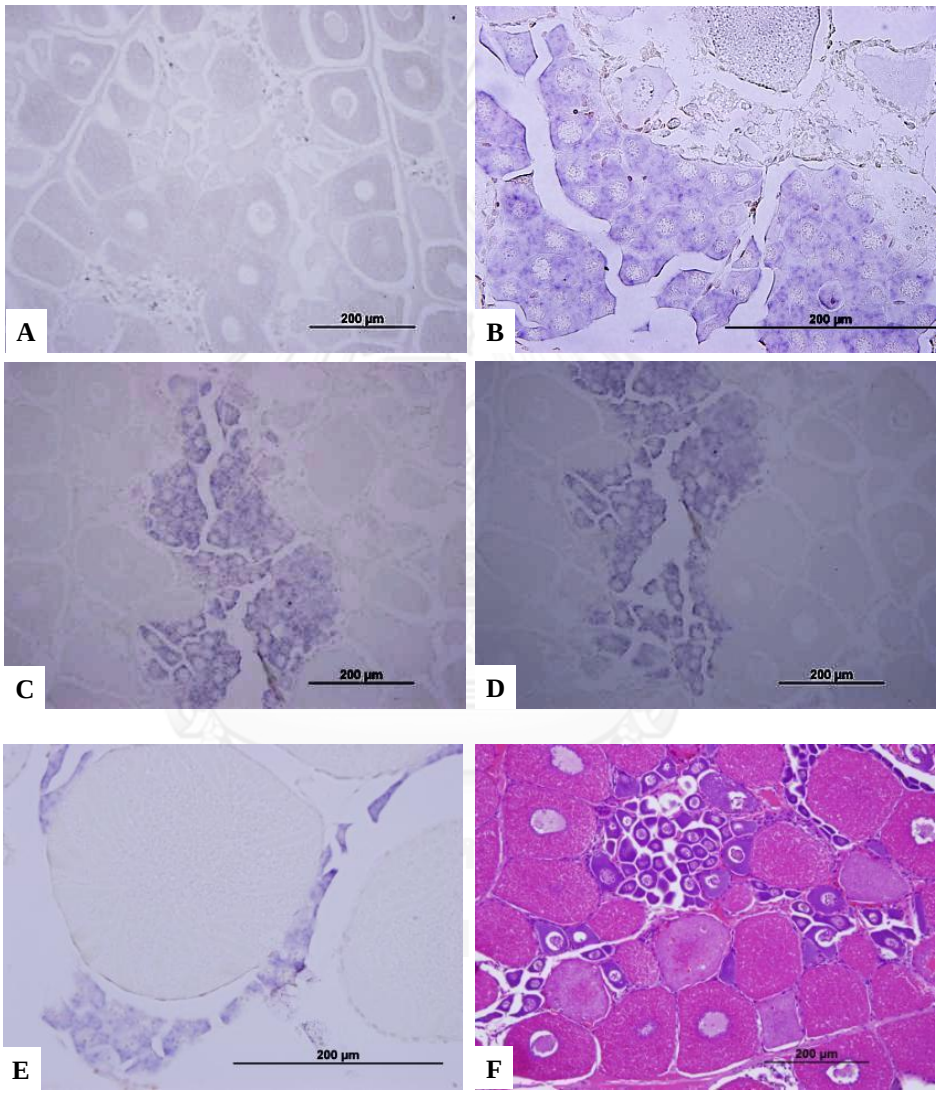

Figure 3. 45 Localization of *PmBystin1* transcript during ovarian development of intact *P. monodon* shrimp visualized by *in situ* hybridization using antisense (B-E) and sense probes (the control; A). Hematoxylin and eosin staining was carried out for identification of oocyte stages (F).

Localization of *PmCdc2* and *PmCdk7* transcripts was examined in both intact and eyestalk-ablated broodstock. The positive signals were observed in ooplasm of previtellogenic oocytes but not in vitellogenic, early cortical rod, and mature oocytes of both intact and eyestalk-ablated broodstock. No signal was found with the sense cRNA probe (Figure 3.47-3.50).

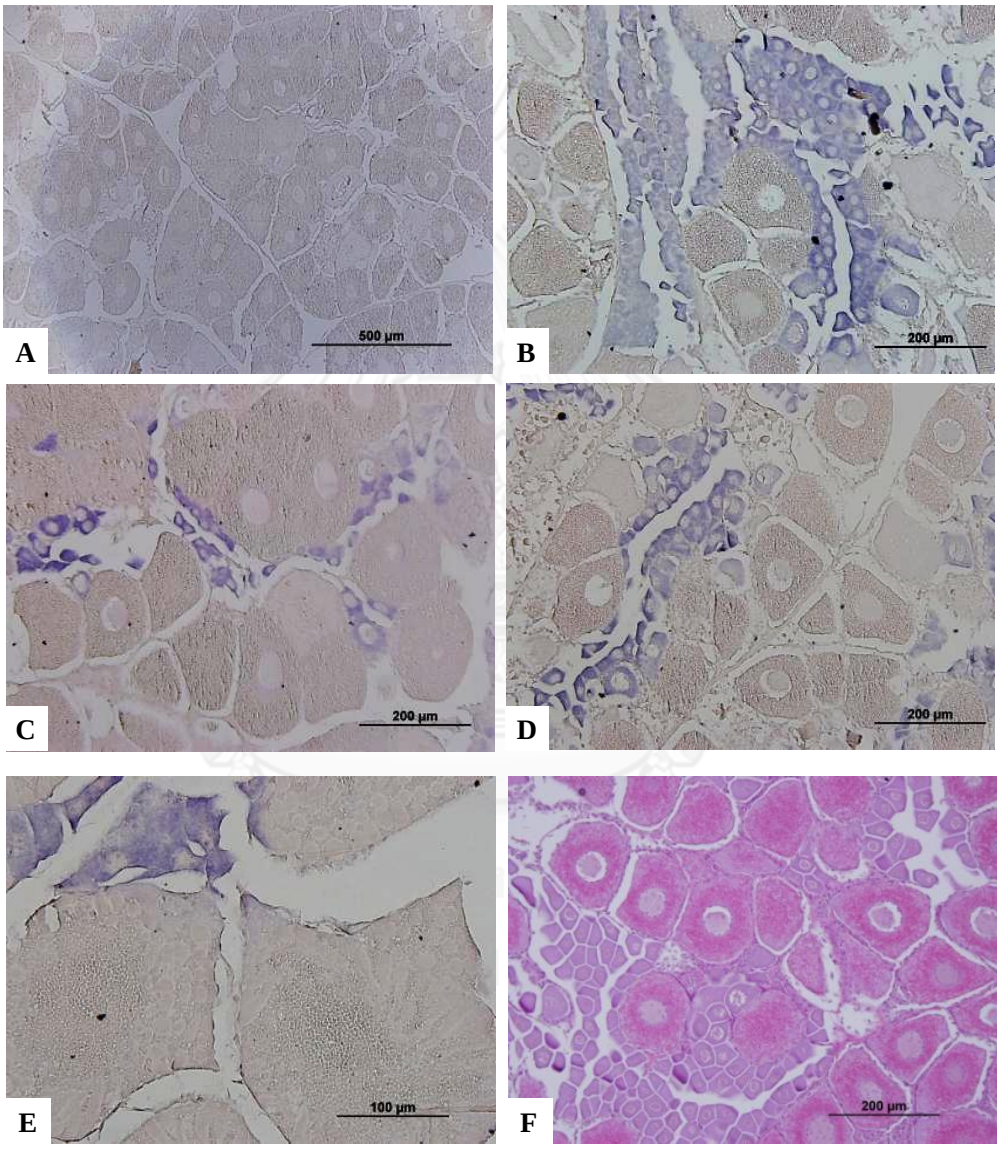

Figure 3. 46 Localization of *PmCdc2* transcript during ovarian development in intact *P. monodon* visualized by *in situ* hybridization using antisense (B-E). The sense probe (A) was included as the control. Hematoxylin and eosin staining was carried out for identification of oocyte stages (F).

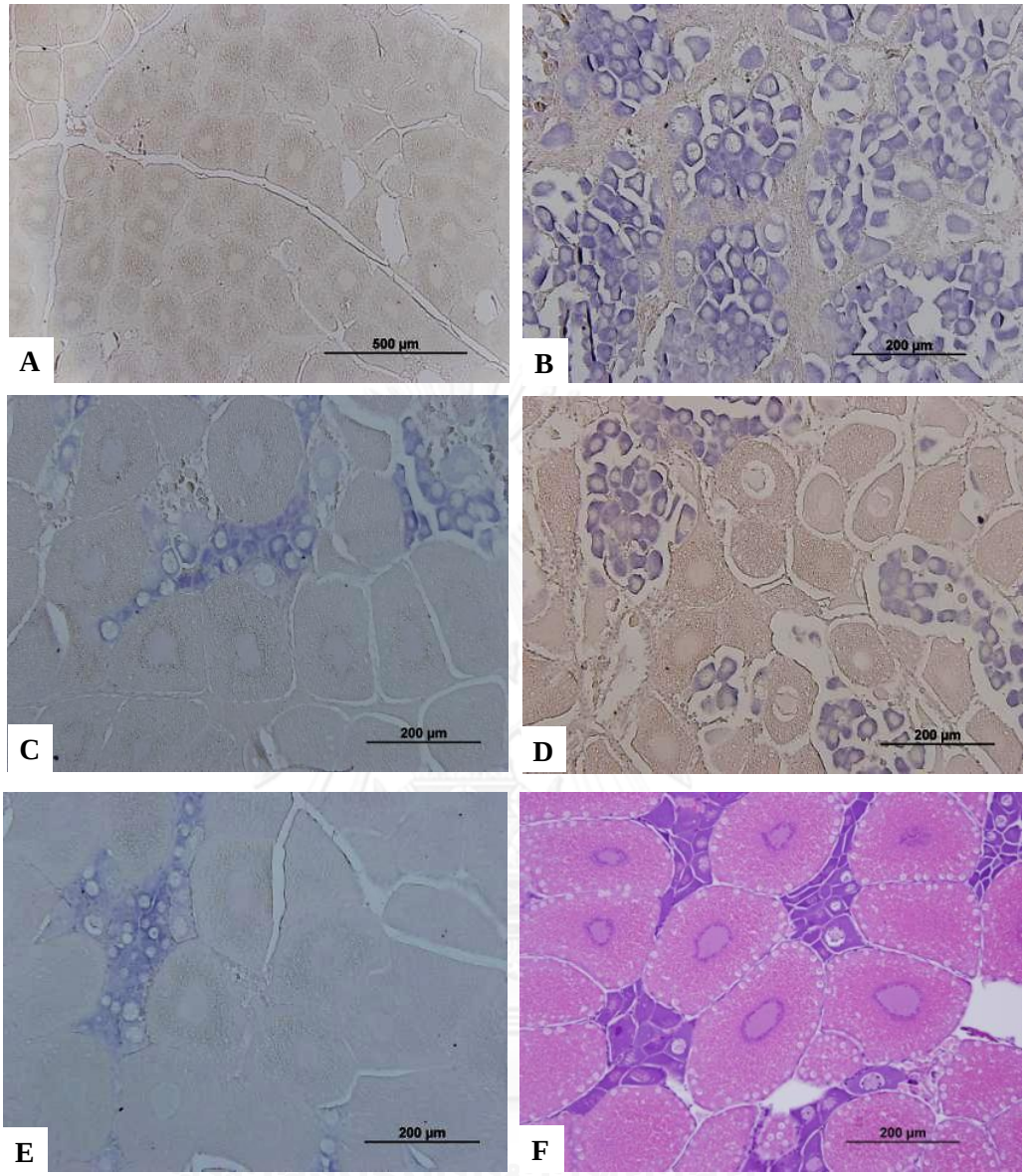

Figure 3. 47 Localization of *PmCdc2* transcript during ovarian development of eyestalk-ablated *P. monodon* visualized by *in situ* hybridization using antisense (B-E). The sense probes (A) was used as the control. (F) Hematoxylin and eosin staining was carried out for identification of oocyte stages.

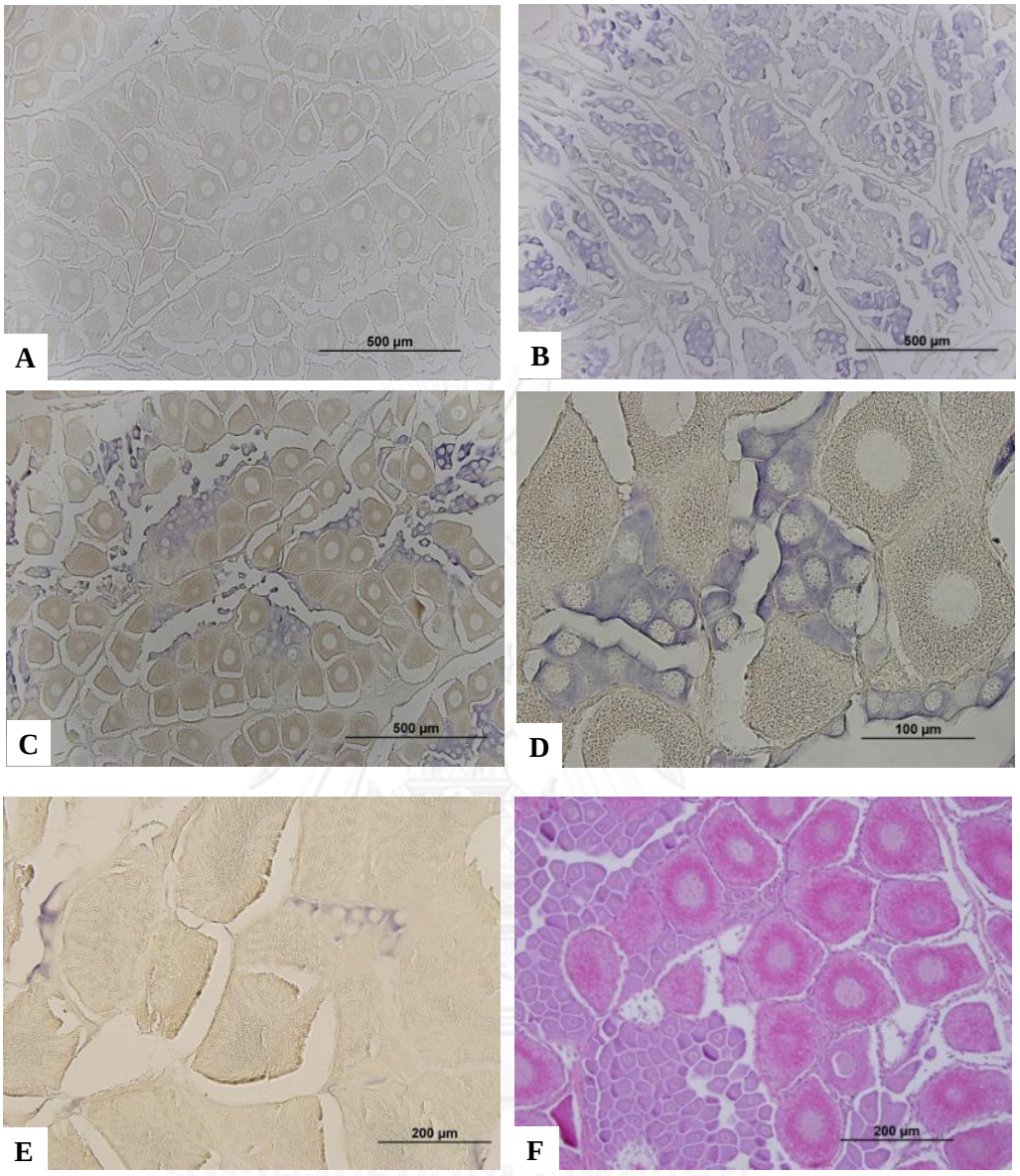

Figure 3. 48 Localization of *PmCdk7* transcript during ovarian development of intact *P. monodon* visualized by *in situ* hybridization using antisense (B-E). The sense probe (A) was used as the control. Hematoxylin and eosin staining was carried out for identification of oocyte stages (F).

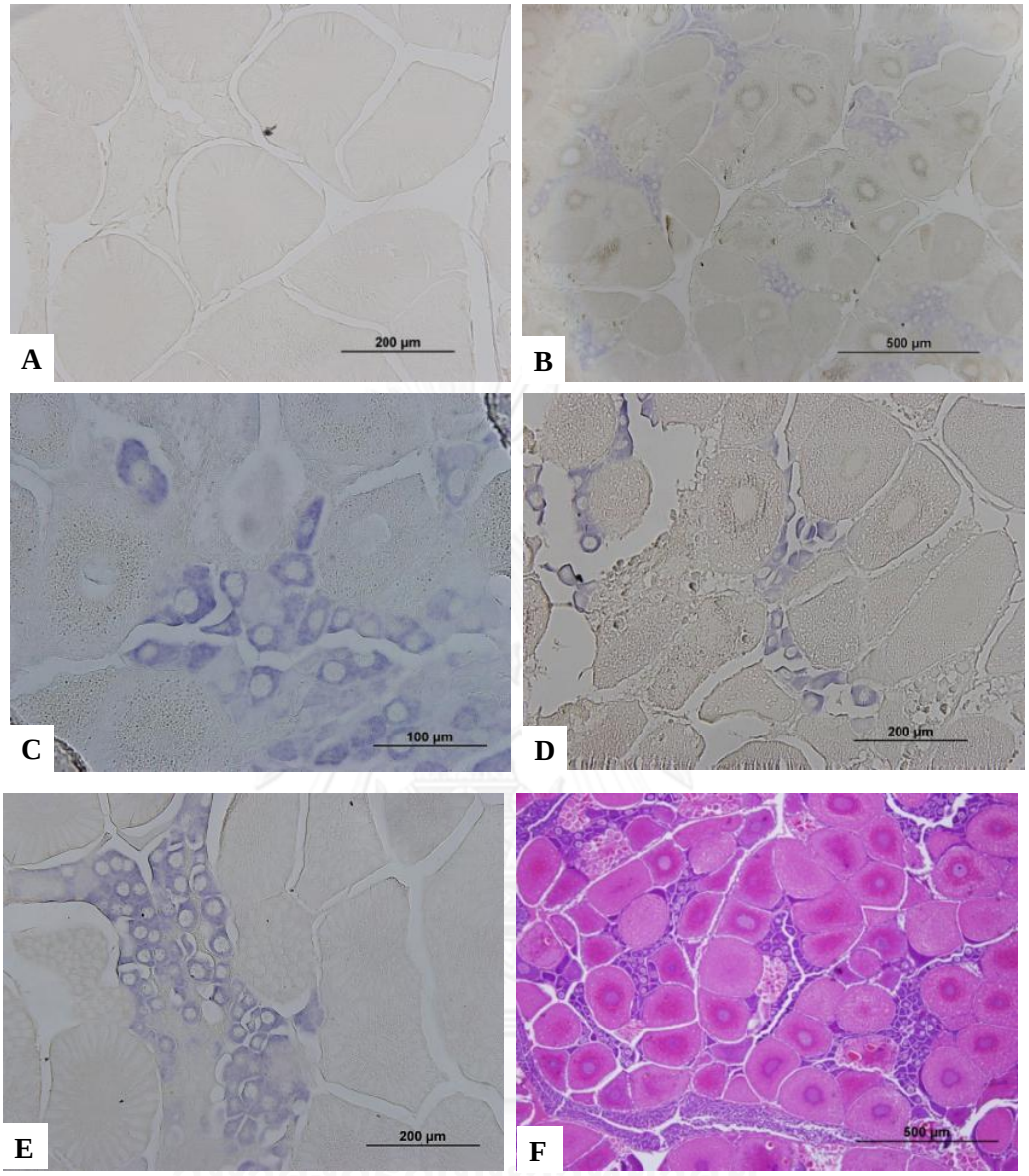

Figure 3. 49 Localization of *PmCdk7* transcript during ovarian development of eyestalk-ablated *P. monodon* visualized by *in situ* hybridization using antisense (B-E) and sense probes (A) used as the control. Hematoxylin and eosin staining was carried out for identification of oocyte stages (F).

3.7 *In vitro* expression of recombinant PmApc11, PmBystin1, PmCdc2, PmCdc20, PmCdk7, PmChk1 and PmRpd3 proteins using the bacterial expression system

3.7.1 Amplification of the insert

A pair of primers for amplification of the complete ORF of *PmApc11*, *PmBystin1*, *PmCdc2*, *PmCdc20*, *PmCdk7*, *PmChk1* and a partial coding sequence covering a function domain of *PmRpd3* was designed. The amplified product of each transcript (Figure 3.50) was ligated to pGEM® -T easy vector and transformed into *Escherichia coli* JM109. The plasmid DNA was extracted and used the template for

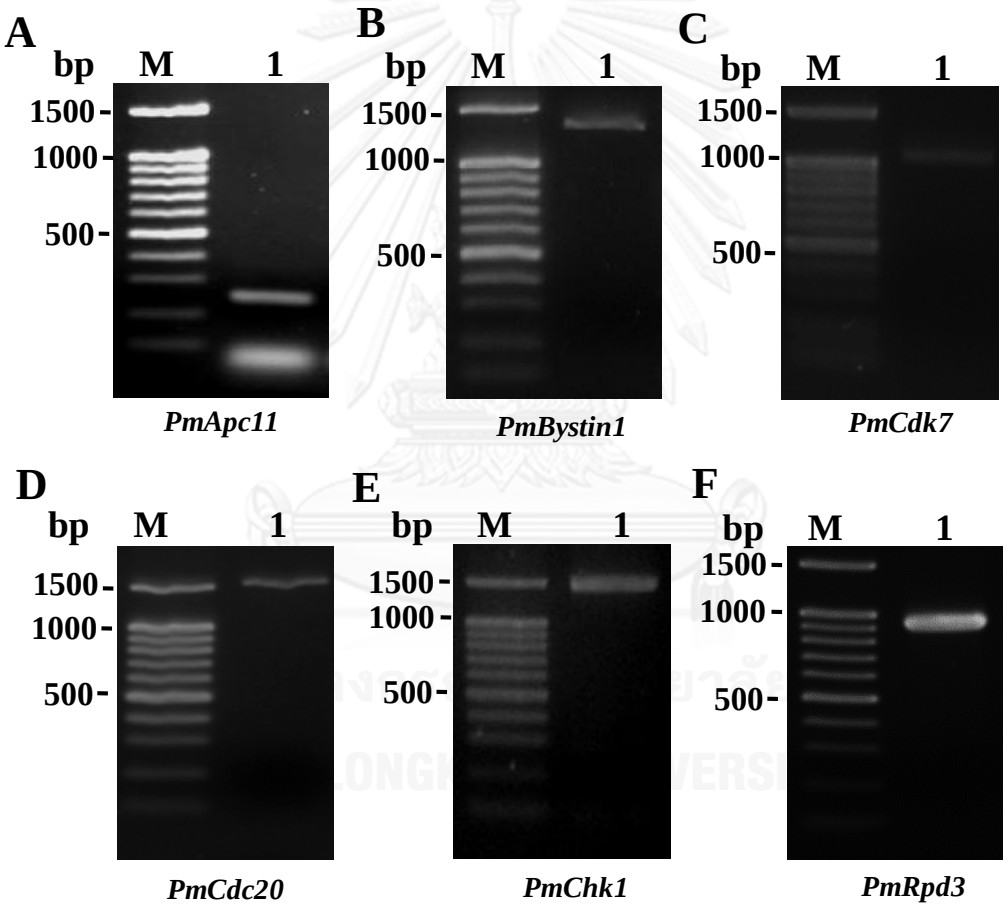

Figure 3. 50 Ethidium bromide-stained agarose gels showing the amplification results of the complete ORF of *PmApc11* (A), *PmBystin1* (B), *PmCdc20* (C), *PmCdk7* (D), *PmChk1* (E) and the partial ORF sequence of *PmRpd3* (F) using the first-stand cDNA of ovaries of wild broodstock as the template. Lands M are a 100 bp DNA ladder.

amplification of the target sequence using primers containing recognition sequences of appropriate restriction enzymes and sequenced to confirm the orientation and nucleotide sequence of a partial recombinant clone (Figure 3.51).

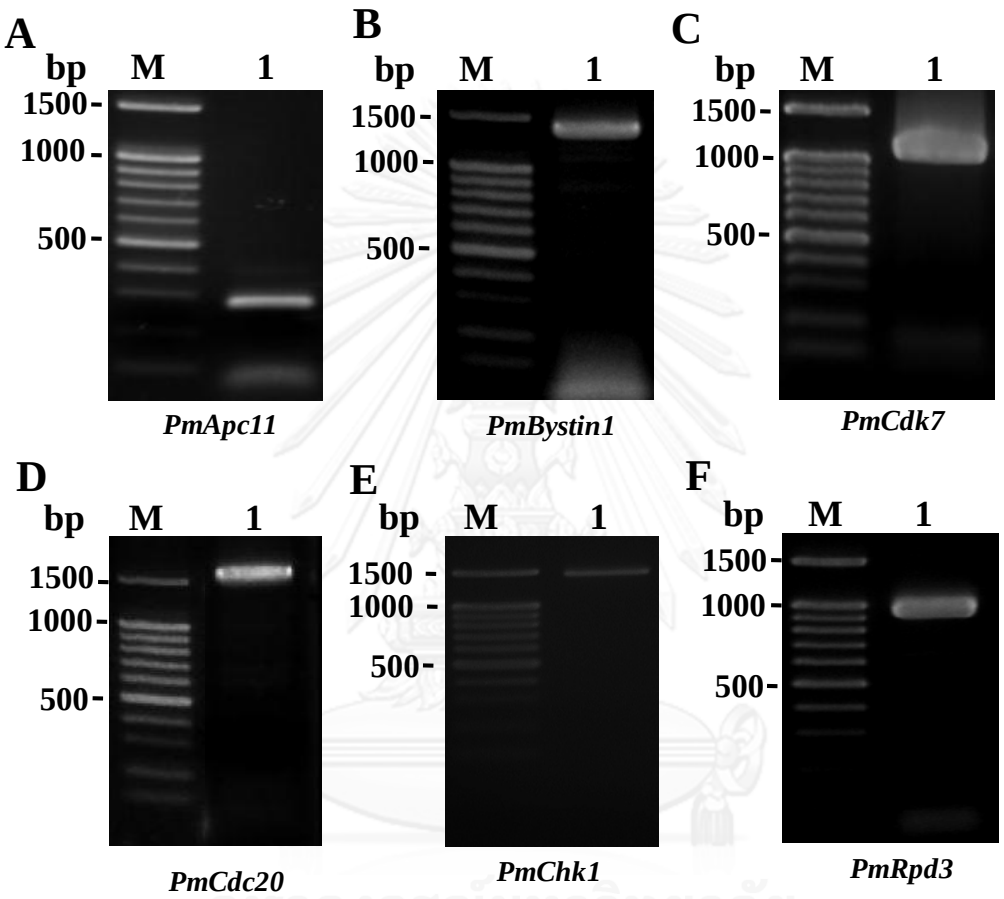

Figure 3. 51 Ethidium bromide-stained agarose gels showing the amplification results of the complete ORF (containing the overhang of recognition restriction enzyme sequences and six-repeated Histidine tag of *PmApc11* (A), *PmBystin1* (B), *PmCdc20* (C), *PmCdk7* (D), *PmChk1* (E) and the partial ORF sequence of *PmRpd3* (F) using the first stand cDNA of ovaries of wild broodstock as the template. A 100 bp DNA ladder (lands M) was used as the marker.

The amplification products of *PmApc11, PmBystin1, PmCdc20* and *PmRpd3* were 255, 1365, 1626 and 912 bp in length corresponding to a polypeptide of 84, 454, 541 and 304 amino acids, respectively. BlastX analysis indicated that these sequences significantly similar to The ORF sequence significantly matched *Apc11* of *Pediculus humanus corporis* (*E*-value = 1.0e-47), *Bystin1* of *Camponotus floridanus* (*E*-value = 1.0e-154), *Cdc20* of *Branchiostoma floridae* (*E*-value = 0.0) and *Rpd3* of *Daphnia pulex* (*E*-value = 0.0) (Figures 3.52 - 3.55), respectively. Gene-specific primers containing the *Nde I* restriction site for the forward primer and *Bam HI* restriction site and six-repeated His tag for reverse primer, were designed.

A

ATGAAGGTGAAGATTAAATCCTGGACGGGAGTGGCTACATGGCGGTGGGTGGCTAATGATGACAGTTGTG
GCATTTGTAGGATGCCCTTTGATGGATGCTGCTCAGATTGTAGGTTGCCAGGTGATGACTGCCCACTAGT
GTGGGGCCAGTGCTCTCACTGTTTCCATATTCACTGCATTATGAAGTGGCTTCAATCTCAACAGCTTCAC
CAGCAGTGTCCAATGTGTCGGCAAGAGTGGAAGTTTAAAGAA**TAA**

B

```
Anaphase-promoting complex subunit 11 [Pediculus humanus corporis]
Sequence ID: ref|XP_002431494.1|Length: 84
Score =157 bits, Expect =1e-47
Identities = 70/84(83%), Positives = 78/84(92%), Gaps = 0/84(0%)
Frame = +1

Query  1    MKVKIKSWTGVATWRWVANDDSCGICRMPFDGCCSDCRLPGDDCPLVWGQCSHCFHIHCI  180
            MK+ I++W GVATWRWVANDD+CGICRMPFD CC+DC+LPGDDCPLVWGQCSHCFHIHCI
Sbjct  1    MKINIRNWNGVATWRWVANDDNCGICRMPFDACCTDCKLPGDDCPLVWGQCSHCFHIHCI  60

Query  181  MKWLQSQQLHQQCPMCRQEWKFKE  252
            MKWL SQQ++  CPMCRQEWKFKE
Sbjct  61   MKWLNSQQINHHCPMCRQEWKFKE  84
```

Figure 3. 52 The complete ORF (A) and similarity search results using blastX (B) of *PmApc11*. Start and stop codons are illustrated in boldface and underlined.

A

ATGGGAAAGATTAAACGTCTGCAGAATGCTGGTGGCAAAGTGCCTCGGCCAGGCCCTCTAGCAGAGCAAA
TTGAAAAATCTGAATATGCACAACCCTCTGCAAGGAAGAAAGTTCGCAGCCAACGCTCTGATGGTGACGA
TGAATTTGTAGAAGGCCAGATGGGGCGTAGCATCTTGAAACAGAGTCAGGCTCAATTGCAGGAGGTTCTT
TTTGAAGACATGGAGAAGGACTTCCCACCTCTTGGGCAGCCGGTTGAGAAATATGAGAGACAACCTCAGA
AGGTGTCTCTCAGCCGAAAATCCAAAGATGCCATTGATGACGAGGAAAGCAGTGACGATGAGAAAGAGGT
TAATGAGATGGATAACCCTGTACCTTGCAATGTAGACAAAGTTGTAAACGATTTTGAGAAGGAATTGGAT
TTAGCCGAAGATGACATGAAAATTCTGGAACACTTCATGAACAAAGACGCACAACCCCAGAGAAAACTAG
CAGACATGTTCCGTGATAAAATCACGGAAAAGCAGACAGACATCCAATCACAAGTGAATGCTAGCACTGT
ACAGACCGTTAACCTTAGTCCAGAGGTGCAAGAAATGTGCTCACAGATTGGGAATGTCTTGTCAAAATAC
AGAAGTGGACCCTTGCCAAAGATGTTCAAGGTAATTCCAAAGATGCGCAACTGGGAAGAACTCGTATACC
TGACAGACCCTGACAAGTGGTCTGCTGCTGCTGTGTACCAGGGTGTTAGAATATTTGTGAGTAACCTCAA
GGAGCCCATGGCACAGCGCTTCTTCAACTTGGTCCTCCTTCCTCGCATACGGGATGACATCTCCTACTAC
AAGCGCCTCAACTTCCATTTGTATCAGGCTATGTGCAAGGCCCTTTTCAAGCCAGGTGCCTTCTTTAAAG
GTGTTTTACTTCCTCTGTGCATGTCCGGTACATGTACTCTTCGAGAAGCTATTATTGTTGGTTCAGTAAT
TGCAAAGAACCACATACCAATTCTGCACTCGGCTGCAACGATACTGAAGATTGCTGAAATGGACTATTCT
GGAGCAAATTCAATATTTTTGAGAATATTTTTTGATAAGAAATATGCCCTCCCATACAGAGTTGTTGATG
CTTGTGTCTACCATTTTATGAGGTTCCAGCATGACCGCCGTGAACTGCCAGTTTTGTGGCATCAAGCCTT
GCTTGTATTTGTCCAAAGATACAAGGAAGATATGAGTCCCGACCAGAAACAAGCCATCATGGATGTCATT
AAATTCCACACTCATTTCACCATCACTGCCGAGGTGAGGAGAGAACTTCTGAATTCCAAGTGCAGAGGTC
AAGATGATGATATGCCAATGATGGTTGATGAG**TAG**

B

Bystin [Camponotus floridanus] Sequence ID: gb|EFN65824.1|Length: 434
Score =457 bits, **Expect =**1e-154
Identities = 230/444(52%), **Positives** = 314/444(70%), **Gaps** = 29/444(6%)
Frame = +1

```
Query  1     MGKIKRLQNAGGKVPRPGPLAEQIEKSEYAQPSARKKVRSQRSDGDDEFVEGQMGRSILK  180
             MGK K+++ + G       L EQIE  +  +P+ R+K+R  R++ ++E+V   + R IL
Sbjct  1     MGKAKKIKVSKGTKESKISLTEQIEIDKAVKPTVRQKIR-HRANDEEEYVAPTLTRRILS  59

Query  181   QSQAQLQEVLFEDMEKDFPPLGQPVEKYERQPQKVSLSRkskdaiddeessddekeVNEM  360
             Q++ Q  E+  E        +G    K E+   K+S                   E+N++
Sbjct  60    QARQQQLEIEEE--------IGLSKPKSEKLTVKLS------------------TELNDV  93

Query  361   DNPVPCNVDKVVN-DFEKELDLAEDDMKILEHFMNKDAQPQRKLADMFRDKITEKQTDIQ  537
             ++    + + V N  + +++ + EDD + L+ FM+KD  P R LAD+  +K+TEK+T+I+
Sbjct  94    EDRSSDDEEPVDNVHYYEDIQINEDDERALQMFMSKDPVPTRTLADIIMEKLTEKKTEIE  153

Query  538   SQV-NASTVQTVNLSPEVQEMCSQIGNVLSKYRSGPLPKMFKVIPKMRNWEELVYLTDPD  714
             +Q  +A T+Q  +L P V+ M   + +VL KYRSG LPK FK++P ++NWE+++Y+TDP
Sbjct  154   TQFSDAGTIQLQDLDPRVKAMYEGVRDVLVKYRSGKLPKAFKIVPSLKNWEQILYITDPP  213

Query  715   KWSAAAVYQGVRIFVSNLKEPMAQRFFNLVLLPRIRDDISYYKRLNFHLYQAMCKALFKP  894
             KWSAA+YQ  RIF SNLK+ MAQRF+NLVLLPRIRDD++ YKRLNFHLYQA+ KALFKP
Sbjct  214   KWSAAAMYQATRIFASNLKDKMAQRFYNLVLLPRIRDDLAEYKRLNFHLYQALRKALFKP  273

Query  895   GAFFKGVLLPLCMSGTCTLREAIIVGSVIAKNHIPILHSAATILKIAEMDYSGANSIFLR  1074
               F KG+LLPL  SGTCTLRE++I+GSVIAKN IPILHS+A ILKIAEMDY+GANSIFLR
```

```
Sbjct  274   AGFMKGILLPLLESGTCTLRESVIIGSVIAKNSIPILHSSAAILKIAEMDYTGANSIFLR  333

Query  1075  IFFDKKYALPYRVVDACVYHFMRFQHDRRELPVLWHQALLVFVQRYKEDMSPDQKQAIMD  1254
              IF DKKYALPYRVVD  V+HF+RF+ D RELPVLWHQALL FVQRYK D+S +QK+AI+
Sbjct  334   IFLDKKYALPYRVVDGVVFHFVRFERDTRELPVLWHQALLTFVQRYKSDISSEQKEAILR  393

Query  1255  VIKFHTHFTITAEVRRELLNSKCR  1326
              +++  +H +IT E+RREL ++KCR
Sbjct  394   LLRKQSHHSITPEIRRELQHAKCR  417
```

Figure 3. 53 The complete ORF (A) and similarity search results using blastX (B) of *PmBystin1*. Start and stop codons are illustrated in boldface and underlined.

A

ATGTCCCACCTTCAGTTTGACGCTAAGCTAAGTGAAGCGTTAAGGATGGACGGAGATTTGAC
GAGGGGGCCAATCCCGAGGTGGCAGCGGAAGGCAATGGAGCAGGGAATGCAACAGCTCTCCA
TAAGCAACGAAAACAGTTTTGTTAACAAGTCCGGTTATAGCAGTCCAAAGTCGGGTAAAACT
CCACGAAGCGGATCTTTCCTTGAGACCAAGAGCCCTGGCCGAGGGAAGTCTCCAAGCAGGTC
CAAGTCGCCAGGTCGCAGGATTCCAAAGCTGACAGTTCGCGGTGCAGGCCAGAAGACTCCCT
CTCTCAAAACTCCCGCCACCCCACATAACCAGCAAGACAGATTCATTCCAAACCGAAGCACC
ACAGATACGGAACGTTCCCACCACCTTTTGGTCACCAGCATGGAGGCTTCGGGAGGAGAAAA
GTCTGCAGAGGAGGATGAAGTGTCCCTGCAGCAGAAAGAATATCAGGAGAAGATGACAGAGA
ACCTAAACGATGGGATAGCACCTGAGTCGAGGGTTTTGTCATTTAAGAGTAAGGCACCACAA
GCAAAAGAAGGACATTTGAACAATCACAAAGTTCTCTACAGTGCTGGAAAACCCACTGTGCC
CAAGGCTGCCACAACAAGACACATTCCCAACATGCCAGAAAAGGTTCTTGATGCTCCAGAAC
TTCTTGATGATTACTATCTTCACCTTCTCGACTGGAGTGTGAACAACCACTTGGCTGTAGCT
CTGGGAAATTCGGTGTATGTTTGGAATGCTGGCGATGGTTCCATTACCCCCCTGTGCCAGCT
GGATGACCCCGACTATATCTGCTCTCTGTCGTGGATTAAGGAAGGTAATGTGCTTGCCATTG
GCAATAGCTCGGGTGTCACACAGCTGTGGGATGTTGCACAACAGAAGCTTGTTCGCTCTATG
GGTGGCCACGAGAGCCGTGTCACCACCCTTTCCTGGAACTCGTACATCCTCTCCTCCGGCTC
TCGCTCAGGACAGATTTTCCACCATGATGTCAGAGTGGCTGAACATCATGTGGCGACCTTAG
CTGGGCATTCGCAGGAGGTCTGTGGTCTAAAGTGGTCTCCTGATGGGCGTTTGCTTGCCTCG
GGTGGAAATGACAATCAGGTAAACATCTGGGATAGCATGAATACTACTCCGGTCCACACGCT
AACTCAACATCAAGCTGCCGTTAAGGCTGTAGCTTGGTGTCCGTGGCAGAACAATCTCCTTG
CAACGGGTGGAGGGACTGCCGACCGCACCATCAGATTGTGGAACTGCACAACTGGAATTTGC
CTTAAAGATACCACAACTAATTCTCAGGTGTCATCCATTGTTTGGTCTGCACACTACAAAGA
GTTCATATCAGGCCATGGATTCTCTAACAATCAGCTGACCATCTGGAAGTACCCATCTATGG
CAAAGGTGGCTGACCTCACAGGTCACACAGGCAGAGTACTGGAGCTGTGTGTGTCTCCTGAT
GGCCAGATGGTAGTGAGTGCAGCTGCCGACGAGACCATCCGGATGTGGAAATGCTGGGCCAT
GGACAAAAAGGACAAGAAACAGGCCGATGCAAACAAAGGCCATCCGATATCCATGCTTGCTC
AGACCATTCGA**TAA**

B.

Cdc20 [Branchiostoma floridae] Sequence ID: gb|AAO85336.1|Length: 536
Score =533 bits, **Expect =** 0.0
Identities = 290/543(53%),**Positives** = 358/543(65%), **Gaps** = 62/543(11%)
Frame = +1

```
Query  1     MSHLQFDAKLSEALRMDGDLTRGPIPRWQRKAMEQGM-------QQLSISNENSFVNKSG  159
             MSHL+F+  +++ LR+D   T GP+PRWQRKAME            L+ S  N  +N SG
Sbjct  1     MSHLKFENDVNQLLRLDSAFTDGPVPRWQRKAMESSRCSGPSNNTSLNSSCRNMSLNVSG  60

Query  160   YS---------------SPKLGKTPRSGSFLETkspgrgkspsrskspgrripkLTVRGA  294
              +               +P   KTPRSG   +T
Sbjct  61    CTPMKTSNRASAKTPSHTPGKAKTPRSGRKSKTP------------------------G  95

Query  295   GQKTP-SRKTPVTPHNQQDRFIPNRSTTDTERSHHLLVTSMEASGGEKSAEEDEVSLQQK  471
               KTP + KTP TP    DRFIPNRS ++ E  H       + +  +   +E+ +S  ++
Sbjct  96    KSKTPGNAKTPKTP--VADRFIPNRSASNFELGH------FKCNNDKVHVDEEMLSPSKQ  147

Query  472   EYQEKMTENLNDGIAPESRVLSFKSKAPQAKEGHLNNHKVLYSAGKPTVPKAATTRHIPN  651
             +YQE M+ENLN  +   S++L++K+KAPQA EG+ NN +VLYS  K        TRHIP
Sbjct  148   QYQEAMSENLNGNVV-NSKILAYKNKAPQAPEGYQNNMRVLYSQTKTPSSTRKVTRHIPQ  206

Query  652   MPEKVLDAPElddyylhlldWSVNNHLAVALGNSVYVWNAGDGSITPLCQLDDP-DYIC  828
             +PE++LDAPE+LDDYYL+LL WS NNHLAVALGNSVY+WNAG G I  L  +  P DY+
Sbjct  207   VPERILDAPEILDDYYLNLLAWSCNNHLAVALGNSVYLWNAGTGDIQQLMSMSGPEDYVS  266

Query  829   SLSWIKEGNVLAIGNSSGVTQLWDVAQQKLVRSMGGHESRVTTLSWNSYILSSGSRSGQI  1008
             ++SWI EGN LAIG+S+   QLWDVA QK VR+M    SRV +L WN YILSSGSR+G I
Sbjct  267   AVSWIAEGNFLAIGSSNAEVQLWDVAAQKRVRNMTSQSSRVGSLDWNVYILSSGSRAGTI  326

Query  1009  FHHDVRVAEHHVATLAGHSQEVCGLKWSPDGRLLASGGNDNQVNIWDSMNT----TPVHT  1176
              HHDVR+A+HHVATL GH+QEVCGLKWSPDGR LASGGNDN +NIW    T     P+H+
Sbjct  327   HHHDVRIADHHVATLDGHTQEVCGLKWSPDGRYLASGGNDNLLNIWGYQCTREGNVPLHS  386

Query  1177  LTQHQAAVKAVAWCPWQNNLLATGGGTADRTIRLWNCTTGICLKDTTTNSQVSSIVWSAH  1356
             LTQHQAAVKA++WCPWQ ++LA+GGGTADR IR WN  TG CL    T SQV SI+WS
Sbjct  387   LTQHQAAVKALSWCPWQASVLASGGGTADRCIRFWNANTGHCLNTVDTKSQVCSILWSKE  446

Query  1357  YKEFISGHGFSNNQLTIWKYPSMAKVADLTGHTGRVLELCVSPDGQMVVSAAADETIRMW  1536
             YKE ISGHGF+NNQLTIWKYP+MAKV +LTGH  RVL + +SPDG  VVSAAADET+R+W
Sbjct  447   YKELISGHGFANNQLTIWKYPTMAKVTELTGHQARVLHMAMSPDGTTVVSAAADETLRLW  506

Query  1537  KCW  1545
             KC+
Sbjct  507   KCF  509
```

Figure 3. 54 The complete ORF (A) and similarity search results using blast*X* (B) of *PmCdc20*. Start and stop codons are illustrated in boldface and underlined.

A

AGTGACATTGGAAATTATTACTACGGCCAGGGCCATCCCATGAAGCCACACAGGATACGTATGACACAC
AACCTCCTCTTGAATTATGGGCTGTACCGCAAGATGGAGATATATAGGCCTCATAAAGCAACTCAAGAT
GAAATGACCAAGTTCCATAGTGATGACTACATCAGGTTTATAAGGTCCATTCGTCCAGATAACATGAAT
GAATACAATAAACAGATGCAAAAGTTTAATGTTGGAGAAGATTGCCCAGTCTTTGATGGCCTGTATGAG
TTTTGTCAGTTATCTTCTGGAGGCTCCATTGCTGGTGCTGTGAAGTTGAACAAACAAGCTTGTGATATT
GCTATTAACTGGGCTGGTGGACTTCATCATGCAAAAAAAAGTGAAGCTTCAGGTTTCTGCTACGTGAAT
GACATTGTGTTAGCTATTTTGGAGCTCCTTAAGTATCACCAGCGAGTTCTGTACATTGATATTGATATT
CATCATGGAGATGGTGTTGAGGAGGCCTTCTACACCACAGACCGTGTAATGACTGTCTCCTTCCACAAG
TATGGAGAGTATTTCCCTGGGACTGGAGACCTAAGGGATATTGGTGCTGGGAAGGGTAAATATTATGCT
GTTAACTTCCCATTAAGAGATGGCATAGATGATGAGAGCTATGACAGCATATTTGTGCCAATAATGACA
AAGGTAATGGAAACCTACCAGCCCTCTGCAATTGTTCTTCAGTGTGGTGCTGACTCTCTCAGTGGAGAC
AGGCTTGGTTGTTTCAACCTCACCCTAAAAGGCCATGCAAAGTGTGTTGAATTTGTCAAGAAGTACAAC
CTTCCCCTACTCTTACTTGGTGGAGGAGGATACACCATCCGTAATGTAGCAAGATGTTGGACTTATGAA
ACGGCTGTTGCTTTA

B

Histone deacetylase Rpd3 protein [Daphnia pulex]

Sequence ID: gb|EFX74892.1|Length: 538
Score =502 bits, **Expect =**0.0
Identities = 286/304(94%), **Positives** = 300/304(98%), **Gaps** = 0/304(0%)
Frame = +1

```
Query  1    SDIGNYYYGQGHPMKPHRIRMTHNLLLNYGLYRKMEIYRPHKATQDEMTKFHSDDYIRFI  180
            SDIGN+YYGQGHPMKPHRIRMTHNLLLNYGLYRKMEIYRPHKAT +EMTKFHSDDYIRF+
Sbjct  18   SDIGNFYYGQGHPMKPHRIRMTHNLLLNYGLYRKMEIYRPHKATAEEMTKFHSDDYIRFL  77

Query  181  RSIRPDNMNEYNKQMQKFNVGEDCPVFDGLYEFCQLSSGGSIAGAVKLNKQACDIAINWA  360
            RSIRPDNM EYNKQMQ+FNVGEDCPVFDGLYEFCQLS+GGS+AGAVKLNKQA +IA+NWA
Sbjct  78   RSIRPDNMTEYNKQMQRFNVGEDCPVFDGLYEFCQLSAGGSVAGAVKLNKQATEIAVNWA  137

Query  361  GGLHHAKKSEASGFCYVNDIVLAILELLKYHQRVLYIDIDIHHGDGVEEAFYTTDRVMTV  540
            GGLHHAKKSEASGFCYVNDIVLAILELLKYHQRVLYIDIDIHHGDGVEEAFYTTDRVMTV
Sbjct  138  GGLHHAKKSEASGFCYVNDIVLAILELLKYHQRVLYIDIDIHHGDGVEEAFYTTDRVMTV  197

Query  541  SFHKYGEYFPGTGDLRDIGAGKGKYYAVNFPLRDGMDDESYDSIFVPIMTKVMETYQPSA  720
            SFHKYGEYFPGTGDLRDIGAGKGKYYAVNFPLRDG+DDESY+ IFVPIM+KVMETYQPSA
Sbjct  198  SFHKYGEYFPGTGDLRDIGAGKGKYYAVNFPLRDGIDDESYEQIFVPIMSKVMETYQPSA  257

Query  721  IVLQCGADSLSGDRLGCFNLTLKGHAKCVEFVKKYNLPllllggggYTIRNVARCWTYET  900
            +VLQCGADSLSGDRLGCFNLTLKGHAKCV+FVKK+NLPLLLLGGGGYTIRNVARCWTYET
Sbjct  258  VVLQCGADSLSGDRLGCFNLTLKGHAKCVDFVKKHNLPLLLLGGGGYTIRNVARCWTYET  317

Query  901  AVAL  912
            AVAL
Sbjct  318  AVAL  321
```

Figure 3. 55 The partial ORF (A) and similarity search results using blast*X* (B) of *PmRpd3*. Start and stop codons are illustrated in boldface and underlined.

The amplification product of *PmCdc2*, *PmCdk7* and *PmCdk1* was 900, 1062 and 1455 bp in length (Figure 3.56-3.58) corresponding to a polypeptide of 299, 353 and 484 amino acids, respectively. Their deduced amino acid sequences significantly matched *Cdc2* of *P. monodon* (*E*-value = 0.0), *Cdc7* of *Bombus impatiens* (*E*-value = 4.0e-169) and *Cdk1* of *Daphnia pulex* (*E*-value = 3.0e-175), respectively. Primer overhang of with *Nhe I/Xho* I + 6X-His, *Nde I/Nco* I + 6X-His and *Bam* HI/*Xho* I + 6X-His of respective genes were designed.

The PCR product of each gene was cloned in to pGEM-T Easy vector and transformed into *E. coli* JM109. The orientation of an insert was confirmed. The recombinant plasmid of each transcript was digested with corresponding restriction enzymes and the product was ligated into the expression vector before transformed in to *E. coli* JM109 and subsequently into *E. coli* BL21 (DE3) codon+ RIPL.

A

ATGGAGGATTACTTACGTATAGAAAAGCTTGGAGAGGGAACATATGGCGTGGTATACAAAGC
CAAGAACCGCAAAAGTGGGAAGTTTGTGGCCATGAAAAAGATCAGACTGGAGAATGAGGAAG
AAGGTGTCCCTTCCACAGCTATCAGAGAAATCTCTCTCCTGAAAGAACTTCAGCATCCCAAC
ATTGTCCTACTAGAAGATGTATTGATGCAGGAGAGCAAACTTTTCCTTGTGTTCGAGTTCCT
CAACATGGATTTGAAGAAATATCTTGACTCTTTGGAATCTGGCAAATATGTAGATAAGAAAC
TTGTGAAA*TCTTA*CTGCTACCAGCTTTTCCAAGGAATTCTCTATTGCCATCAGCGAAGGGTG
CTCCACAGAGATCTCAAACCACAGAATCTCCTCATCAATGAGCAGGGCGTCATAAAGATTGC
TGATTTTGGCCTTGCTCGCGCATTTGGAATCCCAGTGAGAGTGTATACACATGAGGTTGTGA
CTCTGTGGTATCGAGCTCCAGAGGTCCTTCTTGGTTCCTCTCGATACTCCTGTCCTGTTGAT
GTTTGGTCTCTTGGCTGTATATTTGCCGAGATGGTTACTAAACGGCCACTGTTCCATGGTGA
CTCAGAGATTGACCAGCTCTTCAGGATATTCAGAACCTTAACAACCCCCACAGAAGACAACT
GGCCTGGTGTAACACAACTGCAGGACTACAAGGCCAATTTCCCCAAGTGGACTGATTACAAT
CTTGGAAATTCCGTCAAACAGATGGACAGCGATGGCTTGGACCTTTTATCGAAAACACTGAT
CTACGATCCGACTCGAAGGATTTCTGCCAAGGAGGCCCTGAAGCACCCCTACTTTGATGATC
TCGACAAGTCCACTCGTCCAGCCAAGAAT**TAA**

B

Cdc2 [Penaeus monodon] Sequence ID: gb|AGS56255.1|Length: 299
Score = 619bits, **Expect =** 0.0
Identities = 299/299(100%), **Positives** = 299/299(100%), **Gaps** = 0/299(0%),
Frame = +1

```
Query  1    MEDYLRIEKLGEGTYGVVYKAKNRKSGKFVAMKKIRLENEEEGVPSTAIREISLLKELQH  180
            MEDYLRIEKLGEGTYGVVYKAKNRKSGKFVAMKKIRLENEEEGVPSTAIREISLLKELQH
Sbjct  1    MEDYLRIEKLGEGTYGVVYKAKNRKSGKFVAMKKIRLENEEEGVPSTAIREISLLKELQH  60

Query  181  PNIVLLEDVLMQESKLFLVFEFLNMDLKKYLDSLESGKYVDKKLVKSYCYQLFQGILYCH  360
            PNIVLLEDVLMQESKLFLVFEFLNMDLKKYLDSLESGKYVDKKLVKSYCYQLFQGILYCH
Sbjct  61   PNIVLLEDVLMQESKLFLVFEFLNMDLKKYLDSLESGKYVDKKLVKSYCYQLFQGILYCH  120

Query  361  QRRVLHRDLKPQNLLINEQGVIKIADFGLARAFGIPVRVYTHEVVTLWYRAPEVLLGSSR  540
            QRRVLHRDLKPQNLLINEQGVIKIADFGLARAFGIPVRVYTHEVVTLWYRAPEVLLGSSR
Sbjct  121  QRRVLHRDLKPQNLLINEQGVIKIADFGLARAFGIPVRVYTHEVVTLWYRAPEVLLGSSR  180

Query  541  YSCPVDVWSLGCIFAEMVTKRPLFHGDSEIDQLFRIFRTLTTPTEDNWPGVTQLQDYKAN  720
            YSCPVDVWSLGCIFAEMVTKRPLFHGDSEIDQLFRIFRTLTTPTEDNWPGVTQLQDYKAN
Sbjct  181  YSCPVDVWSLGCIFAEMVTKRPLFHGDSEIDQLFRIFRTLTTPTEDNWPGVTQLQDYKAN  240

Query  721  FPKWTDYNLGNSVKQMDSDGLDLLSKTLIYDPTRRISAKEALKHPYFDDLDKSTRPAKN  897
            FPKWTDYNLGNSVKQMDSDGLDLLSKTLIYDPTRRISAKEALKHPYFDDLDKSTRPAKN
Sbjct  241  FPKWTDYNLGNSVKQMDSDGLDLLSKTLIYDPTRRISAKEALKHPYFDDLDKSTRPAKN  299
```

C

```
PmCdc2-O    ATGGAGGATTACTTACGTATAGAAAAGCTTGGAGAGGGAACATATGGCGTGGTATACAAA      60
PmCdc2-T    ATGGAGGATTACTTACGTATAGAAAAGCTTGGAGAGGGAACATATGGCGTGGTATACAAA
            ************************************************************
PmCdc2-O    GCCAAGAACCGCAAAAGTGGGAAGTTTGTGGCCATGAAAAAGATCAGACTGGAGAATGAG      120
PmCdc2-T    GCCAAGAACCGCAAAAGTGGGAAGTTTGTGGCCATGAAAAAGATCAGACTGGAGAATGAG
            ************************************************************
PmCdc2-O    GAAGAAGGTGTCCCCTCCACAGCTATCAGAGAAATCTCTCTCCTGAAAGAACTTCAGCAT      180
PmCdc2-T    GAAGAAGGTGTCCCTTCCACAGCTATCAGAGAAATCTCTCTCCTGAAAGAACTTCAGCAT
            ************ ************************************************
PmCdc2-O    CCCAACATTGTCCTACTAGAAGATGTATTGATGCAGGAGAGCAAACTTTTCCTTGTGTTC      240
PmCdc2-T    CCCAACATTGTCCTACTAGAAGATGTATTGATGCAGGAGAGCAAACTTTTCCTTGTGTTC
            ************************************************************
PmCdc2-O    GAGTTCCTCAACATGGATTTGAAGAAATATCTTGACTCTTTTGAATCTGGCAAATATGTA      300
PmCdc2-T    GAGTTCCTCAACATGGATTTGAAGAAATATCTTGACTCTTTGGAATCTGGCAAATATGTA
            ****************************************** ******************
PmCdc2-O    GATAAGAAACTTGTGAAATCTTACTGCTACCAGCTTTTCCAAGGAATTCTCTATTGCCAT      360
PmCdc2-T    GATAAGAAACTTGTGAAATCTTACTGCTACCAGCTTTTCCAAGGAATTCTCTATTGCCAT
            ************************************************************
PmCdc2-O    CAGCGAAGGGTGCTCCACAGAGATCTCAAACCACAGAATCTCCTCATCAATGAGCAGGGC      420
PmCdc2-T    CAGCGAAGGGTGCTCCACAGAGATCTCAAACCACAGAATCTCCTCATCAATGAGCAGGGC
            ************************************************************
PmCdc2-O    GTCATAAAGATTGCTGATTTTGGCCTTGCTCGCGCATTTGGAATCCCAGTGAGAGTGTAT      480
PmCdc2-T    GTCATAAAGATTGCTGATTTTGGCCTTGCTCGCGCATTTGGAATCCCAGTGAGAGTGTAT
            ************************************************************
PmCdc2-O    ACACATGAGGTTGTGACTCTGTGGTATCGAGCTCCAGAAGTCCTTCTTGGTTCCTCTCGA      540
```

```
PmCdc2-T    ACACATGAGGTTGTGACTCTGTGGTATCGAGCTCCAGAGGTCCTTCTTGGTTCCTCTCGA
            ************************************ **********************
PmCdc2-O    TACTCCTGTCCTGTTGATGTTTGGTCTCTTGGCTGTATATTTGCCGAGATGGTTACTAAA      600
PmCdc2-T    TACTCCTGTCCTGTTGATGTTTGGTCTCTTGGCTGTATATTTGCCGAGATGGTTACTAAA
            ************************************************************
PmCdc2-O    CGGCCACTGTTCCATGGTGACTCAGAGATTGACCAGCTCTTCAGGATATTCAGAACCTTA      660
PmCdc2-T    CGGCCACTGTTCCATGGTGACTCAGAGATTGACCAGCTCTTCAGGATATTCAGAACCTTA
            ************************************************************
PmCdc2-O    ACAACCCCCACAGAAGACAACTGGCCTGGTGTAACACAACTGCAGGACTACAAGGCCAAT      720
PmCdc2-T    ACAACCCCCACAGAAGACAACTGGCCTGGTGTAACACAACTGCAGGACTACAAGGCCAAT
            ************************************************************
PmCdc2-O    TTCCCCAAGTGGACTGATTACAATCTTGGAAATTCCGTCAAACAGATGGACAGCGATGGC      780
PmCdc2-T    TTCCCCAAGTGGACTGATTACAATCTTGGAAATTCCGTCAAACAGATGGACAGCGATGGC
            ************************************************************
PmCdc2-O    TTGGACCTTTTATCGAAAACACTGATCTACGATCCGACTCGAAGGATTTCTGCCAAGGAG      840
PmCdc2-T    TTGGACCTTTTATCGAAAACACTGATCTACGATCCGACTCGAAGGATTTCTGCCAAGGAG
            ************************************************************
PmCdc2-O    GCCCTGAAGCACCCCTACTTTGATGATCTCGACAAGTCCACTCTTCCAGCCAAGAATTAA      900
PmCdc2-T    GCCCTGAAGCACCCCTACTTTGATGATCTCGACAAGTCCACTCGTCCAGCCAAGAATTAA
            ****************************************** ****************
```

D

```
PmCdc2-O    MEDYLRIEKLGEGTYGVVYKAKNRKSGKFVAMKKIRLENEEEGVPSTAIREISLLKELQH  60
PmCdc2-T    MEDYLRIEKLGEGTYGVVYKAKNRKSGKFVAMKKIRLENEEEGVPSTAIREISLLKELQH
            ************************************************************
PmCdc2-O    PNIVLLEDVLMQESKLFLVFEFLNMDLKKYLDSFESGKYVDKKLVKSYCYQLFQGILYCH  120
PmCdc2-T    PNIVLLEDVLMQESKLFLVFEFLNMDLKKYLDSLESGKYVDKKLVKSYCYQLFQGILYCH
            ********************************* ************************
PmCdc2-O    QRRVLHRDLKPQNLLINEQGVIKIADFGLARAFGIPVRVYTHEVVTLWYRAPEVLLGSSR  180
PmCdc2-T    QRRVLHRDLKPQNLLINEQGVIKIADFGLARAFGIPVRVYTHEVVTLWYRAPEVLLGSSR
            ************************************************************
PmCdc2-O    YSCPVDVWSLGCIFAEMVTKRPLFHGDSEIDQLFRIFRTLTTPTEDNWPGVTQLQDYKAN  240
PmCdc2-T    YSCPVDVWSLGCIFAEMVTKRPLFHGDSEIDQLFRIFRTLTTPTEDNWPGVTQLQDYKAN
            ************************************************************
PmCdc2-O    FPKWTDYNLGNSVKQMDSDGLDLLSKTLIYDPTRRISAKEALKHPYFDDLDKSTLPAKN   299
PmCdc2-T    FPKWTDYNLGNSVKQMDSDGLDLLSKTLIYDPTRRISAKEALKHPYFDDLDKSTRPAKN
            ************************************************** ****
```

Figure 3. 56 The complete ORF (A) and similarity search results using blast*X* (B) of *PmCdc2*. Start and stop codons are illustrated in boldface and underlined. Pairwise alignment of the nucleotide (C) and deduced amino acid sequences of PmCdc2 isolated from ovaries and testes is shown (D).

A

ATGGAAGTAGAACAAGAGAAGAAAGGAAGGATTAGAATAGAAGAAAAATTGAAGAGATATGA
GAAGATCGATTTCTTGGGAGAAGGACAGTTTGCCACTGTATATAAGGCTCTTGATGTGGAGA
CCAAGCAGATAGTAGCTGTCAAAAAGATCAAACTAGGTAGCAGAGAGGAGGCAAGGGATGGC
ATCAACCGTACGGCTCTCCGAGAGATCAAGCTCTTGCAGGAGGTCCACCACCCAAACCTCAT
TGGCCTCCTCGATGTCTTTGGCTACAAGTCAAATGTGTCGCTGGTGTTTGATTTCATGGATA
CAGATTTAGAGGTGATCATCAAGGACACAGACAACATCATCCTCACACCCTCCAACATCAAA

GCATATATGATCCAAACATTAAAAGGCTTGGAATTCCTGCATCTTCACTGGATCCTACACAG
AGATCTGAAACCAAACAACCTACTAGTCAATTCAGATGGCATACTTAAAATAGGAGATTTTG
GTCTGGCAAGATTCTTTGGCTCTCCCAACAGACAGTATTCACATCAAGTAGTTACAAGATGG
TACAGGAGTCCAGAGTTGCTGTTTGGCGCGAGATCCTACGGCACAGGGGTAGACATGTGGGC
GATTGGCTGTATCCTGGCGGAGATGTTGGTTCGCTGTCCCTACTTCCCGGGTGACTCTGATC
TAGACCAGCTTACCAGGATCTTCACTGCCCTAGGGACTCCTGGTGATGACGACTGGCCGGAC
ATGACGAAACTTCCCGACTACGTATCATTCAAGCACTTCGAGGGTTCCCCACTGCGAGACCT
CTTTCCTGCTGCCAGTGATGACCTTCTCCAGCTATTGGGGTCTTTGCTCACTATTAATCCTA
TGAAACGATGCAGCTGTACTGAGGCTCTGAAGATGGAGTATTTCAGCAATAAGCCTGTCCCG
ACACCAGGACCTCTTCTTCCTCTCCCACCAACCATTAGACAGAGAAGTGAGGCAGAAAAACC
GTCCCTCAAGCGAAAGATTATTGAAGAGTCTGGCTTTGGAGGTTCCTTAGCAAAGAAGCTTC
AATTC**TAG**

B

cyclin-dependent kinase 7 [Bombus impatiens]
Sequence ID: ref|XP_003490299.1| Length: 338
Score =487 bits, **Expect =**4e-169
Identities = 252/341(74%),**Positives** = 302/341(88%), **Gaps** = 3/341(0%)
Frame = +1

```
Query  37    IEEKLKRYEKIDFLGEGQFATVYKALDVETKQIVAVKKIKLGSREEARDGINRTALREIK  216
             + EKL+RYEKIDFLGEGQFATVYKA D+ET +IVAVKKIK+GSR EARDGINRTALREIK
Sbjct  1     MTEKLRRYEKIDFLGEGQFATVYKAKDIETSKIVAVKKIKVGSRAEARDGINRTALREIK  60

Query  217   LLQEVHHPNLIGLLDVFGYKSNVSLVFDFMDTDLEVIIKDTDNIILTPSNIKAYMIQTLK  396
             LLQE+ H N+IGLLDVFG+KSNVSLVFDFMDTDLE+IIKD+ NI+LT +NIKAYMIQTL+
Sbjct  61    LLQELKHDNVIGLLDVFGHKSNVSLVFDFMDTDLEIIIKDS-NIVLTAANIKAYMIQTLQ  119

Query  397   GLEFLHLHWILHRDLKPNNLLVNSDGILKIGDFGLARFFGSPNRQYSHQVVTRWYRSPEL  576
             GL++LH +WILHRDLKPNNLLVNS+G+LKIGDFGLA+FFGSPNR  +HQVVTRWYRSPEL
Sbjct  120   GLDYLHYNWILHRDLKPNNLLVNSEGVLKIGDFGLAKFFGSPNRINTHQVVTRWYRSPEL  179

Query  577   LFGARSYGTGVDMWAIGCILAEMLVRCPYFPGDSDLDQLTRIFTALGTPGDDDWPDMTKL  756
             L+GAR YGTG+DMWA+GCILAE+L+R P+ PG+SDLDQLTRIF  LGTP ++ WP MT+L
Sbjct  180   LYGARLYGTGIDMWAVGCILAELLLRVPFLPGESDLDQLTRIFQTLGTPTEETWPGMTEL  239

Query  757   PDYVSFKHFEGSPLRDLFPAAsddllqllgslltINPMKRCSCTEALKMEYFSNKpvptp  936
             PD++ FK F G+PL+ +F AA DDLL L+ SLL +NP++RC+C +AL+M YFSNKP PTP
Sbjct  240   PDFIQFKPFPGTPLKHIFTAAGDDLLDLIASLLNVNPLERCTCDQALQMPYFSNKPAPTP  299

Query  937   gpllplppTIRQRSEAEKPSLKRKIIEESGFGGSLAKKLQF  1059
             GP LPLP +++++ E EKPSLKRK++ ES  G SLAK+LQF
Sbjct  300   GPRLPLPTSVKRQPE-EKPSLKRKLL-ESMDGASLAKRLQF  338
```

C

```
PmCdk7-O    ATGGAAGTAGAACAAGAGAAGAAAGGAAGGATTAGAATAGAAGAAAAATTGAAGAGATAT   60
PmCdk7-T    ATGGAAGTAGAACAAGAGAAGAAAGGAAGGATTAGAATAGAAGAAAAATTGAAGAGATAT
            ************************************************************

PmCdk7-O    GAGAAGATCGATTTCTTGGGAGAAGGACAGTTTGCCACTGTATATAAGGCTCTTGATGTG  120
PmCdk7-T    GAGAAGATCGATTTCTTGGGAGAAGGACAGTTTGCCACTGTATATAAGGCTCTTGATGTG
            ************************************************************

PmCdk7-O    GAGACCAAGCAGATAGTAGCTGTCAAAAAGATCAAACTAGGTAGCAGAGAGGAGGCAAGG  180
PmCdk7-T    GAGACCAAGCAGATAGTAGCTGTCAAAAAGATCAAACTAGGTAGCAGAGAGGAGGCAAGG
            ************************************************************

PmCdk7-O    GATGGCATCAACCGTACGGCTCTCCGAGAGATCAAGCTCTTGCAGGAGGTCCACCACCCA  240
PmCdk7-T    GATGGCATCAACCGTACGGCTCTCCGAGAGATCAAGCTCTTGCAGGAGGTCCACCACCCA
            ************************************************************

PmCdk7-O    AACCTCATTGGCCTCCTCGATGTCTTTGGCTACAAGTCAAATGTGTCGCTGGTGTTTGAT  300
PmCdk7-T    AACCTCATTGGCCTCCTCGATGTCTTTGGCTACAAGTCAAATGTGTCGCTGGTGTTTGAT
            ************************************************************

PmCdk7-O    TTCATGGATACAGATTTAGAGGTGATCATCAAGGACACAGACAACATCATCCTCACACCC  360
PmCdk7-T    TTCATGGATACAGATTTAGAGGTGATCATCAAGGACACAGACAACATCATCCTCACGCCC
            ************************************************************ ***

PmCdk7-O    TCCAACATCAAAGCATATATGATCCAAACATTAAAAGGCTTGGAATTCCTGCATCTTCAC  420
PmCdk7-T    TCCAACATCAAAGCATATATGATCCAAACATTAAAAGGCTTGGAATTCCTGCATCTTCAC
            ************************************************************

PmCdk7-O    TGGATCCTACACAGAGATCTGAAACCAAACAACCTACTAGTCAATTCAGATGGCATACTT  480
PmCdk7-T    TGGATCCTACACAGAGATCTGAAACCAAACAACCTACTAGTCAATTCAGATGGCATACTT
            ************************************************************

PmCdk7-O    AAAATAGGAGATTTTGGTCTGGCAAGATTCTTTGGCTCTCCCAACAGACAGTATTCACAT  540
PmCdk7-T    AAAATAGGAGATTTTGGTCTGGCAAGATTCTTTGGCTCTCCCAACAGACAGTATTCACAT
            ************************************************************

PmCdk7-O    CAAGTAGTTACAAGATGGTACAGGAGTCCAGAGTTGCTGTTTGGCGCGAGATCCTACGGC  600
PmCdk7-T    CAAGTAGTTACAAGATGGTACAGGAGTCCAGAATTGCTGTTTGGCGCGAGATCCTACGGC
            ********************************* ****************************

PmCdk7-O    ACAGGGGTAGACATGTGGGCGATTGGCTGTATCCTGGCGGAGATGTTGGTTCGCTGTCCC  660
PmCdk7-T    ACAGGGGTAGACATGTGGGCGATTGGCTGTATCCTGGCGGAGATGTTGGTTCGCTGTCCC
            ************************************************************

PmCdk7-O    TACTTCCCGGGTGACTCTGATCTAGACCAGCTTACCAGGATCTTCACTGCCCTAGGGACT  720
PmCdk7-T    TACTTCCCGGGTGACTCTGATCTAGACCAGCTTACCAGGATCTTCACTGCCCTAGGGACT
            ************************************************************

PmCdk7-O    CCTGGTGATGACGACTGGCCGGACATGACGAAACTTCCCGACTACGTATCATTCAAGCAC  780
PmCdk7-T    CCTGGTGATGACGACTGGCCGGACATGACGAAACTTCCCGACTACGTATCATTCAAGCAC
            ************************************************************

PmCdk7-O    TTCGAGGGTTCCCCACTGCGAGACCTCTTTCCTGCTGCCAGTGATGACCTTCTCCAGCTA  840
PmCdk7-T    TTCGAGGGTTCCCCACTGCGAGACCTCTTTCCTGCTGCCAGTGATGACCTTCTCCAGCTA
            ************************************************************

PmCdk7-O    TTGGGGTCTTTGCTCACTATTAATCCTATGAAACGATGCAGCTGTACTGAGGCTCTGAAG  900
PmCdk7-T    TTGGGGTCTTTGCTCACTATTAATCCTATGAAACGATGCAGCTGTACTGAGGCTCTGAAG
            ************************************************************

PmCdk7-O    ATGGAGTATTTCAGCAATAAGCCTGTCCCGACACCAGGACCTCTTCTTCCTCTCCCACCA  960
PmCdk7-T    ATGGAGTATTTCAGCAATAAGCCTGTCCCGACACCAGGACCTCTTCTTCCTCTCCCACCA
            ************************************************************

PmCdk7-O    ACCATTAGACAGAGAAGTGAGGCAGAAAAACCGTCCCTCAAGCGAAAGATTATTGAAGAG  1020
PmCdk7-T    ACCATTAGACAGAGAAGTGAGGCAGAAAAACCGTCTCTCAAGCGAAAGATTATTGAAGAG
            ********************************** ***********************

PmCdk7-O    TCTGGCTTTGGAGGTTCCTTAGCAAAGAAGCTTCAATTCTAG   1062
PmCdk7-T    TCTGGCTTTGGAGGTTCCTTAGCAAAGAAGCTTCAATTCTAG
            ****************************************
```

D

```
PmCdk7-O     MEVEQEKKGRIRIEEKLKRYEKIDFLGEGQFATVYKALDVETKQIVAVKKIKLGSREEAR   60
PmCdk7-T     MEVEQEKKGRIRIEEKLKRYEKIDFLGEGQFATVYKALDVETKQIVAVKKIKLGSREEAR
             ************************************************************
PmCdk7-O     DGINRTALREIKLLQEVHHPNLIGLLDVFGYKSNVSLVFDFMDTDLEVIIKDTDNIILTP  120
PmCdk7-T     DGINRTALREIKLLQEVHHPNLIGLLDVFGYKSNVSLVFDFMDTDLEVIIKDTDNIILTP
             ************************************************************
PmCdk7-O     SNIKAYMIQTLKGLEFLHLHWILHRDLKPNNLLVNSDGILKIGDFGLARFFGSPNRQYSH  180
PmCdk7-T     SNIKAYMIQTLKGLEFLHLHWILHRDLKPNNLLVNSDGILKIGDFGLARFFGSPNRQYSH
             ************************************************************
PmCdk7-O     QVVTRWYRSPELLFGARSYGTGVDMWAIGCILAEMLVRCPYFPGDSDLDQLTRIFTALGT  240
PmCdk7-T     QVVTRWYRSPELLFGARSYGTGVDMWAIGCILAEMLVRCPYFPGDSDLDQLTRIFTALGT
             ************************************************************
PmCdk7-O     PGDDDWPDMTKLPDYVSFKHFEGSPLRDLFPAASDDLLQLLGSLLTINPMKRCSCTEALK  300
PmCdk7-T     PGDDDWPDMTKLPDYVSFKHFEGSPLRDLFPAASDDLLQLLGSLLTINPMKRCSCTEALK
             ************************************************************
PmCdk7-O     MEYFSNKPVPTPGPLLPLPPTIRQRSEAEKPSLKRKIIEESGFGGSLAKKLQF         353
PmCdk7-T     MEYFSNKPVPTPGPLLPLPPTIRQRSEAEKPSLKRKIIEESGFGGSLAKKLQF
             ***************************************************
```

Figure 3. 57 The complete ORF (A) and similarity search results using blast*X* (B) of *PmCdk7*. Start and stop codons are illustrated in boldface and underlined. Pairwise alignment of the nucleotide (C) and deduced amino acid sequences of PmCdc7 isolated from ovaries and testes is shown (D).

A

ATGGCTGGGCCGGTCACCGAATTTGTGGTGGGGTGGAACGTAGTCCAGACCCTTGGGGAGGG
GGCCTTTGGAGAAGTAAAATTGCTAATCAATAAGGACACTGGGGAGGCAGTTGCCATGAAGA
TGGTGGACTTGGTCAAACATCCAGATGCAGCAGATGCTGTGCGCAAGGAAATATGTCTGCAC
CGCATGTTAAAACATGCAAACATCATAAAATTTTATGGAAGTCGCCGTGAAAATTCAATGCA
GTACATGTTCCTGGAATATGCTGCAGGTGGTGAACTATTTGATCGTATTGAGCCTGACACGG
GCATGCCTCCCCATCAGGCACAGAAGTACTTCAGGGAATTGATCAGTGGTGTGGAATACCTC
CATGGACGGGGTGTTACACACCGGGATCTCAAGCCAGAGAACTTGCTGCTTGACGAGAATGA
CCATCTTAAAATAACAGACTTTGGAATGGCCACTCTCTTCAGACACAATGGGAAGGAACGTG
AATTGGATCGTCGTTGTGGAACAAAACCATATATGGCTCCTGAAGTATTGCTGAGACCCTAT
AATGCTGAACCTGCAGATATTTGGTCTTGTGGAGTGATTCTTGTTGCACTGCTAGCTGGTGA
ATTGCCATGGGATGAACCAACTTTTTCTTGTCCAGAATACACGGCCTGGAAAGACCGAGATT
GTAGGTTGTTCACAACCACACCTTGGACAAAGGTGGACAATCTGGCCCTCTCTCTTTTGCGC
AAGGTATTGAATACTGTACCTAGGCATCGAGCAACAGTACCTCAGGTGAAAGCACATCAGTG
GTTCACAAAGAACTACCACAAATCTTCAGGTTTTGGACGCAGTGCATCGAATGACAGCATGA
CCCCTACTACCAAGCGTGTGTGCAGTGAGCTTGAACGGGAAAACTCCTCATTCTGTTTGGAA
GACATGTCAGCACGGTTAGCATGTTCACAGCCAGAGGCCCCTACATCTGCTTCAATTAATAC

TGTTAATGGTCCTAATGTAGACATGGGGGTTGTGAGCTTCTCGCAACCAGCCCAACCTGACC
AGCTGTTGCTCTCCTCTCAACTTACTCAAAGTACACAAGCAAGTCAAACACCACTGCAGAGG
CTTGTGAAACGCATGACTCGTTTGCTTGTAAGGACCAACCTGGAGGACACCCTAACTCACCT
GGAAGCATTGTTCAACAAGATGAACTACACTTATCGTATGCACAATGTCAATGTTCTTACTG
TAACCACTCTGGATCGACGTGGAGCTCAACTTGTGCTGAAAGCAAGCATACTGGATATGGGC
CAGCATATTCTTGTGGATTTCAGACTTTCAAAAGGATGTGGATTGGATTTTAAACGACATTT
TCTGCGAATTAAAGAGGGTTTATCTCATATAGTAATCAAGGGTCCTGTAACTTGGAATATGG
CTCTAGCAACAAATATGCTACCAGCC**TAA**

B

checkpoint kinase 1 [Daphnia pulex]Sequence ID: gb|AGN95867.1||Length: 498
Score =513 bits, **Expect =**4e-175
Identities = 264/492(54%),**Positives** = 343/492(69%), **Gaps** = 20/492(4%)
Frame = +1

```
Query  13    VTEFVVGWNVVQTLGEGAFGEVKLLINKDTGEAVAMKMVDLVKHPDAADAVRKEICLHRM  192
             V EFV GW+++QTLGEGAFGEVKLL+N  TGEAVAMK++DL KH +AA+ V+KE+C+HRM
Sbjct  14    VIEFVEGWDMIQTLGEGAFGEVKLLVNAKTGEAVAMKVIDLKKHANAAETVKKEVCVHRM  73

Query  193   LKHANIIKFYGSRRENSMQYMFLEYAAGGELFDRIEPDTGMPPHQAQKYFRELISGVEYL  372
             L   ++I+FYG R   + +++FLEYA+GGELFDRIEPD GMP  +AQ+YF++LI+GV YL
Sbjct  74    LNDPHVIRFYGRRENGNFEFIFLEYASGGELFDRIEPDVGMPQVEAQRYFKQLIAGVSYL  133

Query  373   HGRGVTHRDLKPENLLLDENDHLKITDFGMATLFRHNGKERELDRRCGTKPYMAPEVLLR  552
             H RG+ HRD+KPENLLLD ND+LKI+DFGMAT+FR  G+ER LD+RCGT PY+APEVL R
Sbjct  134   HSRGIAHRDIKPENLLLDANDNLKISDFGMATVFRFQGRERHLDKRCGTLPYIAPEVLCR  193

Query  553   PYNAEPADIWSCGVILVALLAGELPWDEPTFSCPEYTAWKDRDCRLFTTTPWTKVDNLAL  732
              Y AEPADIWSCGV+LVA+LAGELPWD P+  CP YT+WK  +C++ T  PWTK+D LAL
Sbjct  194   KYAAEPADIWSCGVVLVAMLAGELPWDVPSNDCPLYTSWK--ECQI-TRLPWTKIDTLAL  250

Query  733   SLLRKVLNTVPRHRATVPQVKAHQWFTKNYHKSSGFGRSASNDSMTPTTKRVCSELEREN  912
             SLLRKVL  +P  R T+ Q+  HQWF K +   S   R+  N    P +KR+CS++
Sbjct  251   SLLRKVLMPLPGKRYTIQQITNHQWFQKKFKVPSTSLRTEEN---MPVSKRLCSDVVDAG  307

Query  913   SSFCLEDMSARLACSQP--------EAPTSASINTVNGPNVDM--GVVSFsqpa---qpd  1053
              S    D +  L+ SQP        +       N    PN  +   + SFSQPA
Sbjct  308   LSPPSSD-ATHLSYSQPGLELFSGSQPVHQNDTNDDQEPNKHLPGAMFSFSQPAHIDDML  366

Query  1054  qlllssqltqstqasqtplqRLVKRMTRLLVRTNLEDTLTHLEALFNKMNYTYRMHNVNV  1233
                   +  T S  +  +PLQRLVKRMTRL+ + + E+ + HL     K+ YT+++H   V
Sbjct  367   LNSQLNTQTASGSSISSPLQRLVKRMTRLVAKVSCEEAIKHLSQQLIKLGYTWKIHTPGV  426

Query  1234  LTVTTLDRRGAQLVLKASILDMGQHILVDFRLSKGCGLDFKRHFLRIKEGLSHIVIKGPV  1413
             +T++T DRR  QLV KA++ DM   +L+DFRLS+GCGLDFKRHFL IK  L+ I+   PV
Sbjct  427   VTISTQDRRKMQLVFKATVYDMQTMVLLDFRLSRGCGLDFKRHFLTIKHKLADILCSAPV  486

Query  1414  TWNMALATNMLP  1449
             TW++A ATN +P
Sbjct  487   TWSIATATNSIP  498
```

Figure 3. 58 The complete ORF (A) and similarity search results using blast*X* (B) of *PmChk1*. Start and stop codons are illustrated in boldface and underlined.

3.7.2 Sequence alignments between the full length cDNA and ORF for expression of recombinant protein

Sequence of the full-length cDNA and an ORF (amplify by *Pfu* polymerase) of each gene were aligned. Sequence alignment indicated that the full-length cDNA of *PmApc11* that contained T, T and T at positions 32, 43 and 50 were substituted by G, G and G in the amplified ORF. As a result, two Leu (positions 11 and 17) in the deduced PmApc11 protein were replaced with Val. A nonsynonymous substitution was observed (T in the full-length can replaced by C at position 1356) in *PmBystin1*. Likewise, a nonsynonymous replacement of C and T by T and C at position 490 and 712 was observed in *PmCdk7*. Nucleotide sequences of the full-length cDNA and amplified complete ORF of *PmCdc20* and *PmChk1* were not differences. Likewise, an identical sequences between the amplified partial ORF and the corresponding region in the full-length cDNA of *PmRpd3* was also observed.

Four nucleotide variants were observed between *PmCdc2* from testes and ovaries where T, G, G and G at positions 135, 281, 519 and 884 of the former were replaced by C, T, A and T in an ORF of the latter. Accordingly, two amino acid variants; Leu (position 94) and Arg (position 295) in the deduced PmCdc2 protein from testes which were replaced with Phe and Leu in that isolated from ovaries, were observed (Figure 3.56C).

Three nucleotide variants were observed between PmCdk7 from ovaries (this study) and testes where A, G and C at positions 357, 573 and 996 of the former were synonymously substituted by G, A and T in the same positions of the latter (Figure 3.57C).

3.7.3 *In vitro* expression of recombinant protein

Recombinant PmApc11, PmBystin1, PmCdc2, PmCdc20, PmCdk7, PmChk1 and PmRpd3 proteins was *in vitro* expressed in the bacterial expression system. Inducted express protein with 0.1 mM IPTG for time course 1, 2, 3, 6, 12 and 24 hours were examined.

The recombinant PmApc11 (11 kDa), PmBystin1 (52 kDa), PmCdc2 (34 kDa), PmCdc20 (59 kDa), PmCdk7 (40 kDa), PmChk1 (74 kDa) and PmRpd3 (34 kDa) were expressed since 1 hours post induction of IPTG (1.0 mM) (Figure 3.59 -3.66). All recombinant proteins except rPmCdc20 was stably expressed at 1 – 24 hour post induction. The rPmCdc20 seemed to be degraded at 6, 12 and 24 hours post induction (Figure 3.62).

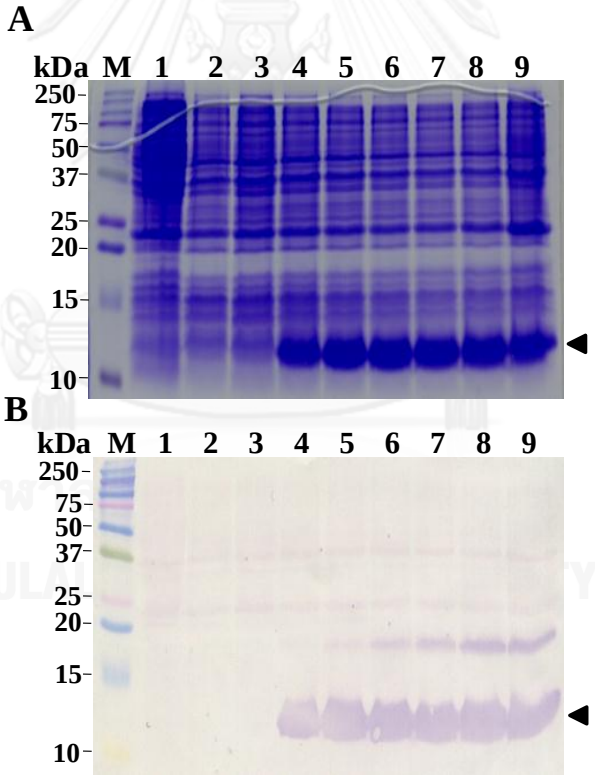

Figure 3. 59 18% SDS-PAGE (A) and Western blot (B) showing *in vitro* expression of the recombinant PmApc11 protein with pET29a vectors in *E. coli* BL21-CodonPlus (DE3)-RIPL at 0,1,2,3,6,12 and 24 hours after induction (lanes 3- 9). *E. coli* BL21-CodonPlus (DE3)-RIPL and pET29a in *E. coli* BL21-CodonPlus (DE3)-RIPL (lanes 1 and 2) were included as the negative controls. Arrowheads indicated the expected protein products.

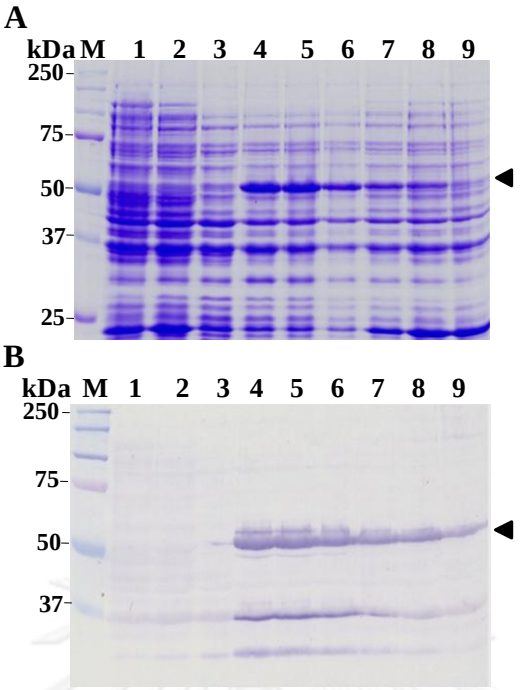

Figure 3. 60 12% SDS-PAGE (A) and Western blot analysis (B) showing *in vitro* expression of rPmBystin1 protein (pET32a) vectors after induction with 1.0 mM IPTG for 0, 1, 2, 3, 6, 12 and 24 hours (lanes 3- 9). *E. coli* BL21-CodonPlus (DE3)-RIPL and pET32a in *E. coli* BL21-CodonPlus (DE3)-RIPL (lanes 1 and 2) were included as the negative controls. Arrowheads indicated the expected protein products

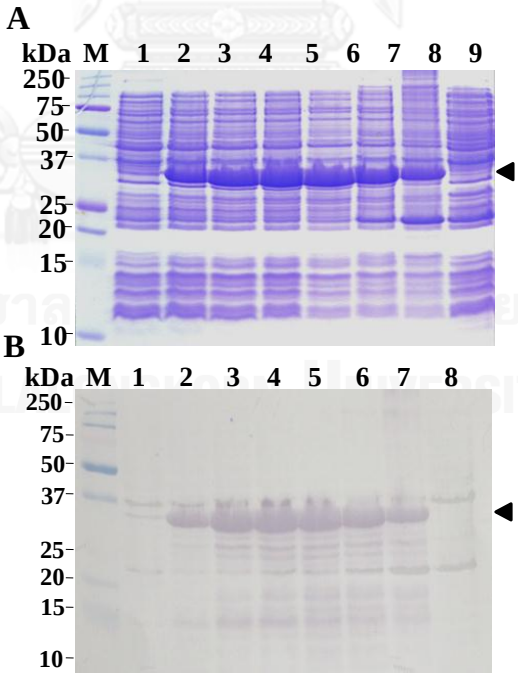

Figure 3. 61 15% SDS-PAGE (A) and Western blot analysis (B) showing *in vitro* expression of rPmCdc2 protein (pET17b) at 0, 1, 2, 3, 6, 12 and 24 hours after induction with 1.0 mM IPTG (lanes 1-7). The pET17b in *E. coli* BL21-CodonPlus (DE3)-RIPL (lanes 8) was included as the negative control. Arrowheads indicated the expected protein products.

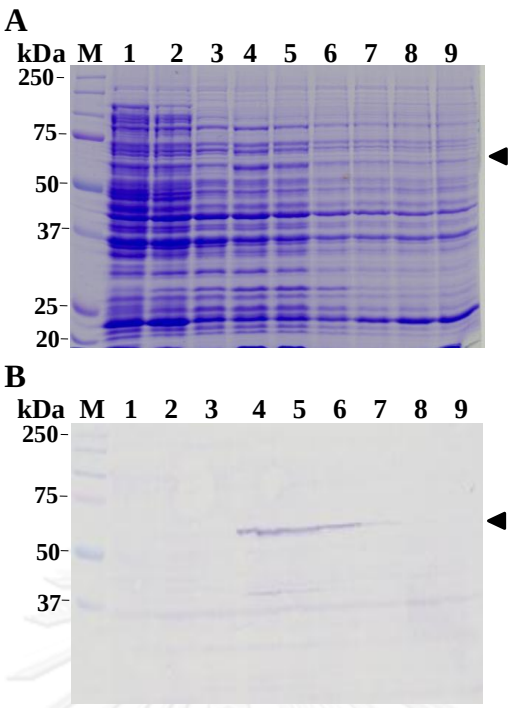

Figure 3. 62 12% SDS-PAGE (A) and Western blot analysis (B) showing *in vitro* expression of rPmCdc20 protein (pET32a) after induction with 1.0 mM IPTG for 0, 1, 2, 3, 6, 12 and 24 hours (lanes 3- 9). *E. coli* BL21-CodonPlus (DE3)-RIPL and pET32a in *E. coli* BL21-CodonPlus (DE3)-RIPL (lanes 1 and 2) were included as the negative control. Arrowheads indicated the expected protein products.

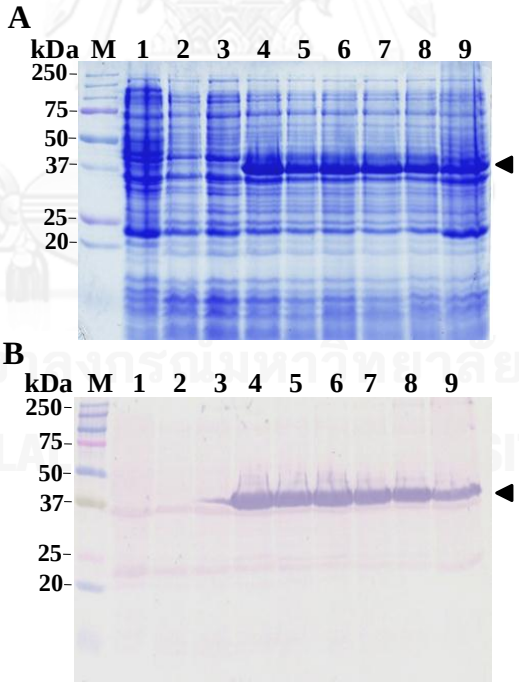

Figure 3. 63 15% SDS-PAGE (A) and Western blot analyis (B) showing in vitro expression of rPmCdk7 protein (pET29a) at 0, 1, 2, 3, 6, 12 and 24 hours after induction with 1.0 mM IPTG (lanes 3- 9) *E. coli* BL21-CodonPlus (DE3)-RIPL and pET29a in *E. coli* BL21-CodonPlus (DE3)-RIPL (lanes 1 and 2) were included as the negative control. Arrowheads indicated the expected protein products.

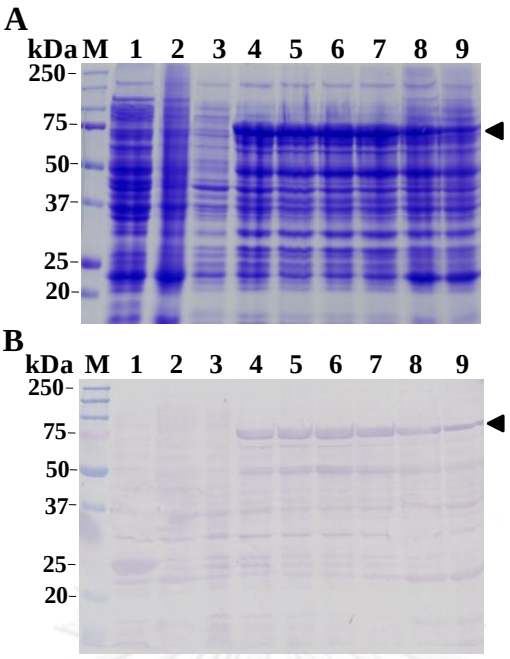

Figure 3. 64 12% SDS-PAGE (A) and Western blot analysis (B) showing *in vitro* expression of rPmChk1 protein (pGEX4T-1) after induction with 1.0 mM IPTG for 0, 1, 2, 3, 6,12 and 24 hours (lanes 3- 9) *E. coli* BL21-CodonPlus (DE3)-RIPL and pGEX4T-1 in *E. coli* BL21-CodonPlus (DE3)-RIPL (lanes 1 and 2) were included as the negative controls. Arrowheads indicated the expected protein products.

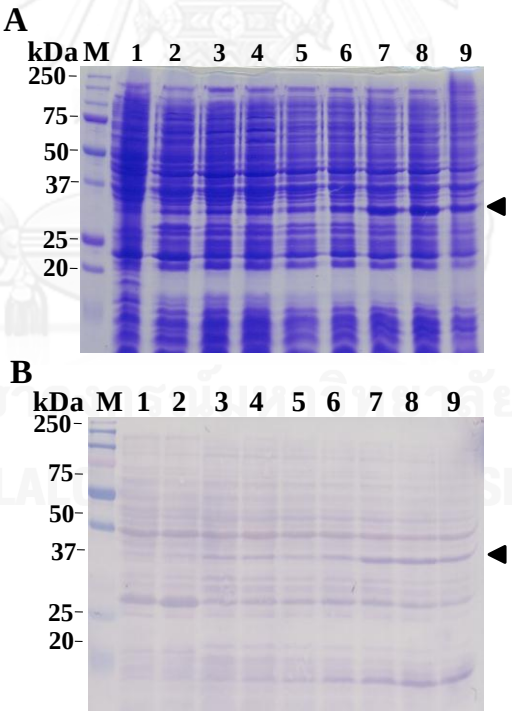

Figure 3. 65 12% SDS-PAGE (A) and Western blot (B) showing *in vitro* expression of rPmRpd3 protein (pET 17b) at 0, 1, 2, 3, 6, 12 and 24 hours after induction with 1.0 mM IPTG (lanes 3- 9) *E. coli* BL21-CodonPlus (DE3)-RIPL and pET 17b in *E. coli* BL21-CodonPlus (DE3)-RIPL (lanes 1 and 2) were included as the negative controls. Arrowheads indicated the expected protein products.

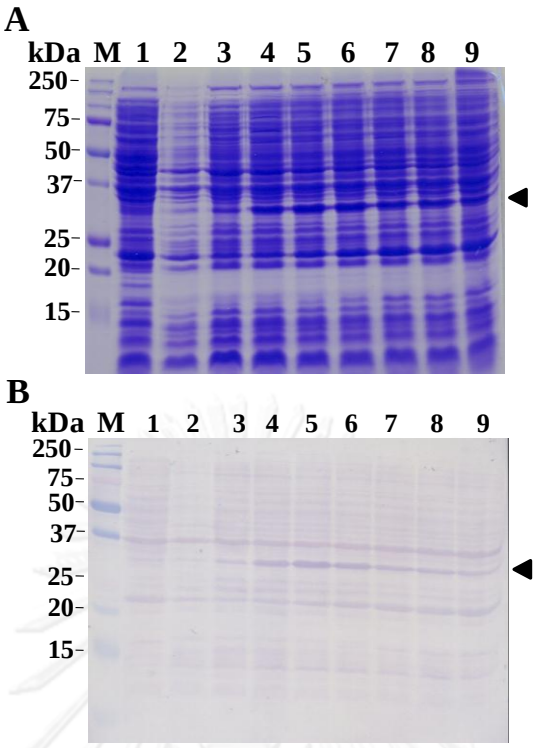

Figure 3. 66 12% SDS-PAGE (A) and Western blot analysis (B) showing *in vitro* expression of rPmRpd3 protein (pET 29a) after induction with 1.0 mM IPTG for 0, 1, 2, 3, 6, 12 and 24 hours (lanes 3- 9). *E. coli* BL21-CodonPlus (DE3)-RIPL and pET 29a in *E. coli* BL21-CodonPlus (DE3)-RIPL (lanes 1 and 2) were included as the negative controls. Arrowheads indicated the expected protein products.

3.8 Expression of rPmApc11, rPmBystin1, rPmCdc2, rPmCdc20, rPmCdk7, rPmChk1 and rPmRpd3 proteins in soluble and insoluble fractions

Recombinant clones of PmApc11, PmBystin1, PmCdc2, PmCdc20, PmCdk7, PmChk1 and PmRpd3 were cultured at 37°C. Soluble and insoluble fractions were separated to identify the forms of expressed recombinant proteins. The rPmApc11, rPmBystin1, rPmCdc2, rPmCdc20, rPmChk1 and rPmRpd3 were solely expressed in the inclusion bodies while rPmCdk7 was expressed in both soluble and (majorly) insoluble forms (Figure 3.67 - 3.73).

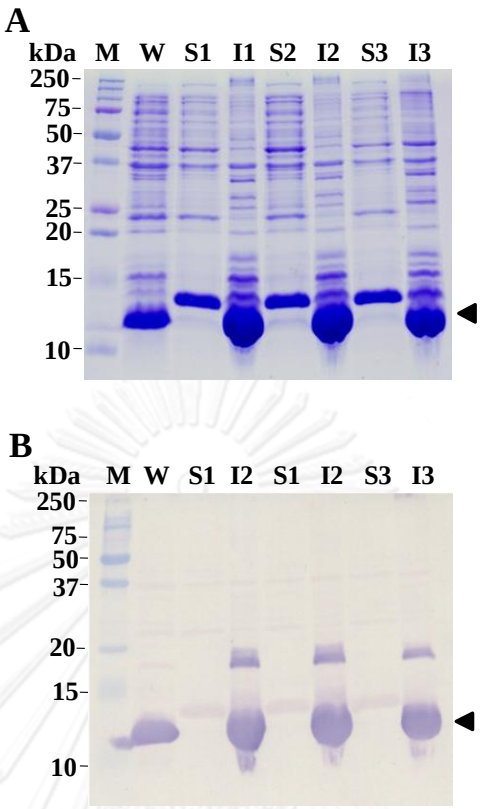

Figure 3. 67 18% SDS-PAGE (A) and Western blot analysis (B) showing expression of rPmApc11 after induction with 1.0 mM IPTG for 2 hours at 37°C. Lane W = whole cells, Lanes S = soluble protein fractions and Lanes I = insoluble protein fractions of clone no. 1, 2 and 3, respectively (15 µg protein). Arrowheads indicated the expected protein products.

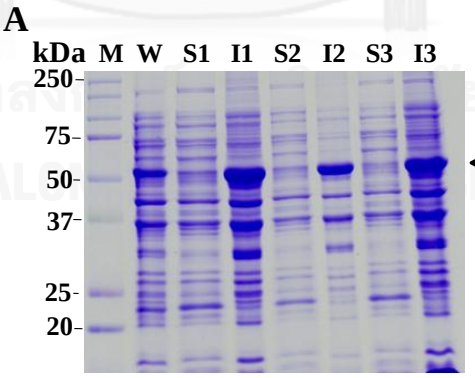

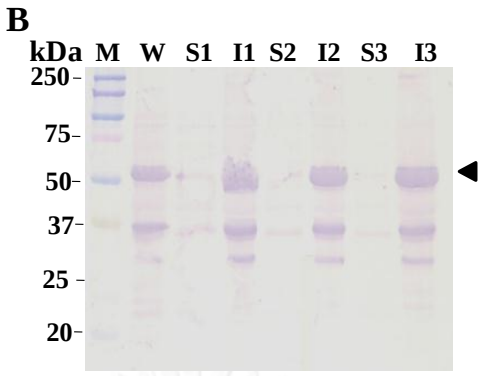

Figure 3. 68 15% SDS-PAGE (A) and Western blot analysis (B) showing expression of rPmBystin1 after induction with 1.0 mM IPTG induction for 2 hours at 37°C. Lane W = whole cells, Lanes S = soluble protein fractions and Lanes I = insoluble protein fractions of clone no. 1, 2 and 3, respectively (15 µg protein). Arrowheads indicated the expected protein products.

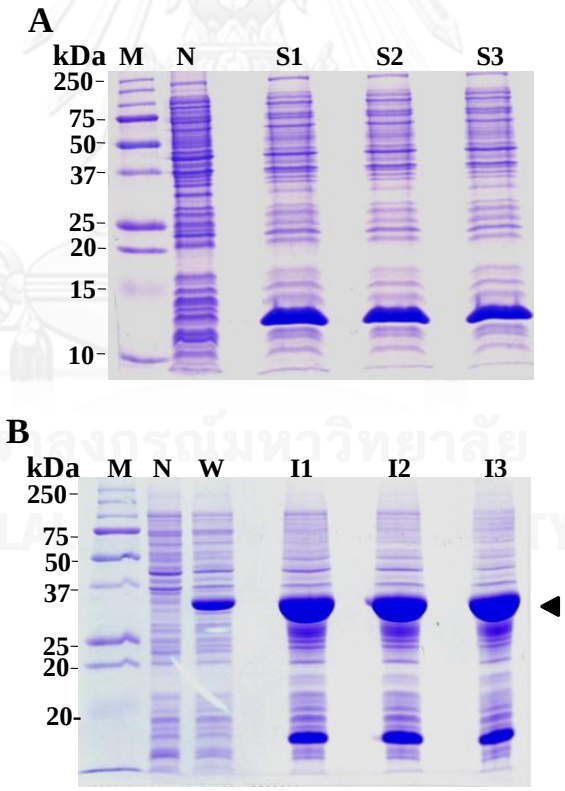

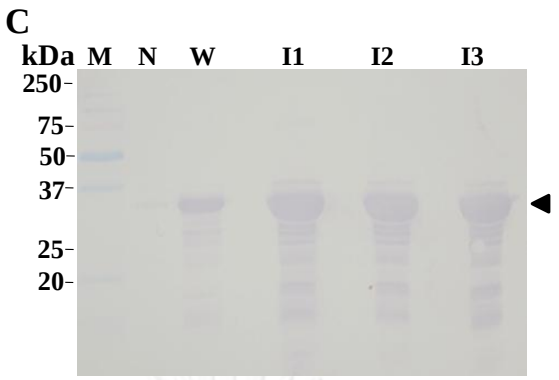

Figure 3. 69 15% SDS-PAGE (A, B) and Western blot analysis (C) showing expression of rPmCdc2 after induction with 1.0 mM IPTG for 2 hours at 37°C. Lane N = pET 17b in *E. coli* BL21-CodonPlus (DE3)-RIPL, Lane W = whole cells, Lanes S = soluble protein fractions and Lanes I = insoluble protein fractions of clone no. 1, 2 and 3, respectively (15 µg protein). Arrowheads indicated the expected protein products.

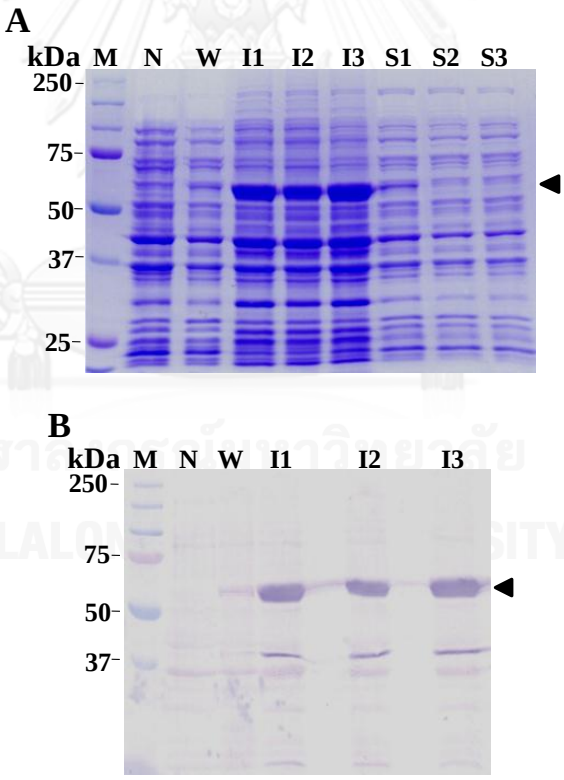

Figure 3. 70 12% SDS-PAGE (A) and Western blot analysis (B) showing expression of rPmCdc20 after induction with 1.0 mM IPTG for 2 hours at 37°C. Lane1 = pET 32a in *E. coli* BL21-CodonPlus (DE3)-RIPL, Lane 2 = whole cells, Lanes S = soluble fractions

and Lanes I = insoluble fractions of clone 1, 2 and 3, respectively (15 µg protein). Arrowheads indicated the expected protein products.

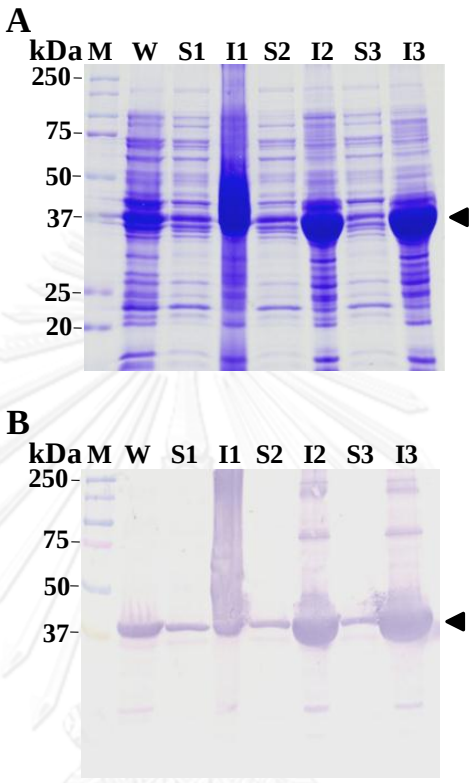

Figure 3. 71 15% SDS-PAGE (A) and Western blot analysis (B) showing expression of rPmCdk7 after induction with 1.0 mM IPTG for 2 hours at 37°C as the insoluble protein. Lane W = whole cells, Lanes S = soluble fractions and Lanes I = insoluble fractions of clone no. 1, 2 and 3, respectively (15 µg protein). Arrowheads indicated the expected protein products.

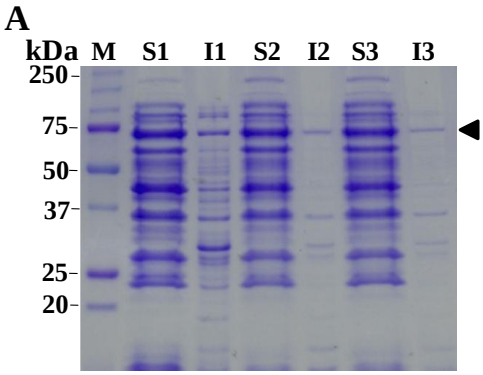

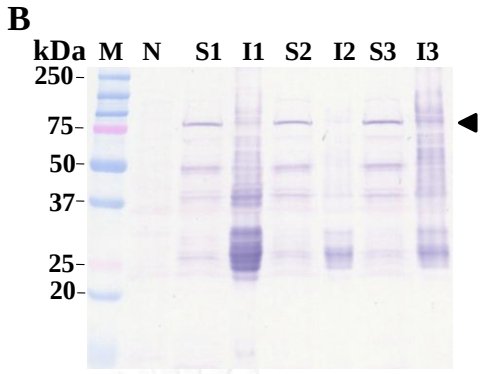

Figure 3. 72 15% SDS-PAGE (A) and Western blot analysis (B) showing expression of rPmChk1 after induction with 1.0 mM IPTG for 2 hours at 37°C as the soluble protein. Lane N = pGEX4T-1 in *E. coli* BL21-CodonPlus (DE3)-RIPL, Lanes S = soluble fractions and Lanes I = insoluble fractions of clone 1, 2 and 3, respectively (15 µg protein). Arrowheads indicated the expected protein products.

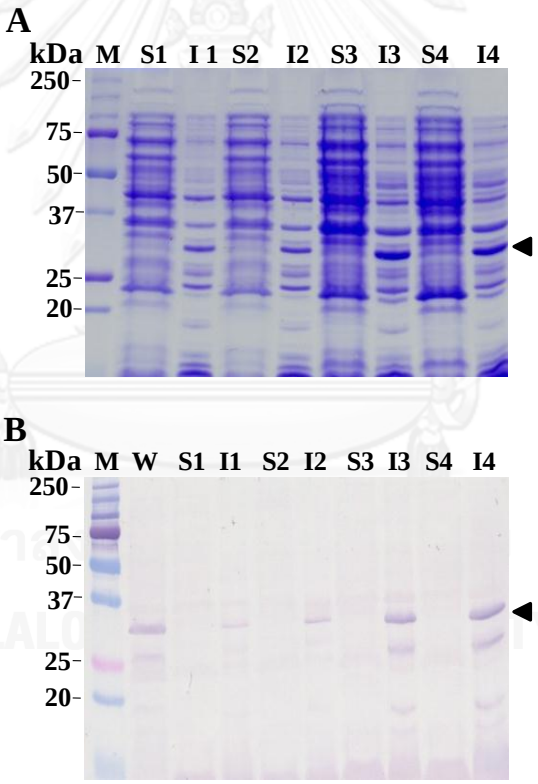

Figure 3. 73 15% SDS-PAGE (A) and Western blot analysis (B) showing expression of rPmRpd3 after induction with 1.0 mM IPTG induction for 2 hours at 37°C. Lane W = whole cells of PmRpd3 in pET17b, Lanes S1, S2 = soluble fractions in pET17b, Lanes I1, I2 = insoluble fractions in pET17b, Lanes S3, S4 = soluble fractions in pET29a, Lanes I3, I4 = insoluble fractions in pET29a of clone no. 1 and 2, respectively (15 µg protein). Arrowheads indicated the expected protein products.

3.9 Purification of the recombinant proteins

As can be seen from the previous section, recombinant proteins in this study were expressed in the insoluble form. Therefore, they were further purified under the denaturing conditions (20 mM sodium phosphate, 500 mM NaCl, and 20 mM imidazole, pH 7.4 with 8 M urea) using HiTrap Chelating HP affinity chromatography. Each fraction of the washing and eluting step (20 mM sodium phosphate, 500 mM NaCl and 500 mM imidazole, pH 7.4 and 8M urea) were analyzed by SDS-PAGE and Western blotting. The purified protein was stored at -20°C.

The crude rPmApc11, rPmBystin1, rPmCdc2, rPmCdc20, rPmCdk7, rPmRpd3 and rPmChk1 proteins were purified as described above (Figure 3.74 - 3.80) and a single discrete band of 11 kDa, 52 kDa, 34 kDa, 59 kDa, 40 kDa, 34 kDa and 75 KDa were obtained, respectively (Figure 3.81), respectively.

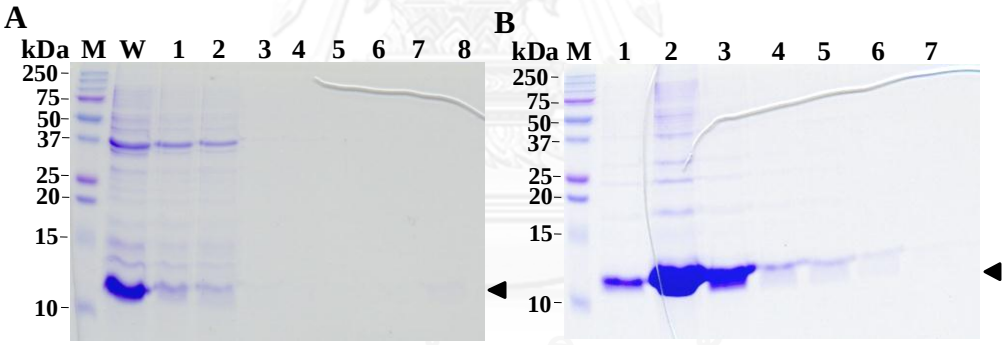

Figure 3. 74 Purification of rPmApc11 under the denaturing conditions. Recombinant proteins were examined using 18% SDS-PAGE (A-B). Panel A, lane W = whole cells, lane 1 = the insoluble fraction before pass through the column, lane 2 = the insoluble fraction after pass through the column, lanes 3 and 4 = the first wash (20mM imidazole) fractions 1 and 10, lanes 5 and 6 = the second wash (40 mM) fractions 1 and 5, and lanes 7 and 8 = the third wash (80 mM) fractions 1 and 5, respectively. Lanes 1-7 (B) = eluted protein fractions 1-7, respectively.

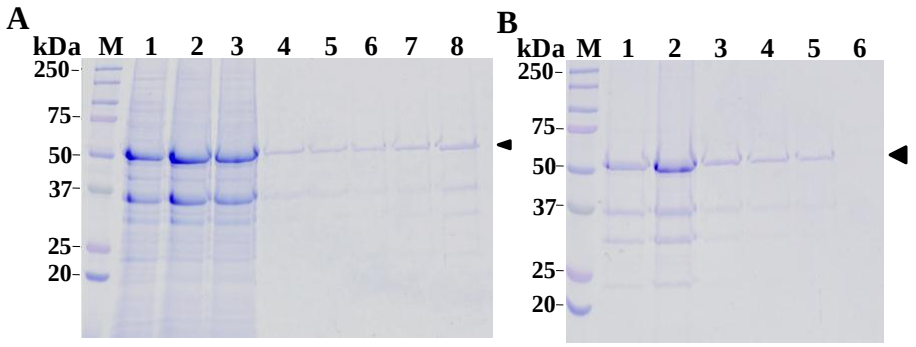

Figure 3. 75 Purification of rPmBystin1 under the denaturing conditions. Recombinant proteins were examined using 12% SDS-PAGE (A-B) lane 1 = the insoluble fraction before pass through the column, lane 2 = the insoluble fraction after pass through the column, lanes 3 and 4 = the first wash (20 mM imidazole) fractions 1 and 10, lanes 5, 6 = the second wash (40 mM) fractions 1 and 5, and lanes 7 and 8 = the third wash (80 mM) fractions 1 and 5, respectively. Lanes 1-6 (B) = eluted protein fractions 1-6, respectively.

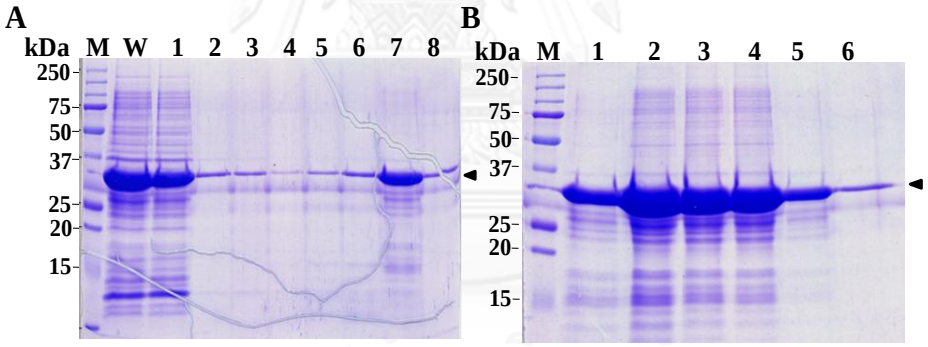

Figure 3. 76 Purification of rPmCdc2 under the denaturing conditions. Recombinant proteins were examined using 15% SDS-PAGE (A-B). Panel A, lane W = whole cells, lane 1 = the insoluble fraction before pass through the column, lane 2 = the insoluble fraction after pass through the column, lanes 3 and 4 = the first wash (20 mM imidazole) fractions 1 and 10, lanes 5, 6 = the second wash (40 mM) fractions 1 and 5, and lanes 7 and 8 = the third wash (80 mM) fractions 1 and 5, respectively. Lanes 1-6 (B) = eluted protein fractions 1-6, respectively.

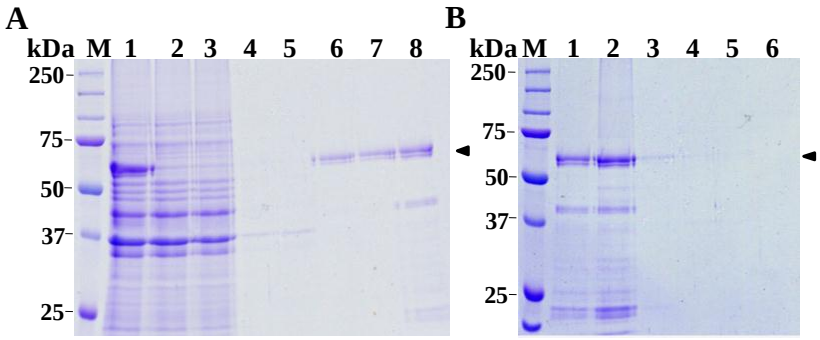

Figure 3. 77 Purification of rPmCdc20 under the denaturing conditions. Recombinant proteins were examined using 12% SDS-PAGE (A-B); Panel A, lane 1 = the insoluble fraction before pass through the column, lane 2 = the insoluble fraction after pass through the column, lanes 3 and 4 = the first wash (20 mM imidazole) fractions 1 and 10, lanes 5 and 6 = the second wash (40 mM) fractions 1 and 5, and lanes 7 and 8 = the third wash (80 mM) fractions 1 and 5, respectively. Lanes 1-6 (B) = eluted protein fractions 1-6, respectively.

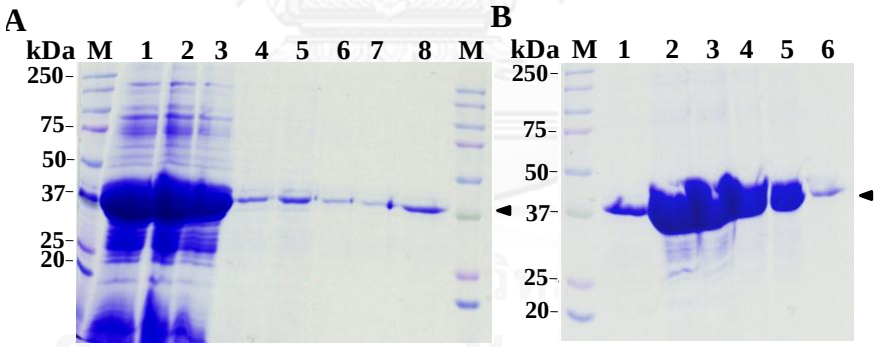

Figure 3. 78 Purification of rPmCdk7 under the denaturing conditions. Recombinant proteins were examined using 12% SDS-PAGE (A-B). Panel A, lane 1 = the insoluble fraction before pass through the column, lane 2 = the insoluble fraction after pass through the column, lanes 3 and 4 = the first wash (20 mM) fractions 1 and 10, lanes 5, 6 = the second wash (40 mM) fractions 1 and 5, and lanes 7 and 8 = the third wash (80 mM) fractions 1 and 5, respectively. Lanes 1-6 (B) = eluted protein fractions 1-6, respectively.

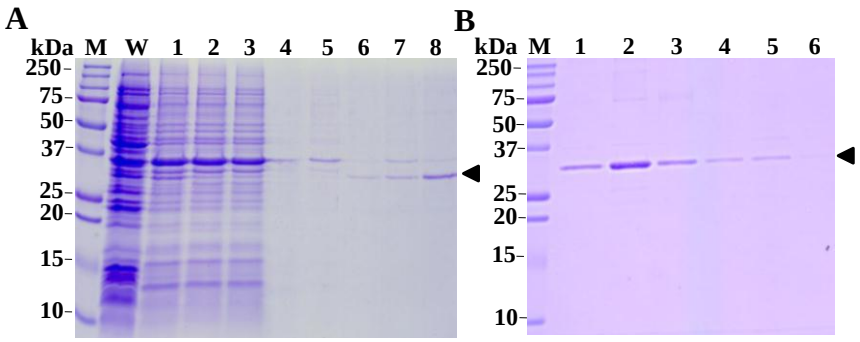

Figure 3. 79 Purification of rPmRpd3 under the denaturing conditions. Recombinant proteins were examined using 15% SDS-PAGE (A-B). Panel A lane W = whole cells, lane 1 = the insoluble fraction before pass through the column, lane 2 = the insoluble fraction after pass through the column, lanes 3 and 4 = the first wash (20 imidazole) fractions 1 and 10, lanes 5 and 6 = the second wash (40 mM) fractions 1 and 5, and lanes 7 and 8 = the third wash (80 mM) fractions 1 and 5, respectively. Lanes 1-6 (B) = eluted protein fractions 1-7, respectively.

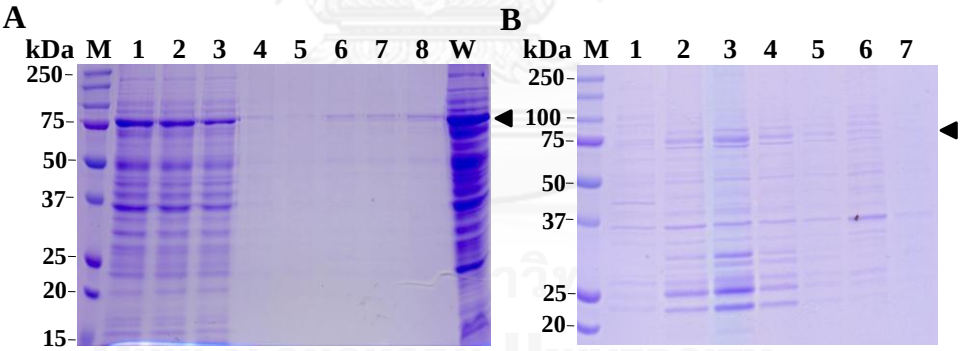

Figure 3. 80 Purification of rPmChk1 under the non-denaturing conditions. Recombinant proteins were examined using 12% SDS-PAGE (A-B). Panel A, lane W = whole cells, lane 1 = the soluble fraction before pass through the column, lane 2 = the soluble fraction after pass through the column, lanes 3 and 4 = the first wash (20 mM imidazole) fractions 1 and 10, lanes 5 and 6 = the second wash (40 mM) fractions 1 and 5, and lanes 7 and 8 = the third wash (80 mM) fractions 1 and 5, respectively. B lanes 1-7 = eluted protein fractions 1-7, respectively.

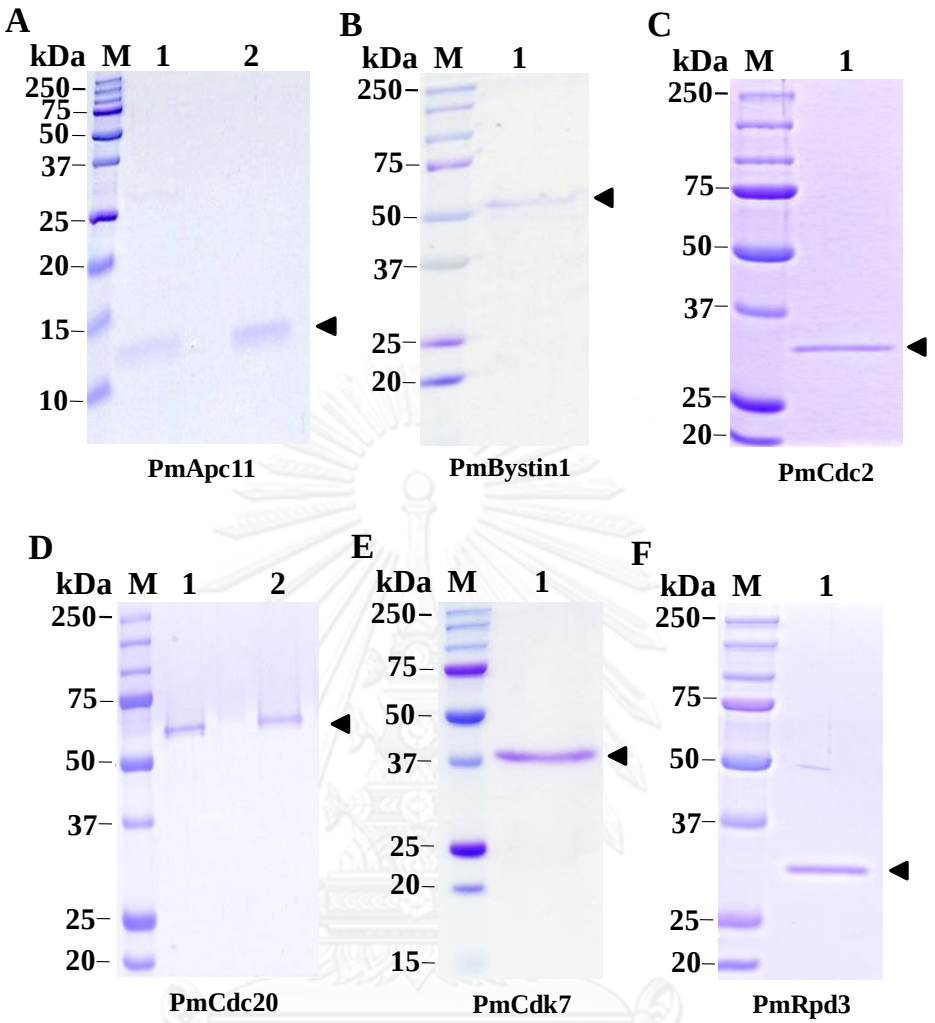

Figure 3. 81 SDS-PAGE showing purification of rPmApc11 (A), rPmBystin1 (B), rPmCdc2 (C), rPmCdc20 (D), rPmCdk7 (E) and rPmRpd3 (F) in the denaturing conditions using a His GraviTrap kit.

3.10 Polyclonal antibody production against recombinant proteins

Rabbit anti-rPmBystin1, anti-rPmCdc2, anti-rPmCdc20, anti-rPmCdk7 and anti-rPmRpd3 PAb were produced by the Faculty of Associated Medical Sciences, Chiang Mai University. Polyclonal antibodies against recombinant proteins in this study were quite difficult to generated and several repeated administration of the antigens were required. The titers of anti-rPmBystin1 (5 doses), anti-rPmCdc2 (6 doses), anti-rPmCdc20 (4 doses), anti-rPmCdk7 (5 doses) and anti-rPmRpd3 (6 doses) are shown by Table 3.1. The crude polyclonal antibody was further filtrated using 0.22 μM membrane and stored at -20°C.

Table 3. 1 Titers of anti-rPmBystin1, anti-rPmCdc2, anti-rPmCdc20, anti-rPmCdk7 and anti-rPmRpd3 after rabbits were immunized with antigen (recombinant protein) measured by the direct ELISA assay (OD_{450}).

	Polyclonal antibody			
	Coated		Uncoated	
Dilution of serum	Pre-immunized serum (OD_{450})*	Immunized serum (OD_{450})**	Pre-immunized serum (OD_{450})	Immunized serum (OD_{450})
1. rPmBystin1				
1:500	0.068	3.123	0.040	0.214
1:2000	0.029	2.702	0.023	0.078
1:8000	0.015	1.674	0.013	0.030
1:32000	0.011	0.715	0.012	0.019
2. rPmCdc2				
1:500	0.056	2.197	0.033	0.065
1:2000	0.024	1.625	0.010	0.026
1:8000	0.014	0.764	0.005	0.008
1:32000	0.013	0.242	0.003	0.007
3. rPmCdc20				
1:500	0.086	3.095	0.088	0.089
1:2000	0.022	1.750	0.024	0.032
1:8000	0.010	0.657	0.010	0.022
1:32000	0.007	0.206	0.008	0.013
4. rPmCdk7				
1:500	0.090	2.389	0.051	0.046
1:2000	0.040	1.498	0.023	0.020
1:8000	0.018	0.526	0.011	0.015
1:32000	0.010	0.161	0.007	0.007
5. rPmRpd3				
1:500	0.078	1.407	0.055	0.079
1:2000	0.033	0.807	0.021	0.044
1:8000	0.013	0.448	0.009	0.023
1:32000	0.018	0.306	0.003	0.022

*Pre-immunized serum = serum from normal rabbit

**Immunized serum = serum from rabbit injected with the recombinant protein

3.11 Specificity and sensitivity of purified anti-PmCdc2 PAb and anti-PmCdk7 PAb

Anti-rPmCdc2 and anti-rPmCdk7 PcAb gave positive immunoreactive signals with the target (rPmCdc2 or rPmCdk7) but did not cross-react with non-target proteins including rPmDRK which contained the Src homolog domains, SH2 and SH3, rPmPKACB which contained a protein kinase domain, rPmCdc2 which contained a S_TKc domain, rPmCyB which contained a cyclin domain, rPmSema which contained a semaphorin domain and rPmRpd3 which contained a Hist_deacetyl domain (Figure 3.82A and 3.83A). When the detection sensitivity for the produced anti-PmCdc2 and anti-PmCdk7 antibody were tested, positive reactions were observed with 0.03 - 1 µg of both rPmCdc2 and rPmCdk7 (Figure 3.82B and 3.83B).

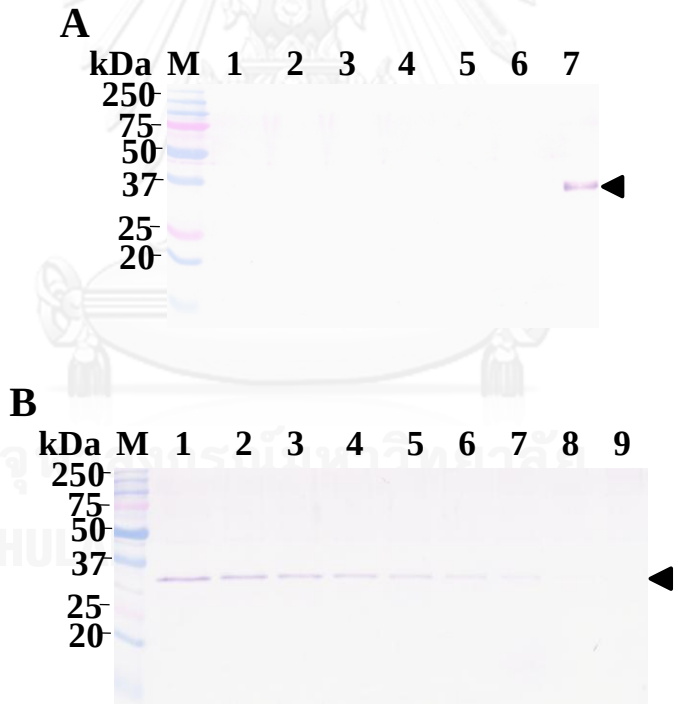

Figure 3. 82 Specificity of anti-rPmCdc2 PAb was tested against various recombinant proteins (0.2 µg) of *P. monodon* including rPmDRK, PmPKACB, rPmCdc2, rPmCyB, rPmSema, rPmRpd3 and rPmCdc2 (A). The sensitivity of anti-rPmCdc2 PAb against varying amounts of rPmCdc2 protein (1, 0.8, 0.6, 0.4, 0.2, 0.1, 0.05, 0.03, 0.01 µg, lanes 1-9, respectively; B)

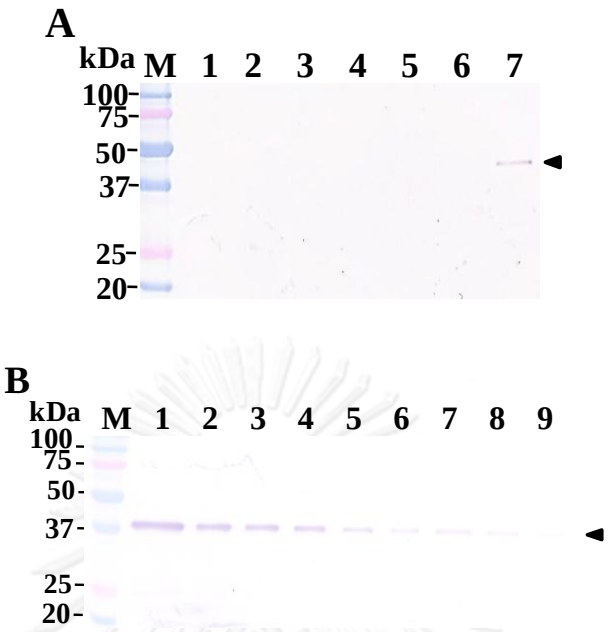

Figure 3. 83 Specificity of anti-rPmCdk7 PAb was tested against various recombinant proteins (0.2 µg) of *P. monodon* including rPmDRK, PmPKACB, rPmCdc2, rPmCyB, rPmSema, rPmRpd3 and rPmCdk7 (A). The sensitivity of anti-rPmCdk7 PAb against varying amounts of rPmCdk7 protein (1, 0.8, 0.6, 0.4, 0.2, 0.1, 0.05, 0.03, 0.01 µg, lanes 1-9, respectively; B).

Western blot analysis using anti-rPmCdk7 PAb revealed a discrete band of 67 kDa in various stages of ovaries in both intact and eyestalk-ablated shrimp. Antigen-antibody competition experiment was carried out to determine the specificity of anti-PmCdk7 PAb. The positive immmunoreactive band was observed from 2.5, 5, 10 and 20 µg total ovarian proteins whether or not the purified antibody was used in competition with 1 µg rPmCdk7. Increasing competition of rPmCdk7 to 2.5 µg resulted in the disappearance of the positive band in 2.5 and 5 µg total ovarian proteins. Disappearance of the positive signal was observed when the purified antibody was used in competition with 5 and 10 µg rPmCdk7. This confirmed the specificity of anti-PmCdk7 PAb against the 67 kDa band (Figure 3.84).

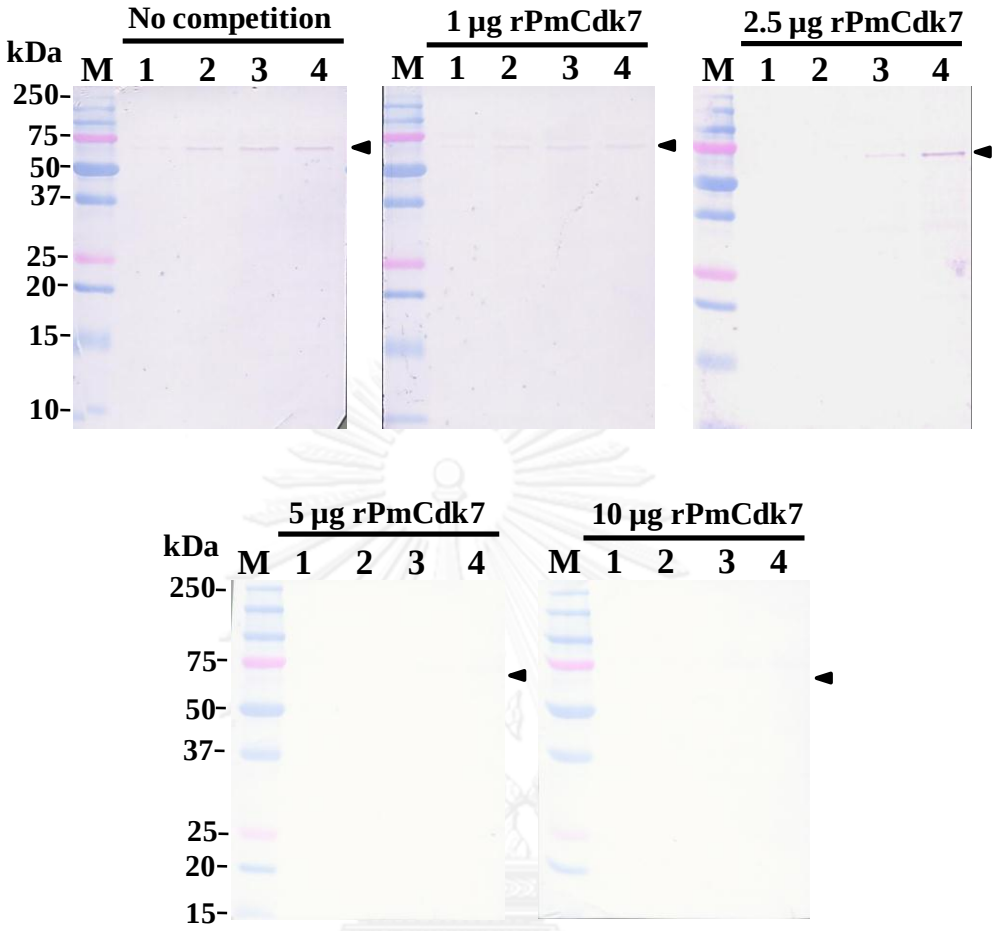

Figure 3. 84 Competitive binding assays with rPmCdk7 PAb was carried out using rPmCdk7. Western blot analysis of the purified anti-PmCdk7 PAb (3.5 ml, 1:100) pre-mixed with 0, 1, 2.5, 5 or 10 µg of rPmCdk7 and used against 2.5, 5, 10 and 20 µg total ovarian proteins (lanes 1–4, respectively) of a female shrimp with vitellogenic ovaries (stage II) and showing complete competitive blocking at 5 and 10 µg rPmCdk7.

3.12 Expression profiles of anti-rPmBystin1, anti-rPmCdc2, anti-rPmCdc20, anti-rPmCdk7 and anti-rPmRpd3 protein during ovarian development of *P. monodon*

Crude anti-rPmBystin1, anti-rPmCdc2, anti-rPmCdc20, anti-rPmCdk7 and anti-rPmRpd3 PAb generated non-specific bands when directly applied for western blot analysis. These antibodies were further purified where anti-rPmBystin1, anti-rPmCdc2

and anti-rPmCdc20 PAb was purified by using a protein A method while anti-rPmCdk7 PAb was purified by an affinity-chromatographic approach.

Western blot analysis indicated that PmBystin1 (52 kDa) was expressed in ovaries of juveniles and stages I-IV and post spawning ovaries of intact broodstock and in stages II-IV ovaries in eyestalk-ablated broodstock. In addition, a smaller band of approximately 50 kDa were observed along with a 52 kDa band in stages I-IV and II-IV in respective group of broodstock. A 43 kDa band was also observed in stges II-IV ovaries of both groups and in post-spawning ovaries in intact broodstock. This suggested the possible modification of PmBystin1 during vitellogenesis and maturation of ovarian development in *P. monodon* (Figure 3.85).

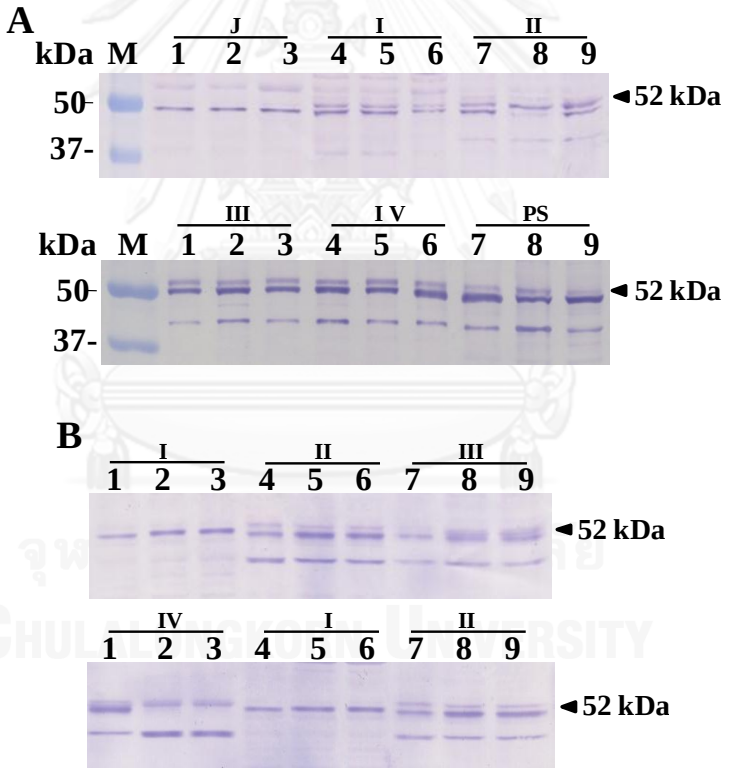

Figure 3. 85 Western blot analysis of anti-rPmBystin1 PAb (1:200) against 20 µg of total proteins extracted from ovaries of cultured juveniles (lanes 1-3, A), intact broodstock (lanes 1–9, A) and eyestalk-ablated (lanes 1–9, B) broodstock of *P. monodon*. Lanes J = juveniles, I–IV = stages I, II, III and IV ovaries, respectively. Lanes M = a protein standard.

Anti-rPmCdc2 PAb revealed the expected 34 kDa band (both phosphorylated and non-phosphorylated forms) along with a smaller band of approximately 23 kDa in juveniles and broodstock shrimp having different stages of ovarian development. The expression of the 34 kDa PmCdc2 was reduced relative to stages I and II in stages III and IV in intact broodstock (Figures 3.86A). In eyestalk-ablated broodstock, its expression was lower in stages II–IV compared to that of stage I ovaries (Figures 3.86B).

Using phospho-Cdc2 (Thr161) PAb, the positive signal of 34 kDa (active form) was found in all stages of ovaries in intact broodstock. Surprisingly, the phophorylated PmCdc2 was also observed in juvenile shrimp (Figure 3.86C). This antibody did not generated a 23 kDa band and it did not recognized rPmCdc2 (non-phosphorylated protein).

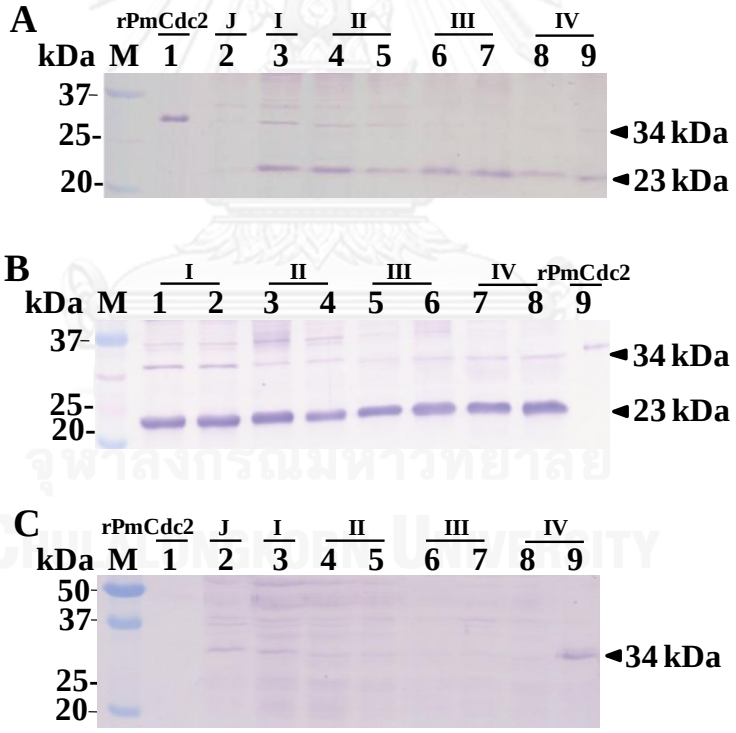

Figure 3. 86 Western blot analysis of anti-rPmCdc2 PAb (1:200) and phospho-Cdc2 (Thr161) PAb (1:300, C) against 30 µg of total proteins extracted from ovaries of cultured juveniles (lanes 2, A and C), intact broodstock (lanes 3–9, A and C) and eyestalk-ablated broodstock (lanes 1–8, B) of *P. monodon*. Purified rPmCdc2 was included as the positive control (lanes 1A and 9B). Lanes J = juveniles, I–IV = stages I, II, III and IV ovaries, respectively. Lanes M = a protein standard.

In intact broodstock, the phosphorylated PmCdc2 protein was relatively low in stages I–III and it was increased in the mature stage of ovarian development (Figure 3.87A). Interestingly, comparably abundant levels were observed in different stages of ovarian development in eyestalk-ablated broodstock (Figure 3.87B).

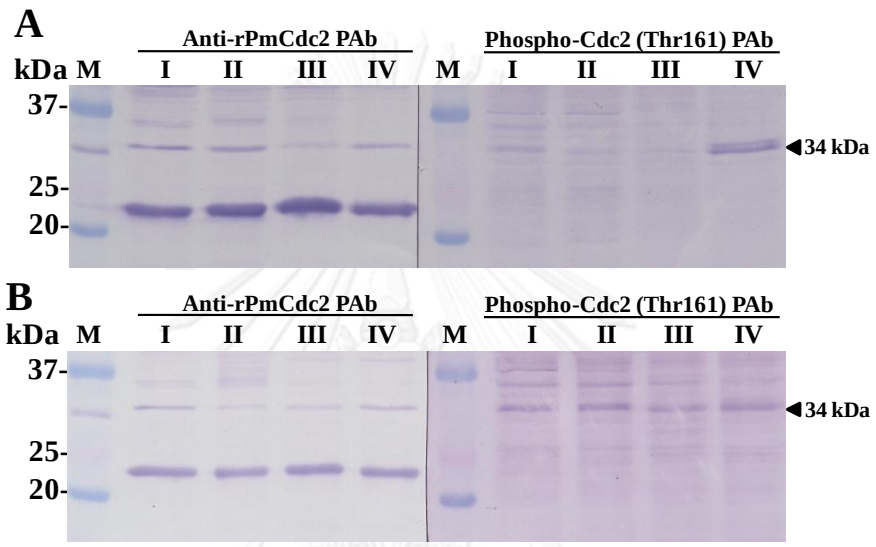

Figure 3. 87 Western blot analysis of anti-rPmCdc2 PAb (1:200) and phospho-Cdc2 (Thr161) PAb (1:200) against total proteins (30 µg) extracted from different stages of ovaries of intact broodstock (A) and eyestalk-ablated broodstock (B) of wild *P. monodon*. Ovarian proteins from each stage were size-fractionated in the same gel. The transferred membrane was cut to two halves and examined by different antibodies. I-IV = stages I, II, III and IV ovaries. Lanes M = a protein standard.

Western blot analysis of anti-rPmCdc20 PAb revealed the expected 59 kDa band in juveniles and broodstock that exhibited different stages of ovarian development. The immunoreactive signal seemed to reduced in stage III ovaries in intact broodstock and in stages III and IV ovaries in eyestalk-ablated broodstock (Figures 3.88).

Anti-PmCdk7 PAb generated the positive immunoreactive band of 67 kDa in stage I-IV of ovaries in both wild intact broodstock and eyestalk-ablated broodstock. PmCdk7 was not differentially expressed during ovarian development in *P. monodon*

broodstock. Nevertheless, the positive signals were not observed in juvenile ovaries. (Figure 3.89, A-C).

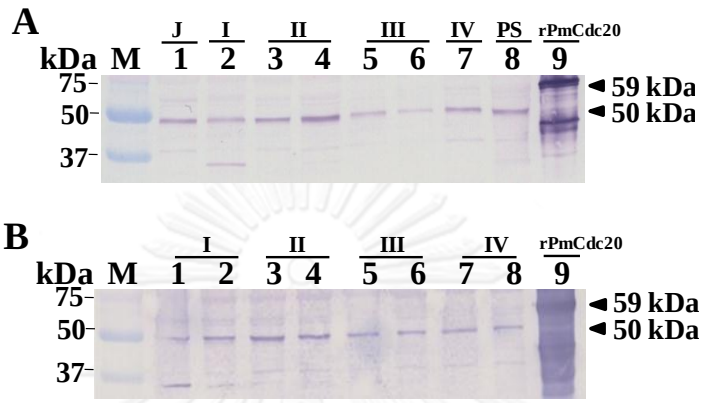

Figure 3. 88 Western blot analysis of anti-rPmCdc20 PAb (1:200) against 20 µg of total proteins extracted from ovaries of cultured juveniles (lane 1, A), intact broodstock (lanes 2-8, A) and eyestalk-ablated broodtock (lanes 1–8, B) of *P. monodon*. The rPmCdc20 was included as the positive control (lanes 1A and 9B). Lanes J = juveniles, I–IV = stages I, II, III and IV ovaries, respectively. Lanes M = a protein standard.

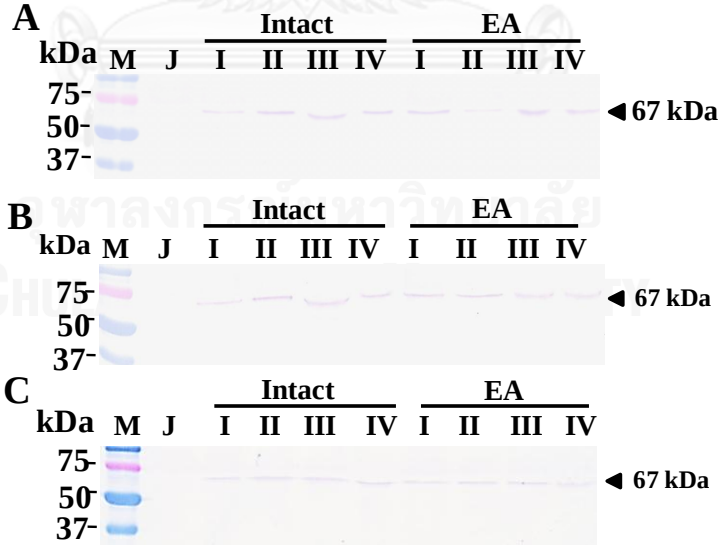

Figure 3. 89 Western blot analysis of anti-rPmCdk7 PAb (1:100) against 30 µg of total proteins extracted from different stages of ovaries of juvenile shrimp (J, *N* = 3), intact broodstock (*N* = 3 each of stages I–IV) and eyestalk-ablated broodstock (EA, *N* = 3 each of stages I–IV) of *P. monodon*. Lane M = a protein standard.

Western blot analysis of anti-rPmRpd3 PAb revealed the expected 42 kDa band in stage I and the signals reduced in more mature stages of ovaries in intact broodstock. The immunoreactive signal seemed reduce in stage III and IV ovaries in eyestalk-ablated broodstock (Figure 3.90, A and B).

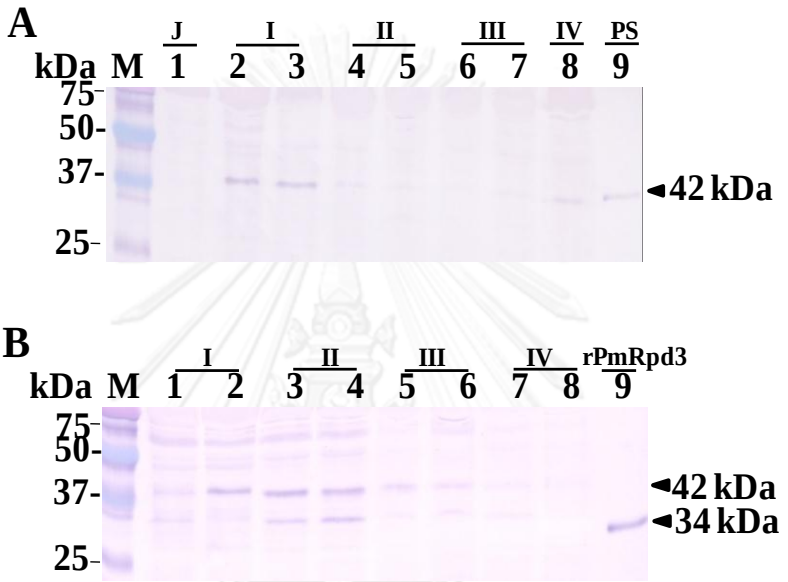

Figure 3. 90 Western blot analysis of anti-rPmRpd3 PAb (1:100) against 30 µg of total proteins extracted from ovaries of cultured juveniles (lane 1, A), intact broodstock (lanes 2-9, A) and eyestalk-ablated broodtock (lanes 1–8, B) of *P. monodon*. The rPmRpd3 was included as the positive control (lanes 9B). Lanes J = juveniles, I–IV = stages I, II, III and IV ovaries, respectively. Lanes M = a protein standard.

3.13 Characterization of recombinant and immunoreactive proteins using nanoESI-LC-MS/MS

3.13.1 Characterization of recombinant proteins

Peptide sequencing using nanoESI-LC-MS/MS was applied for verification of recombinant proteins generated in this study. Results indicated that a recombinant protein of 40 kDa (PmCdk7) significantly matched Cdk7 of *P. monodon* (gi|000049788, Mascot score = 69, $P < 0.05$; Figure 3.91), while that of 59 kDa (rPmCdc20) significantly matched Cdc20 of *Saccoglossus Kowalevskii* (gi|000037222, Mascot score = 85, $P < 0.05$; Figure 3.92) and a 34 kDa rPmRpd3 significantly matched Hdac (Rpd3) of *Neogonodactylus Oerstedii* (gi|000056754, Mascot score = 85, $P < 0.05$; Figure 3.93)

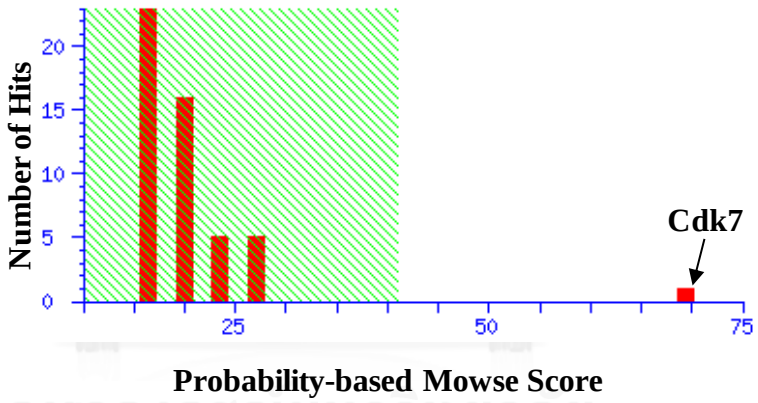

Figure 3. 91 The recombinant PmCdk7 (40 kDa) were analyzed by nanoESI-LC-MS/MS. Sequences inferred from the mass spectra were searched against a redundant *P. monodon* translated protein database. The Mowse score is −10 log (P), where P is the probability that the observed match is a random event. The height of each bar represents the number of proteins in the database matched within a score range. The matches falling outside the shaded area, where the *P* value < 0.05 are considered to be significant. Bars representing a 40 kDa band significantly matched Cdk7 of *Apis mellifera* (score = 69).

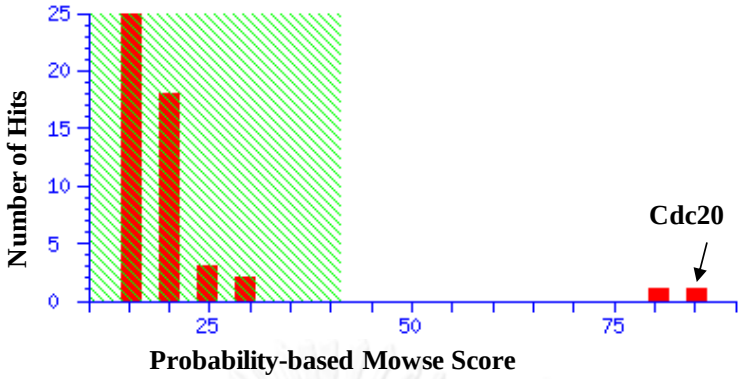

Figure 3. 92 The recombinant PmCdc20 59 kDa were analyzed by nanoESI-LC-MS/MS. Sequences inferred from the mass spectra were searched against a redundant *P. monodon* translated protein database. The Mowse score is −10 log (P), where P is the probability that the observed match is a random event. The height of each bar represents the number of proteins in the database matched within a score range. The matches falling outside the shaded area, where the *P* value < 0.05 are considered to be significant. Bars representing a 59 kDa band significantly matched Cdc20 of *Saccoglossus Kowalevskii* (score = 85).

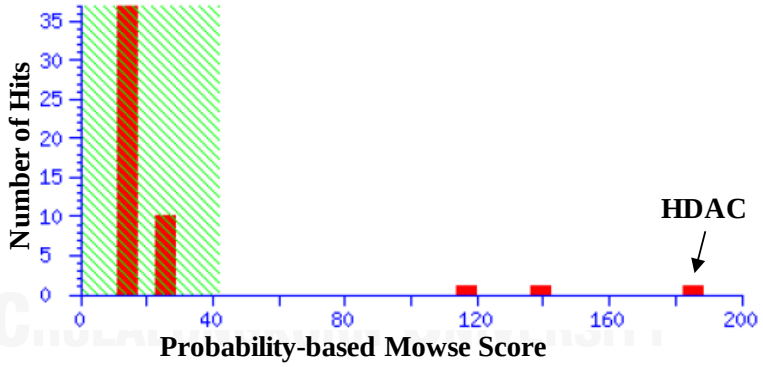

Figure 3. 93 The rPmHdac (also called rPmRpd3, 34 kDa) were analyzed by nanoESI-LC-MS/MS. Sequences inferred from the mass spectra were searched against a redundant *P. monodon* translated protein database. The Mowse score is −10 log (P), where P is the probability that the observed match is a random event. The height of each bar represents the number of proteins in the database matched within a score range. The matches falling outside the shaded area, where the *P* value < 0.05 are considered to be significant. Bars representing a 34 kDa band significantly matched Hdac of *Neogonodactylus Oerstedii* (score = 185).

3.13.2 Identification of immunoreactive proteins from western blot analysis

Results from peptide sequencing indicated that a positive immunoreactive band of 34 kDa band against Anti-rPmCdc2 PAb significantly matched Cdc2 of *P. monodon* (gi|000049788, Mascot score = 46, $P < 0.05$; Figure 3.94A) while a 23 kDa significantly matched ribosomal protein S3 (RPS3) of *Solea senegalensis* (gi|000036949, Mascot score = 119; $P < 0.05$) and S3Ae ribosomal protein (RPS3Ae) of *Tribolium castaneum* (gi|000004257, Mascot score = 49; $P < 0.05$; Figure 3.94B).

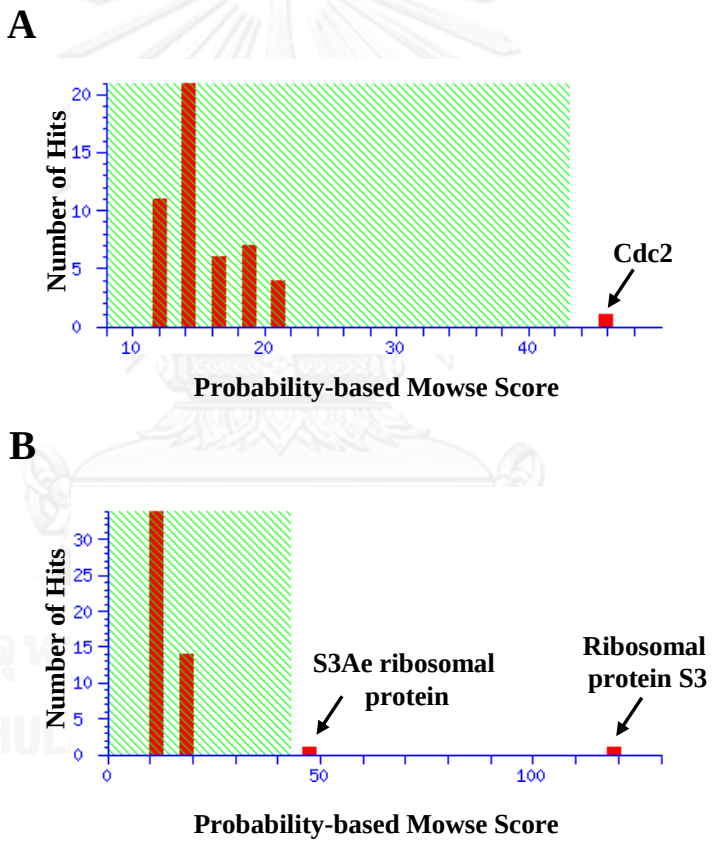

Figure 3. 94 The positive bands of 34 and 23 kDa of PmCdc2 were analyzed by ESI-LCMS/MS. Sequences inferred from the mass spectra were searched against a redundant *P. monodon* translated protein database. The Mowse score is −10 log (P), where P is the probability that the observed match is a random event. The height of each bar represents the number of proteins in the database matched within a score range. The matches falling outside the shaded area, where the *P* value < 0.05 are considered to be significant. Bars representing a 34 kDa band significantly matched

Cdc2 of *Penaeus monodon* (score = 46, A). Results from a 23 kDa band revealed two bars significantly matches unknown proteins (scores = 119 and 49, B).

An imunoreactive band of 52 kDa generated from Western blot analysis of total ovarian proteins against anti-rPmBystin1 PAb significantly matched Bystin1 of *Nasonia vitripennis* (gi|000009321, Mascot score = 192, $P < 0.05$; figure 3.95).

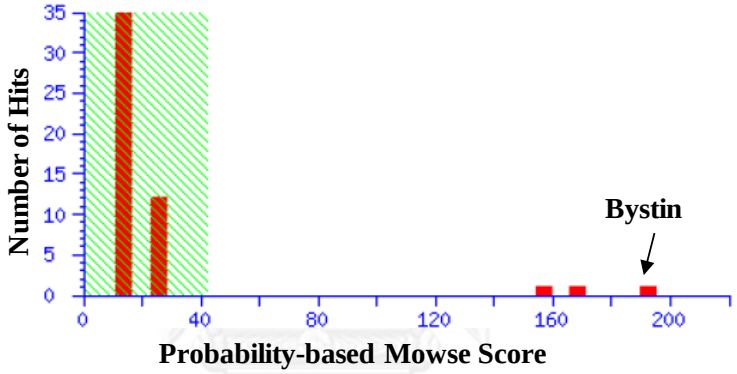

Figure 3. 95 The rPmBystin1 52 kDa were analyzed by ESI-LCMS/MS. Sequences inferred from the mass spectra were searched against a redundant *P. monodon* translated protein database. The Mowse score is -10 log (P), where P is the probability that the observed match is a random event. The height of each bar represents the number of proteins in the database matched within a score range. The matches falling outside the shaded area, where the *P* value < 0.05 are considered to be significant. Bars representing a 52 kDa band significantly matched Bystin1 of *Nasonia vitripennis* (score = 192).

3.14 Localization of PmCdk7 protein and phospho-Cdc2 (Thr161) during ovarian development of *P. monodon*

Immunofluorescence was carried out for localization of PmCdk7 and phosphorylated PmCdc2 (active form) during ovarian development of intact and eyestalk-ablated broodtock of *P. monodon*.

The positive signals of PmCdk7 were detected in follicular layers and ooplasm of previtellogenic oocytes in both intact and eyestalk-ablated shrimp (Figure 3.96 and 3.97). In vitellogenic oocytes, PmCdk7 was localized in both ooplasm and nucleus. Interestingly, PmCdk7 was found in nucleo-cytoplasmic compartments, the cytoskeletal architecture and at the cortical rods in early cortical rod and mature oocytes of both intact and eyestalk-ablated broodstock. No immunoreactive signal was found in ovaries incubated with the preimmune serum (Figure 3.96 and 3.97).

Anti-Phospho-Cdc2 (Thr161) PcAb gave the positive imunoreactive signals in ooplasm of previtellogenic and vitellogenic oocytes in both intact and eyestalk-ablated shrimp (Figure 3.98 and 3.99). Phosphorylated PmCdc2 was also localized in follicular cells surrounding vitellogenic oocytes. In addition, it was localized around the cortical rod in nearly mature and mature oocytes. No immunoreactive signal was found in ovaries when incubated with the preimmune serum (Figure 3.98 and 3.99).

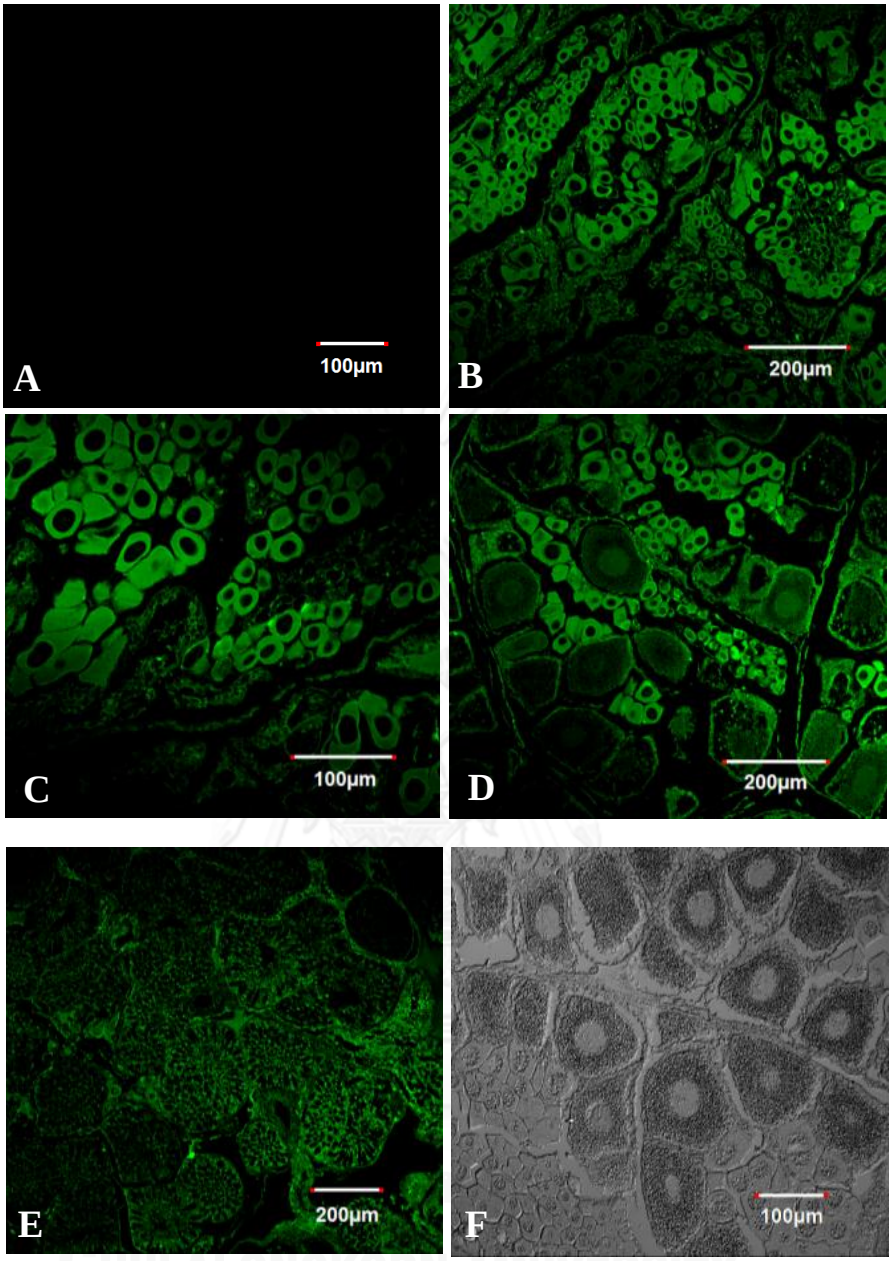

Figure 3. 96 Localization of PmCdk7 protein in ovaries of intact broodstock of *P. monodon* revealed by immunofluorescence against anti-rPmCdk7 PAb. Goat anti-rabbit IgG labeled with Alexa 488 was used as the second antibody. Ovarian tissue sections incubated with the preimmune serum were used as the negative control (A and F).

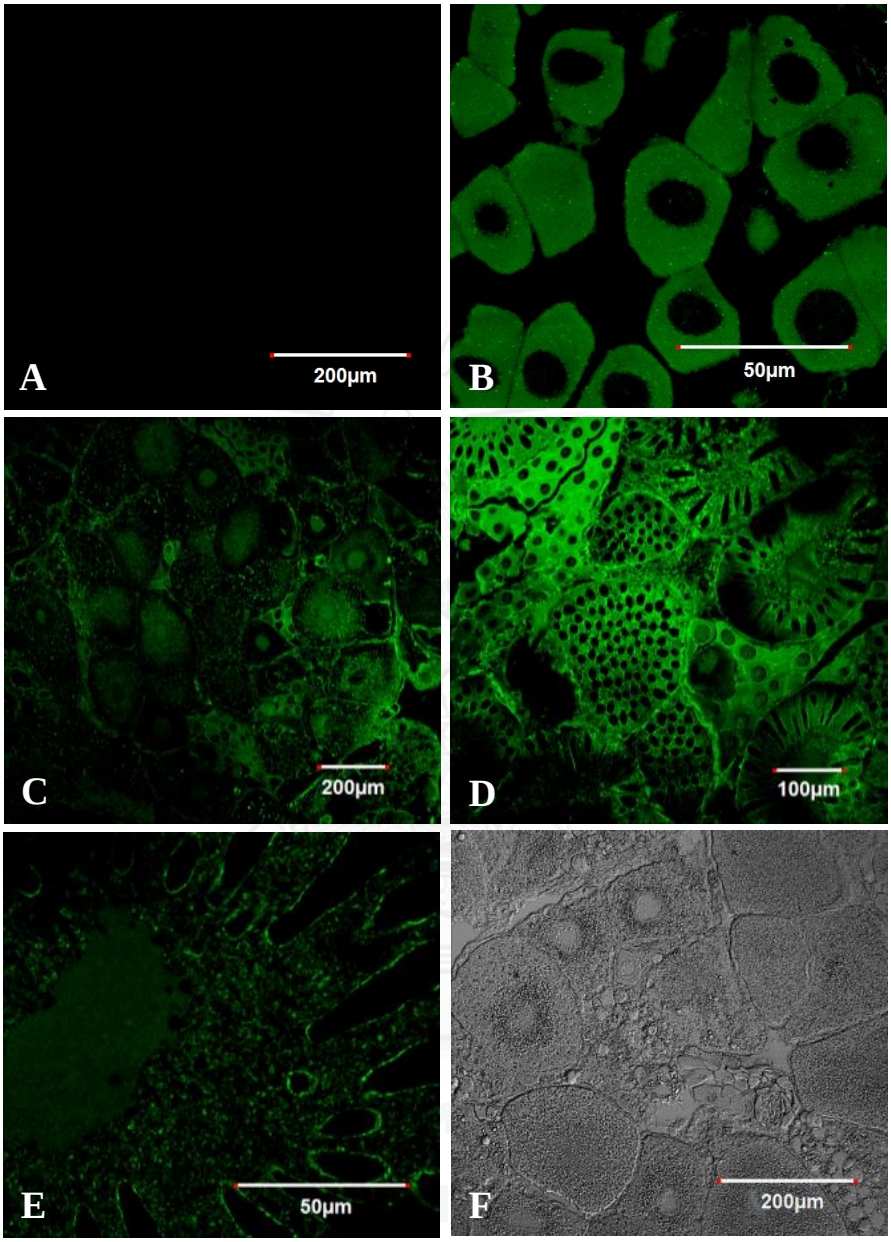

Figure 3. 97 Localization of PmCdk7 protein in ovaries of eyestalk-ablated broodstock of *P. monodon* revealed by immunofluorescence against anti-rPmCdk7 PAb. Goat anti-rabbit IgG labeled with Alexa 488 was used as the second antibody. Ovarian tissue sections incubated with the preimmune serum were used as the negative control (A and F).

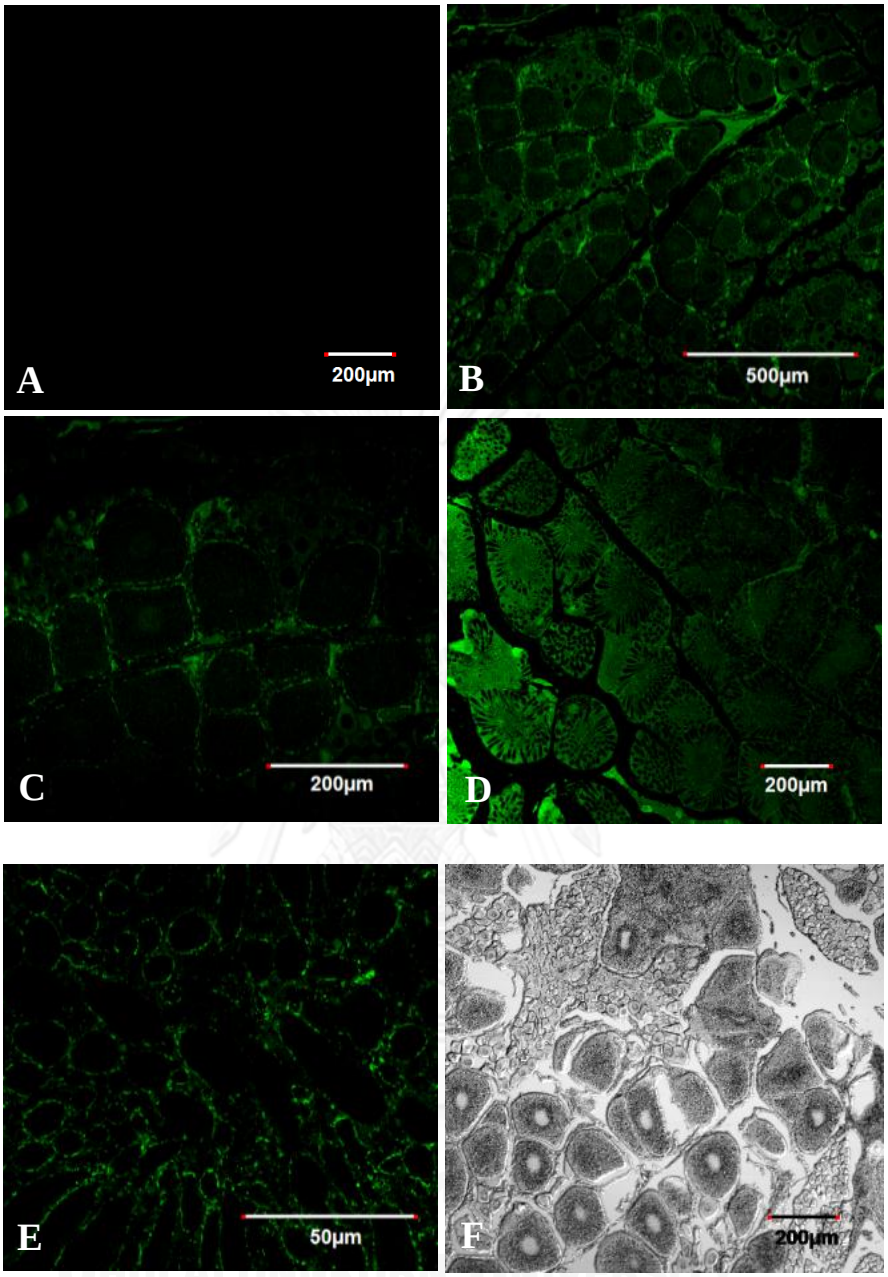

Figure 3. 98 Localization of phosphorylated PmCdc2 protein in ovarian tissue sections of intact broodstock of *P. monodon* revealed by immunofluorescence against anti-phospho-Cdc2 (Thr161) PAb. Goat anti-rabbit IgG labeled with Alexa 488 was used as the second antibody. Ovarian tissue sections incubated with the preimmune serum were used as the negative control (A and F).

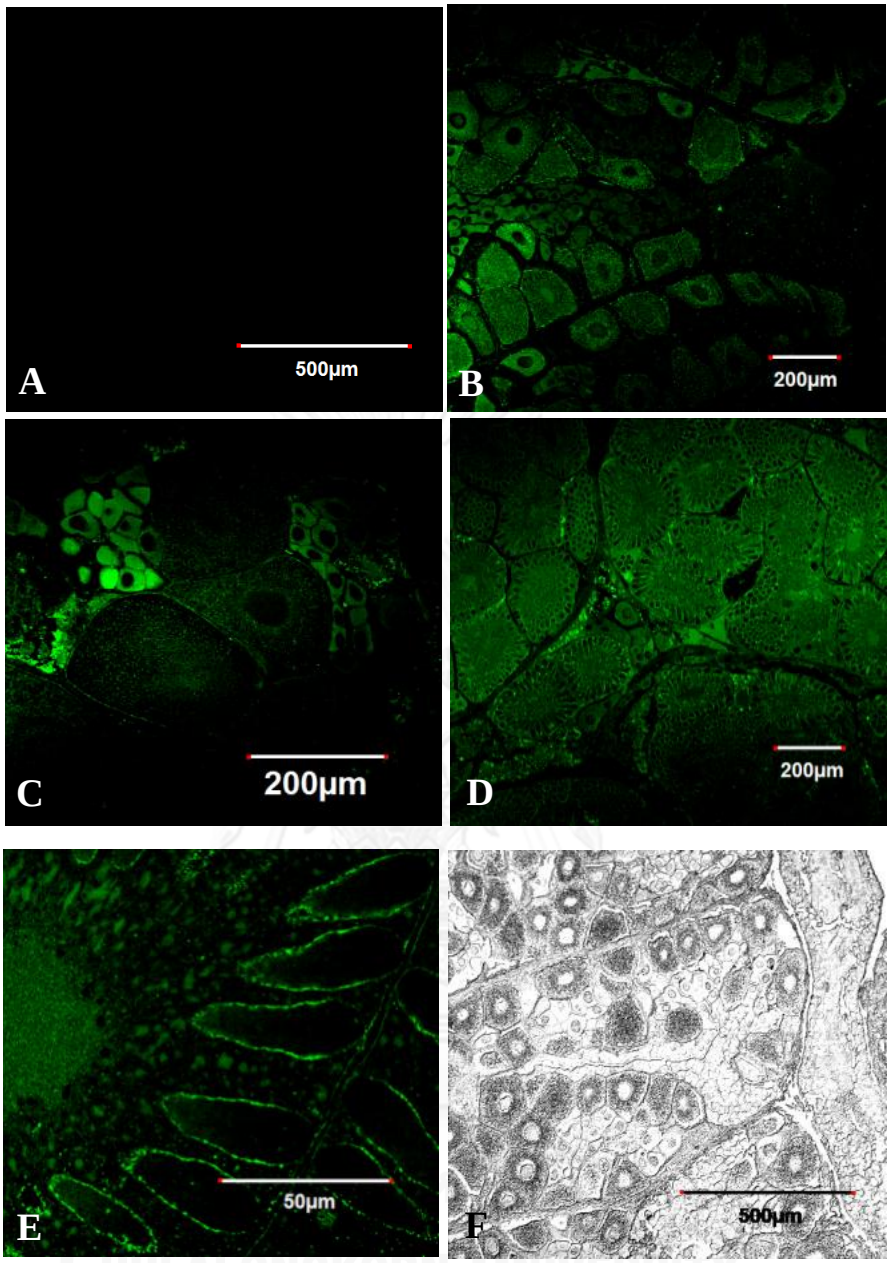

Figure 3. 99 Localization of phosphorylated PmCdc2 protein in ovarian tissue sections of eyestalk-ablated broodstock of *P. monodon* revealed by immunofluorescence against anti-phospho-Cdc2 (Thr161) PAb. Goat anti-rabbit IgG labeled with Alexa 488 was used as the second antibody. Ovarian tissue sections incubated with the preimmune serum were used as the negative control (A and F).

CHAPTER IV
DISCUSSION

Molecular mechanisms underlying meiotic maturation of oocytes and ovarian development of penaeid shrimp are still unknown. Accordingly, knowledge of the molecular mechanisms and functional involvement of reproduction-related genes and proteins in ovarian development is necessary for better understanding of the reproductive maturation of *P. monodon* to resolve the major constraint on reduced degrees of maturation of this economically important species in captivity.

4.1 Isolation and primary structure of the full-length cDNA of *PmCdc2*, *PmCdk7*, *PmCdc16* and *PmCdk5*

Cyclin-dependent kinases (Cdks) associated primary role in eukaryotic cell cycle progression. Cdk subunits with their cognate cyclins subunit typically involves in different stages of cell cycle progression (Child et al., 2010b; Honda et al., 1993). The activity of Cdks depends on the association with cyclins and are regulated by phosphorylation on certain key tyrosine and threonine residues

Recently, the full-length cDNA of *Cdc2* of the Chinese mitten crab (*Eriocheir sinensis*) was isolated (Qiu and Liu, 2009) and it was 1364 bp in length containing an ORF of 900 bp deducing to a polypeptide of 299 amino acids with calculated molecular weight of 34.7 kDa. Subsequently, the full-length cDNA of *Cdc2* in the mud crab (*Scylla paramamosain*) was identified and characterized. The *Sp-Cdc2* was 1593 bp in length with an ORF of 900 bp corresponding to a deduced protein of 299 amino acids (Han et al., 2012).

In *P. monodon*, the full-length cDNA of *PmCdc2* was formerly identified by EST analysis of the testis cDNA library (GenBank accession no. EU492538) (Leelatanawit et al., 2009). The complete ORF of *PmCdc2* from ovaries was characterized in this study and its ORF length was identical with that of PmCdc2 from testes. The conserved phosphorylation sites of Thr14, Tyr15 and Thr161 residues

were found in both transcripts. The potential *N*-linked glycosylation site was not found in the deduced PmCdc2 protein. The catalytic domain of serine/threonine kinases (S_TKc) was found at positions 4–287 of the deduced PmCdc2 protein. The PSTAIRE (positions 45-51) and DFG (positions 146-148) which are related with the cyclin binding, and GxGxxGxV (GEGTYGVV, positions 11-18) elements which is involved in ATP binding (De Bondt et al., 1993) were also found.

The meiotic maturation of animal oocytes is controlled by the MPF (Okano-Uchida et al., 1998). In most species, cytoplasmic MPF is maintained in the inactive form (called pre-MPF) by inhibitory phosphorylation of Cdc2 at Thr14 and Tyr15 by Myt1 kinase and at Thr161 by cyclin-activating kinase (CAK), a complex of Cyclin-dependent kinase 7 (Cdk7)/cyclin H or Cdk7/cyclin H/Mat 1 (Elledge and Harper, 1998; Patel and Simon, 2010; Tassan et al., 1995). Dephosphorylation of Thr14 and Tyr15 residues of Cdc2 by Cdc25 phosphatase lead to the resumption of meiotic maturation of oocytes (Clarke et al., 1992; Dunphy et al., 1988; Dunphy and Kumagai, 1991; Jessus et al., 1991; Mueller et al., 1995). Alternatively, a different mechanism of oocyte resumption has been reported in some amphibians and fishes where Cdc2 presents as a monomer with no phosphorylation due to the absence of cyclin B in immature oocytes. Only Thr161 phosphorylation by CAK is required for MPF activation (Hirai et al., 1992; Honda et al., 1993; Kobayashi et al., 1991; Yamashita et al., 1995). In addition, CAK also acts as a transcriptional regulator in association with the transcription factor II H (TFIIH) (Nigg, 1996; Sclafani, 1996). In zebrafish, the function of CAK is especially important during the early development and *Cdk7* and *Cyclin H* mRNAs were shown to be maternally loaded (Liu et al., 2007).

The full-length cDNA of ovarian *PmCdk7* was also characterized in this study. Its deduced amino acid sequence was identical to that previously identified in testes (Leelatanawit et al., 2009). Two potential polyadenylation signal sequences (AATAAA) were found in *PmCdk7* suggesting the possible selective polyadenylation usage. The T-loop (positions 164-191) which is a region of major conformational difference between active and inactive forms were found in the deduced PmCdc7 protein as in other Cdk proteins of *P. monodon*, for example, PmCdc2 (DFGLARAFGIPVRVYTHEVVT LWYRAPE located at positions 146-173, accession no. EU492538; (Phinyo et al., 2013)

and PmCdk2 (DFGLARAFCLPLRVYTHEVVTLWYRAPE located at positions 146-173, this study). T-loop phosphorylation favors a kinase conformation which allows the access of substrate to the active site (Morgan and De Bondt, 1994; Taylor et al., 1992). Cdk7 is unusual among Cdks because dual phosphorylation in the T-loop (e.g. at S170 and T176 in *Xenopus* Cdk7 and positions Ser164 and Thr170 in *Drosophila* Cdk7 is required for its activation (Larochelle et al., 2001; Martinez et al., 1997). Therefore, the actual positions for activating phosphorylation of PmCdk7 should be further determined.

In addition, the full-length cDNA of *PmCdk2* was characterized and reported for the first time in *P. monodon*. The amino sequence of PmCdk2 contained PSTALRE (positions 47-53) and DFG (position 146-148) which are related with the cyclin subunit binding lead to the realignment of essential ATP binding residues into an active conformation (Child et al., 2010a; De Bondt et al., 1993; Holmes and Solomon, 1996). The T-loop are found difference position in other cyclin-dependent kinase genes as described previously. T-loop displacement is ensured by direct phosphorylation of conserved Thr161 residues within the T-loop (PmCdk2 at Thr161, PmCdc2 at Thr161, PmCdk7 at Ser173 and Ser179) (Devault et al., 1995; Martinez et al., 1997; Tassan et al., 1995).

The full-length cDNA of ovarian *PmCdc16* contains five copies of the tetratricopeptide repeat (TPR) motif. The TPR domain containing serine/threonine protein phosphatase PP5, a protein motif involved important as interface for protein/protein interactions (Dobson et al., 2001; Ollendorff and Donoghue, 1997). In most species (yeast, *Drosophila* and *Xenopus*), Cdc16 are known subunit to bind with Cdc23, Cdc24, Cdc27 and other APC. The complex also called Anaphase-promoting complex or cyclosome (APC/C) with binding to Cdc20 (WD40 domain; the so call Fizzy), the E3 ubiquitin ligase for ubiquitination process to cyclins (Kallio et al., 1998; Lorca et al., 1998; Sigrist and Lehner, 1997).

The full-length cDNA sequence of *PmCdk5* was also characterized. A DUF773 domain which the function is unknown was observed but the S_TKc domain was not

found in the deduced PmCdk5 protein. This suggested that PmCdk5 may play different roles from other Cdks.

Cyclin-dependent kinase 5 (Cdk5) is primarily associated with brain development (Musa et al., 1998; Ohshima et al., 1996) but it is also implicated in lens and muscle differentiation. Cdk5 was also expressed in mouse ovary, and explored the possibility that it plays a role in that reproductive tissue. Western blotting and immunohistochemistry indicated that the known Cdk5 activator, p35, is also present in the mouse ovary. Cdk5 and p35 were detected in oocytes at all stages of the follicle. While Cdk5 was present In the cytoplasm and nucleus of the oocyte, p35 was observed only in the cytoplasm. Immunoprecipitation and histone H1 kinase assays revealed that they form an ovarian complex with considerable kinase activity. Phosphorylation assays showed that several ovarian proteins are substrates for Cdk5/p35 *in vitro*. In addition, p35-associated Cdk5 activity plays an important role in the ovary, where it regulates cell differentiation and apoptosis as it does in the brain (Lee et al., 2004; Zhang et al., 1997).

Acetylation and deacetylation of histones involve cell cycle regulation and differentiation. In *Drosophila*, *groucho* (*gro*) encodes a transcriptional corepressor that has critical roles in many development processes. Gro and Rpd3 form a complex *in vivo* and that they interact directly via the glycine/proline rich (GP) domain in Gro. Cell culture assays demonstrate that Rpd3 potentiates repression by the GP domain. Furthermore, experiments employing a histone deacetylase inhibitor, as well as a catalytically inactive form of Rpd3, imply that histone deacetylase activity is required for efficient Gro-mediated repression. Finally, mutations in *gro* and *rpd3* have synergistic effects on embryonic lethality. In this study, the full-length cDNA of *PmRpd3* was isolated and reported for the first time in *P. monodon*. Its deduced sequence contained the histone deacetylase domain (Chen et al., 1999).

4.2 Expression levels of cell cycle-regulating and reproduction-related genes and proteins during ovarian development of *P. monodon*

The development of oocytes consists of a series of complex cellular events, in which different genes are expressed to ensure the proper development of oocytes

and to store transcripts and proteins as maternal factors for early embryogenesis (Qiu et al., 2005). The expression levels of *PmCdc2*, *PmCdk7*, *PmChk1* and *PmBystin1* mRNA in ovaries were significantly higher in broodstock than in juveniles ($P < 0.05$) suggesting that these genes are involved in oogenesis. Importantly, the expression level of *PmCdc2*, *PmCdk7*, *PmChk1* and *PmBystin1* in stages I–IV ovaries of eyestalk-ablated broodstock was greater than that of the same ovarian stages in intact broodstock ($P < 0.05$).

In *Marsupenaeus japonicus*, eyestalk-ablation caused an increase in the mRNA levels of vitellogenin and cortical rod protein in ovaries (Okumura et al., 2006; Tsutsui et al., 2005). The circumstance suggested that and *PmChk1* should play an important role in reproductive development and maturation and gonad inhibiting hormone (GIH) affected the transcription of these genes in ovaries of *P. monodon* (Meusy and Payen, 1988). Accordingly, the expression profiles of *PmCdc2*, *PmCdk7*, *PmChk1* and *PmBystin1* may be used as molecular indicators for investigation of the progression in reproductive maturation of female *P. monodon* adults as a consequence of maturation-inducing feed and/or exogenous hormone/ neurotransmitter administration.

Generally, complex Cdk2-Cyclin E inhibits APC/C-Cdc20 activity to promote the degradation of cyclin B (Marston and Amon, 2004). In *P. monodon*, the expression level of *PmCdk2* mRNA in stages I and II ovaries of intact broodstock was greater than that in the same stages in eyestalk-ablated broodstock. However, the expression during late vitellogenesis and maturation was not different. The circumstance supported the evidence that eyestalk ablation allow easier progression of oocyte/ovaries development by allowing the accumulation of cyclin B during previtellogenic and early vitellogenic stages.

The expression levels of *PmCdc16* mRNA were significantly higher in juveniles than in broodstock ($P < 0.05$). The expression profiles of *PmCdc16* in intact and eyestalk-ablated broodstock of *P. monodon* were not different. This further suggested that *PmCdc16* may play more important roles in mitotic rather than meiotic cell cycle.

The expression level of *PmRpd3* in ovaries was significantly greater than that in juveniles. Its expression profile was roughly similar with that of *PmRpd3* where eyestalk ablation resulted in the decrease of *PmRpd3* transcription during vitellogenesis and final maturation of ovaries of broodstock. Based on the fact that *PmRpd3* is functionally involved as a transcriptional corepressor, a lower expression of this gene may allow the progression of ovarian development of *P. monodon*.

4.3 *In vivo* and *in vitro* effects of serotonin (5-HT) and treatment on transcription of *PmBystin1*, *PmCdc2* and *PmCdk7* in ovaries *P. monodon*.

Unilateral eyestalk ablation is used in practice to induce ovarian maturation in *P. monodon*. However, this technique affects egg quality and the high mortality rates of spawners (Benzie, 1998; Okumura, 2004). Therefore, the induction of reproductive maturation and spawning of captive *P. monodon* without the use of eyestalk ablation is a long-term goal for the industry (Quackenbush, 2001).

5-HT injection induced ovarian maturation in the crayfish, *Procambarus clarkii* with 5-HT injections and induced ovarian maturation in the lobster, *Homarus americanus* (Fingerman, 1997; Kulkarni et al., 1992), the giant freshwater prawn, *Macrobrachium rosenbergii* (Meeratana et al., 2006), the Pacific white shrimp *Litopenaeus vannamei*, (Vaca and Alfaro, 2000) as well as *P. semisulcatus* (Aktas and Kumlu, 2005). Alfaro et al. (2004) reported that injection of combined 5-HT and dopamine antagonist, spiperone stimulated ovarian maturation, spawning and the release of the maturation promoting hormone in *L. stylirostris* and *L. vannamei*.

In *P. monodon*, exogenous 5-HT injection promoted the expression of various reproduction-related genes in ovaries of domesticated shrimp including *adipose differentiation-related protein* (*PmADRP*) which play the functional role in neutral lipid accumulation of oocytes during oogenesis at 48 hpi (Sittikankaew et al., 2010), *broad-complex* (*PmBr-c*) which is the early ecdysone responsive gene, at 24 hpi (Buaklin et al., 2013), *small androgen receptor interacting protein* (*PmSARIP*) which play a role in the sex steroid pathway, at 3-72 hpi and *GTP binding protein alpha*

subunit Go (*PmG*α_o) which is functional important in meiotic signal transduction pathway of oocytes, at 6-12 hpi (Yocawibon, 2011).

Molecular effects of 5-HT on expression of the cell cycle gene, *PmCdc2* and *PmCdk7* in ovaries of domesticated 18-month-old shrimp were examined. An immediate effect of 5-HT injection (50 µg/g body weight) on the expression level of *PmCdc2* was found at 1 hpi implying the rapid induction to compensate low relative expression levels of this gene during uninduced reproductive development in this species. Nevertheless, 5-HT injection resulted in upregulation of *PmCdk7* at 6-12 hpi ($P < 0.01$). Results in the present study confirms molecular effects of 5-HT on transcription of genes functional involved in the signal transduction and indicated that 5-HT may directly enhance meiotic maturation of oocytes in *P. monodon* by stimulation of the MPF (a complex of Cdc2 and Cyclin B) via the activity of PmCdk7 (and its partner, Cyclin H and/or MAT1 which are still not identified and characterized in *P. monodon*). Likewise, 5-HT injection significant promoted the *PmBystin1* mRNA level at 6-12 hpi ($P < 0.01$). This suggested similar effects of 5-HT injection and eyestalk ablation on the induction of genes in the signal transduction pathways.

Makkapan et al. (2011) reported that 5-HT promoted the expression of ovarian ribosomal protein *L10a* (*RPL10a*), *shrimp ovarian peritrophin* (*SOP*) and *translational controlled tumor protein* (*TCTP*) in the banana shrimp (*Fenneropenaeus merguiensis*) both *in vitro* (1 µg/ml for up to 4 h after incubation, $P < 0.05$) and *in vivo* (for which a low concentration of 1 µg/g body weight was more potent than 50 µg/g body weight at 5 and/or 10 days post-injection). In addition, shrimp injection with a low level of 5-HT (1 µg/g bodyweight) induced increased hemolymph levels of methyl farnesoate (MF) that is recognized as a crustacean hormone functionally involved in ovarian development.

In this study, ovarian tissue culture was set up the conventional morphological examination of sections stained with hematoxylin and eosin was used for morphological observation of ovarian cells. The results indicated that morphological characters of ovaries fragment seemed to be slightly changes after the

ovarian explants were maintained for 24 h. Therefore, more appropriate conditions for culture of ovarian tissue should be further optimized.

The presence of vertebrate-type steroids has been documented in almost all invertebrate groups including crustaceans (Cardoso et al., 1997; Lafont, 1991; Lehoux and Sandor, 1970). Progesterone and 17α-hydroxyprogesterone administration induced ovarian maturation and spawning in *Metapenaeus ensis* (Yano, 1985; Yano, 1987). The conversion of progesterone into 17β-estradiol was reported in *Marsupenaeus japonicus* (Summavielle et al., 2003). Progesterone levels in the hemolymph were shown to fluctuate closely with that of the serum vitellogenin level during ovarian maturation stages of *P. monodon* (Quinitio et al., 1994) implying its controlling role in vitellogenesis.

The expression level of *PmCdc2* in cultured ovarian explants treated with different concentrations of 17α, 20β-DHP (0.1, 1.0 and 10.0 µg/ml) was examined. The preliminary results did not show significant effects of progesterone treatment at these concentrations ($P > 0.05$). Similarly, treatment of 5-HT (1.0 and 15.0 µg/ml) did not affect the expression of *PmCdc2 in vitro* ($P > 0.05$) in all time intervals ($P > 0.05$).

4.4 Expression of rPmBystin1, rPmCdc2, rPmCdc20, rPmCdk7 and rPmRpd3 protein during ovarian development of *P. monodon*

Recombinant PmApc11, PmBystin1, PmCdc2, PmCdc20, PmCdk7, PmChk1 and PmRpd3 were successfully expressed in the bacterial expression system. All except PmChk1 was expressed in the soluble form. The gel-purified recombinant proteins were subjected to the polyclonal antibody production in rabbit but that of rPmApc11 was not successfully produced. In addition, commercially available anti-phospho-Cdc2 (Thr161) PAb was purchased and included for determination of the active form of PmCdc during ovarian development of *P. monodon*.

Western blot analysis using anti-rPmCdc2 PAb revealed the expected 34 kDa band (non-phosphorylated form referring to the inactive protein) and a smaller band of 23 kDa in each juvenile and broodstock shrimp examined. In the rainbow trout, the expected band of 34 kDa was positively detected by anti-Cdc2-PSTAIRE PAb

when immature testes and ovaries were examined. However, the discrete band of 27 kDa was observed in mature testes. It was suspected that the translated PmCdc2 protein in ovaries of *P. monodon* (34 kDa) was further digested by a peptidase to generate a smaller protein of 23 kDa, therefore, both 34 and 23 kDa bands were further examined by nanoESI–LC/MS–MS and the results indicated that the expected band was the PmCdc2 protein but a smaller band was ribosomal protein S3 (RPS3). It is surprising that anti-PmCdc2 PAb reacted strongly with a homologue of RPS3 protein where it did not give the positive reaction with other cell cycle-related recombinant proteins of *P. monodon*, for example cyclin-dependent kinase 7 (Cdk 7), cell division cycle 20 (Cdc20) and cyclin B.

The phospho-Cdc2 (Thr161) PAb give the positive signal against the 34 kDa band but not the 23 kDa band and recombinant PmCdc2 protein. Previous studies illustrated multiple forms of the Cdc2 protein resulting from different degrees of phosphorylation at Thr14, Tyr15 and Thr161 (Choi et al., 1991; Ihara et al., 1998). Typically, two different migrating bands were found. The inactive 35 kDa form has three phosphorylated sites at Thr161, Tyr15 and Thr14 and the active 34 kDa form has only one phosphorylated site at Thr161 (Ihara et al., 1998; Kajiura et al., 1993; Qiu et al., 2008) which are found only in mature oocytes (Choi et al., 1991; Ihara et al., 1998).

In *P. monodon*, the active PmCdc2 protein was found at all stages of ovarian development. In intact broodstock, the expression profiles of active PmCdc2 protein were observed in stages I–III ovaries and the level was increased in the mature stage of ovarian development. Degeneration of developing ovaries without maturation and spawning during reproductive development is the major constraint in captive *P. monodon*. Low level of active PmCdc2 proteins in late vitellogenesis suggested its insufficient amount to lead to GVBD reflecting difficulties in reproductive maturation of *P. monodon* in captivity. In contrast, abundant expression of the active PmCdc2 protein was observed in stages I–IV of eyestalk-ablated broodstock further suggesting that an additional level of active PmCdc2 protein is probably required for rapid development and maturation of this species.

In the mitten crab, both 35 (presumably phosphorylated Cdc2 protein at Thr14, Tyr15 and Thr161) and 34 kDa (presumably phosphorylated Cdc2 protein at Thr161) bands were found from ovarian proteins of juveniles and all developmental stages of broodstock when analyzed by anti-Cdc2-PSTAIRE PAb (Han et al., 2012). This implied that the activation of *E. sinensis* Cdc2 required dephosphorylation of Thr14 and Tyr15 by Cdc25 as reported in *Xenopus* and sea urchin. Our results using the phospho-Cdc2 (Thr161) PAb revealed the positive signal at 34 kDa in immature and mature ovaries. Therefore, we propose that meiotic resumption of oocyte in *P. monodon* is regulated by the single phosphorylation of Thr161 in PmCdc2 possibly by Cdk-activating kinase (CAK) rather than dephosphorylation of Thr14 and Tyr15 by Cdc25.

Anti-rPmCdk7 PAb gave the immunoreactive band against rPmCdk7 but not other recombinant proteins including PmCdc2 that also contains a S_TKc domain. The detection limit of anti-rPmCdk7 PAb was approximately 0.03 µg of rPmCdk7. An immunoreactive band of 67 kDa was obtained when anti-PmCdk7 PAb was tested against total ovarian proteins of *P. monodon* broodstock. Antigen-antibody competition experiments illustrated that the anti-PmCdk7 PAb was specific for a 67 kDa protein. Western blot analysis showed that PmCdk7 was not expressed in premature ovaries of 4-month-old juveniles. In adults, the expression level of PmCdk7 seemed to be increased during the maturation stage of ovarian development in both intact and eyestalk-ablated broodstock. The information agrees with the level of phosphorylated PmCdc2 where the most intense signal (34 kDa) was also in mature (stage IV) ovaries (Phinyo et al., 2013).

Anti-rPmBystin1 PAb gave the positive immunoreactive band of 52 kDa in stages I-IV ovaries of intact broodstock and stages II-IV ovaries of eyestalk-ablated broodstock. In addition, a smaller band of approximately 50 kDa and 43 kDa were observed along with a 52 kDa band in stages I-IV ovaries of intact broodstock and stages II-IV ovaries of eyestalk-ablated broodstock.

Aoki et al. (2006) produced anti-bystin PAb against a synthesis peptide (MEKLTEKQTEVETVC). An immunoreactive band 50 kDa (active bystin) and 25 kDa

(unknown) were found in mouse uterus tissues. The smaller band of 25 kDa may be a bystin variant or a fragment generated from a 50 kDa protein by proteolysis. Similarly, modification of PmBystin1 may have occurred during ovarian development of *P. monodon*.

A single immunoreactive bands of 50 kDa was found when anti-rPmCdc20 was tested against total ovarian proteins of *P. monodon*. This positive band was smaller than that (59 kDa) from analysis of anti-rCdc20 against rCdc20 protein. The expression of a 50 kDa band seemed to decrease during late vitellogenesis and maturation of *P. monodon*.

4.5 Localization of *PmCdc2*, *PmCdk7* and *PmBystin1* transcripts during ovarian development of *P. monodon*

In situ hybridization was used to determine the location of *PmCdc2*, *PmCdk7* and *PmBystin1* transcripts in ovaries of *P. monodon*. The positive signals of *PmCdc2* and *PmCdk7* transcripts were found in ooplasm of previtellogenic oocytes but not in vitellogenic, early cortical rod, and mature oocytes of both intact and eyestalk-ablated broodstock.

In the rainbow trout (*Oncorhynchus mykiss*), *Cdc2* transcripts were found in cytoplasm in previtellogenic oocytes, but concentrated in nucleus of vitellogenic oocytes (Qiu et al., 2008). In addition, The *Cdc2* of green mud crab (*Scylla paramamosain*) was localized transcripts in cytoplasm of oogonia and follicle cells. Results implied that *SpCdc2* play the important role in meiosis of oocytes and mitosis of the follicular cells (Han et al., 2012).

The *PmBystin1* mRNA was localized in ooplasm of previtellogenic and vitellogenic oocytes. In *Drosophila*, *Bystin* was localized in nurse cells but not in follicle cells (Stewart and Nordquist, 2005). The localized *PmBystin1* mRNA support gene and protein expression analysis in that *PmBystin1* may play the important role on ovarian development of *P. monodon*.

The finding further suggested that *PmCdc2*, *PmCdk7* and *PmBystin1* plays a role in oogenesis and ovarian development of *P. monodon*. Typically, stages of

oocytes within a single ovarian lobe are not synchronous (Medina et al., 1996). Accordingly, the ovarian developmental stage was determined based on the predominant oocyte type in a particular specimen. Contradictory results from quantitative real-time PCR and in situ hybridization on the disappearance of *PmCdc2*, *PmCdk7* and *PmBystin1* hybridization signals in ooplasm of more mature stages of oocytes may have been due to the significant increase in oocyte size as oogenesis proceeds. Moreover, quantification of PmMAPK1 mRNA profiles was examined based on cDNA template from the ovarian tissue, whereas in situ hybridization revealed subcellular localization of the PmMAPK1 transcript. Technically, *in situ* hybridization detects gene expression with much lower sensitivity than real-time quantitative PCR.

4.6 Localization of PmCdk7 protein and phospho-Cdc2 (Thr161) during ovarian development of *P. monodon*

Immunofluorescence gave the interesting issue on the translocation of PmCdk7 proteins during oogenesis in *P. monodon*. Immunoreactive signals for the PmCdk7 protein were observed in the ooplasm of previtellogenic oocytes. During vitellogenesis, PmCdk7 was found in ooplasm and a translocation to the nucleus was also observed. Nuclear translocation of PmCdk7 is supported by its additional roles in transcription and DNA repair by association with the transcription factor TFIIH (Nigg, 1996; Svejstrup, 2010). After GVBD, the protein was observed at the nucleo-cytoplasmic compartment, the cytoskeletal architecture and cortical rods of oocytes.

Cortical rods of penaeid shrimp are precursors of egg jelly investment composing of different proteins (e.g. thrombospondin and peritrophin) (Kruevaisayawan et al., 2007a). Cortical rods are released during spawning when ovulated eggs contact with seawater and form a jelly investment around the eggs in penaeid species (Clark et al., 1990; Pongtippatee et al., 2007; Yano and Hoshino, 2006). The functional roles of cortical rods in the induction of the sperm acrosome reaction in *P. monodon* were recently reported (Kruevaisayawan et al., 2007a). The findings in this study further suggest that PmCdk7 protein may have functionally involved in fertilization and embryogenesis of *P. monodon*.

Injection of flag-tagged *Cdk7* mRNA into porcine oocytes resulted in a more rapid activation of MPF than in the non-injected oocytes. In the *Xenopus*, immunoreactive of Cdk7 was localized in the germinal vesicle of *Xenopus* oocytes (Brown et al., 1994; Fujii et al., 2011).

Immunoreactive signals for phospho-Cdc2 (Thr161) PAb against phosphorylation of threonine 161 of Cdc2 protein were observed in the ooplasm of previtellogenic oocytes in *P. monodon*. In mature oocytes, the phosphorylated signals were observed around cortical rods.

In the mitten crab, the total Cdc2 signals (phosphorylated and non-phosphorylated forms) were visualized in ooplasm of previtellogenic oocytes. In vitellogenic oocytes, the weak signals were observed in ooplasm but the strong signals were found in germinal vesicle (GV). At late vitellogenesis stage, the signal is predominant in GV and less in ooplasm, these suggested that the crab Cdc2 protein is exclusively cytoplasmic in previtellogenic oocyte and then relocates into nucleus at vitellogenesis stage and finally accumulates on the meiotic spindle at the final stages of oocyte maturation. Similarly, Cdc2 proteins in *Cherax quadricarinatus* and rainbow trout (*Oncorhynchus mykiss*) were relocated from the cytoplasm to the nucleus during ovarian development (Qiu and Liu, 2009; Qiu et al., 2008; Wang et al., 2013).

In this thesis, the expression and localization of various reproduction-related genes and proteins were examined and they implicated the functional important role on development of ovaries and ovaries of *P. monodon*. The basic knowledge obtained in this study allow functional characterization of reproduction-related gene products on ovarian and oocyte development for better understanding of the reproductive maturation of female *P. monodon* in captivity.

CHAPTER V
CONCLUSIONS

1. The full-length cDNA of various cell cycle-regulating genes were characterized. The full length of *PmCdc16*, *PmCdk2*, *PmCdk5* and *PmRpd3* were contained 2068, 1763, 1758 and 1949 bp with an ORF of 1332, 921, 1524 and 1452 bp corresponding to a polypeptide of 443, 306, 507 and 483 amino acids, respectively. The deduced proteins have a theoretical molecular weight (MW) of 50.11, 34.93, 58.25 and 54.66 kDa, respectively.

2. *PmCdc2*, *PmCdk2, PmCdk7*, *PmChk1 PmBystin1*, and *PmRpd3* were more abundantly expressed in broodstock more than juveniles while the expression profile of *PmCdc16* was expressed in the opposite direction. Eyestalk ablation resulted in an increasing of *PmCdc2*, *PmCdk7*, *PmChk1* and *PmBystin1* transcription but decreasing *PmCdk2* and *PmRpd3* transcription. Nevertheless, it had no effect on the expression of *PmCdc16*.

3. Exogenous 5-HT injection (50 µg/g body weight) induced the expression level of *PmBystin1*, *PmCdc2* and *PmCdk7* at 6-48, 1 and 6-12 hpi.

4. *In vitro* incubation of 5-HT (1 and 15 µg/ml) and 17α, 20β-DHP (0.1, 1.0 and 10.0 µg/ml) did not affect the expression level of *PmCdc2* in cultured ovarian explants.

5. *In situ* hybridization indicated that *PmCdc2* and *PmCdk7* were localized in ooplasm of previtellogenic oocytes in both intact and eyestalk-ablated broodstock while *PmBystin1* was localized in the ooplasm of previtellogenic and vitellogenic oocytes.

7. Polyclonal antibodies against PmBystin1, PmCdc20, PmCdk7 and PmRpd3 were successfully produced in rabbit. Western blot analysis suggested that PmBystin1, PmCdc2, PmCdc20, PmCdk7 and PmRpd3 play the important roles during ovarian development of *P. monodon*.

8. Immunofluorescence indicated that PmCdk7 and phosphorylated Cdc2 were localized in ooplasm and around cortical rods. The results implied that PmCdk7 and PmCdc2 involved in meiotic resumption and cytoskeletal architecturing of *P. monodon* of oocytes.

REFERENCES

Aktas, M., and Kumlu, M. (2005). Gonadal maturation and spawning of *Penaeus semisulcatus* by hormone injection. *Turk. J. Zool.* **29**, 193-199.

Alfaro, J., Zúñiga, G., and Komen, J. (2004). Induction of ovarian maturation and spawning by combined treatment of serotonin and a dopamine antagonist, spiperone in *Litopenaeus stylirostris* and *Litopenaeus vannamei*. *Aquaculture* **236**, 511-522.

Aoki, R., Suzuki, N., Paria, B. C., Sugihara, K., Akama, T. O., Raab, G., Miyoshi, M., Nadano, D., and Fukuda, M. N. (2006). The Bysl gene product, bystin, is essential for survival of mouse embryos. . *FEBS Lett.* **580**, 6062-6068.

Bailey-Brook, J. H., and Moss, S. M. (1992). "Penaeid taxonomy, biology and zoogeography; in Marine Shrimp Culture," Elsevier Science Publishers, Amsterdam, Netherlands.

Benzie, J. A. H. (1998). Penaeid genetics and biotechnology. *Aquaculture* **164**, 23-47.

Bradfield, J., Berlin, R. L., Rankin, S. M., and Keeley, L. (1989). Cloned cDNA and antibody for an ovarian cortical granule polypeptide of the shrimp *Penaeus vannamei*. *Biol. Bull.* **177**, 344-349.

Bradford, M. M. (1976). A rapid and sensitive method for the quantitation of microgram quantities of protein utilizing the principle of protein-dye binding. *Anal. Biochem*. **72**, 248-254.

Brown, A. J., Jones, T., and Shuttleworth, J. (1994). Expression and activity of p40MO15, the catalytic subunit of cdk-activating kinase, during *Xenopus* oogenesis and embryogenesis. *Cell Res*. **5**, 921-932.

Brusca, R. C., and Brusca, G. J. (1990). " Invertebrates.," Sinauer Associates, Inc., Massachusetts,.

Buaklin, A. (2010). Characterization and expression of *O-methyltransferase* and *broad complex* genes and proteins in the giant tiger shrimp *Penaeus monodon*, PhD Thesis Chulalongkorn University, Thailand.

Buaklin, A., Sittikankaew, K., Mensveta, P., and Klinbunga, S. (2013). Characterization and expression analysis of the Broad-complex (Br-c) gene of the giant tiger shrimp *Penaeus monodon*. *Comp. Biochem. Physiol. part B* **164**, 280-289.

Cahill, M. A. (2007). Progesterone receptor membrane component 1: an integrative review. *J. Steroid Biochem. Mol. Biol.* **150**, 16-36.

Cardoso, A. M., Barros, C. M. F., Ferrer Correia, A. J., Cardoso, J. M., Cortez, A., Carvalho, F., and Baldaia, L. (1997). Identification of vertebrate type steroid hormones in the shrimp *Penaeus Japonicas* by tandem mass spectrometry and sequential product ion scanning. *J. Am. Soc. Mass Spectrom.* **8**, 365-370.

Chen, Y., Tseng, D., Ho, P., and Kuo, C. (1999). Site of vitellogenin synthesis determined from a cDNA encoding a vitellogenin fragment in the freshwater giant prawn, *Macrobrachium rosenbergii*. *Mol. Reprod. Dev.* **54**, 215-222.

Child, E. S., Hendrychova, T., McCague, K., Futreal, A., Otyepka, M., and Mann, D. J. (2010a). A cancer-derived mutation in the PSTAIRE helix of cyclin-dependent kinase 2 alters the stability of cyclin binding. *Biochem. Biophys. Acta.* **1803**, 858-864.

Child, E. S., Hendrychova, T., McCague, K., Futreal, A., Otyepka, M., and Mann, D. J. (2010b). A cancer-derived mutation in the PSTAIRE helix of cyclin-dependent kinase 2 alters the stability of cyclin binding. *Biochim. Biophys. Acta*. **1803**, 858-64.

Choi, T., Aoki, F., Mori, M., Yamashita, M., Nagahama, Y., and Kohmoto, K. (1991). Activation of $p34^{cdc2}$ protein kinase activity in meiotic and mitotic cell cycles in mouse oocytes and embryos. *Development* **113**, 789-795.

Clark, J. W. H., Yudin, A. I., Lynn, J. W., Griffin, F. J., and Pillai, M. C. (1990). Jelly layer formation in Penaeoidean shrimp eggs. *Biol. Bull.* **178**, 295-299.

Clarke, P. R., Leiss, D., Pagano, M., and Karsentil, E. (1992). Cyclin A- and cyclin B-dependent protein kinases are regulated by different mechanisms in *Xenopus* egg extracts. *EMBO J.* **11**, 1751-1761.

De Bondt, H. L., Rosenblatt, J., Jancarik, J., Jones, H. D., Morgan, D. O., and Kim, S. H. (1993). Crystal structure of cyclin-dependent kinase 2. *Nature* **363**, 595-602.

De Smedt, V., Poulhe, R., Cayla, X., Dessauge, F., Karaiskou, A., Jessus, C., and Ozon, R. (2002). Thr-161 phosphorylation of monomeric Cdc2 regulation by protein phosphatase 2C *in Xenopus* oocytes. . *J. Biol. Chem.*, 28592-28600.

Devault, A., Martinez, A., Fesquet, D., Labbe, J., Morin, N., Tassan1, J., Nigg1, E. A., Cavadore, J., and Doree, M. (1995). MAT1 ('menage a trois') a new RING finger protein subunit stabilizing cyclin H-cdk7 complexes in starfish and *Xenopus* CAK. *EMBO J.* **14**, 5027-5036.

Dobson, S., Kar, B., Kumar, R., Adams, B., and Barik, S. (2001). A novel tetratricopeptide repeat (TPR) containing PP5 serine/threonine protein phosphatase in the malaria parasite, Plasmodium falciparum. *BMC Microb.* 1-30.

Dunphy, W. G., Brizuela, L., Beach, D., and Newport, J. (1988). The *Xenopus* Cdc2 protein is a component of MPF, a cytoplasmic regulator of mitosis. *Cell* **54**, 423-431.

Dunphy, W. G., and Kumagai, A. (1991). The Cdc25 protein contains an intrinsic phosphatase activity. *Cell* **67**, 189-196.

Elledge, S. J., and Harper, J. W. (1998). The role of protein stability in the cell cycle and cancer. *Biochim. Biophys. Acta.* **1377**, 61-70.

Engelmann, F. (1994). "Invertebrates: hormone-regulated gonadal activity," National Research Council of Canada.

Fairs, N. J., Quinlan, P. T., and Goad, L. J. (1990). Changes in ovarian unconjugated and conjugated steroid titers during vitellogenesis in *Penaeus monodon*. *Aquaculture* **89**, 83-99.

Fingerman, M. (1997). Roles of neurotransmitters in regulating reproductive hormone release and gonadal maturation in decapod crustaceans. *J. Inver. Rep. Dev.* **31**, 47-54.

Fingerman, M., Nagabhushanam, R., and Sarojini, R. (1993). Vertebrate-type hormones in crustaceans: localization, identification and functional significance. *Zool. Sci.* **18**, 13-29.

Fujii, W., Nishimura, T., Kano, K., Sugiura, K., and Naito, K. (2011). CDK7 and CCNH are components of CDK-activating kinase and are required for meiotic progression of pig oocytes. *Biol Reprod.* **85**, 1124-32.

Fukuda, M., Miyoshi, M., and Nadano, D. (2008). The role of bystin in embryo implantation and in ribosomal biogenesis. *Cell Mol. life Sci.* **65**, 92-99.

Fukuda, M. N., and Sugihara, K. (2007). Signal transduction in human embryo implantation. *Cell Cycle-landes Biosci.* **6**, 1153.

Gautier, J., Minshull, J., Lohka, M., Glotzer, M., Hunt, T., and Maller, J. L. (1990). Cyclin is a component of maturation-promoting factor from *Xenopus*. *Cell* **60**, 487-494.

Grøndahl, C. (2008). Oocyte maturation. *Dan. Med. Bull.* **55**, 1-16.

Hallak, H., Seiler, A. E., Green, J. S., Ross, B. N., and Rubin, R. (2000). Association of Heterotrimeric Gi with the Insulin-like Growth Factor-I Receptor Release of Gβγ subunits upon receptor activation. J. Biol. Chem. **275**, 2255-2258.

Han, K., Dai, Y., Zou, Z., Fu, M., Wang, Y., and Zhang, Z. (2012). Molecular characterization and expression profiles of cdc2 and cyclin B during oogenesis and spermatogenesis in green mud crab (*Scylla paramamosain*). *Comp. Biochem. Physiol. B Biochem. Mol. Biol*. **163**, 292-302.

Hassig, C. A., Tong, J. K., Fleischer, T. C., Owa, T., Grable, P. G., Ayer, D. E., and Schreiber, S. L. (1998). A role for histone deacetylase activity in HDAC1-mediated transcriptional repression. *Proc. Natl. Acad. Sci.* **95**, 3519-3524.

Hirai, T., Yamashita, M., Yoshikuni, M., Lou, Y. H., and Nagahama, Y. (1992). Cyclin B in fish oocytes: its cDNA and amino acid sequences, appearance during maturation, and induction of $p34^{cdc2}$ activation. *Mol. Reprod. Dev.* **33**, 131-140.

Holmes, J. K., and Solomon, M. J. (1996). A Predictive scale for evaluating Cyclin-dependent Kinase substrates a comparison of $p34^{cdc2}$ and $p33^{cdk2}$. *J. Biol. Chem.* **271**, 25240-25246.

Honda, R., Ohba, Y., Nagata, A., Okayama, H., and Yasuda, H. (1993). Dephosphorylation of human $p34^{cdc2}$ kinase on both Thr-14 and Tyr-15 by human cdc25B phosphatase. *FEBS letts.* **318**, 331-334.

Huberman, A. (2000). Shrimp endocrinology. A review. *Aquaculture* **191**, 191-208.

Ihara, J., Yoshida, N., Tanaka, T., Mita, K., and Yamashita, M. (1998). Either cyclin B1 or B2 is necessary and sufficient for inducing germinal vesicle breakdown during frog (*Rana japonica*) oocyte maturation. *Mol. Rreprod. Dev.* **50**, 499-509.

Jessus, C., Pime, H., Haccard, O., Lint, J. V., Goris, J., Merlevede, W., and Ozon, R. (1991). Tyrosine phosphorylation of $p34^{cdc2}$ and p42 during meiotic maturation of *Xenopus* oocyte antagonistic action of okadaic acid and 6-DAMP. *Development*, 813-820.

Kajiura, H., Yamashita, M., Katsu, Y., and Nagahama, Y. (1993). Isolation and Characterization of Goldfish cdc2, a Catalytic Component of Maturation-Promoting Factor. *Dev. Growth Diff.* **35**, 647-654.

Kallio, M., Weinstein, J., Daum, J. R., Burke, D. J., and Gorbsky, G. J. (1998). Mammalian p55CDC mediates association of the spindle checkpoint protein Mad2 with the cyclosome/anaphase-promoting complex, and is involved in regulating anaphase onset and late mitotic events. *J. cell Biol*. **141**, 1393-1406.

Karoonuthaisiri, N., Sittikankeaw, K., Preechaphol, R., Kalachikov, S., Wongsurawat, T., Uawisetwathana, U., Russo, J. J., Ju, J., Klinbunga, S., and Kirtikara, K. (2009). ReproArray GTS: A cDNA microarray for identification of reproduction-related genes in the giant tiger shrimp *Penaeus monodon* and characterization of a

novel *nuclear autoantigenic sperm protein* (NASP) gene. *Comp. Biochem. Physiol. Part D* **4**, 90-99.

Keller, G., Paige, C., Gilboa, E., and Wagner, E. F. (1984). Expression of a foreign gene in myeloid and lymphoid cells derived from multipotent haematopoietic precursors. *Nature* **318**, 149-154.

King, J. E. (1998). A study of the reproductive organs of the common marine shrimp, *Penaeus setiferus* (Linnaeus). *The Biological Bulletin* **94**, 244-262.

Kirby, K. S. (1956). A new method for the isolation of ribonucleic acids from mammalian tissues. *Biochem. J.* **64**, 405-408.

Kishimoto, T. (2003). Cell-cycle control during meiotic maturation. *Curr. Opin. Cell Biol.* **15**, 654-663.

Klinbunga, S., Sittikankaew, K., Yuvanatemiya, V., Preechaphol, R., Prasertlux, S., Yamano, K., and Menasveta, P. (2009). Molecular cloning and expression analysis of *ovary-specific transcript 1* (*Pm-OST1*) of the giant tiger shrimp, *Penaeus monodon. Zool. Sci.* **26**, 783-790.

Klinbunga, S., Sodsuk, S., Penman, D., and McAndrew, B. (1996). An improved protocol for total DNA isolation and visualisation of mtDNA-RFLP (s) in tiger prawn, *Penaeus monodon*. *Thai J Aquat. Sci*. **3**, 36-41.

Kobayashi, H., Minshull, J., Ford, C., Golsteyn, R., Poon, R., and Hunt, T. (1991). On the synthesis and destruction of A-and B-type cyclins during oogenesis and meiotic maturation in *Xenopus laevis. J. Cell Biol.* **114**, 755-765.

Kraft, C., Herzog, F., Gieffers, C., Mechtler, K., Hagting, A., Pines, J., and Peters, J. M. (2003). Mitotic regulation of the human anaphase-promoting complex by phosphorylation. *EMBO J.* **22**, 6598-6609.

Kruevaisayawan, H., Vanichviriyakit, R., Weerachatyanukul, W., Magerd, S., Withyachumnarnkul, B., and Sobhon, P. (2007a). Biochemical characterization and physiological role of cortical rods in black tiger shrimp, *Penaeus monodon*. *Aquaculture* **270**, 289-298.

Kruevaisayawan, H., Vanichviriyakit, R., Weerachatyanukul, W., Magerd, S., Withyachumnarnkul, B., and Sobhon, P. (2007b). Biochemical characterization and physiological role of cortical rods in black tiger shrimp, *Penaeus monodon*. *Aquaculture* **270**, 289-298.

Kruevaisayawan, H., Vanichviriyakit, R., Weerachatyanukul, W., Withyachumnarnkul, B., Chavadej, J., and Sobhon, P. (2010). Oogenesis and formation of cortical rods in the black tiger shrimp, *Penaeus monodon*. *Aquaculture* **301**, 91-98.

Kulkarni, G. K., Nagabhushanam, R., Amaldoss, G., Jaiswal, R. G., and Fingerman, M. (1992). *In vitro* stimulation of ovarian development in the red swamp crayfish, *Procambarus clarkii* (Girard), by 5-hydroxytryptamine. *Invert. Reprod. Dev.* **21**, 231-240.

Laemmli, U. K. (1970). Cleavage of structural proteins during the assembly of the head of bacteriophage T4. *Nature* **227**, 680-685.

Lafont, R. (1991). Reverse endocrinology, or "hormones" seeking functions. *Insect Biochemistry* **21**, 697-721.

Lagger, S., Meunier, D., Mikula, M., Brunmeir, R., Schlederer, M., Artaker, M., Pusch, O., Egger, G., Hagelkruys, A., and Mikulits, W. (2010). Crucial function of histone deacetylase 1 for differentiation of teratomas in mice and humans. *EMBO J.* **29**, 3992-4007.

Larochelle, S., Chen, J., Knights, R., Pandur, J., Morcillo, P., Erdjument-Bromage, H., Tempst, P., Suter, B., and Fisher, R. P. (2001). T-loop phosphorylation stabilizes the CDK7–cyclin H–MAT1 complex in vivo and regulates its CTD kinase activity. *EMBO J.* **20**, 3749-3759.

Larochelle, S., Pandur, J., Fisher, R. P., Salz, H. K., and Suter, B. (1998). Cdk7 is essential for mitosis and for *in vivo* Cdk-activating kinase activity. *Genes Dev.* **12**, 370-381.

Lee, K.-Y., Rosales, J. L., Lee, B.-C., Chung, S.-H., Fukui, Y., Lee, N.-S., Lee, K.-Y., and Jeong, Y.-G. (2004). Cdk5/p35 expression in the mouse ovary. *Molecules & Cells* **17**, 17-22.

Leelatanawit, R. (2008). Identification and characterization of genes functionally related to growth and reproduction of the giant tiger shrimp *Penaeus monodon*, Phd Thesis. Chulalongkorn University, Thailand.

Leelatanawit, R., Sittikankeaw, K., Yocawibun, P., Klinbunga, S., Roytrakul, S., Aoki, T., Hirono, I., and Menasveta, P. (2009). Identification, characterization and expression of sex-related genes in testes of the giant tiger shrimp *Penaeus monodon*. *Comp. Biochem. Physiol. A* **152**, 66-76.

Lehoux, J. G., and Sandor, T. (1970). The occurrence of steroids and steroid-metabolising enzyme system in invertebrates. *Steroids* **16**, 141-171.

Lin, C. K., and Nash, G. L. (1996). "Asian shrimp news collected " Asian Shrimp Culture Council, Bangkok, Thailand.

Liu, Q. Y., Wu, Z. L., Lv, W. J., Yan, Y. C., and Li, Y. P. (2007). Developmental expression of cyclin H and Cdk7 in zebrafish: the essential role of cyclin H during early embryo development. *Cell Res*. **17**, 163-73.

Lorca, T., Castro, A., Martinez, A. M., Vigneron, S., Morin, N., Sigrist, S., Lehner, C., Dorée, M., and Labbé, J. C. (1998). Fizzy is required for activation of the APC/cyclosome in *Xenopus* egg extracts. *EMBO J.* **17**, 3565-3575.

Lozano, J. C., Schatt, P., Verge, V., Gobinet, J., Villey, V., and Peaucellier, G. (2010). CDK5 is present in sea urchin and starfish eggs and embryos and can interact with p35, cyclin E and cyclin B3. *Mol. Reprod. Dev.* **77**, 449-61.

Makkapan, W., Maikaeo, L., Miyazaki, T., and Chotigeat, W. (2011). Molecular mechanism of serotonin via methyl farnesoate in ovarian development of white shrimp: *Fenneropenaeus merguiensis* de Man. *Aquaculture* **321**, 101-107.

Marston, A. L., and Amon, A. (2004). Meiosis: cell-cycle controls shuffle and deal. *Nat Rev. Mol. Cell Biol.* **5**, 983-97.

Martinez, A. M., Afshar, M., Martin, F., Cavadore, J. C., Labbé, J. C., and Doree, M. (1997). Dual phosphorylation of the T-loop in cdk7: its role in controlling cyclin H binding and CAK activity. *EMBO J.* **16**, 343-354.

Masui, Y. (1985). "Meiotic arrest in animal oocytes," Academic Press, San Diego.

Mattson, M. P., and Spaziani, E. (1985). 5-Hydroxytryptamine mediates release of moltinhibiting hormone activity from isolated crab eyestalk ganglia. *Biol. Bull.***169**, 246-255.

Medina, A., Vila, Y., Mourente, G., and Rodríguez, A. (1996). A comparative study of the ovarian development in wild and pond-reared shrimp, *Penaeus kerathurus* (Forskål, 1775). *Aquaculture* **148**, 63-75.

Meeratana, P., Withyachumnarnkul, B., Damrongphol, P., Wongprasert, K., Suseangtham, A., and Sobhon, P. (2006). Serotonin induces ovarian maturation in giant freshwater prawn broodstock, *Macrobrachium rosenbergii* de Man. *Aquaculture* **260**, 315-325.

Meusy, J. J., and Payen, G. G. (1988). Female reproduction in Malacostracan Crustacea. *Zool. Sci.* **5**, 217-265.

Miura, F., Kawaguchi, N., Sese, J., Toyoda, A., Hattori, M., Morishita, S., and Ito, T. (2006). A large-scale full-length cDNA analysis to explore the budding yeast transcriptome. *PNAS* **103**, 17846-17851.

Mohamed, K. H. (1970). Synopsis of biological data on the jumbo tiger prawn *Penaeus monodon* Fabricius 1798. *FAO Fish. Rep.* **4**, 1251 - 1266.

Morgan, D. O., and De Bondt, H. L. (1994). Protein kinase regulation: insights from crystal structure analysis. *Curr. Opin. Cell Biol.* **6**, 239-246.

Mueller, P. R., Coleman, T. R., Kumagai, A., and Dunphy, W. G. (1995). Myt1: a membrane-associated inhibitory kinase that phosphorylates Cdc2 on both threonine-14 and tyrosine-15. *Sci.* **270**, 86-90.

Musa, F. R., Tokuda, M., Kuwata, Y., Ogawa, T., Tomizawa, K., Konishi, R., Takenaka, I., and Hatase, O. (1998). Expression of Cydin-Dependent Kinase 5 and Associated Cyclins in Leydig and Sertoli Cells of the Testis. *J. Androl.* **19**, 657-666.

Nebreda, A. R., and Ferby, I. (2000). Regulation of the meiotic cell cycle in oocytes. *Curr. Opin. Cell Biol.* **12**, 666-675.

Nelson, J. (2008). "Structure and function in cell signalling," John Willey & Son Ltd, The Altrium, Southern Gate, Chichester, England.

Nigg, E. A. (1996). Cyclin-dependent kinase 7: at the cross-roads of transcription, DNA repair and cell cycle control? *Curr. Opin. Cell Biol.* **8**, 312-317.

Nigg, E. A. (2001). Mitotic kinases as regulators of cell division and its checkpoints. *Nature reviews Mol. Cell Biol.* **2**, 21-32.

Oe, T., Nakajo, N., Katsuragi, Y., Okazaki, K., and Sagata, N. (2001). Cytoplasmic occurrence of the Chk1/Cdc25 pathway and regulation of Chk1 in *Xenopus* oocytes. *Dev. Biol*. **229**, 250-61.

Ohshima, T., Ward, J. M., Huh, C.-G., Longenecker, G., Pant, H. C., Brady, R. O., Martin, L. J., and Kulkarni, A. B. (1996). Targeted disruption of the cyclin-dependent kinase 5 gene results in abnormal corticogenesis, neuronal pathology and perinatal death. *PNAS* **93**, 11173-11178.

Okano-Uchida, T., Sekiai, T., Lee, K.-s., Okumura, E., Tachibana, K., and Kishimoto, T. (1998). *In Vivo* Regulation of Cyclin A/Cdc2 and Cyclin B/Cdc2 through Meiotic and Early Cleavage Cycles in Starfish. *Dev. Biol.* **197**, 39-53.

Okumura, T. (2004). Perspectives on hormonal manipulation of shrimp reproduction. *JARQ* **38**, 49-54.

Okumura, T., Kim, Y. K., Kawazoe, I., Yamano, K., Tsutsui, N., and Aida, K. (2006). Expression of vitellogenin and cortical rod proteins during induced ovarian development by eyestalk ablation in the kuruma prawn, *Marsupenaeus japonicus*. *Comparative Biochemistry and Physiology Part A: Mol. Integrative Physiol.* **143**, 246-253.

Ollendorff, V., and Donoghue, D. J. (1997). The serine/threonine phosphatase PP5 interacts with CDC16 and CDC27, two tetratricopeptide repeat-containing subunits of the anaphase-promoting complex. *J. Biol. Chem.* **272**, 32011-32018.

Papin, C., Rouget, C., Lorca, T., Castro, A., and Mandart, E. (2004). XCdh1 is involved in progesterone-induced oocyte maturation. *Dev. Biol.* **272**, 66-75.

Patel, S. A., and Simon, M. C. (2010). Functional Analysis of the Cdk7· Cyclin H· Mat1 Complex in Mouse Embryonic Stem Cells and Embryos. *J. Biol. Chem.* **285**, 15587-15598.

Phinyo, M., Visudtiphole, V., Roytrakul, S., Phaonakrop, N., Jarayabhand, P., and Klinbunga, S. (2013). Characterization and expression of *cell division cycle 2 (Cdc2)* mRNA and protein during ovarian development of the giant tiger shrimp *Penaeus monodon*. *Gen. and Comp. Endocrinol.* **193**, 103-111.

Pongtippatee, P., Vanichviriyakit, R., Chavadej, J., Plodpai, P., Pratoomchart, B., Sobhon, P., and Withyachumnarnkul, B. (2007). Acrosome reaction in the sperm of the black tiger shrimp *Penaeus monodon* (Decapoda, Penaeidae). *Aquaculture Research* **38**, 1635-1644.

Preechaphol, R. (2008). Identification of genes related to ovarian development of thegiant tiger shrimp *Penaeus monodon,* PhD. Thesis, Chulalongkorn University, Thailand.

Preechaphol, R., Leelatanawit, R., Sittikankeaw, K., Klinbunga, S., Khamnamtong, B., Puanglarp, N., and Menasveta, P. (2007). Expressed sequence tag analysis for identification and characterization of sex-related genes in the giant tiger shrimp *Penaeus monodon*. *J. of Biochem. Mol. Biol.* **40**, 501-510.

Qiu, G.-F., Yamano, K., and Unuma, T. (2005). Cathepsin C transcripts are differentially expressed in the final stages of oocyte maturation in kuruma prawn *Marsupenaeus japonicus*. *Comp. Biochem. and Physiol. Part B* **140**, 171-181.

Qiu, G. F., and Liu, P. (2009). On the role of Cdc2 kinase during meiotic maturation of oocyte in the Chinese mitten crab, *Eriocheir sinensis*. *Comp. Biochem. Physiol.* **152**, 243-8.

Qiu, G. F., Ramachandra, R. K., Rexroad, C. E., 3rd, and Yao, J. (2008). Molecular characterization and expression profiles of cyclin B1, B2 and Cdc2 kinase during oogenesis and spermatogenesis in rainbow trout (*Oncorhynchus mykiss*). *Anim. Reprod. Sci*. **105**, 209-25.

Quackenbush, L. S. (2001). Yolk synthesis in the marine shrimp, *Penaeus vannamei*. *Am. Zool.* **41**, 458-464.

Quinitio, E., Hara, T. A., Yamaguchi, K., Fuji, A., and (1994). Changes in the steroid hormone and vitellogenin levels during the gametogenic cycle of the giant tiger shrimp, *Penaeus monodon*. *Comp. Biochem. Physiol. part C.* **109**, 21-26.

Rankin, S. M., Bradfield, J. Y., and Keeley, L. L. (1989). Ovarian protein synthesis in the South American white shrimp, *Penaeus vannamei*, during the reproductive cycle. *Int. J. Reprod.* **15**, 27-33.

Rao, K. R., and Fingerman, M. (1970). Action of biogenic amines on chromatophores, II. Analysis of the response of erythrophores in fiddler crab, Uca pugilator, to indolealkylamines and eyestalk hormone. *Comp. Gen. Pharmacol.* **1**, 117-126.

Richardson, B., Engel, G., Donatsch, P., and Stadler, P. (1984). Identification of serotonin M-receptor subtypes and their specific blockade by a new class of drugs. *Nature* **316**, 126-131.

Rodríguez, E. M., Medesani, D. A., Greco, L. S. L., and Fingerman, M. (2002). Effects of some steroids and other compounds on ovarian growth of the red swamp crayfish, *Procambarus clarkii*, during early vitellogenesis. *J. of Exp. Zool.* **292**, 82-87.

Rosenberry, B. (1997). "World Shrimp Farming 1997. Shrimp News International, San Diego.

Sambrook, J., and Russell, D. W. (2001). "Molecular Cloning," Cold Spring Harbor Laboratory Press, New York, USA.

Sarojini, R., Nagabhushanam, R., and Fingerman, M. (1995). Mode of action of the neurotransmitter 5-hydroxytryptamine in stimulating ovarian maturation in the red swamp crayfish, *Procambarus clarkii*: An *in vivo* and *in vitro* study. *J. Exp. Zool.* **271**, 395-400.

Sclafani, R. A. (1996). Cyclin dependent kinase activating kinases. *Curr. Opin. Cell Biol.* **8**, 788-794.

Sharma, P., Sharma, M., Amin, N. D., Albers, R. W., and Pant, H. C. (1999). Regulation of cyclin-dependent kinase 5 catalytic activity by phosphorylation. *Proc. Natl. Acad. Sci.* **96**, 11156-11160.

Sherr, C. J., and Roberts, J. M. (2004). Living with or without cyclins and cyclin-dependent kinases. *Genes Dev.* **18**, 2699-711.

Shih, J.-T. (1997). Sex steroid-like substances in the ovaries, hepatopancreases, and body fluid of female Mictyris brevidactylus. *Zool. Stu.* **36**, 136-145.

Sigrist, S. J., and Lehner, C. F. (1997). *Drosophila* fizzy-related down regulates mitotic cyclins and is required for cell proliferation arrest and entry into endocycles. *Cell* **90**, 671-681.

Silva Gunawardene, Y. I. N., Chow, B. K. M., He, J. G., and Chan, S. M. (2001). The shrimp, FAMeT cDNA is encoded for a putative enzyme involved in the

methylfarnesoate (MF) biosynthetic pathway and is temporally expressed in the eyestalk of different sexes. *Insect. Biochem. Mol. Bio.* **131**, 1115-1124.

Sittikankaew, K., Preechaphol, R., Yocawibun, P., Yamano, K., and Klinbunga, S. (2010). Identfication, characterization and expression of *adipose differentiation-related protein (ADRP)* gene and protein in ovaries of the giant tiger shrimp *Penaeus monodon*. *Aquaculture* **308**, 591-599.

Stewart, M. J., and Nordquist, E. K. (2005). Drosophila Bys is nuclear and shows dynamic tissue-specific expression during development. *Dev. Genes Evol*. **215**, 97-102.

Sugihara, K., Sugiyama, D., Byrne, J., Wolf, D. P., Lowitz, K. P., Kobayashi, Y., Kabir-Salmani, M., Nadano, D., Aoki, D., and Nozawa, S. (2007). Trophoblast cell activation by trophinin ligation is implicated in human embryo implantation. *PNAS* **104**, 3799-3804.

Summavielle, T., Rocha Monteiro, P. R., Reis-Henriques, M. A., and Coimbra, J. (2003). In vitro metabolism of steroid hormones by ovary and hepatopancreas of the crustacean peneid shrimp *Marsupenaeus japonicus*. *Scientia Marina (Barcelona)* **67**, 299-306.

Svejstrup, J. Q. (2010). The interface between transcription and mechanisms maintaining genome integrity. *Trends biochem.* **35**, 333-338.

Tan-Fermin, J. D., and Pudadera, R. A. (1989). Ovarian maturation stages of the wild giant tiger prawn, *Penaeus monodon* Fabricius. *Aquaculture* **77**, 229-242.

Tassan, J.-P., Jaquenoud, M., Fry, A., Frutiger, S., Hughes, G., and Nigg, E. (1995). In vitro assembly of a functional human CDK7-cyclin H complex requires MAT1, a novel 36 kDa RING finger protein. *EMBO J.* **14**, 5608.

Taylor, S., Knighton, D., Zheng, J., Ten Eyck, L., and Sowadski, J. (1992). Structural framework for the protein kinase family. *Ann. Rev. Cell Biol.* **8**, 429-462.

Towbin, H., Staehelin, T., and Gordon, J. (1979). Electrophoretic transfer of proteins from polyacrylamide gels to nitrocellulose sheets: procedure and some applications. *Proc. Natl Acad. Sci.* **76**, 4350-4354.

Tsutsui, N., Kim, Y. K., Jasmani, S., Ohira, T., Wilder, M. N., and Aida, K. (2005). The dynamics of vitellogenin gene expression differs between intact and eyestalk ablated kuruma prawn Penaeus (*Marsupenaeus*) *japonicus*. *Fish. Sci.* **71**, 249-256.

Vaca, A. A., and Alfaro, J. (2000). Ovarian maturation and spawning in the white shrimp, *Penaeus vannamei*, by serotonin injection. *Aquaculture* **182**, 373-385.

van Leuken, R., Clijsters, L., and Wolthuis, R. (2008). To cell cycle, swing the APC/C. *Biochim. Biophys. Acta.* **1786**, 49-59.

Visudtiphole, V., Klinbunga, S., and Kirtikara, K. (2009). Molecular characterization and expression profiles of *cyclin A* and *cyclin B* during ovarian development of the giant tiger shrimp *Penaeus monodon*. *Comp. Biochem. Physiol. Part A:* **152**, 535-543.

Vodermaier, H. C., Gieffers, C., Maurer-Stroh, S., Eisenhaber, F., and Peters, J.-M. (2003). TPR Subunits of the Anaphase-Promoting Complex Mediate Binding to the activator protein CDH1. *Curr. Biol.* **13**, 1459-1468.

Voronina, E., and Wessel, G. M. (2003). The Regulation of Oocyte Maturation. Dev. Biol. **58**, 53-110.

Wang, L. M., Zuo, D., Lv, W. W., Wang, D. L., Liu, A. J., and Zhao, Y. (2013). Characterization of Cdc2 kinase in the red claw crayfish (*Cherax quadricarinatus*): evidence for its role in regulating oogenesis. *Gene* **515**, 258-65.

Warrier, S. R., Tirumalai, R., and Subramoniam, T. (2001). Occurrence of vertebrate steroids, estradiol 17β and progesterone in the reproducing females of the mud crab *Scylla serrata*. *Comp. Biochem. Physiol. Part A* **130**, 283-294.

Wei, F. Y., Tomizawa, K., Ohshima, T., Asada, A., Saito, T., Nguyen, C., Bibb, J. A., Ishiguro, K., Kulkarni, A. B., Pant, H. C., Mikoshiba, K., Matsui, H., and Hisanaga, S. (2005). Control of cyclin-dependent kinase 5 (Cdk5) activity by glutamatergic regulation of p35 stability. *J Neurochem.* **93**, 502-12.

Whitfield, Z. J., Chisholm, J., Hawley, R. S., and Orr-Weaver, T. L. (2013). A meiosis-specific form of the APC/C promotes the oocyte-to-embryo transition by decreasing levels of the Polo kinase inhibitor matrimony. *PLoS Biol.* **11**, e1001648.

Withyachumnarnkul, B., Boonsaeng, V., Flegel, T. W., Panyim, S., and Wongteerasupaya, C. (1998). "Domestication and selective breeding of *Penaeus monodon* in Thailand," National Center for Genetic Engineering and Biotechnology, Bangkok.

Wongprasert, K., Asuvapongpatana, S., Poltana, P., Tiensuwan, M., and Withyachumnarnkul, B. (2006). Serotonin stimulates ovarian maturation and spawning in the black tiger shrimp *Penaeus monodon*. *Aquaculture* **261**, 1447-1454.

Yamamoto, T. M., Iwabuchi, M., Ohsumi, K., and Kishimoto, T. (2005). APC/C-Cdc20-mediated degradation of cyclin B participates in CSF arrest in unfertilized *Xenopus* eggs. *Dev. Biol.* **279**, 345-55.

Yamano, K., Qiu, G.-F., and Unuma, T. (2004). Molecular cloning and ovarian expression profiles of thrombospondin, a major component of cortical rods in ature oocytes of penaeid shrimp, *Marsupenaeus japonicus*. *Biol. Rreprod.* **70**, 1670-1678.

Yamashita, M. (2000). Toward Modeling of a General Mechanism of MPF Formation during oocyte maturation in vertebrates. *Zool. Sci.* **17**, 841-851.

Yamashita, M., Kajiura, H., Tanaka, T., Onoe, S., and Nagahama, Y. (1995). Molecular mechanisms of the activation of maturation-promoting factor during goldfish oocyte maturation. *Develop. Biol.* **168**, 62-75.

Yano, I. (1985). Induced ovarian maturation and spawning in greasyback shrimp, *Metapenaeus ensis*, by progesterone. *Aquaculture* **47**, 223-229.

Yano, I. (1987). Effect of 17-a-OH-progesterone on vitellogenin secretion in kuruma prawn, *Penaeus japonicus. Aquaculture* **61**, 46-57.

Yano, I., and Hoshino, R. (2006). Effects of 17 β-estradiol on the vitellogenin synthesis and oocyte development in the ovary of kuruma prawn (*Marsupenaeus japonicus*). *Comp. Biochem. and Physiol. Part A:* **144**, 18-23.

Yocawibon, P. (2011). Cloning and expression analysis of genes in the G protein pathway in the black tiger shrimp *Penaeus monodon*, Ms. D Thesis. Chulalongkorn University, Thailand.

Zapata, V., LopezGreco, L. S., Medesani, D., and Rodriguez, E. M. (2003). Ovarian growth in the crab, Chasmagnathusgranulata induced by hormones and neuroregulators throughout the year, *In vivo* and *in vitro* studies. *Aquaculture* **224**, 339-353.

Zhang, Q., Ahuja, H. S., Zakeri, Z. F., and Wolgemuth, D. J. (1997). Cyclin-dependent kinase 5 is associated with apoptotic cell death during development and tissue remodeling. *Develop. Biol.* **183**, 222-233.

APPENDIX

APPENDIX A

Expression of reproduction-related genes analyzed by quantitative real-time PCR

Table A1 The relative expression level of *PmBystin1* in ovaries of wild intact and eyestalk-ablated *P. monodon*.

Sample		Mean conc.		Ratio (target / *EF-1α*)	Average	SD
		PmBystin1	*EF-1α*			
Juvenile	JNOV4	2.80E+04	6.06E+06	4.62E-03	5.17E-03	1.23E-03
	JNOV5	1.34E+04	3.34E+06	4.02E-03		
	JNOV6	2.27E+04	5.40E+06	4.21E-03		
	JNOV7	4.26E+04	6.39E+06	6.66E-03		
	JNOV14	4.13E+04	6.54E+06	6.32E-03		
N-BD-Stage I	BU14OV8	6.26E+04	6.91E+06	9.07E-03	8.79E-03	2.55E-04
	BU14OV15	4.45E+04	5.20E+06	8.57E-03		
	BU14OV18	4.95E+04	5.67E+06	8.73E-03		
N:BD-Stage II	BFNOV25	3.27E+04	2.60E+06	1.26E-02	1.22E-02	5.13E-04
	BFNOV31	5.40E+04	4.67E+06	1.16E-02		
	BFNOV33	4.61E+04	3.75E+06	1.23E-02		
N:BD-Stage III	BFNOV1	1.62E+04	1.40E+06	1.16E-02	1.12E-02	1.26E-03
	BFNOV7	1.45E+04	1.43E+06	1.01E-02		
	BFNOV18	2.52E+04	2.54E+06	9.90E-03		
	BFNOV23	2.73E+04	2.42E+06	1.13E-02		
	BFNOV24	2.89E+04	2.22E+06	1.30E-02		
N:BD-Stage IV	BFNOV9	1.17E+04	6.93E+05	1.70E-02	1.37E-02	1.70E-03
	BFNOV10	7.01E+03	5.59E+05	1.26E-02		
	BFNOV11	9.41E+03	7.12E+05	1.32E-02		
	BFNOV14	1.35E+04	8.84E+05	1.53E-02		
	BFNOV15	8.43E+03	6.56E+05	1.28E-02		
	BFNOV16	1.04E+04	8.09E+05	1.28E-02		
	BFNOV17	8.90E+03	6.50E+05	1.37E-02		
	BFNOV20	8.04E+03	6.81E+05	1.18E-02		
N:Post-	BFNOV30	5.67E+04	4.97E+06	1.14E-02	1.20E-02	1.08E-03

Sample		Mean conc.		Ratio (target / *EF-1α*)	Average	SD
		PmBystin1	*EF-1α*			
spawning						
	BFNOV34	8.83E+04	6.43E+06	1.37E-02		
	BFNOV37	6.57E+04	5.27E+06	1.25E-02		
	BFNOV39	7.02E+04	6.26E+06	1.12E-02		
	BFNOV40	4.21E+04	3.73E+06	1.13E-02		
EA:BD-Stage I	BFEAOV15	3.40E+04	2.10E+06	1.62E-02	1.78E-02	1.89E-03
	WFEA4	3.87E+04	1.89E+06	2.04E-02		
	WFEA33	1.55E+04	9.31E+05	1.66E-02		
	BFEAOV18	3.40E+04	2.10E+06	1.79E-02		
EA:BD-Stage II	WFEA1	2.52E+04	1.53E+06	1.65E-02	1.69E-02	1.10E-03
	WFEA6	2.84E+04	1.54E+06	1.85E-02		
	WFEA29	1.92E+04	1.20E+06	1.59E-02		
	WFEA24	2.47E+04	1.39E+06	1.78E-02		
	WFEA30U	1.87E+04	1.13E+06	1.66E-02		
	WFEA30L	1.68E+04	1.07E+06	1.57E-02		
	WFEA27U	3.35E+04	2.11E+06	1.59E-02		
	WFEA2	4.63E+04	2.56E+06	1.81E-02		
EA:BD-Stage III	WFEA12	1.99E+04	1.09E+06	1.83E-02	1.83E-02	8.90E-04
	WFEA18	2.51E+04	1.27E+06	1.97E-02		
	WFEA19	2.98E+04	1.64E+06	1.82E-02		
	WFEA26	2.36E+04	1.29E+06	1.83E-02		
	WFEA31U	1.32E+04	7.65E+05	1.73E-02		
	WFEA31L	9.59E+03	5.62E+05	1.71E-02		
	WFEA25	2.01E+04	1.06E+06	1.89E-02		
EA:BD-Stage IV	WFEA13	1.62E+04	6.87E+05	2.36E-02	2.05E-02	2.46E-03
	WFEA15	1.02E+04	5.65E+05	1.81E-02		
	WFEA16	2.00E+04	8.84E+05	2.27E-02		
	WFEA11	1.48E+04	7.78E+05	1.91E-02		
	WFEA14	1.37E+04	7.18E+05	1.91E-02		

Table A2 The relative expression level of *PmCdc2* in ovaries of wild intact and eyestalk-ablated *P. monodon*.

Sample		Mean conc.		Ratio (target / *EF-1α*)	Average	SD
		PmCdc2	*EF-1α*			
Juvenile	JNOV4	4.75E+03	6.06E+06	7.83E-04	7.51E-04	8.18E-05
	JNOV5	2.16E+03	3.34E+06	6.45E-04		
	JNOV6	3.97E+03	5.40E+06	7.36E-04		
	JNOV14	5.48E+03	6.54E+06	8.38E-04		
N-BD-Stage I	BU14OV8	1.20E+04	6.91E+06	1.74E-03	2.07E-03	3.97E-04
	BU14OV15	9.63E+03	5.20E+06	1.85E-03		
	BU14OV18	1.16E+04	5.67E+06	2.04E-03		
	BFNOV22	1.10E+04	4.17E+06	2.63E-03		
N:BD-Stage II	BFNOV25	1.09E+04	2.60E+06	4.20E-03	3.20E-03	8.67E-04
	BFNOV31	1.25E+04	4.67E+06	2.67E-03		
N:BD-Stage II	BFNOV33	1.02E+04	3.75E+06	2.73E-03		
N:BD-Stage III	BFNOV1	5.09E+03	1.40E+06	3.63E-03	3.13E-03	4.09E-04
	BFNOV7	4.66E+03	1.43E+06	3.26E-03		
	BFNOV18	6.59E+03	2.54E+06	2.59E-03		
	BFNOV23	8.00E+03	2.42E+06	3.31E-03		
	BFNOV24	6.33E+03	2.22E+06	2.85E-03		
N:BD-Stage IV	BFNOV8	2.59E+03	7.56E+05	3.43E-03	4.02E-03	5.35E-04
	BFNOV9	3.35E+03	6.93E+05	4.83E-03		
	BFNOV10	1.97E+03	5.59E+05	3.53E-03		
	BFNOV11	2.94E+03	7.12E+05	4.13E-03		
	BFNOV14	3.76E+03	8.84E+05	4.25E-03		
	BFNOV15	2.52E+03	6.56E+05	3.84E-03		
	BFNOV16	2.64E+03	8.09E+05	3.26E-03		
	BFNOV17	2.87E+03	6.50E+05	4.42E-03		
	BFNOV20	3.05E+03	6.81E+05	4.48E-03		
N:BD Post-spawning	BFNOV30	1.22E+04	4.97E+06	2.45E-03	2.73E-03	3.41E-04
	BFNOV34	2.04E+04	6.43E+06	3.18E-03		
	BFNOV37	1.54E+04	5.27E+06	2.93E-03		
	BFNOV39	1.47E+04	6.26E+06	2.35E-03		
	BFNOV40	1.02E+04	3.73E+06	2.73E-03		

Sample		Mean conc.		Ratio (target /	Average	SD
		PmCdc2	*EF-1α*	*EF-1α*)		
EA:BD-Stage I	BFEAOV15	1.24E+04	2.10E+06	5.88E-03	4.83E-03	7.77E-04
	WFEA4	7.60E+03	1.89E+06	4.01E-03		
	WFEA33	4.33E+03	9.31E+05	4.65E-03		
	BFEAOV18	3.69E+03	7.75E+05	4.77E-03		
EA:BD-Stage II	WFEA1	6.06E+03	1.53E+06	3.97E-03	4.26E-03	3.63E-04
	WFEA6	6.04E+03	1.54E+06	3.93E-03		
	WFEA29	5.57E+03	1.20E+06	4.63E-03		
	WFEA24	6.47E+03	1.39E+06	4.67E-03		
	WFEA30U	4.69E+03	1.13E+06	4.16E-03		
	WFEA30L	4.20E+03	1.07E+06	3.92E-03		
	WFEA27L	1.01E+04	2.22E+06	4.54E-03		
	WFEA22	9.94E+03	2.40E+06	4.14E-03		
	WFEA2	9.83E+03	2.56E+06	3.84E-03		
	WFEA21	1.06E+04	2.21E+06	4.80E-03		
EA:BD-Stage III	WFEA12	5.55E+03	1.09E+06	5.11E-03	4.59E-03	6.23E-04
	WFEA18	6.28E+03	1.27E+06	4.94E-03		
	WFEA19	6.99E+03	1.64E+06	4.25E-03		
EA:BD-Stage III	WFEA26	6.04E+03	1.29E+06	4.67E-03		
	WFEA28	5.63E+03	1.25E+06	4.49E-03		
	WFEA31U	2.81E+03	7.65E+05	3.67E-03		
	WFEA31L	2.03E+03	5.62E+05	3.60E-03		
	WFEA10	5.91E+03	1.32E+06	4.49E-03		
	WFEA17	5.43E+03	1.03E+06	5.29E-03		
	WFEA25	5.73E+03	1.06E+06	5.39E-03		
EA:BD-Stage IV	WFEA13	4.04E+03	6.87E+05	5.87E-03	5.27E-03	7.17E-04
	WFEA15	2.55E+03	5.65E+05	4.51E-03		
	WFEA16	5.43E+03	8.84E+05	6.14E-03		
	WFEA11	4.01E+03	7.78E+05	5.15E-03		
	WFEA14	3.36E+03	7.18E+05	4.68E-03		

Table A3 The relative expression level of *PmCdc16* in ovaries of wild intact and eyestalk-ablated *P. monodon*

Sample		Mean conc.		Ratio (target / *EF-1α*)	Average	SD
		PmCdc16	*EF-1α*			
Juvenile	JNOV05	2.47E+04	8.07E+04	3.06E-01	2.03E-01	7.07E-02
	JNOV12	4.45E+03	2.60E+04	1.71E-01		
	BU5OV13	4.26E+04	2.90E+05	1.47E-01		
	BU5OV14	4.71E+04	2.50E+05	1.88E-01		
N-BD-Stage I	BFNOV32	4.25E+04	9.10E+05	4.67E-02	5.22E-02	1.16E-02
	WFNOV9	2.03E+04	4.56E+05	4.44E-02		
	BFNOV22	3.62E+04	5.51E+05	6.56E-02		
N:BD-Stage II	WFNOV5	2.80E+04	5.32E+05	5.27E-02	5.22E-02	1.24E-02
	WFNOV2	2.66E+04	4.27E+05	6.24E-02		
	WFNOV3	2.82E+04	4.75E+05	5.94E-02		
	WFNOV24	3.96E+04	7.68E+05	5.15E-02		
	WFNOV27	2.01E+04	3.64E+05	5.54E-02		
	WFNOV26	8.85E+02	2.82E+04	3.13E-02		
	WFNOV15	1.43E+04	2.49E+05	5.77E-02		
	WFNOV25	5.41E+02	1.67E+04	3.24E-02		
	WFNOV14	1.83E+04	3.74E+05	4.89E-02		
	WFNOV16	2.07E+04	2.93E+05	7.06E-02		
N:BD-Stage III	WFNOV13	1.83E+04	3.32E+05	5.53E-02	6.24E-02	6.89E-03
	WFNOV12	2.13E+04	3.00E+05	7.10E-02		
	WFNOV11	8.11E+03	1.25E+05	6.50E-02		
	WFNOV21	2.18E+04	3.93E+05	5.54E-02		
	WFNOV22	1.54E+04	2.34E+05	6.55E-02		
N:BD-Stage IV	WFNOV20	2.51E+04	3.88E+05	6.49E-02	5.20E-02	1.11E-02
	WFNOV18	1.15E+04	2.25E+05	5.13E-02		
	WFNOV10	6.10E+03	1.50E+05	4.06E-02		
	WFNOV19	3.47E+03	6.18E+04	5.62E-02		
	WFNOV08	6.08E+03	9.88E+04	6.16E-02		
	WFNOV06	1.62E+03	4.32E+04	3.75E-02		
N:BD Post-spawning	WFNOV01	2.27E+04	3.68E+05	6.16E-02	5.09E-02	1.99E-02
	WFNOV04	2.46E+04	3.90E+05	6.32E-02		

Sample		Mean conc.		Ratio (target / EF-1α)	Average	SD
		PmCdc16	*EF-1α*			
	WFNOV17	2.02E+04	7.26E+05	2.79E-02		
EA:BD-Stage I	WFEA04	4.61E+03	1.08E+05	4.28E-02	3.88E-02	8.74E-03
	WFEA06	6.41E+03	1.43E+05	4.49E-02		
	WFEA02	8.86E+03	3.08E+05	2.88E-02		
EA:BD-Stage II	WFEA27U	5.51E+03	1.40E+05	3.93E-02	4.35E-02	9.87E-03
	WFEA27L	8.17E+03	1.83E+05	4.46E-02		
	WFEA21	9.08E+03	2.38E+05	3.82E-02		
	WFEA05	5.95E+03	1.09E+05	5.44E-02		
	WFEA20	5.42E+03	1.03E+05	5.28E-02		
	WFEA24	2.79E+03	9.93E+04	2.81E-02		
	WFEA30U	2.08E+03	3.71E+04	5.60E-02		
	WFEA30L	1.80E+03	6.00E+04	2.99E-02		
	WFEA18	5.21E+03	9.77E+04	5.33E-02		
	WFEA28	4.63E+03	1.26E+05	3.67E-02		
	WFEA19	1.04E+04	2.32E+05	4.48E-02		
EA:BD-Stage III	WFEA26	1.17E+03	6.09E+04	1.93E-02	2.77E-02	6.40E-03
	WFEA32U	7.63E+02	2.44E+04	3.12E-02		
	WFEA32L	4.74E+02	2.03E+04	2.33E-02		
	WFEA17	1.29E+04	3.63E+05	3.56E-02		
	WFEA25	3.24E+03	9.46E+04	3.42E-02		
	WFEA09	1.42E+03	4.64E+04	3.06E-02		
	WFEA31U	1.24E+03	6.45E+04	1.93E-02		
	WFEA31L	9.67E+02	3.42E+04	2.83E-02		
EA:BD-Stage IV	WFEA13	3.07E+03	3.51E+04	8.73E-02	5.22E-02	2.86E-02
	WFEA11	3.11E+03	4.90E+04	6.35E-02		
	WFEA16	3.11E+03	1.17E+05	2.66E-02		
	WFEA15	1.20E+03	3.84E+04	3.13E-02		

Table A4 The relative expression level of *PmCdk2* in ovaries of wild intact and eyestalk-ablated *P. monodon*

Sample		Mean conc.		Ratio (target / *EF-1α*)	Average	SD
		PmCdk2	*EF-1α*			
Juvenile	JNOV14	2.14E+04	2.62E+06	8.16E-03	2.88E-02	2.43E-02
	JNOV07	9.04E+04	2.56E+06	3.53E-02		
	JNOV06	2.44E+04	2.16E+06	1.13E-02		
	JNOV05	8.07E+04	1.34E+06	6.03E-02		
N-BD-Stage I	BFNOV32	1.00E+06	9.10E+05	1.10E+00	1.15E+00	3.31E-01
	WFNOV9	3.84E+05	4.56E+05	8.43E-01		
	BFNOV22	8.27E+05	5.51E+05	1.50E+00		
N:BD-Stage II	WFNOV5	5.46E+05	5.32E+05	1.03E+00	1.25E+00	3.23E-01
	WFNOV2	5.03E+05	4.27E+05	1.18E+00		
	WFNOV3	6.53E+05	4.75E+05	1.37E+00		
	WFNOV24	7.29E+05	7.68E+05	9.49E-01		
	WFNOV27	4.48E+05	3.64E+05	1.23E+00		
	WFNOV26	2.43E+04	2.82E+04	8.62E-01		
	WFNOV15	3.53E+05	2.49E+05	1.42E+00		
	WFNOV14	3.73E+05	3.74E+05	9.97E-01		
	WFNOV16	4.81E+05	2.93E+05	1.64E+00		
	WFNOV23	5.85E+05	3.13E+05	1.87E+00		
N:BD-Stage III	WFNOV13	2.48E+05	3.32E+05	7.48E-01	7.42E-01	2.18E-01
	WFNOV12	1.56E+05	3.00E+05	5.21E-01		
	WFNOV21	3.76E+05	3.93E+05	9.56E-01		
N:BD-Stage IV	WFNOV20	2.65E+05	3.88E+05	6.83E-01	6.89E-01	1.26E-01
	WFNOV18	1.82E+05	2.25E+05	8.09E-01		
	WFNOV10	1.12E+05	1.50E+05	7.49E-01		
	WFNOV08	5.11E+04	9.88E+04	5.17E-01		
N:BD Post-spawning	WFNOV01	6.88E+05	3.68E+05	1.87E+00	1.26E+00	5.46E-01
	WFNOV04	4.27E+05	3.90E+05	1.10E+00		
	WFNOV17	5.90E+05	7.26E+05	8.13E-01		
EA:BD-Stage I	WFEA4	1.77E+06	2.80E+06	6.32E-01	5.41E-01	1.22E-01
	WFEA33	8.72E+04	2.16E+05	4.03E-01		
	WFEA6	2.18E+06	3.70E+06	5.89E-01		

Sample		Mean conc.		Ratio (target /	Average	SD
		PmCdk2	*EF-1α*	*EF-1α*)		
EA:BD-Stage II	WFEA1	3.48E+05	6.16E+05	5.66E-01	7.15E-01	1.53E-01
	WFEA21	6.00E+05	8.34E+05	7.19E-01		
	WFEA29	2.31E+05	4.01E+05	5.76E-01		
	WFEA5	3.47E+05	4.49E+05	7.73E-01		
	WFEA20	5.55E+05	6.70E+05	8.29E-01		
	WFEA24	2.34E+05	4.63E+05	5.07E-01		
	WFEA18	3.16E+05	5.84E+05	5.41E-01		
	WFEA28	2.05E+06	2.43E+06	8.44E-01		
	WFEA19	1.04E+06	1.59E+06	6.53E-01		
	WFEA26	3.49E+05	4.60E+05	7.60E-01		
	WFEA27U	4.58E+05	6.20E+05	7.39E-01		
	WFEA27L	4.90E+05	7.65E+05	6.40E-01		
	WFEA30U	2.96E+05	3.82E+05	7.76E-01		
	WFEA30L	2.79E+05	2.56E+05	1.09E+00		
EA:BD-Stage III	WFEA32U	2.11E+05	3.69E+05	5.71E-01	6.60E-01	1.72E-01
	WFEA32L	1.81E+05	3.92E+05	4.63E-01		
	WFEA31U	2.77E+05	3.49E+05	7.94E-01		
	WFEA31L	2.37E+05	2.73E+05	8.68E-01		
	WFEA10	7.01E+05	9.39E+05	7.47E-01		
	WFEA25	3.20E+05	3.72E+05	8.59E-01		
	WFEA08	5.25E+04	1.26E+05	4.15E-01		
	WFEA09	1.68E+05	3.25E+05	5.16E-01		
	WFEA12	4.68E+05	6.65E+05	7.03E-01		
EA:BD-Stage IV	WFEA11	2.43E+05	3.23E+05	7.53E-01	7.91E-01	7.45E-02
	WFEA14	2.16E+05	2.46E+05	8.77E-01		
	WFEA15	1.80E+05	2.41E+05	7.43E-01		

Table A5 The relative expression level of *PmCdk7* in ovaries of wild intact and eyestalk-ablated *P. monodon*

Sample		Mean conc.		Ratio (target / EF-1α)	Average	SD
		PmCdk7	*EF-1α*			
Juvenile	JNOV4	9.56E+04	6.06E+06	1.58E-02	1.70E-02	9.03E-04
	JNOV5	5.62E+04	3.34E+06	1.68E-02		
	JNOV6	9.84E+04	5.40E+06	1.82E-02		
	JNOV7	1.07E+05	6.39E+06	1.67E-02		
	JNOV14	1.15E+05	6.54E+06	1.75E-02		
N-BD-Stage I	BU14OV8	1.19E+05	6.91E+06	1.72E-02	1.77E-02	1.95E-03
	BU14OV15	8.95E+04	5.20E+06	1.72E-02		
	BU14OV18	8.96E+04	5.67E+06	1.58E-02		
	BFNOV22	8.51E+04	4.17E+06	2.04E-02		
N:BD-Stage II	BFNOV31	8.97E+04	4.67E+06	1.92E-02	1.72E-02	4.64E-03
	BFNOV33	7.70E+04	3.75E+06	2.05E-02		
	BFNOV38	8.16E+04	6.87E+06	1.19E-02		
N:BD-Stage III	BFNOV1	3.59E+04	1.40E+06	2.56E-02	2.29E-02	1.92E-03
	BFNOV7	3.42E+04	1.43E+06	2.39E-02		
	BFNOV18	5.21E+04	2.54E+06	2.05E-02		
	BFNOV23	5.44E+04	2.42E+06	2.25E-02		
	BFNOV24	4.94E+04	2.22E+06	2.22E-02		
N:BD-Stage IV	BFNOV8	1.84E+04	7.56E+05	2.44E-02	2.88E-02	3.15E-03
	BFNOV9	2.17E+04	6.93E+05	3.14E-02		
	BFNOV10	1.31E+04	5.59E+05	2.34E-02		
	BFNOV14	2.69E+04	8.84E+05	3.04E-02		
	BFNOV15	1.94E+04	6.56E+05	2.96E-02		
	BFNOV16	2.31E+04	8.09E+05	2.86E-02		
	BFNOV17	2.05E+04	6.50E+05	3.16E-02		
	BFNOV20	2.08E+04	6.81E+05	3.06E-02		
N:BD Post-spawning	BFNOV30	9.33E+04	4.97E+06	1.88E-02	1.98E-02	2.13E-03
	BFNOV34	1.13E+05	6.43E+06	1.76E-02		
	BFNOV37	1.21E+05	5.27E+06	2.29E-02		

Sample		Mean conc.		Ratio (target / EF-1α)	Average	SD
		PmCdk7	*EF-1α*			
	BFNOV39	1.16E+05	6.26E+06	1.86E-02		
	BFNOV40	7.81E+04	3.73E+06	2.09E-02		
EA:BD-Stage I	YLBOV06	6.30E+04	1.38E+06	4.57E-02	4.54E-02	2.72E-03
	WFEA4	8.05E+04	1.89E+06	4.25E-02		
	WFEA33	4.46E+04	9.31E+05	4.79E-02		
EA:BD-Stage II	WFEA27U	8.52E+04	2.11E+06	4.04E-02	4.55E-02	3.17E-03
	WFEA6	6.58E+04	1.54E+06	4.27E-02		
	WFEA1	6.60E+04	1.53E+06	4.33E-02		
EA:BD-Stage II	WFEA29	5.55E+04	1.20E+06	4.61E-02		
	WFEA5	6.22E+04	1.23E+06	5.07E-02		
	WFEA20	7.29E+04	1.59E+06	4.58E-02		
	WFEA24	6.20E+04	1.39E+06	4.47E-02		
	WFEA30U	5.48E+04	1.13E+06	4.86E-02		
	WFEA30L	5.09E+04	1.07E+06	4.75E-02		
EA:BD-StageIII	WFEA18	5.83E+04	1.27E+06	4.58E-02	5.65E-02	1.75E-02
	WFEA19	7.35E+04	1.64E+06	4.47E-02		
	WFEA28	5.92E+04	1.25E+06	4.72E-02		
	WFEA26	6.43E+04	7.51E+05	8.57E-02		
	WFEA31U	3.62E+04	7.65E+05	4.73E-02		
	WFEA31L	2.62E+04	5.62E+05	4.67E-02		
	WFEA12	5.23E+04	6.71E+05	7.79E-02		
EA:BD-StageIV	WFEA11	3.80E+04	7.78E+05	4.88E-02	5.10E-02	4.46E-03
	WFEA13	3.68E+04	6.87E+05	5.36E-02		
	WFEA14	3.48E+04	7.18E+05	4.84E-02		
	WFEA15	2.64E+04	5.65E+05	4.68E-02		
	WFEA16	5.09E+04	8.84E+05	5.76E-02		

Table A6 The relative expression level of *PmChk1* in ovaries of wild intact and eyestalk-ablated *P. monodon*

Sample		Mean conc.		Ratio (target / EF-1α)	Average	SD
		PmChk1	*EF-1α*			
Juvenile	JNOV4	1.48E+04	6.06E+06	2.44E-03	2.15E-03	5.42E-04
	JNOV5	6.58E+03	3.34E+06	1.97E-03		
	JNOV6	7.11E+03	5.40E+06	1.32E-03		
	JNOV7	1.46E+04	6.39E+06	2.29E-03		
	JNOV14	1.79E+04	6.54E+06	2.74E-03		
N-BD-Stage I	BU14OV8	2.24E+05	6.91E+06	3.25E-02	2.89E-02	9.32E-03
	BU14OV15	1.04E+05	5.20E+06	2.00E-02		
	BU14OV18	1.29E+05	5.67E+06	2.27E-02		
	BFNOV22	1.68E+05	4.17E+06	4.03E-02		
N:BD-Stage II	BFNOV25	1.72E+05	2.60E+06	6.59E-02	5.12E-02	1.30E-02
	BFNOV31	1.92E+05	4.67E+06	4.11E-02		
	BFNOV33	1.75E+05	3.75E+06	4.67E-02		
N:BD-Stage III	BFNOV1	5.89E+04	1.40E+06	4.19E-02	4.25E-02	2.02E-03
	BFNOV7	6.56E+04	1.43E+06	4.60E-02		
	BFNOV18	1.05E+05	2.54E+06	4.13E-02		
	BFNOV23	1.02E+05	2.42E+06	4.23E-02		
	BFNOV24	9.11E+04	2.22E+06	4.10E-02		
N:BD-Stage IV	BFNOV8	3.29E+04	7.56E+05	4.35E-02	4.89E-02	8.45E-03
	BFNOV9	4.71E+04	6.93E+05	6.80E-02		
	BFNOV10	2.62E+04	5.59E+05	4.69E-02		
	BFNOV11	3.65E+04	7.12E+05	5.12E-02		
	BFNOV14	4.48E+04	8.84E+05	5.06E-02		
	BFNOV15	2.53E+04	6.56E+05	3.86E-02		
	BFNOV16	3.35E+04	8.09E+05	4.15E-02		
	BFNOV17	3.32E+04	6.50E+05	5.10E-02		
	BFNOV20	3.30E+04	6.81E+05	4.85E-02		
N:BD Post-spawning	BFNOV30	1.68E+05	4.97E+06	3.37E-02	3.74E-02	6.03E-03
	BFNOV34	2.61E+05	6.43E+06	4.06E-02		
	BFNOV37	2.44E+05	5.27E+06	4.64E-02		
	BFNOV39	1.99E+05	6.26E+06	3.17E-02		

Sample		Mean conc.		Ratio (target / EF-1α)	Average	SD
		PmChk1	*EF-1α*			
	BFNOV40	1.29E+05	3.73E+06	3.46E-02		
EA:BD-Stage I	YLBOV06	9.17E+04	1.38E+06	6.65E-02	5.83E-02	1.97E-02
	BFEAOV18	6.06E+04	2.10E+06	2.88E-02		
	WFEA4	1.33E+05	1.89E+06	7.03E-02		
	WFEA33	6.29E+04	9.31E+05	6.76E-02		
EA:BD-Stage II	WFEA27U	1.66E+05	2.11E+06	7.85E-02	7.50E-02	8.38E-03
	WFEA6	9.76E+04	1.54E+06	6.34E-02		
	WFEA1	1.09E+05	1.53E+06	7.11E-02		
	WFEA29	9.37E+04	1.20E+06	7.78E-02		
	WFEA5	9.66E+04	1.23E+06	7.87E-02		
	WFEA20	1.43E+05	1.59E+06	8.99E-02		
	WFEA24	9.04E+04	1.39E+06	6.52E-02		
	WFEA30U	9.14E+04	1.13E+06	8.09E-02		
	WFEA30L	7.50E+04	1.07E+06	6.99E-02		
EA:BD-StageIII	WFEA18	8.94E+04	1.27E+06	7.03E-02	7.13E-02	1.92E-02
	WFEA19	1.35E+05	1.64E+06	8.19E-02		
	WFEA28	9.76E+04	1.25E+06	7.79E-02		
EA:BD-StageIII	WFEA32U	5.76E+04	1.09E+06	5.30E-02		
	WFEA9	6.05E+04	1.29E+06	4.68E-02		
	WFEA31U	5.18E+04	7.65E+05	6.77E-02		
	WFEA31L	3.58E+04	5.62E+05	6.36E-02		
	WFEA12	7.29E+04	6.71E+05	1.09E-01		
EA:BD-StageIV	WFEA11	5.95E+04	7.78E+05	7.64E-02	6.71E-02	1.36E-02
	WFEA13	4.87E+04	6.87E+05	7.08E-02		
	WFEA14	5.72E+04	7.18E+05	7.96E-02		
	WFEA15	2.57E+04	5.65E+05	4.54E-02		
	WFEA16	5.60E+04	8.84E+05	6.34E-02		

Table A7 The relative expression level of *PmRpd3* in ovaries of wild intact and eyestalk-ablated *P. monodon*

Sample		Mean conc.		Ratio (target / EF-1α)	Average	SD
		PmRpd3	*EF-1α*			
Juvenile	JNOV05	5.85E+00	3.60E+05	1.62E-05	6.57E-03	8.41E-03
	JNOV06	4.56E+03	4.04E+05	1.13E-02		
	JNOV07	3.52E+03	4.86E+05	7.24E-03		
	JNOV08	6.19E+00	2.25E+05	2.76E-05		
	JNOV09	1.12E+01	1.93E+05	5.79E-05		
	JNOV10	1.64E+04	7.86E+05	2.08E-02		
N-BD-Stage I	BUFOV03	2.81E+04	7.83E+05	3.59E-02	3.46E-02	8.14E-03
	BUFOV04	3.46E+04	1.26E+06	2.76E-02		
	AGYLOV01	5.28E+04	2.27E+06	2.32E-02		
	AGYLOV04	5.61E+04	1.47E+06	3.81E-02		
	AGYLOV02	5.35E+04	1.16E+06	4.62E-02		
	BUFOV32	3.11E+04	8.55E+05	3.64E-02		
N:BD-Stage II	ASPOV10	5.08E+04	3.66E+05	1.39E-01	1.46E-01	3.32E-02
	ASPOV06	6.70E+04	7.34E+05	9.13E-02		
	BFNOV38	4.27E+04	2.62E+05	1.63E-01		
	BFNOV35	4.89E+04	2.94E+05	1.67E-01		
	BFNOV31	6.74E+04	3.94E+05	1.71E-01		
N:BD-Stage III	BFNOV18	1.72E+04	2.99E+05	5.75E-02	8.53E-02	3.50E-02
	BFNOV03	1.47E+04	2.38E+05	6.18E-02		
	BFNOV04	2.66E+04	2.05E+05	1.30E-01		
	BFNOV24	1.83E+04	1.80E+05	1.01E-01		
	BFNOV05	2.89E+04	2.48E+05	1.17E-01		
	BFNOV01	1.79E+04	3.95E+05	4.52E-02		
N:BD-Stage IV	BFNOV02	1.20E+04	9.25E+04	1.30E-01	1.39E-01	4.42E-02
	BFNOV10	1.09E+04	7.78E+04	1.40E-01		
	BFNOV12	1.16E+04	1.30E+05	8.88E-02		
	BFNOV20	1.16E+04	7.12E+04	1.63E-01		
	BFNOV16	6.86E+03	7.31E+04	9.38E-02		
	BFNOV17	9.40E+03	4.28E+04	2.20E-01		
	BFNOV13	1.26E+04	9.10E+04	1.38E-01		
N:BD Post-	BFNOV34	4.59E+04	6.06E+05	7.58E-02	1.08E-01	3.44E-02

Sample		Mean conc.		Ratio (target / EF-1α)	Average	SD
		PmRpd3	*EF-1α*			
spawning						
	BFNOV37	3.97E+04	2.87E+05	1.38E-01		
	BFNOV39	3.70E+04	4.60E+05	8.05E-02		
	BFNOV40	3.49E+04	2.55E+05	1.37E-01		
EA:BD-Stage I	YLBOV06	2.34E+04	4.54E+05	5.15E-02	6.11E-02	1.66E-02
	BFEAOV18	1.74E+04	2.59E+05	6.71E-02		
	BFEAOV15	5.92E+04	6.85E+05	8.64E-02		
	WFEAOV4	3.56E+04	6.20E+05	5.74E-02		
	WFEAOV33	1.34E+04	3.10E+05	4.31E-02		
EA:BD-Stage II	WFEAOV27U	3.66E+04	6.88E+05	5.32E-02	5.20E-02	1.07E-02
	WFEAOV6	1.57E+04	5.06E+05	3.10E-02		
	WFEAOV1	2.73E+04	5.02E+05	5.44E-02		
	WFEAOV29	1.83E+04	3.98E+05	4.59E-02		
	WFEAOV5	2.44E+04	4.06E+05	6.02E-02		
	WFEAOV20	3.50E+04	5.23E+05	6.70E-02		
	WFEAOV24	2.20E+04	4.57E+05	4.82E-02		
	WFEAOV30U	2.30E+04	3.74E+05	6.15E-02		
	WFEAOV30L	1.66E+04	3.56E+05	4.65E-02		
EA:BD-Stage III	WFEAOV18	2.04E+04	4.20E+05	4.85E-02	5.65E-02	1.34E-02
	WFEA19	4.02E+04	5.39E+05	7.46E-02		
	WFEA28	2.90E+04	4.14E+05	7.00E-02		
	WFEA26	1.96E+04	4.27E+05	4.60E-02		
	WFEA32U	1.20E+04	2.25E+05	5.32E-02		
	WFEA9	1.93E+04	2.51E+05	7.66E-02		
	WFEA31U	1.32E+04	2.56E+05	5.16E-02		
	WFEA31L	8.11E+03	1.90E+05	4.28E-02		
	WFEA12	1.63E+04	3.60E+05	4.52E-02		
EA:BD-Stage IV	WFEA11	1.47E+04	2.60E+05	5.64E-02	7.06E-02	1.95E-02
	WFEA13	1.92E+04	2.31E+05	8.34E-02		
	WFEA14	1.63E+04	2.41E+05	6.77E-02		
	WFEA15	9.30E+03	1.91E+05	4.88E-02		
	WFEA16	2.84E+04	2.95E+05	9.65E-02		

Table A8 *In vivo* effect of 5-HT treatment on transcription of *PmBystin1* in ovaries *P. monodon*

Sample	Mean conc.		Ratio (target /	Average	SD
	PmBystin1	*EF-1α*	*EF-1α*)		
5HT_NS-1	4.86E+03	6.31E+04	7.70E-02	8.46E-02	9.11E-03
5HT_NS-2	2.49E+04	3.25E+05	7.67E-02		
5HT_NS-3	7.01E+04	7.44E+05	9.42E-02		
5HT_NS-4	3.47E+05	3.83E+06	9.05E-02		
5HT_0-1	4.37E+04	6.38E+05	6.85E-02	7.41E-02	1.38E-02
5HT_0-2	1.86E+04	3.24E+05	5.74E-02		
5HT_0-3	4.37E+04	5.26E+05	8.31E-02		
5HT_0-4	1.03E+05	1.18E+06	8.74E-02		
5HT_1-1	1.25E+04	1.78E+05	7.01E-02	6.82E-02	2.11E-02
5HT_1-2	7.20E+03	1.74E+05	4.14E-02		
5HT_1-3	2.57E+04	2.76E+05	9.30E-02		
5HT_1-5	7.39E+04	1.08E+06	6.83E-02		
5HT_3-1	1.13E+04	2.07E+05	5.43E-02	1.67E-01	2.29E-01
5HT_3-2	7.88E+03	4.77E+05	1.65E-02		
5HT_3-4	7.00E+03	1.62E+04	4.31E-01		
5HT_6-1	1.41E+04	2.23E+04	6.34E-01	1.95E+00	1.43E+00
5HT_6-2	1.27E+05	3.19E+04	3.98E+00		
5HT_6-3	1.35E+04	8.28E+03	1.64E+00		
5HT_6-4	2.81E+04	1.81E+04	1.55E+00		
5HT12-1	1.07E+05	1.70E+04	6.28E+00	2.43E+00	2.63E+00
5HT12-2	2.83E+04	1.69E+04	1.67E+00		
5HT12-3	4.33E+03	1.31E+04	3.30E-01		
5HT12-4	3.52E+04	2.45E+04	1.43E+00		
5HT_24-1	2.81E+04	2.48E+04	1.13E+00	1.57E+00	1.04E+00
5HT_24-3	2.86E+04	1.60E+04	1.79E+00		
5HT_24-4	1.02E+05	3.51E+04	2.91E+00		
5HT_24-4	1.02E+05	3.51E+04	2.91E+00		
5HT_24-5	1.18E+04	2.55E+04	4.63E-01		
5HT_48-1	4.37E+04	1.31E+04	3.32E+00	1.98E+00	1.30E+00
5HT_48-2	1.59E+04	2.43E+04	6.54E-01		
5HT_48-5	4.54E+04	1.61E+04	2.83E+00		

Sample	Mean conc.		Ratio (target / EF-1α)	Average	SD
	PmBystin1	*EF-1α*			
5HT_48-6	5.46E+04	4.94E+04	1.11E+00		

Table A9 *In vivo* effect of 5-HT treatment on transcription of *PmCdc2* in ovaries *P. monodon*

Sample	Mean conc.		Ratio (target / EF-1α)	Average	SD
	PmCdc2	*EF-1α*			
5HT_NS-1	4.22E+03	5.82E+05	7.26E-03	3.89E-03	2.35E-03
5HT_NS-2	9.13E+03	3.23E+06	2.82E-03		
5HT_NS-3	2.81E+04	7.83E+06	3.58E-03		
5HT_NS-4	6.94E+04	3.67E+07	1.89E-03		
5HT_0-1	4.14E+04	4.87E+06	8.51E-03	9.08E-03	2.53E-03
5HT_0-2	1.03E+04	1.66E+06	6.18E-03		
5HT_0-3	6.10E+04	4.95E+06	1.23E-02		
5HT_0-4	9.79E+04	1.05E+07	9.32E-03		
5HT_1-1	3.39E+04	7.44E+05	4.55E-02	2.58E-02	2.51E-02
5HT_1-2	4.78E+04	9.64E+05	4.96E-02		
5HT_1-3	1.02E+04	2.52E+06	4.05E-03		
5HT_1-5	3.72E+04	8.94E+06	4.16E-03		
5HT_3-1	2.96E+04	2.08E+06	1.42E-02	1.08E-02	4.16E-03
5HT_3-2	3.41E+04	2.42E+06	1.41E-02		
5HT_3-2	3.58E+04	3.91E+06	9.15E-03		
5HT_3-4	1.42E+04	2.51E+06	5.65E-03		
5HT_6-1	3.69E+04	3.70E+06	9.96E-03	9.26E-03	3.14E-03
5HT_6-2	5.08E+04	1.09E+07	4.64E-03		
5HT_6-3	5.05E+04	4.49E+06	1.13E-02		
5HT_6-4	1.24E+05	1.11E+07	1.12E-02		
5HT12-1	8.46E+04	2.28E+07	3.71E-03	7.78E-03	3.25E-03
5HT12-2	8.83E+04	8.75E+06	1.01E-02		
5HT12-3	1.69E+04	2.56E+06	6.62E-03		
5HT12-4	7.88E+04	7.36E+06	1.07E-02		
5HT_24-1	5.26E+04	8.11E+06	6.49E-03	6.04E-03	1.64E-03

Sample	Mean conc.		Ratio (target / EF-1α)	Average	SD
	PmCdc2	*EF-1α*			
5HT_24-3	7.13E+04	9.72E+06	7.33E-03		
5HT_24-4	1.14E+05	3.13E+07	3.64E-03		
5HT_24-5	2.65E+04	3.95E+06	6.70E-03		
5HT_48-1	9.76E+04	1.63E+07	5.98E-03	6.11E-03	2.61E-03
5HT_48-2	2.52E+04	8.26E+06	3.06E-03		
5HT_48-5	6.33E+04	6.71E+06	9.44E-03		
5HT_48-6	6.82E+04	1.14E+07	5.99E-03		

Table A10 *In vivo* effect of 5-HT treatment on transcription of *PmCdk7* in ovaries *P. monodon*

Sample	Mean conc.		Ratio (target / EF-1α)	Average	SD
	PmCdk7	*EF-1α*			
5HT_NS-1	1.05E+04	6.31E+04	1.66E-01	1.09E-01	4.81E-02
5HT_NS-2	4.22E+04	3.25E+05	1.30E-01		
5HT_NS-3	5.78E+04	7.44E+05	7.77E-02		
5HT_NS-4	2.36E+05	3.83E+06	6.16E-02		
5HT_0-1	4.95E+04	6.38E+05	7.76E-02	7.30E-02	3.84E-03
5HT_0-2	2.27E+04	3.24E+05	7.00E-02		
5HT_0-3	3.93E+04	5.26E+05	7.47E-02		
5HT_0-4	8.22E+04	1.18E+06	6.96E-02		
5HT_1-1	1.28E+04	1.78E+05	7.16E-02	7.58E-02	3.63E-02
5HT_1-2	7.82E+03	1.74E+05	4.50E-02		
5HT_1-3	3.53E+04	2.76E+05	1.28E-01		
5HT_1-5	6.37E+04	1.08E+06	5.89E-02		
5HT_3-1	1.50E+04	2.07E+05	7.25E-02	1.23E+00	1.96E+00
5HT_3-2	1.06E+04	4.77E+05	2.23E-02		
5HT_3-4	1.12E+04	1.62E+04	6.87E-01		
5HT_6-1	1.93E+04	2.23E+04	8.67E-01	1.54E+00	6.24E-01
5HT_6-2	6.55E+04	3.19E+04	2.06E+00		
5HT_6-3	1.73E+04	8.28E+03	2.09E+00		
5HT_6-4	2.09E+04	1.81E+04	1.15E+00		
5HT12-1	4.81E+04	1.70E+04	2.83E+00	1.38E+00	1.04E+00
5HT12-2	2.32E+04	1.69E+04	1.37E+00		

Sample	Mean conc.		Ratio (target / EF-1α)	Average	SD
	PmCdk7	*EF-1α*			
5HT12-4	2.23E+04	2.45E+04	9.09E-01		
5HT_24-1	2.08E+04	2.48E+04	8.36E-01	1.39E+00	6.97E-01
5HT_24-3	3.13E+04	1.60E+04	1.95E+00		
5HT_24-4	7.12E+04	3.51E+04	2.03E+00		
5HT_24-5	1.89E+04	2.55E+04	7.39E-01		
5HT_48-1	2.92E+04	1.31E+04	2.22E+00	1.42E+00	8.63E-01
5HT_48-2	1.58E+04	2.43E+04	6.52E-01		
5HT_48-5	3.40E+04	1.61E+04	2.12E+00		
5HT_48-6	3.46E+04	4.94E+04	7.02E-01		

Table A11 *In vitro* effect of 5-HT treatment on transcription of *PmCdc2* in ovaries *P. monodon*

Sample	Mean conc.		Ratio (target / EF-1α)	Average	SD
	PmCdc2	*EF-1α*			
NC0-1	4.92E+04	9.92E+05	4.96E-02	5.39E-02	2.51E-02
NC0-2	7.49E+04	9.27E+05	8.08E-02		
NC0-3	8.21E+04	2.11E+06	3.90E-02		
NC24-1	9.37E+04	1.56E+06	5.99E-02	4.87E-02	1.51E-02
NC24-2	1.23E+05	2.25E+06	5.47E-02		
NC24-3	6.33E+04	2.01E+06	3.16E-02		
NC48-1	3.75E+04	6.44E+05	5.83E-02	5.19E-02	2.24E-02
NC48-2	1.08E+05	1.54E+06	7.04E-02		
NC48-3	1.45E+04	5.40E+05	2.69E-02		
1-5HTVC0-1	5.46E+04	1.13E+06	4.83E-02	4.97E-02	1.40E-02
1-5HTVC0-2	6.17E+04	9.58E+05	6.43E-02		
1-5HTVC0-3	6.20E+04	1.71E+06	3.64E-02		
1-5HT0-1	7.01E+04	1.12E+06	6.28E-02	4.90E-02	1.20E-02
1-5HT0-2	1.25E+05	2.93E+06	4.28E-02		
1-5HT0-3	7.41E+04	1.79E+06	4.14E-02		
1-5HT30m-1	3.54E+04	5.80E+05	6.09E-02	4.46E-02	1.45E-02
1-5HT30m-2	7.45E+04	1.87E+06	3.99E-02		
1-5HT30m-3	7.34E+04	1.81E+06	4.07E-02		
1-5HT2-1	3.76E+04	6.08E+05	6.19E-02	5.23E-02	1.42E-02

Sample	Mean conc.		Ratio (target / EF-1α)	Average	SD
	PmCdc2	*EF-1α*			
1-5HT2-2	5.19E+04	8.80E+05	5.90E-02		
1-5HT2-3	5.97E+04	1.66E+06	3.60E-02		
1-5HT6-1	7.17E+04	1.21E+06	5.93E-02	5.22E-02	2.00E-02
1-5HT6-2	1.42E+05	2.10E+06	6.76E-02		
1-5HT6-3	8.75E+04	2.95E+06	2.96E-02		
1-5HT12-1	1.01E+05	1.56E+06	6.48E-02	5.94E-02	1.78E-02
1-5HT12-2	1.40E+05	1.90E+06	7.38E-02		
1-5HT12-3	7.35E+04	1.86E+06	3.95E-02		
1-5HT24-1	7.04E+04	1.18E+06	5.95E-02	6.03E-02	2.30E-02
1-5HT24-2	1.76E+05	2.11E+06	8.36E-02		
1-5HT24-3	5.95E+04	1.58E+06	3.77E-02		
1-5HT48-1	1.37E+04	2.68E+05	5.11E-02	4.49E-02	9.99E-03
1-5HT48-2	1.58E+05	3.14E+06	5.03E-02		
1-5HT48-3	4.84E+04	1.45E+06	3.34E-02		
15-5HTVC0-1	3.39E+04	7.25E+05	4.68E-02	4.97E-02	1.65E-02
15-5HTVC0-2	1.01E+05	1.50E+06	6.74E-02		
15-5HTVC6-3	7.09E+04	2.03E+06	3.49E-02		
15-5HT0-1	5.52E+04	1.03E+06	5.34E-02	4.28E-02	9.24E-03
15-5HT0-2	7.52E+04	2.05E+06	3.67E-02		
15-5HT0-3	6.64E+04	1.74E+06	3.83E-02		
15-5HT30m-1	5.34E+04	8.96E+05	5.97E-02	4.54E-02	1.31E-02
15-5HT30m-2	5.37E+04	1.26E+06	4.27E-02		
15-5HT30m-3	6.34E+04	1.86E+06	3.40E-02		
15-5HT2-1	5.39E+04	1.05E+06	5.13E-02	4.02E-02	9.74E-03
15-5HT2-2	9.71E+04	2.72E+06	3.57E-02		
15-5HT2-3	4.67E+04	1.40E+06	3.35E-02		
15-5HT6-1	7.32E+04	1.13E+06	6.48E-02	4.73E-02	1.55E-02
15-5HT6-2	1.17E+05	2.83E+06	4.15E-02		
15-5HT6-3	9.28E+04	2.62E+06	3.55E-02		
15-5HT12-1	9.19E+04	1.25E+06	7.36E-02	4.84E-02	2.19E-02
15-5HT12-2	1.18E+05	3.12E+06	3.79E-02		
15-5HT12-3	8.33E+04	2.47E+06	3.37E-02		
15-5HT24-1	5.31E+04	9.05E+05	5.87E-02	4.77E-02	1.02E-02
15-5HT24-2	1.65E+05	3.61E+06	4.59E-02		

Sample	Mean conc.		Ratio (target / EF-1α)	Average	SD
	PmCdc2	*EF-1α*			
15-5HT24-3	6.23E+04	1.62E+06	3.84E-02		
15-5HT48-1	2.61E+04	5.47E+05	4.76E-02	4.60E-02	1.24E-02
15-5HT48-2	1.94E+05	3.38E+06	5.75E-02		
15-5HT48-3	3.13E+04	9.51E+05	3.29E-02		

Table A12 *In vitro* effect of 17α, 20β-DHP treatment on transcription of *PmCdc2* in ovaries *P. monodon*

Sample	Mean conc.		Ratio (target / EF-1α)	Average	SD
	PmCdc2	*EF-1α*			
NC0-2	1.85E+04	8.18E+06	2.26E-03	2.87E-03	7.77E-04
NC0-4	2.77E+04	7.92E+06	3.49E-03		
NC0-5	3.73E+04	1.04E+07	3.58E-03		
NC0-6	6.65E+04	3.12E+07	2.13E-03		
NC24-2	4.72E+04	1.28E+07	3.69E-03	3.43E-03	8.59E-04
NC24-4	2.69E+04	7.14E+06	3.76E-03		
NC24-5	4.56E+04	1.11E+07	4.10E-03		
NC0-24	8.47E+04	3.90E+07	2.17E-03		
VC0-2	3.02E+04	1.32E+07	2.29E-03	2.64E-03	3.84E-04
VC0-4	1.02E+04	3.94E+06	2.58E-03		
VC0-5	5.07E+04	1.66E+07	3.05E-03		
VC1-2	4.60E+04	1.27E+07	3.62E-03	3.59E-03	8.31E-04
VC1-4	2.42E+04	5.50E+06	4.41E-03		
VC1-5	4.51E+04	1.64E+07	2.75E-03		
VC3-2	3.99E+04	8.93E+06	4.47E-03	3.79E-03	5.99E-04
VC3-4	2.34E+04	6.50E+06	3.60E-03		
VC3-5	8.88E+04	2.68E+07	3.31E-03		
VC6-2	4.35E+04	1.30E+07	3.35E-03	2.90E-03	8.07E-04
VC6-4	1.18E+04	5.97E+06	1.97E-03		
VC6-5	7.10E+04	2.09E+07	3.40E-03		
VC12-2	4.22E+04	1.37E+07	3.08E-03	2.73E-03	3.29E-04
VC12-4	5.43E+03	2.24E+06	2.42E-03		

Sample	Mean conc.		Ratio (target / EF-1α)	Average	SD
	PmCdc2	*EF-1α*			
VC12-5	6.88E+04	2.56E+07	2.69E-03		
VC24-2	4.47E+04	1.38E+07	3.24E-03	3.24E-03	2.27E-04
VC24-4	2.77E+04	9.20E+06	3.01E-03		
VC24-5	6.20E+04	1.79E+07	3.46E-03		
0.1-DHP0-2	2.38E+04	8.74E+06	2.72E-03	3.29E-03	1.65E-03
0.1-DHP0-4	1.73E+04	5.84E+06	2.96E-03		
0.1-DHP0-5	6.62E+04	1.17E+07	5.65E-03		
0.1-DHP0-6	5.93E+04	3.26E+07	1.82E-03		
0.1-DHP1-2	2.88E+04	8.28E+06	3.47E-03	3.03E-03	4.90E-04
0.1-DHP1-4	3.77E+04	1.20E+07	3.14E-03		
0.1-DHP1-5	7.34E+04	2.31E+07	3.18E-03		
0.1-DHP1-6	8.09E+04	3.47E+07	2.33E-03		
0.1-DHP3-2	2.09E+04	4.98E+06	4.19E-03	3.10E-03	9.11E-04
0.1-DHP3-4	2.27E+04	9.05E+06	2.51E-03		
0.1-DHP3-5	8.14E+04	2.34E+07	3.48E-03		
0.1-DHP3-6	7.85E+04	3.56E+07	2.21E-03		
0.1-DHP6-2	4.60E+04	1.85E+07	2.49E-03	2.50E-03	6.65E-04
0.1-DHP6-4	8.06E+03	4.15E+06	1.94E-03		
0.1-DHP6-5	8.14E+04	2.37E+07	3.43E-03		
0.1-DHP6-6	7.32E+04	3.45E+07	2.12E-03		
0.1-DHP12-2	4.25E+04	1.27E+07	3.35E-03	2.87E-03	5.26E-04
0.1-DHP12-4	1.52E+04	6.00E+06	2.53E-03		
0.1-DHP12-5	8.01E+04	2.44E+07	3.28E-03		
0.1-DHP12-6	7.80E+04	3.38E+07	2.31E-03		
0.1-DHP24-2	7.28E+04	2.19E+07	3.32E-03	2.83E-03	7.15E-04
0.1-DHP24-4	3.60E+04	1.05E+07	3.43E-03		
0.1-DHP24-5	5.78E+04	2.15E+07	2.69E-03		
0.1-DHP24-6	9.44E+04	5.04E+07	1.87E-03		
1-DHP0-2	3.39E+04	1.36E+07	2.49E-03	2.34E-03	3.78E-04
1-DHP0-4	1.27E+04	5.55E+06	2.29E-03		
1-DHP0-5	4.10E+04	1.50E+07	2.73E-03		
1-DHP0-6	6.70E+04	3.64E+07	1.84E-03		
1-DHP1-2	3.76E+04	1.35E+07	2.79E-03	2.74E-03	6.69E-04

Sample	Mean conc.		Ratio (target / EF-1α)	Average	SD
	PmCdc2	*EF-1α*			
1-DHP1-4	3.90E+04	1.28E+07	3.04E-03		
1-DHP1-5	6.09E+04	1.83E+07	3.33E-03		
1-DHP1-6	5.10E+04	2.85E+07	1.79E-03		
1-DHP3-2	4.07E+04	1.62E+07	2.51E-03	2.66E-03	9.98E-04
1-DHP3-4	1.63E+04	6.24E+06	2.60E-03		
1-DHP3-5	6.57E+04	1.65E+07	3.98E-03		
1-DHP3-6	3.91E+03	2.51E+06	1.56E-03		
1-DHP6-2	2.75E+04	6.81E+06	4.03E-03	2.78E-03	1.03E-03
1-DHP6-4	9.93E+03	3.93E+06	2.53E-03		
1-DHP6-5	5.10E+04	1.69E+07	3.02E-03		
1-DHP6-6	5.62E+04	3.63E+07	1.55E-03		
1-DHP12-2	6.40E+04	1.88E+07	3.40E-03	2.85E-03	8.97E-04
1-DHP12-4	1.91E+04	6.25E+06	3.06E-03		
1-DHP12-5	7.91E+04	2.32E+07	3.41E-03		
1-DHP12-6	6.84E+04	4.48E+07	1.53E-03		
1-DHP24-2	6.18E+04	2.17E+07	2.85E-03	2.52E-03	8.18E-04
1-DHP24-4	2.02E+04	8.68E+06	2.33E-03		
1-DHP24-5	6.92E+04	2.03E+07	3.41E-03		
1-DHP24-6	4.83E+04	3.26E+07	1.48E-03		
10-DHP0-2	1.81E+04	7.75E+06	2.33E-03	2.47E-03	1.03E-03
10-DHP0-4	2.79E+04	9.51E+06	2.94E-03		
10-DHP0-5	8.05E+04	2.29E+07	3.51E-03		
10-DHP0-6	3.80E+04	3.43E+07	1.11E-03		
10-DHP1-2	4.40E+04	1.18E+07	3.72E-03	2.90E-03	1.14E-03
10-DHP1-4	1.51E+04	5.59E+06	2.69E-03		
10-DHP1-5	7.26E+04	1.91E+07	3.80E-03		
10-DHP1-6	4.94E+04	3.62E+07	1.36E-03		
10-DHP3-2	2.92E+04	9.18E+06	3.18E-03	2.90E-03	8.42E-04
10-DHP3-4	3.12E+04	8.16E+06	3.82E-03		
10-DHP3-5	6.58E+04	2.37E+07	2.78E-03		
10-DHP3-6	5.91E+04	3.27E+07	1.81E-03		
10-DHP6-2	4.63E+04	1.51E+07	3.07E-03	2.50E-03	6.35E-04
10-DHP6-4	3.35E+04	1.21E+07	2.77E-03		

Sample	Mean conc.		Ratio (target / EF-1α)	Average	SD
	PmCdc2	*EF-1α*			
10-DHP6-5	3.38E+04	1.32E+07	2.56E-03		
10-DHP6-6	4.68E+04	2.93E+07	1.60E-03		
10-DHP12-2	3.52E+04	1.12E+07	3.14E-03	2.61E-03	8.02E-04
10-DHP12-4	3.96E+04	1.53E+07	2.59E-03		
10-DHP12-5	1.00E+05	3.10E+07	3.23E-03		
10-DHP12-6	6.53E+04	4.40E+07	1.48E-03		
10-DHP24-2	3.96E+04	1.08E+07	3.66E-03	3.13E-03	1.24E-03
10-DHP24-4	4.12E+04	9.42E+06	4.37E-03		
10-DHP24-5	4.13E+04	1.36E+07	3.04E-03		
10-DHP24-6	4.80E+04	3.30E+07	1.45E-03		

VITA

Miss Mahattanee Phinyo was born on November 01, 1983 in Chonburi Province. She graduated with the degree of Bachelor of Science with second class honors from the Faculty of Marine Technology, Burapha University in 2006 and the degree of Master of Science from the Program in Biotechnology, Chulalongkorn University in 2009.

Publications during graduate study

International Journals

Phinyo, M., Visudtiphole, V., Roytrakul, S., Phaonakrop, N., Jarayabhand, P. and Klinbunga, S. 2013. Characterization and expression of cell division cycle 2 (Cdc2) mRNA and protein during ovarian development of the giant tiger shrimp Penaeus monodon. Gen. Comp. Endocrinol. 193: 103-111.

Phinyo, M., Nounurai, P., Hiransuchalert, R., Jarayabhand, P., Klinbunga, S. 2014. Characterization and expression analysis of Cyclin-dependent kinase 7 (Cdk7) gene and protein in ovaries of the giant tiger shrimp Penaeus monodon. (submitted).

International Conferences

Phinyo, M., Visudtiphole, V., Jarayabhand, P. and Klinbunga, S. 2012. Characterization and expression of cell division cycle 2 (Cdc2) mRNA and protein during ovarian development of the giant tiger shrimp Penaeus monodon, The 9th Asia-Pacific Marine Biotechnology Conference (APMBC) 2012. Kochi, Japan, July 13-16, 2012.

Phinyo, M., Suwannarangsee, S., Burapatana, V. and Chulalaksananukul, W. 2008.Double mutagenesis by EMS and UV radiation of Trichoderma reesei TISTR 3081to enhance cellulase activity. The 13th Biological Sciences Graduate Congress. National University of Singapore, Singapore, December 15-17, 2008.

National Conferences

Phinyo, M., Hiransuchalert, R., Jarayabhand, P. and Klinbunga, S. 2012. Characterization and expression analysis of Bystin1 gene and protein in ovaries of the giant tiger shrimp Penaeus monodon, The 38th Congress on Science and Technology of Thailand (STT). Chiangmai, Thailand, October 17-19, 2012.

Phinyo, M., Suwannarangsee, S., Burapatana, V. and Chulalaksananukul, W. 2008. Cellulase activity enhancement of Trichoderma reesei TISTR 3081 by induced mutation with EMS and UV radiation, Proceedings of 4th Naresuan Research Conference 2008. Naresuan University, Phitsanulok, Thailand, July 28-29, 2008.